9950-441

DOE/JPL 954853-80/80
Distribution Category UC

FINAL REPORT

on the

INVESTIGATION OF PROPOSED PROCESS SEQUENCE FOR THE ARRAY AUTOMATED ASSEMBLY TASK - PHASES I & II

Covering the Period

October 1, 1977 - June 30, 1980

JPL Contract 954853
CDRL 011

Prepared by:

Nick Mardesich
Alec Garcia
Kim Eskenas

Approved by:

William E. Taylor, Manager
Process Development and Engineering

of

SPECTROLAB, INC.
12500 Gladstone Avenue
Sylmar, CA 91342

August 1980

The JPL Low-Cost Silicon Solar Array Project is sponsored by the U. S. Department of Energy and forms part of the Solar Photovoltaic Conversion Program to initiate a major effort toward the development of low-cost solar arrays. This work was performed for the Jet Propulsion Laboratory, California Institute of Technology by agreement between NASA and DOE.

ACKNOWLEDGEMENTS

This final report is the accumulation of a three-year effort to develop a low cost process to fabricate photovoltaic cells. The authors wish to acknowledge

Ernst Aerni
Stefanie Allison
Margaret Beck
Steven Bunyan
Bob Edwards
Charles Gay
Eleanor Gee
William Kimberly
Ivan Lawrence
Angel Pepe
Wilma Shipp
William Sipperly
Linda Stone
Boon Wong

for their contribution to this development program.

TABLE OF CONTENTS

Table of Contents (Cont'd)

Table of Contents (Cont'd)

LIST OF TABLES

List of Tables (Cont'd)

List of Tables (Cont'd)

List of Tables (Cont'd)

List of Tables (Cont'd)

List of Tables (Cont'd)

List of Tables (Cont'd)

List of Tables (Cont'd)

List of Tables (Cont'd)

LIST OF FIGURES

List of Figures (Cont'd)

List of Figures (Cont'd)

List of Figures (Cont'd)

List of Figures (Cont'd)

List of Figures (Cont'd)

1.0 SUMMARY

A selected process sequence for the low cost fabrication of photovoltaic modules was defined during this contract. Each part of the process sequence was looked at regarding its contribution to the overall dollars per watt cost. During the course of the research done, some of the initially included processes were dropped due to technological deficiencies. The printed dielectric diffusion mask, codiffusion of the n+ and p+ regions, wrap-around front contacts and retention of the diffusion oxide for use as an AR coating were all the processes that were removed for this reason. Other process steps were retained to achieve the desired overall cost and efficiency. Square wafers, a polymeric spin-on PX-10 diffusion source, a p+ back surface field and silver front contacts are all processes that have been recommended for use in this program. The printed silver solderable pad for making contact to the aluminum back was replaced by an ultrasonically applied tin-zinc pad. Also, the texturized front surface was dropped as inappropriate for the sheet silicon likely to be available in 1986.

Progress has also been made on the process sequence for module fabrication. A shift from bonding with a conformal coating to laminating with ethylene vinyl acetate and a glass superstrate is recommended for further module fabrication.

The processes that were retained for the selected process sequence, spin-on diffusion, print and fire aluminum p+ back, clean, print and fire silver front contact and apply tin pad to aluminum back, were evaluated for their cost contribution.

The finalized process sequence is shown schematically on page 1A and in Table 3.21-1, page 295. The process specifications for the finalized process sequence are shown in Appendix F. The Format A's for SAMICS calculations of the finalized process are shown in Appendix G.

PROCESS SEQUENCE

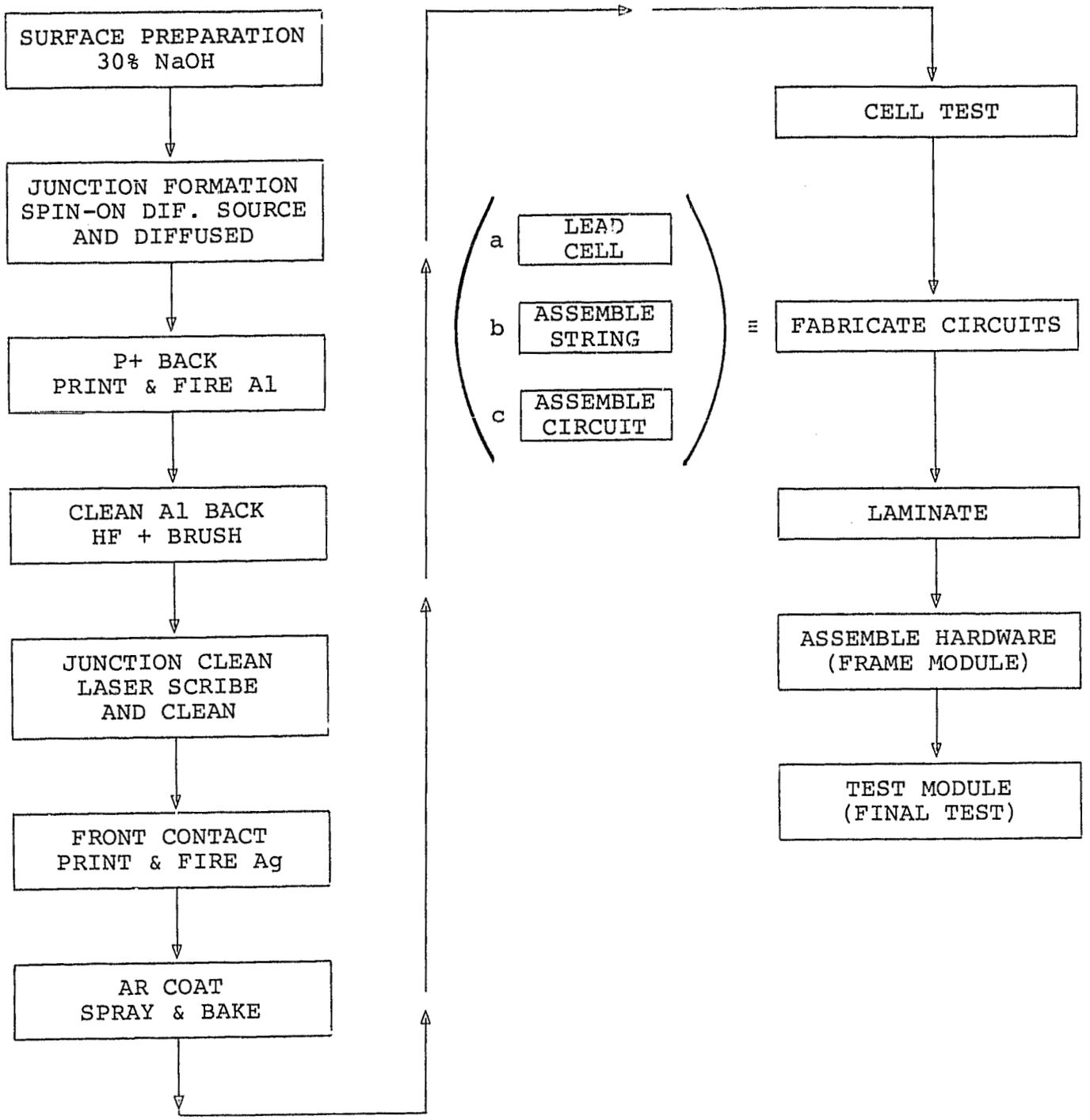

2.0 INTRODUCTION

This Final Report describes an investigation of the state of technology readiness for a selected process sequence for the low cost fabrication of photovoltaic modules. The investigation constituted a part of Phases 1 and 2 of the Array Automated Assembly Task, Low Cost Silicon Solar Array Project. This report covers the period from October 1, 1977 through June 30, 1980.

2.1 TECHNICAL OVERVIEW OF CELL DESIGN AND PROCESS SEQUENCE

The proposed cell design and selected process sequence are outlined in Table 2.1-1. Discussion of the module design and process sequence is presented in a subsequent section. In order to make clear what was proposed, operations which would be performed on one piece of automated equipment and regarded as one process have been subdivided. Thus printing a pattern and firing it have been indicated as separate steps, although the work might be performed at one station.

The design included shaped cells in order to achieve the goal of 12-13% module efficiency. Spectrolab's plan included the use of texturized surfaces, conforming to the conclusions of the Phase 1 studies which stated that this is advantageous. Texturizing is already well developed for (100) oriented single crystal material. Sheet or ribbon input materials have a different orientation however, and for these it will be necessary to develop a suitable texturing process.

The cell design included a p+ back field obtained from a printed aluminum source. The n+ diffusion was to be obtained from a phosphorus doped polymer source. An innovative approach to the junction formation process was included: namely, the use of a preferred masking dielectric on the edge of the cell. This was intended to

Table 2.1-1

CELL DESIGN AND PROCESS SEQUENCE

1. Design:

   Shaped, size 25-100 cm^2 (4-16 in^2)
   Texturized surface
   n+ junction diffusion
   p+ back surface field
   Printed contact Metallization
   Wraparound contacts
   η_c = 15% (28°C, 100 mW/cm^2)

2. Process Sequence:

   1) Texture etch
   2) Print edge masking dielectric
   3) Fire edge masking dielectric
   4) Print back aluminum
   5) Apply front polymer dopant
   6) Fire junction and back surface field sources
   7) Print back isolation dielectric
   8) Fire back isolation dielectric
   9) Print contact pads
   10) Print front grid pattern and wraparound conductors
   11) Fire contact pads, grid pattern and wraparound conductors
   12) Test cells

permit the codiffusion of the n+ and p+ regions without the need for an edge etch. As a further innovation, the diffusion oxide was to be retained for use as an antireflection coating. The process sequence proposed here thus was intended to eliminate the following process operations: Separate p and n diffusions, edge and/or back etching, diffusion oxide removal and a separate AR coating step.

A further anticipated use for the edge masking dielectric was as an insulation layer for wraparound contacts. At this point an additional printing and firing operation was introduced to locate dielectric pads for the wraparound contacts on the back aluminum. Solderable contacting pads on the aluminum back were to be printed next. Front metallization grids and wraparound conductors were then printed. For this we proposed using thick film paste formulated for adherence and contact through the diffusion oxide. Finally, the front contact grids and solderable contacts on the back side would be cofired to complete the cell fabrication.

As a result of the investigation, some of these design elements and process steps have been eliminated on the basis of technological deficiencies. These eliminations include:

- Printed dielectric diffusion mask
- Codiffusion of the n+ and p+ regions
- Wraparound front contacts
- Retention of the diffusion oxide for use as an AR coating

The printed silver solderable pad for making contact to the aluminum back was replaced by an ultrasonically applied tin-zinc pad. The texturized front surface has been dropped as inappropriate for the sheet silicon likely to be available in 1986. Plasma etching is proposed as a treatment to provide a standard reproducible incoming surface to the process sequence.

The remaining processes provide a cost effective procedure for a large volume, low cost production operation. However, the eliminations require the injection of suitable processes for junction clean-up and AR coating. The process sequence and alternates shown in Table 2.1-2 are recommended for further development and evaluation.

2.2 TECHNICAL OVERVIEW OF MODULE DESIGN AND PROCESS SEQUENCE

The module design and selected process sequence are shown in Table 2.2-1. The module design was comprised of a 24 by 48 inch (60 x 120 cm) tempered glass superstrate. Square shaped cells enabled achievement of the 12% module efficiency goal.

The module structure used a thin bond line adhesive to attach the solar cells to the glass superstrate. Since silicone adhesives are known to be technically feasible, and the thin bond line minimizes costs, they were included in the preliminary design. However, alternative adhesives were to be evaluated in a search for greater cost effectiveness. Interconnect conductors were to be thin copper foil or ribbons. A simple automatic reflow soldering operation permitted by the wraparound techniques was to be used to position both contacts on the back sides of the cells. A conformal coating provided the encapsulation and rear surface. The module assembly was to be completed by mounting the superstrate in an aluminum extrusion frame.

The search for an alternate adhesive material was unsuccessful. Inability to bond a low cost conformal coating material in combination with rapid progress in developing ethylene vinyl acetate as an encapsulant material by Springborn Laboratories on another contract with JPL resulted in a recommendation to shift attention to module fabrication by lamination using EVA as the encapsulant material.

Table 2.1-2

PROCESS SEQUENCE

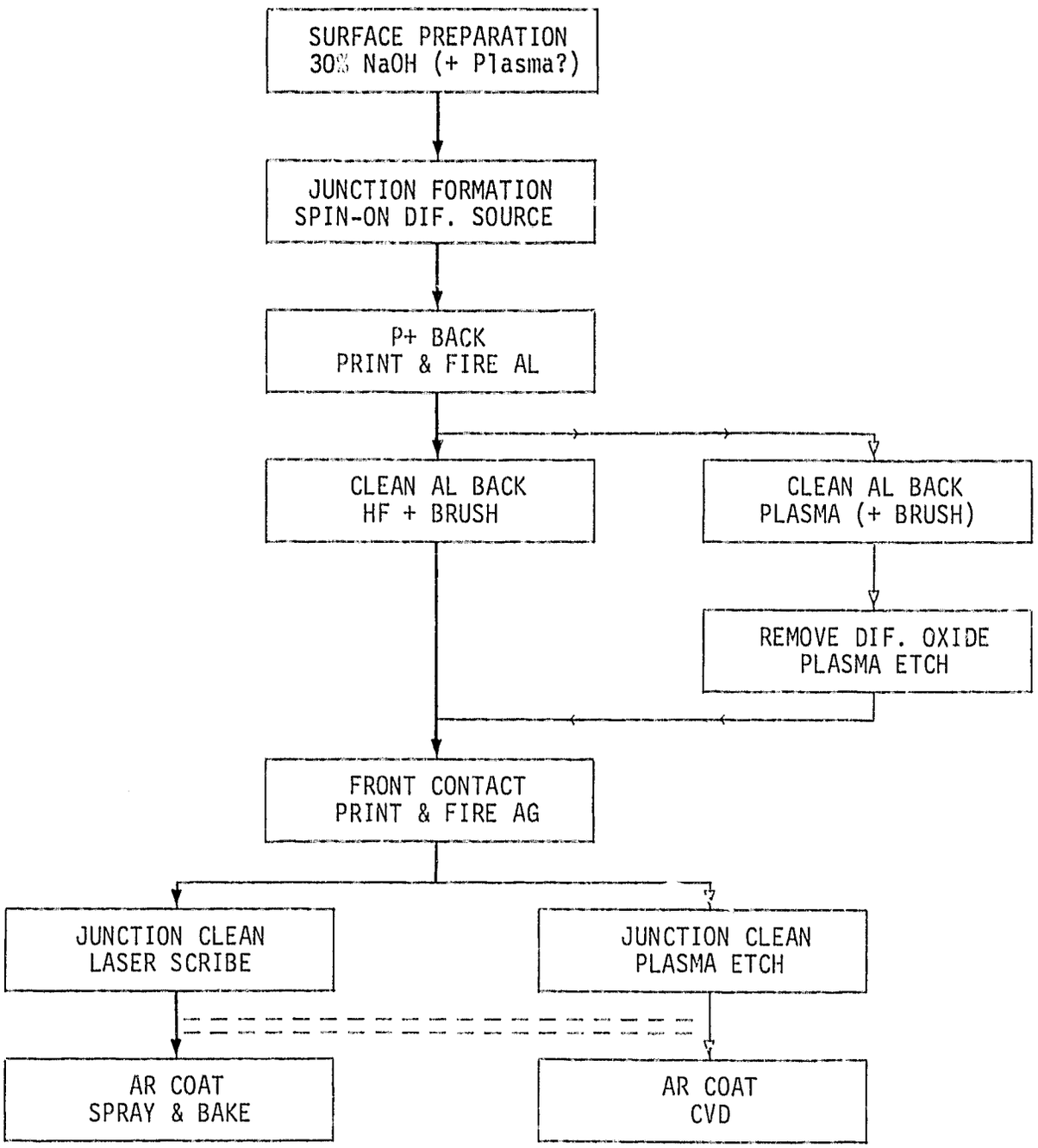

Table 2.2-1

MODULE DESIGN AND PROCESS SEQUENCE

1. Design

   Size 60 x 120 cm (2 x 4 ft)
   Tempered glass superstrate
   Cells attached by polymeric adhesive
   Preformed circuit interconnects
   3 mil polymeric conformal coating
   Aluminum extrusion frame
   η_m = 12%

2. Process Sequence*

   13. AR treat superstrate glass
   14. Mount cells on superstrate
   15. Cure adhesive
   16. Apply interconnects
   17. Apply conformal coat
   18. Cure conformal coat
   19. Mount in frame
   20. Test module

*Process sequence numbers continue from the cell area (Table 2.1-1)

3.0 TECHNICAL DISCUSSION

3.1 INTRODUCTION

The work performed and corresponding experimental results are described in the following sections. Insofar as practical, a section is devoted to each element of the design concept and process sequence. Each section is preceded by summarizing conclusions and recommendations pertaining to the experimental work and analysis.

A separate section (3.22) is devoted to a cost analysis of the surviving cell fabrication processes using the IPEG equation. Since attention was shifted from the adhesive coating lay-up module fabrication procedure to a lamination process, a similar cost analysis for the module assembly was not performed.

3.2 SILICON INGOT EVALUATION

3.2.1 Recommendations

The recommended method of silicon ingot evaluation is to compare incoming wafers to control wafers from Spectrolab crystals. The use of this technique was shown to provide a reliable means of silicon wafer evaluation.

3.2.2 Work Performed

Ingots (100) orientation procured from a variety of vendors have been sliced at Spectrolab. To evaluate the two ingots received, wafers were processed into cells simultaneously with control wafers from Spectrolab crystals. The standard process sequence shown in Table 2.1-2 was used to fabricate these cells except that laser scribing was performed prior to front contact printing, and the AR coating step was omitted. Square, 2.12" wafers from different ingot lots were chemically etched prior to front printing, and simultaneously processed with the 3" round wafers.

An example of an ingot evaluation is given in Table 3.2-1. This run indicates that Dymat silicon is equivalent to the control Spectrolab silicon. The cells had an average efficiency of 10.3% (equivalent to 13.8% with AR coating).

Table 3.2-1

INGOT EVALUATION

Lot #	Vendor	Bulk ρ (Ω-cm)	Ag Fire Temp ^{o}C	Sheet ρ ($\Omega/\square$)	V_{oc} (mV)	I_{sc} (mA)	I_{500} (mA)
Laser Scribed							
7.59.9 A	SL*	1-3	700	27-38	603	670	584
7.59.9 B	Dymat	1-3	700	28-33	603	673	586
7.59.9 C	Dymat	1-3	700	27-32	600	662	580

3.3 WAFER SHAPE

3.3.1 Recommendations

To achieve the most cost effective encapsulation and module assembly, cells should be a shape suitable for achieving 100% nesting efficiency. Several of the silicon sheet processes being developed will lead to natural square or rectangular wafers. If sheet material is obtained from Czochralski crystals, shaping into "modified" (partially shaped) hexagons will be required. The optimum degree of shaping will depend on the ratio of module costs to sheet material and shaping costs. Based upon cost data taken during this report period, it appears that shaping of cells is not cost effective (see Figure 3.3-B).

We recommend that further process development and evaluation work make use of square shaped wafers to ensure that cell processes are compatible with sheet material that will be available in 1986. A more detailed discussion is given in Appendix A.

3.3.2 Work Performed

In order to achieve the program goal of $.70/peak watt (1980 dollars), high module efficiency will be required. This implies a high nesting efficiency to avoid encapsulation costs associated with non-productive interstitial areas. It is possible that by 1986 sheet material will be available from ribbon or sheet crystal growth processes in square or rectangular shape which can be closely packed, however, low cost Czochralski crystal processes are also a possible source of silicon sheet material in 1986. In this case shaping square or hexagonal wafers (or cells) from the natural round shape will incur costs associated with the shaping operation and the generation of silicon scrap. Shaping will only be effective to the extent that the encapsulation costs saved by reduced interstitial areas are not off-set by the shaping and material scrap costs.

An analysis was made of the optimum shaping of squared wafers from cylindrical Czochralski crystals as a function of the relative costs of silicon material and photovoltaic module and system related costs. For the purposes of this analysis it was assumed that the shaping would be accomplished by slabbing off four sides of the crystal to form a square section with truncated (rounded) corners. This procedure eliminates the cell processing costs which would be associated with the discarded silicon if the cells were shaped after processing. It also provides the maximum salvage value for the discarded silicon.

The module geometry associated with one cell is shown in Figure 3.3-A. The circular segments, A_S, outside of the square correspond to the areas of discarded silicon. The corners of the square, A_I, which are truncated by the circle, correspond to interstitial areas which incur module and system related costs, but which do not generate any power.

For interpretive purposes it is convenient to consider the ratio of the size of the circle to that of the square rather than the angle θ as a measure of the degree or extent of shaping:

$$\alpha = \frac{R}{Y_o} = \frac{1}{\cos\theta} \qquad (1)$$

The range of α will be from 1 (perfect circle, no shaping) to 1.414 (perfect square).

The total cost per watt will be

$$C_w = C_w^o + S_w^o A_S' + M_w^o A_I' \qquad (2)$$

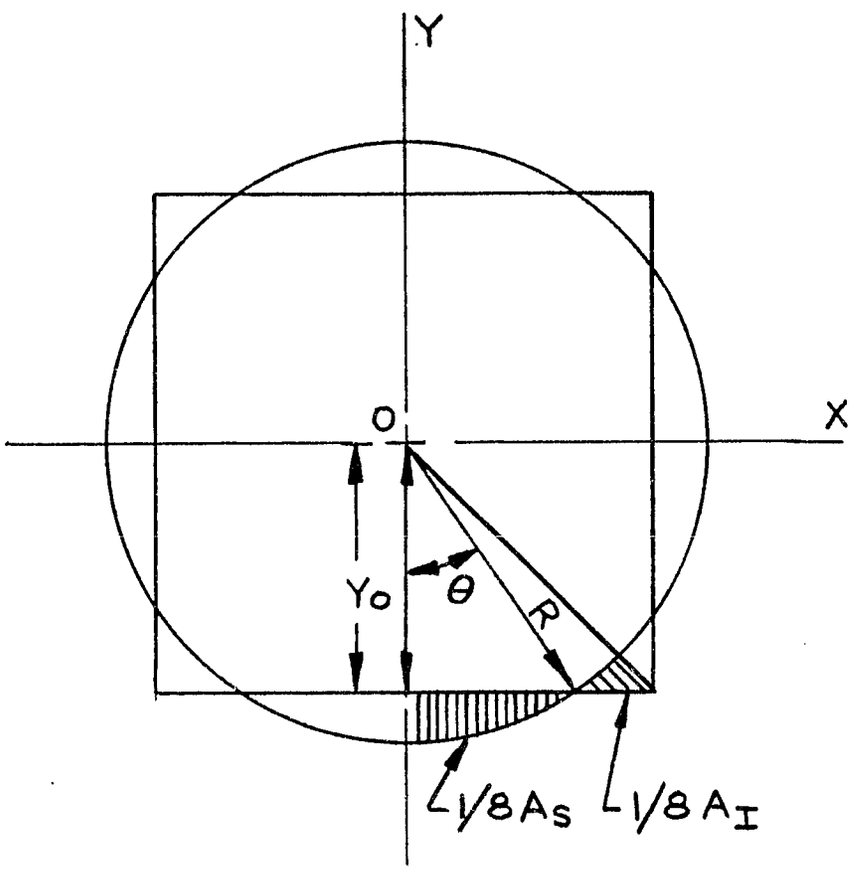

Figure 3.3-A. MODULE GEOMETRY OF UNIT CELL

where C_W^o = Cost per watt assuming perfect nesting without shaping costs

S_W^o = Cost per watt for silicon

A_S' = Fractional area of silicon discarded

M_W^o = Module and system associated cost per watt

A_I' = Fractional area of module not occupied

and where the superscript o indicates costs assuming perfect nesting without shaping costs.

The incremental costs for shaping will be:

$$\Delta C_W = S_W^o A' + M_W^o A_I' = f(\alpha) \qquad (3)$$

Equation (3) will have a minimum at some value of α which will be determined by the ratio of module to silicon costs:

$$\frac{\Delta C_W}{S_W^o} = A_S' + \beta A_I' = f(\alpha) \qquad (4)$$

where $$\beta = M_W^o / S_W^o$$

Shaping will be favored if the module costs are large compared to the silicon cost.

The relation between $\frac{\Delta C_W}{S_W^o}$ and α (Equation 4) is derived in Appendix A and shown graphically for $\beta = 1.0$ in Figure 3.3-B.

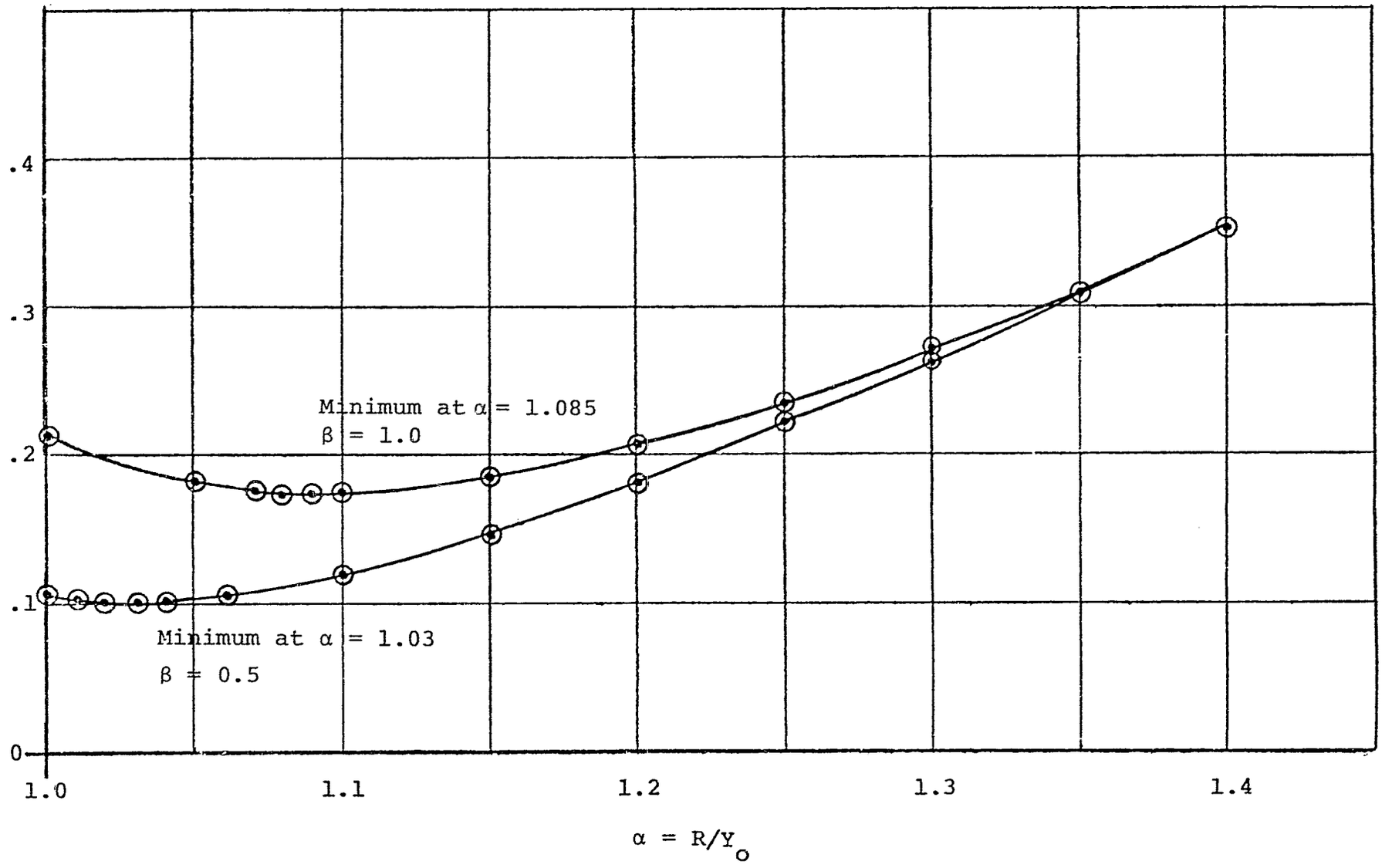

Figure 3.3-B. INCREMENTAL COSTS ASSOCIATED WITH SHAPING MODIFIED SQUARES FROM CIRCULAR CRYSTALS

The α location of the minimum cost as a function of the rate is shown in Figure 3.3-C (derivation in Appendix A). LSA cost projections suggest it is unlikely that β will ever be larger than 1. For example, a typical recent cost allocation for a $.50/watt (1975 dollars) strawman model budgeted $0.177 for silicon and $0.164 for module costs[1] (β = 0.927). The area of interest in Figure 3.3-C is therefore that indicated by the small square between β = 1.0, corresponding to α = 1.03 and α = 1.085. The optimum trimming will thus generate wafers in which the length of arc at the truncated corners is comparable to larger than the length of the flat sides.

From Figures 3.3-B and 3.3-C it will be seen that the optimum shape will be nearer to a circle than a square. This implies that there will be significant incremental costs. Incremental costs for a number of assumptions regarding interim silicon and module costs are summarized in Table 3.3-1. Similar results have been obtained for shaping modified hexagons from circular discs[2].

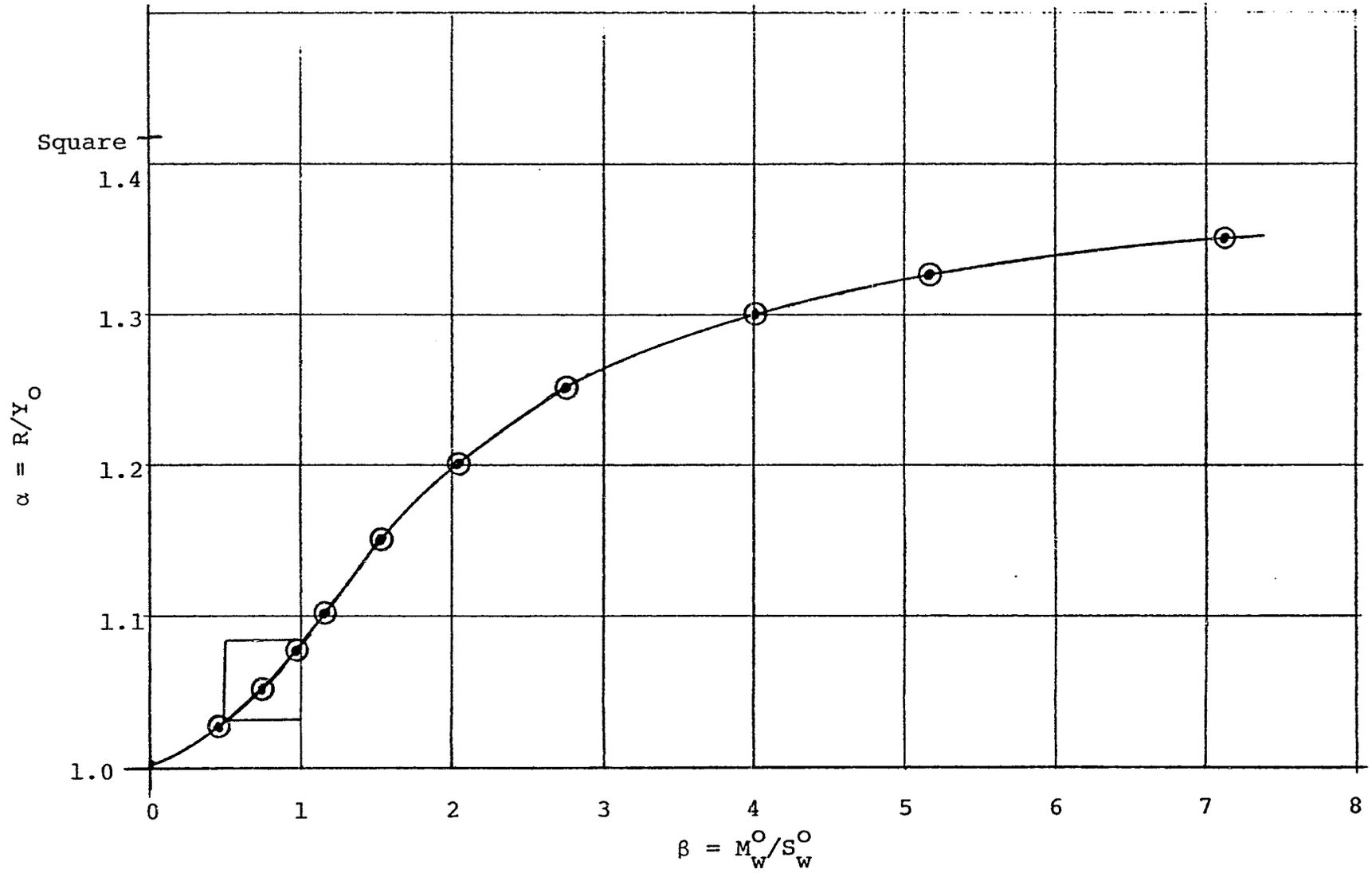

Figure 3.3-C. α LOCATION OF THE MINIMUM INCREMENTAL COST FOR SHAPING MODIFIED SQUARES FROM CIRCULAR CRYSTALS AS A FUNCTION OF THE RATIO OF MODULE TO SILICON COSTS.

Table 3.3-1

INCREMENTAL COSTS ASSOCIATED WITH SHAPING
MODIFIED SQUARES FROM CIRCULAR CRYSTALS

Silicon Cost $/Watt	Cost Ratio $\beta = M_w^o/S_w^o$	Size Ratio at Cost Min. $\alpha = R/Y_o$	Minimum Incremental Cost
2.00	0.5	1.0287	$0.200
2.00	1.0	1.0851	0.351
2.00	2.0	1.1966	0.515
1.00	0.5	1.0287	$0.100
1.00	1.0	1.0851	0.176
1.00	2.0	1.1966	0.257
0.20	0.5	1.0287	$0.020
0.20	1.0	1.0851	0.035
0.20	2.0	1.1966	0.051

3.4 SURFACE PREPARATION

3.4.1 Recommendations

A variety of silicon sheet processes are being worked on, some of which do not have surface orientations suitable for texture etching. We recommend that further process development and evaluation use non-textured wafers with a variety of surface orientations to ensure that processes selected for use in the 1986 plant will be compatible with the sheet material available at that time.

Assuming sheet material is delivered to a cell company with surfaces free from saw damages, it will be desirable to treat the sheet surfaces to establish a standard surface condition prior to diffusion. Plasma etching of non-surface damaged wafers such as EFG and Web with SF_6 is the recommended method of preparing these wafers for junction formation. For surfaces with extensive saw damage, we recommend a 30% NaOH etch.

3.4.2 Work Performed

Silicon wafers, which had been sliced using slurry-fed gang cutting methods, were etched in sodium hydroxide for varying times to determine the minimum quantity of material removal necessary for damage elimination. The (100) orientation, one ohm-cm material used in this study, was then diffused and fabricated into solar cells using standard controlled aerospace processes. 2 cm by 2 cm cells were cut from the processed round wafers and tested without AR coating. Since a distorted layer of silicon has a low minority carrier diffusion length, the output of a cell is adversely affected by any residual cutting damage. In addition, the high

leakage current caused by abraded silicon cells also results in curve shape degradation. Current at the 500 mV load point was used as a measure of residual surface damage.

Four surface preparation procedures were examined:

Group	Pre-Etch Boiling 30% NaOH	Texturizing Etch 80°C 2% NaOH*	Material Removed per Side	Sample
1	0	55 Min.	0.0009 inch	29 cells
2	90 Sec.	55 Min.	0.002 inch	26 cells
3	180 Sec.	55 Min.	0.003 inch	30 cells
4	270 Sec.	55 Min.	0.004 inch	28 cells

*20% by volume Isopropyl alcohol

Open circuit voltage, short circuit current and current at 500 mV were measured under AM1 Xenon source illumination. The results are summarized in Table 3.4-1.

These data (Table 3.4-1) suggest that the power at load is as large with a one-step texture etch as it is with a multi-stage etching process (Groups 2, 3, 4). Moreover, there appears to be the advantage of a narrower distribution of output power and possibly fewer units lost in the form of outliers. The latter would undoubtedly be rejects in a manufacturing operation.

Table 3.4-1

V_{oc}, I_{sc} AND I_{500} FOR 4 GROUPS OF CELLS GIVEN DIFFERENT SURFACE PREPARATIONS

		V_{oc} mV	I_{sc} mA/cm^2	I_{500} mA/cm^2	Rejects %
Group 1	$\bar{x}$	607.6	137.5	130.8	6.9
	σ	2.78	2.01	2.60	-
Group 2	$\bar{x}$	605.2	143.0	127.2	3.9
	σ	5.12	2.67	9.93	-
Group 3	$\bar{x}$	603.1	139.2	119.6	16.7
	σ	5.76	2.59	10.45	-
Group 4	$\bar{x}$	606.6	142.7	130.3	
	σ	4.54	2.01	7.91	

We tentatively attribute the larger variance of I_{500} for the more heavily etched samples to an increased probability of surface damage occurring between the junction diffusion and front collector metallization steps. Visual observation of the textured surface reveals that the parts treated by the one-step process have a somewhat coarse and more irregular structure. The greater number of smaller and more uniformly sized tetrahedral peaks formed in a multi-stage sequence will be more susceptible to damage in subsequent processing. Such damage would result in varying degrees of junction shunting, depending on the nature of the damage and its location. Such shunting would also have adverse effects on open circuit voltage and could account for the greater variance of that parameter for Groups 2, 3, and 4.

Another effect of pre-etching is the development of a rocky or pillowed structure, with local square shaped areas which are in some cases recessed and in others standing in relief. This structuring is barely noticeable for Group 2 in contrast to Groups 3 and 4, where it is quite pronounced. It may be that the elevated blocks are susceptible to more severe damage during subsequent processing, which could account for the increased incidence of outliers in Groups 3 and 4.

The more perfectly texturized surfaces of Groups 2, 3 and 4 would be expected to trap incident radiation more efficiently and hence to have higher short circuit current than Group 1. There is some evidence of this, but it is not sufficient to offset a degradation in curve shape for the pre-etched cells. This tendency toward curve shape degradation is probably attributable to the damage effects which have been discussed in the previous paragraphs.

The surface topography of these cells was investigated with a Scanning Electron Microscope to distinguish between surfaces generated with the use of a pre-etch to remove surface damage and those produced by direct texture etching of slurry-sawed wafers. Cells

were selected for examination to include a high output and a low output cell from three surface treatment groups. The cells, their treatment and electrical parameters are identified in Table 3.4-2.

All three groups had been etched and/or texturized with solutions of NaOH. A hot, aqueous 30% NaOH solution etches the surface fairly uniformly, but leaves pits about 50 μm in diameter. A hot 2% NaOH, 20% Isopropyl Alcohol, texturing solution has a negligible etch rate in the (111) direction which leaves the (100) surface with four sided pyramids. The rate at which these NaOH solutions attack the surface is dependent on the amount of surface damage, the temperature of the solution, the solution concentration, the relative free-bond density and the solute molecule diffusion through the reaction boundary layer.

The first pair of cells was prepared by slurry-fed ganged slicing followed by cleaning and texture etching with 2% alcoholic NaOH at 80°C for 55 minutes. Figures 3.4-A(a) and 3.4-A(b) show a typical surface region of the higher output solar cell; the surface appears to be free of pitting. The pyramids are broad and have a distribution ranging from 0.2 to 15 μm with the two extremes disproportionately represented. An average surface section of the lower output solar cell has pits of about 50 μm in diameter (Figure 3.4-B(a)) and has a slightly higher density of small pyramids (Figure 3.4-B(b)).

The second pair of cells was prepared in a manner similar to Group 1 but had a 30% NaOH treatment at 110°C for 1.5 minutes prior to the texturing treatment. The high output device has pits of 30 to 60 μm (Figure 3.4-C(a)). Small pyramids of about 4 μm in base width diameter and a narrow size distribution appear on the surface (Figure 3.4-C(b)). There seems to be a larger number of deeper pits of the same diameter in the low output solar cell (Figure 3.4-D(a)). The pyramid morphology and density seems to be about the same as that of the high output solar cell (Figure 3.4-D(b)).

Table 3.4-2

CELLS EXAMINED BY SEM FOR SURFACE TOPOGRAPHY

No.	Pre-Etch Boiling 30% NaOH Minutes	Texture Etch 80°C 2% NaOH* Seconds	E_{oc} Volts	I_{sc} mA	I_{500} mA
1	0.0	55	.612	135	131
2	0.0	55	.604	140	125
3	1.5	55	.612	143	136
4	1.5	55	.602	140	118
5	5.5	55	.613	142	138
6	5.5	55	.599	144	114

*20% by volume Isopropyl Alcohol

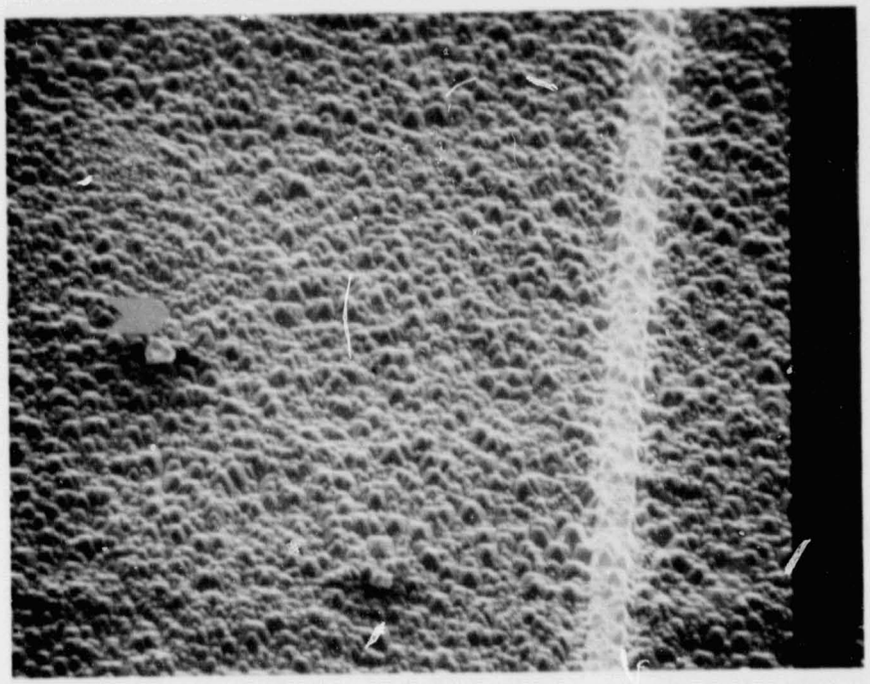

Figure 3.4-A(a) 200X

Figure 3.4-A(b) 500X

Figure 3.4-A. Surface Topography of High Output Solar Cell Prepared by Texture Etching with No Prior Damage Removed

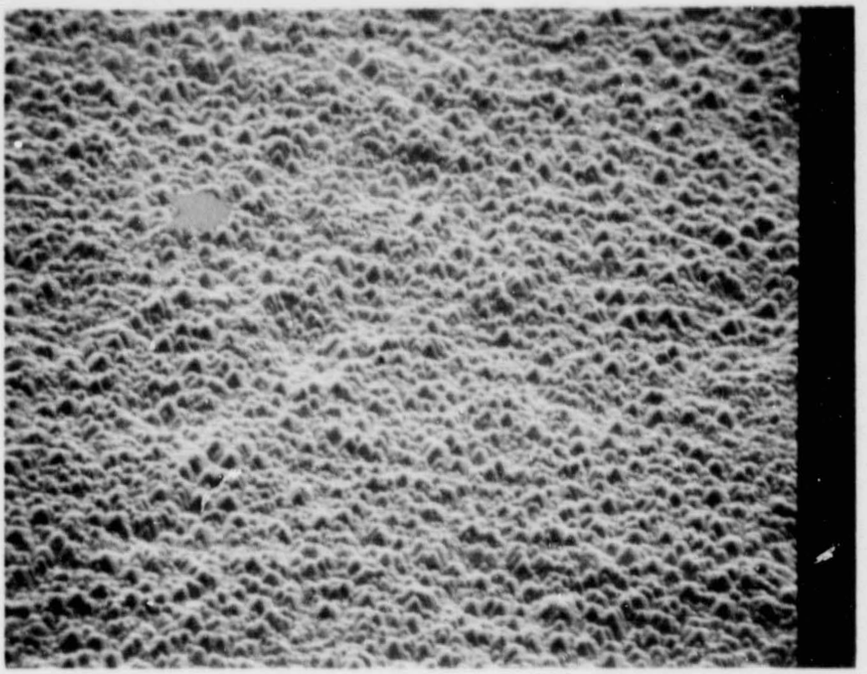

Figure 3.4-B(a) 200X

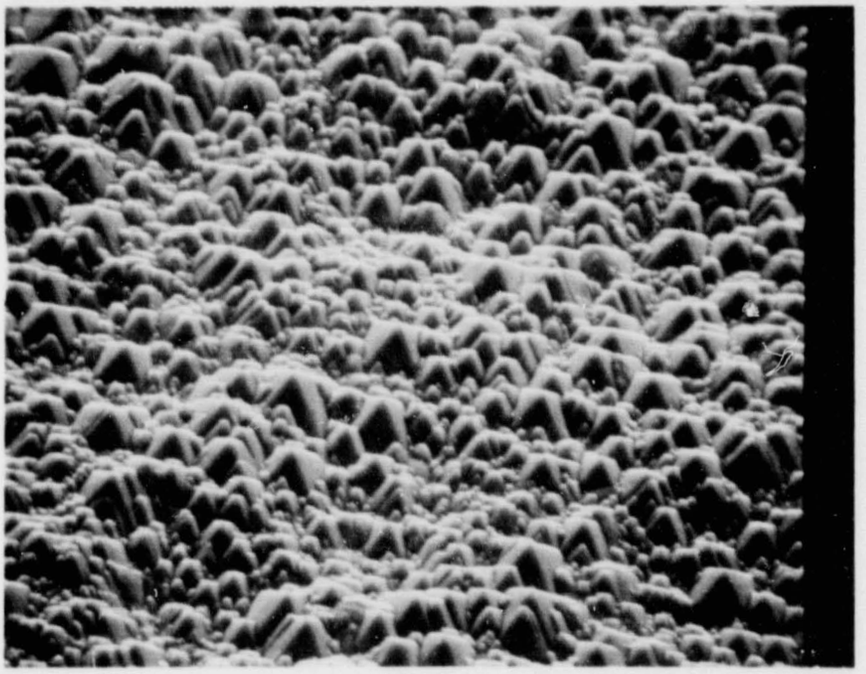

Figure 3.4-B(b) 500X

Figure 3.4-B. Surface Topography of Low Output Solar Cell Prepared by Texture Etching with No Prior Damage Removed

Figure 3.4-C(a) 200X

Figure 3.4-C(b) 500X

Figure 3.4-C. Surface Topography of High Output Solar Cell Prepared by Texture Etch After 1.5 Minutes in 30% NaOH Solution at 110°C

Figure 3.4-D(a) 200X

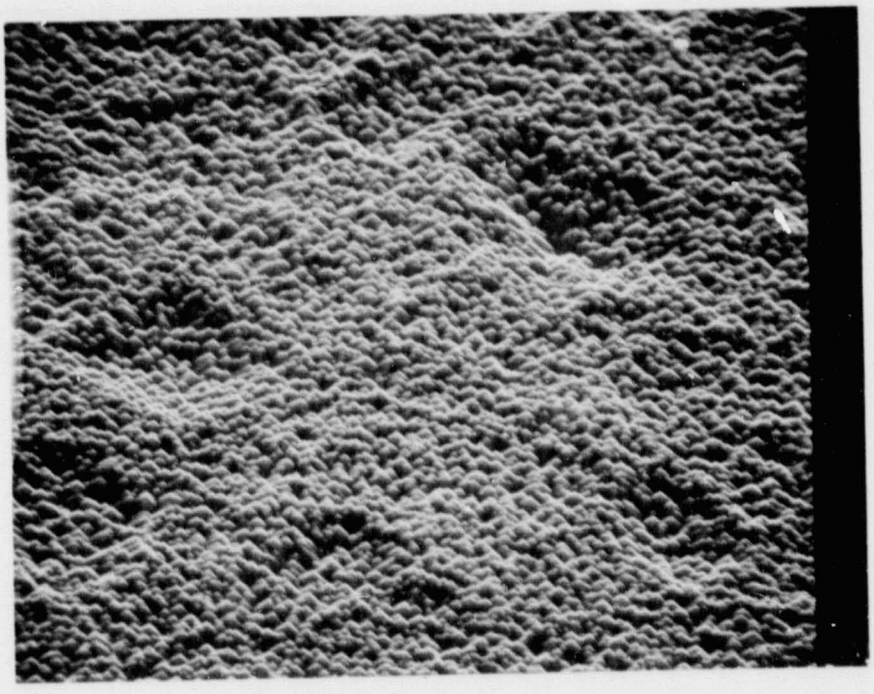

Figure 3.4-D(b) 500X

Figure 3.4-D. Surface Topography of Low Output Solar Cells Prepared by Texture Etching After 1.5 Minutes in 30% NaOH Solution at 110°C

The third pair of cells had a 5.5 minute 30% NaOH etching treatment prior to texturing. An average surface section of the high output solar cell has very deep 25 μm pits (Figure 3.4-E(a)). The pyramids appear very thin with most of the base diameters being either large ≈ 12 μm or small ≈ 4 μm (Figure 3.4-E(b)). The low output cell does not have many pits (Figure 3.4-F(a)) but does have the same thin shaped pyramids (Figure 3.4-F(b)).

The best solar cells appeared to have minimal pitting with large broad pyramids, height to base diameter ratio of about 0.5 to 1.0. However there does not appear to be a significant difference in the observable surface structure of high and low output cells.

Differences in etch treatment prior to texturizing lead to differences in observable structure which may be significant in terms of cell output. The overall yield of high output solar cells was degraded as more pretexturing treatment occurred. Also the yield of good cells progressed: Group 1 > Group 2 > Group 3. The small thin pyramids observed with long pre-etch times may be more susceptible to mechanical damage during the fabrication of the cell, thus resulting in more recombination centers or shunting and poor yield.

An additional wafer surface preparation test was performed with ingots procured from Wacker (10 ohm-cm). These ingots were sectioned into 2.125" cubes and sliced to produce wafers with a (110) surface orientation. The normal 30% NaOH etching treatment for 20 minutes resulted in the removal of 6 mils from the surface. (100) wafers generally lose 3 mils in 20 minutes. This treatment produced a partially textured surface. This surface preparation would produce an irregular surface if applied to EFG ribbons or polycrystalline wafers since these materials have numerous surface orientations. Assuming sheet material is delivered to a

Figure 3.4-E(a) 200X

Figure 3.4-E(b) 500X

Figure 3.4-E. Surface Topography of High Output Solar Cell Prepared by Texture Etching After 5.5 Minutes in 30% NaOH Solution at 110°C

Figure 3.4-F(a) 200X

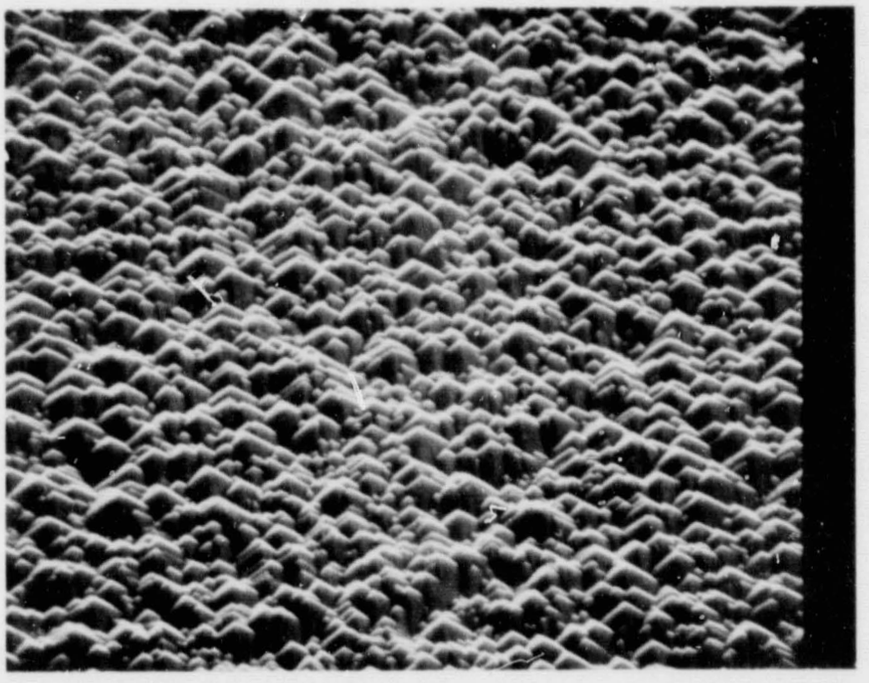

Figure 3.4-F(b) 500X

Figure 3.4-F. Surface Topography of Low Output Solar Cell Prepared by Texture Etching After 5.5 Minutes in 30% NaOH at 110°C

cell company with surfaces free of saw damage, it will be desirable to treat sheet surfaces to establish a standard surface condition which is constant with time. Plasma etching was investigated as a possible technique for creating such a standard state.

An evaluation of plasma etching non-surface damaged wafers (i.e., EFG and Web wafers) prior to junction formation was conducted in order to prepare dirty or oxidized wafers for the junction formation step. Sawed CZ wafers were first etched in NaOH to remove surface damage. These wafers were then divided into two groups; one for controls, and one for plasma etching in Freon 14 and 8% oxygen (F_{14} + 8% O_2) or sulfur hexafluoride (SF_6).

The group of wafers set aside for plasma etching was placed in an open area to accumulate dust and other foreign matter. After a period of one week these wafers were separated into four subgroups, two of which were plasma etched in F_{14} + 8% O_2 for 4 and 8 seconds, and the remaining two were plasma etched in SF_6 for 4 and 8 seconds. Junctions were formed in the four groups by spinning on PX-10, drying and diffusing the wafers. The plasma etched and control wafers were then processed together through the remaining steps of the baseline processing sequence. Table 3.4-3 lists the resultant data of the experiment.

It is evident that cells etched with F_{14} + 8% O_2 were inferior to the controls in most cases. The cells etched in SF_6 were as good as the controls in most cases.

These results indicate that plasma etching with SF_6 may be an effective method of preparing a non-surface damaged wafer for junction formation. In the case of saw damaged wafers, plasma etching is not cost effective, since long periods of etching are required. Hot NaOH is the most economical method of removing sawed surface damage.

Table 3.4-3

PLASMA ETCHING OF NON-DAMAGED WAFERS
PRIOR TO JUNCTION FORMATION

(No AR Coating)

Etching Conditions		V_{oc} (mV)	I_{sc} (mA)	I_{500} (mA)	R_{sh} (Ω)
F_{14} + 8% O_2	4 Secs.	586	657	239	15.9
	8 Secs.	598	703	526	30.7
		596	689	591	24.8
		597	696	471	30.7
	Ave.	597	696	529	28.7
SF_6	4 Secs.	600	700	616	43.5
		599	714	495	21.6
		601	715	602	22.9
	Ave.	600	710	571	29.3
	8 Secs.	599	719	488	32.5
		602	714	627	31.6
		599	713	571	15.6
	Ave.	600	715	562	26.6
Conventional Etch		606	722	607	38.1
		604	708	601	35.2
		598	693	424	14.4
		602	709	575	39.0
		603	697	581	50.0
		602	711	588	64.0
	Ave.	603	706	562	40.0

3.5 DIFFUSION MASK PROCESS

3.5.1 Recommendations

Many difficulties were encountered in attempting to develop a printable dielectric paste which would act as a barrier for the diffusion of the N+ and P+ dopants and could therefore be used to eliminate the junction cleaning process. Although dielectric pastes were developed which act as barriers for diffusion, we were not able to obtain satisfactory cell output curves. We conclude that this process is not at a suitable state of readiness.

3.5.2 Work Performed - Dielectric Paste Development*

The following criteria were selected for guiding the development of the diffusion masking dielectric:

1. Maturation (firing temperature = 850 - 900°C)
2. Barrier to phosphorus migration
3. Thermal coefficient of linear expansion, 3.9 to 4.6 x 10^{-6} per °C
4. Good melting properties
5. Stability with respect to water
6. Stability with respect to silicon at the maturation temperature
7. Structural and chemical stability with respect to thermal cycling in subsequent processing

The low expansion coefficient of silicon (3.9 to 4.6 x 10^{-6}/°C) dictates the use of glasses whose compositions can be modified to obtain expansion values below 4 x 10^{-6}/°C. The glasses must mature within

*For a more detailed discussion see Appendix B.

the selected temperature ranges and exhibit the required physical characteristics when applied to silicon. In general, the expansion coefficients of glasses are inversely proportional to the maturation temperature. Low expansion glasses usually have high maturation temperatures.

The glass systems investigated were selected based on the following considerations:

1. Those with low expansion coefficients which would mature within the required temperature limits; and

2. Coating systems with acceptable maturation temperatures and composition which can be altered to reduce the expansion coefficient and not affect the firing characteristics.

Based on criteria (1), (2), and (3), five families of glasses were selected as potential candidates. The initial compositions are shown in Table 3.5-1.

Series 1 - Beta Spodumene Glasses

This family of glass was selected because of low expansion characteristics and low viscosity at about 1090°C. Additionally, prescription of spodumene promotes thermal stability.

Series 2 - Magnesia-Alumina Borosilicate Glasses

These glasses are based on a commercial composition which has a calculated expansion coefficient of $3.9 \times 10^{-6}/^{\circ}C'$ and a maturation temperature of 1010°C.

Table 3.5-1

STARTING COMPOSITIONS OF DIFFUSION MASKING DIELECTRICS

Series	1E-1	2E-1	3E-1	5E-1	7E-1
Oxide			Equivalents		
BaO	-	-	0.133	-	0.395
Li_2O	0.811	-	-	0.149	-
MgO	0.189	0.875	0.783	-	0.436
CaO	-	0.125	0.043	0.080	0.085
ZnO	-	-	0.041	0.055	0.084
Na_2O	-	-	-	0.505	-
K_2O	-	-	-	0.211	-
Total	1.000	1.000	1.000	1.000	1.000
B_2O_3	-	1.382	1.753	0.644	0.766
Al_2O_3	0.282	0.330	-	-	-
P_2O_5	0.340	-	-	-	-
	-	-	-	-	-
SiO_2	3.023	2.334	1.016	2.669	0.857
TiO_2	-	-	-	1.178	-
			Mol Percent		
BaO	-	-	3.52	-	15.06
Li_2O	17.46	-	-	2.71	-
MgO	4.07	17.34	20.79	-	16.62
CaO	-	2.48	1.14	1.46	3.24
ZnO	-	-	1.09	1.00	3.20
Na_2O	-	-	-	9.20	-
K_2O	-	-	-	3.84	-
B_2O_3	-	27.39	46.51	11.73	29.20
Al_2O_3	6.07	6.54	-	-	-
P_2O_5	7.32	-	-	-	-
SiO_2	65.08	46.25	26.96	48.61	32.67
TiO_2	-	-	-	21.45	-

Series 3 - Baria-Magnesia Borosilicate

This series has a maturation temperature of 100°C and a low expansion due to the high content of MgO, B_2O_3 and SiO_2. This series is similar to Series 7, although the latter has a higher BaO and lower MgO, and B_2O_3 content.

Series 5 - Titania Precipitated Glass

This glass, when smelted and water quenched (i.e., cooled quickly) is transparent. When it is matured on a substrate and cooled slowly (air-quenched) through 620°C and 700°C the titania crystallizes as a mixture of anatase and rutile. This structure is a prime contributor to thermal stability of the coating.

Series 7 - Baria Magnesia Borosilicate

These glasses are similar to those in Series 3; except that initially they contained a higher quantity of BaO and lower quantity of MgO and SiO_2. They are therefore "softer" glasses and would tend to have lower maturation temperature than those of Series 3. The Series 7 glasses are lithia and sodium free.

The investigation of variations of these series is described in detail in Appendix B.

Diffusion Barrier Tests and Cell Fabrication

Series 5E-7 and 5E-8 (Table 3.5-2) were evaluated as diffusion barriers by subjecting P-type silicon wafers to a diffusion cycle using Emulsitone N-250 phosphorus diffusion source. The silicon surface under the barrier coated areas was tested by staining techniques and resistivity measurement. No evidence of phosphorus penetration was detected.

Table 3.5-2

SERIES 5 COMPOSITIONS

Oxide	5E-7	5E-8	5E-7-1	5E-7-1P[3]
		Equivalent		
Na_2O	.271[1]	.219	.270[1]	.217[1]
K_2O	.088	.093	.088	.088
CaO	.216	.234	.216	.216
Li_2O	.276[2]	.292	.276[2]	.276[2]
ZnO	.150	.162	.150	.150
Total	1.000	1.000	1.000	1.000
B_2O_3	2.752	2.932	2.752	2.752
TiO_2	1.393	1.489	-	-
SiO_2	7.338	7.823	8.731	8.731
		Mol Percent		
Na_2O	2.16	1.65	2.16	2.16
K_2O	0.70	0.70	0.70	0.70
CaO	1.73	1.77	1.73	1.73
Li_2O	2.21	2.20	2.21	2.21
ZnO	1.20	1.22	1.20	1.20
B_2O_3	22.05	22.14	22.05	22.05
TiO_2	11.16	11.24	-	-
SiO_2	58.78	59.07	69.94	69.94
Expansion Coefficient ($\times 10^{-6}/^{o}C$)	5.2	5.2	3.5	3.5

(1) Na_2O added as 0.366 NaF (equivalents)

(2) Li_2O added as .479 LiF (equivalents)

(3) Glass smelted in platinum crucible

Attempts were then made to integrate this mask into the process sequence:

Print and fire mask

Diffuse

Print and fire aluminum back

Cells produced with compositions 5E-7 and 5E-8 were very inferior. Tests of a reformulation in which the titania was replaced by silica (Composition 5E-7-1) were tested with equally dismal results. The use of a platinum crucible for the frit fabrication did not improve the result.

These cell fabrication experiments were repeated with some modification of process sequence and extended to include composition 7E-8-1, Table 3.5-3. Two different process sequences were used as outlined in Table 3.5-4. The essential difference in the two sequences is the use of a printed aluminum back intermediate step in the second sequence.

The effects of potential titania, clay crucible and alkali metal contamination were investigated by fabricating cells using Process 1 (no aluminum) and pastes 5E-7, 5E-7-1 P and 7E-8-1. Cell characteristics at AM1 and 28^{o}C are reported in Table 3.5-5. It should be noted that the 5 series samples were run as a group, while the 7 series units were processed at a subsequent date.

The data obtained in this series of experiments completely fail to support the hypotheses of contamination arising from the titania, clay crucible or alkali metal ions. The best results were seen with original 5E-7 dielectric, with each attempt at refinement resulting in poorer characteristics. E-I curves for the cells with contact firing times of 20 seconds are shown in Figure 3.4-A. Although the best cells obtained here were relatively inferior, they were far superior to those obtained in the original evaluation. In that experiment the use of an aluminum back was included.

Table 3.5-3

COMPOSITION OF SERIES 7E-8-1 DIFFUSION MASKING DIELECTRICS

(Equivalents)

Oxide	7E-8-1
BaO	0.260
ZnO	0.055
CaO	0.056
MgO	0.629
PbO	---
Total	1.000
Al_2O_3	---
B_2O_3	0.506
SiO_2	0.433

Table 3.5-4

PROCESS SEQUENCES FOR EVALUATING
DIFFUSION MASKING DIELECTRICS

1	2
a) Print and dry diffusion dielectric	a) same
b) Fire diffusion dielectric (7 minutes @ 880°C)	b) same
c) Diffuse wafer (phosphine) (60 minutes at 850°F)	c) same
d) Back etch wafer	d) Print aluminum, dry and fire (10 seconds at 900°C)
e) Remove dielectric with HF	e) Remove aluminum with concentrated HCl
f) Print front contact and dry (TFS A256 + 2% N diffusol)	f) same
g) Print back contact and dry (TFS A256 + 2% N diffusol)	g) same
h) Fire front and back contact (20 seconds at 700°C)	h) same

Table 3.5-5

Cell characteristics at AM1 and 28° for cells fabricated with exposure to diffusion masking dielectric during the diffusion step (Process Sequence 1, Table 3.5-4). Reported values are the averages of the number of cells in parentheses.

Contact Firing Time (sec)	5E-7	5E-7-1	5E-7-1 P	7E-8-1
		V_{oc} (mV)		
10	596 (1)	597 (1)	-	-
15	593 (2)	592.5 (2)	558 (1)	-
20	594 (1)	587 (1)	581 (1)	585.7 (3)
25	594 (1)	587 (1)	581 (1)	588.6 (3)
		I_{sc} (mA)		
10	661 (1)	655 (1)	640 (1)	-
15	657.5 (2)	670 (2)	647.5 (2)	-
20	655 (1)	663 (1)	633 (1)	660.3 (3)
25	682 (1)	677 (1)	638 (1)	671 (3)
		I_{475} (mA)		
10	421 (1)	373 (1)	355 (1)	-
15	565.5 (2)	535.5 (2)	432 (2)	-
20	540 (1)	485 (1)	370 (1)	465.3 (3)
25	592 (1)	519 (1)	202 (1)	537.3 (3)

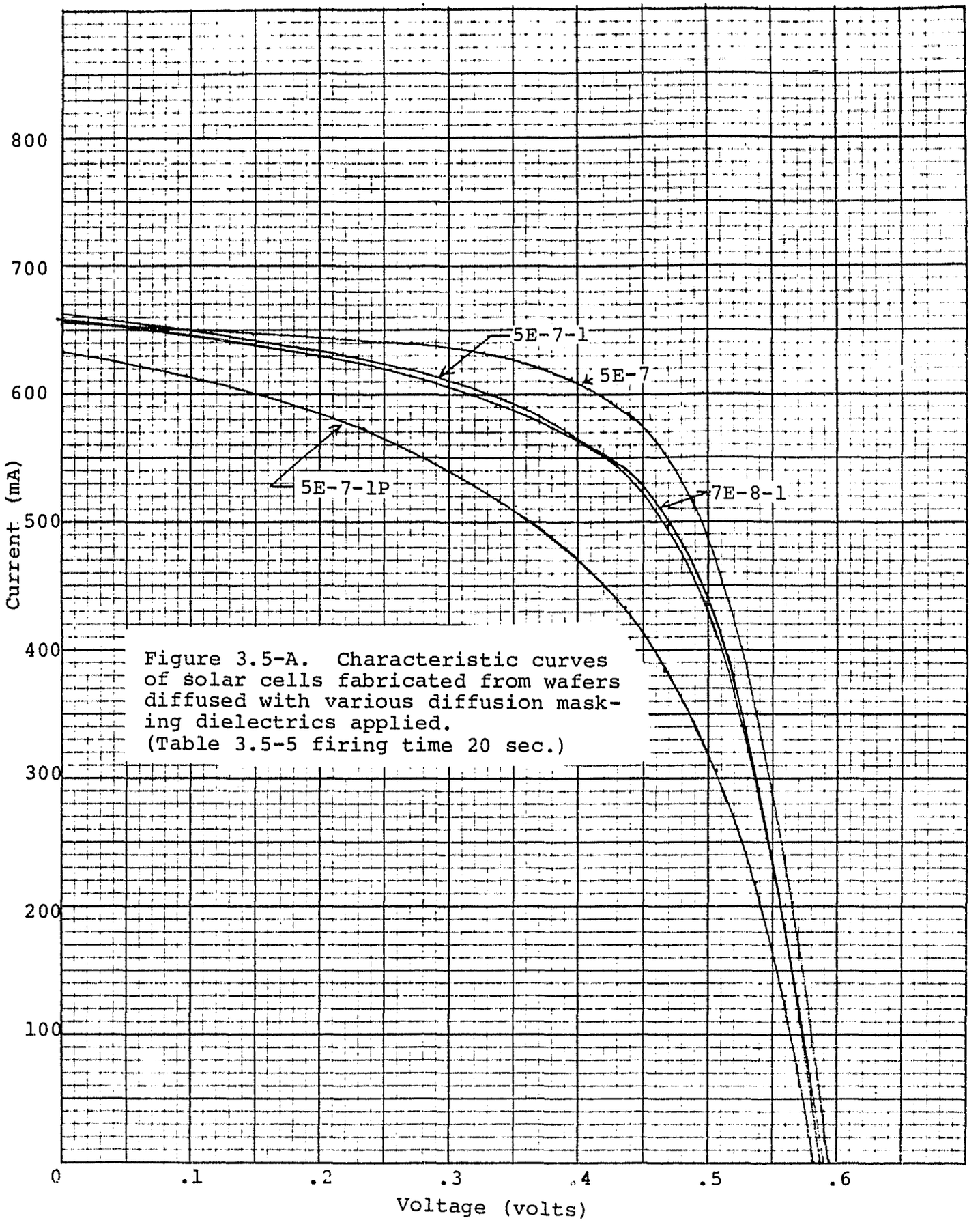

Figure 3.5-A. Characteristic curves of solar cells fabricated from wafers diffused with various diffusion masking dielectrics applied. (Table 3.5-5 firing time 20 sec.)

Cells were next fabricated using process sequences 1 and 2 (Table 3.5-4) and formulations 5E-7 and 5E-8. Cell characteristics at AM1 and 28°C are reported in Table 3.5-6. The major problem with curve shape in this experiment appeared to be a very low shunt resistance. This was verified by estimating the shunt resistance using the dark reverse current on a number of cells. These estimates, also reported in Table 3.5-6, were all below 10 ohms in contrast to a normal value of 120 ohms or more.

In this experiment the introduction of aluminum back contacts into the process sequence had an adverse impact on the solar cell characteristics, however, the cells fabricated using the 5E-7 dielectric and process sequence 1 were decidedly inferior to those obtained in the previous experiment. This result suggests the presence of an unidentified process variable which was not being controlled.

The cells fabricated with 5E-8 dielectric and aluminum backs were edge etched in order to determine the extent to which additional leakage might be attributed to edge shunting. Cell characteristics before and after edge etching are compared in Table 3.5-7 with those for cells fabricated from the same paste without the aluminum back (process sequence 1). The edge etching process substantially improved the performance of the cells fired for 20 seconds. Examination of the individual cell data showed that the poor result for the 25 second firing time group was due to one cell whose current at load dropped from 330 mA to 149 mA during the edge etching process.

One further attempt was made to produce cells and/or identify the source of difficulties using the process sequence and controls given in Table 3.5-8.

Table 3.5-6

Effect of aluminum firing on cell characteristics of cells fabricated with exposure to diffusion masking dielectric during the diffusion step (Table 3.5-4). Reported values are the averages for the number of cells given in parentheses.

Contact Firing Time (sec)	5E-7		5E-8	
	Process 1	Process 2	Process 1	Process 2
		V_{oc}-mV		
20	561.0 (5)	448.4 (5)	583.8 (5)	546.3 (3)
25	568.7 (3)	448.4 (5)	576.7 (3)	575.7 (3)
		I_{sc} (mA)		
20	674.4 (5)	649.0 (5)	666.6 (5)	662.0 (3)
25	659.0 (3)	613.7 (3)	651.3 (3)	655.0 (3)
		I_{475} (mA)		
20	312.2 (5)	228.4 (5)	502.8 (5)	263.3 (3)
25	348.7 (3)	125.0 (3)	458.0 (3)	381.7 (3)
		R_{sh} Ohms		
20	3.0 (1)	1.2 (2)		
25	2.1 (1)		4.4 (3)	

Table 3.5-7

Effect of edge etching on cell characteristics of aluminum back contact cells. Reported data are averages for the number of cells indicated in parentheses.

Process Sequence *	2	2	1
Edge Treatment	None	Etched	None
Contact Firing Time		V_{oc} (mV)	
20 sec	546.3 (3)	584.3 (3)	583.8 (5)
25	575.7 (3)	560.7 (3)	576.7 (3)
		I_{sc} (mA)	
20 sec	662.0 (3)	570.0 (3)	666.6 (5)
25	655.0 (3)	666.7 (3)	651.3 (3)
		I_{475} (mA)	
20 sec	263.3 (3)	482.7 (3)	502.8 (5)
25	381.7 (3)	342.7 (3)	458.0 (3)

*See Table 3.5-4

Table 3.5-8

PROCESS SEQUENCE USED TO EVALUATE
DIFFUSION MASKING DIELECTRIC

1.	Texture etch
2.	Print and dry masking dielectric (edge of wafer)
3.	Fire diffusion masking dielectric
4.	Phosphine diffuse wafers
5.	HF back of wafers
6.	Print, dry and fire aluminum paste (Ampal 631 aluminum paste)
7.	HF wafers
8.	Remove unconsolidated aluminum powder and clean wafers
9.	Print, dry and fire front silver paste
9a.	Dice 1.4" squares (controls only)
10.	Test cells

Control Set 1 omitted Step 2

Control Set 2 omitted Steps 2 and 3

Control cells were processed in parallel, in an attempt to determine the exact modes of failure. The first set of control wafers omitted Step 2 to determine whether the wafers might experience front surface contamination at this point. A second set of control wafers omitted Steps 2 and 3, to determine whether the presence of dielectric in the diffusion tube might create problems. Control cells required an edge clean-up which was provided by cutting 1.4" squares between Steps 9 and 10.

Five types of masking dielectrics (5E-7, 5E-7-1, 5E-8, 7E-20 and 7E-24) were evaluated using this sequence. The results are given in Table 3.5-9. In every case cells with masking dielectric had a poor output as compared to the control cells. A number of cells from each group showed evidence of front silver contact peeling, which was attributed to poor cleaning procedures in Step 8.

The 5 series dielectric had a low output at load, and portions of the aluminum back contact had peeled on the 5E-7. This peeling of the aluminum contact occurs adjacent to the diffusion mask dielectric. Sanding the edges of the cells to improve output was not advantageous. Edge clean-up by sawing squares was not feasible with the diffusion dielectric, which fouled the dicing saw blade. The 7 series dielectric devitrified and cracked during the diffusion step, which resulted in cells of low output. Sanding the edges of the cells improved the output, indicating that the 7 series dielectric is not an effective phosphine diffusion barrier. All of the cells produced with a dielectric had an erratic output at load which was attributed to high back contact resistance. This contact resistance was reduced by ultrasonically soldering tin pads to the back, opposite the front contact pads.

The results of this experiment indicate that these diffusion mask dielectrics are detrimental to the cell's output and also have detrimental effects on the aluminum back surface field. Three of

Table 3.5-9

RESULTS OF CELL FABRICATION TEST OF DIFFUSION MASKING DIELECTRICS

Sample	V_{oc} mV	I_{sc} mA/cm^2	I_{500} mA/cm^2	R_{sh} ohms
5E7-1	521 - 576	27.4 - 28.8	10.9 - 16.2	1.5 - 3.0
Control 1	600 - 603	29.9 - 31.1	19.1 - 25.5	11.3 - 12.6
Control 2	Cells Broke			
5E7	488 - 557	16.6 - 30.7	0 - 14.7	2.0 - 2.8
Control 1	591 - 604	30.6 - 31.5	21.4 - 26.0	8.1 - 33.1
Control 2	Cells Broke			
5E8	518 - 582	19.1 - 28.3	6.3 - 12.4	2.8 - 7.3
Control 1	598 - 603	31.2 - 31.9	18.8 - 25.9	18.1 - 104.1
Control 2	598 - 603	29.8 - 31.2	0 - 26.8	28.7 - 36.5
7E20	550 - 581	19.2 - 27.1	6.3 - 17.7	3.3 - 5.9
Control 1	599 - 606	31.4 - 31.5	22.5 - 27.0	15.1 - 33.1
Control 2	599 - 604	29.1 - 31.6	25.1 - 26.9	29.8 - 42.7
7E24	521 - 594	25.4 - 30.7	7.0 - 24.6	1.8 - 5.4
Control 1	600	31.7	26.1	36.8
Control 2	597 - 598	30.5 - 31.2	25.3 - 25.9	20 - 32.9

the dielectrics (5E-7-1, 5E-8 and 7E-24) were then selected for further verification of these results. Cells were processed in accordance with the schedule shown in Table 3.5-8, except for an additional cleaning in a dilute solution of acetic acid at Step 8. These cells did not experience any front silver contact peeling, but did experience aluminum peeling associated with shear failure of the silicon. These cells had a reasonably high short circuit current (I_{sc} above 600 mA), but low open circuit voltage (V_{oc}) and output at load (I_{500}), Table 3.5-10. The application of the tin solder pad did not produce any noticeable improvement (Table 3.5-11). These cells were subsequently edge etched, which improved the short circuit current, open circuit voltage and output at load. The dark reverse current at 500 mV was measured in order to estimate shunt resistance (R_{sh}). The shunt resistance for all the cells was too low (1-4 Ω) for good solar cell performance.

We concluded from these experiments that:

1) The dielectrics are not a sufficient barrier to electrical conduction because of either conduction under, through or over the dielectric.

2) The silicon-dielectric interaction introduces detrimental effects into the bulk silicon which cause a low shunt resistance.

3) The aluminum-dielectric interaction causes peeling of the back aluminum-silicon contact possibly by interfering with the regrowth of the back surface field.

4) Some of the dielectrics studied react with the phosphine diffusion agent which causes the dielectric to devitrify.

The extent of the problems associated with the dielectrics are too great to enable this process to be classed as suitable for inclusion in the process sequence.

Table 3.5-10

AVERAGE VALUES OF PARAMETERS OF 2.12" ROUND CELLS
FABRICATED WITH VARIOUS DIFFUSION MASKING DIELECTRICS

Dielectric	N	As Fabricated			After Edge Etch			
		V_{oc} mV	I_{sc} mA	I_{500} mA	V_{oc} mV	I_{sc} mA	I_{500} mA	R_{sh} ohms
5E7-1	9	558.2	648.0	194.0	584.0	660.4	406.8	2.89
5E8	8	534.8	641.8	96.6	577.2	667.6	345.6	2.09
7E24	5/4	531.6	615.2	74.8	571.0	632.2	265.8	1.83

Table 3.5-11

EFFECT OF TIN SOLDER PAD ON CURRENT OUTPUT AT LOAD POINT, DIFFUSION MASKING DIELECTRIC TEST 2.12 INCH ROUND CELLS, NO AR COATING

Dielectric	I_{500} (mA)	
	Al Contact	Sn Solder Pad
5E7-1	326	370
	315	348
	247	248
5E7	204	237
	61	83
	67	-0-
	61	105
5E8	130	243
	113	283
	-0-	171
	58	144
7E20	315	403
	124	146
	200	227
	274	334
	148	144
7E24	159	35
	-0-	Broken
	317	419
	298	381
	490	509
	400	560*
	364	547*

*Cell edge sanded

3.6 DIFFUSION PROCESS

3.6.1 Recommendations

The N-250 diffusion source was found to be satisfactory for use on texturized, screen printed cells as applied by spinning or air-brush spraying and diffused in the temperature range from 850°C to 900°C. The recommended diffusion source for non-texturized, screen printed cells is Accuspin® PX-10, due to inconsistent results obtained with N-250. Initial work with I-R furnace drying and firing spin-on PX-10 was very encouraging, and further experimental development work in this area is recommended. Preliminary work with spraying PX-10 diffusion source with a hand held Paasche airbrush indicates that PX-10 may be utilized as either a spray-on or spin-on source.

3.6.2 Work Performed

Preliminary tests were made with two phosphorus sources as alternatives to gaseous sources. Emulsitone Emitter Source N-250 (Emulsitone Co., Whippany, New Jersey) yielded cells with properties similar to those obtained with our aerospace process gaseous PH_3 source. The second alternative source was a Transene 1020N Phosphorus Diffusant Preform (Transene Co., Inc., Rowley, Massachusetts) which gave results somewhat inferior to those obtained with the spin-on and gaseous sources.

The Emulsitone N-250 source was applied to texturized round (2 inch) and square (2 cm) wafers at a spin rate of 3000 RPM. The wafers were sliced from 2-3 ohm-cm boron doped crystals. The coated wafers were baked for 10 minutes at 125°C and then diffused for 30 minutes at 850°C in a flowing nitrogen-oxygen

gas mixture (500cc/min N_2, 20 cc/min O_2). The other cell processing steps consisted of standard controlled aerospace solar cell processing methods, without AR coating. Measurements of open circuit voltage, short circuit current and current at 300 mV were made using AM1 Xenon illumination. Results obtained with the square cells are reported in Table 3.6-1.

The Transene 1020N Phosphorus Diffusant Preform is comprised of a thin (2.5 mils) disc impregnated with a phosphorus compound. A sample of cells was prepared with these preforms using the same diffusion conditions, cell processing and measurement techniques as were used with the Emulsitone source. Results are reported in Table 3.6-2.

A small control sample was prepared using the PH_3 source used in our normal aerospace cell processing. In this case the diffusion cycle consisted of 5 minutes pre-heat, 20 minutes deposition, and 10 minutes of further drive-in, all at 850°C. Gas flow conditions were the same as in the previous runs, as were the other cell processing and measurement techniques. Results are reported in Table 3.6-3 where the standard deviation is replaced by its unbiased estimate, s_x.

Examination of cells processed with the Transene 1020N source showed that the tetrahedral peaks and edges had been rounded by a corrosive or dissolution process and that residual stains, which could not be removed with hydrofluoric acid, appeared erratically on the cell surfaces. Both of these processes would have a negative impact on short circuit and load point current.

The Emulsitone N-250 diffusion source was successfully applied by air brush spraying and contact transfer techniques to yield

Table 3.6-1

DIFFUSION DATA

Emulsitone N-250 Spin-On Source

2 cm Square Wafer

	V_{oc} mV	I_{sc} mA	I_{300}
	580	137	136
	581	138	136
	584	137	136
	584	136	136
	587	136	135
	579	136	135
	593	136	135
	579	136	134
	586	134	134
	584	134	134
	583	135	134
	589	135	134
	582	135	134
	587	134	133
	586	134	133
	584	134	133
	583	134	133
	586	132	132
	593	132	131
	576	132	131
	586	132	131
	584	134	131
	585	128	127
	558	137	137*
$\bar{x}$	584.0	134.4	133.4
σ	3.91	2.14	2.12

*Cells treated as outliers, data not included in calculated statistical parameters.

Table 3.6-2

DIFFUSION DATA

Transene 1020N Phosphorus Diffusant Preform

2 cm Square Wafer

V_{oc} mV	I_{sc} mA	I_{300} mA
588	140	140
590	140	140
589	138	138
590	137	136
585	137	136
586	134	134
590	133	133
589	133	132
584	134	132
586	133	131
585	131	130
586	129	129
584	129	128
587	129	128
587	126	122
582	121	121
589	121	120
578	119	119
587	117	117
583	116	116
585	116	116
590	112	111
288	001	001*
$\bar{x}$ 586.4	128.4	127.7
σ 2.98	8.40	8.39

*Cells treated as outliers, data not included in calculated statistical parameters.

Table 3.6-3

DIFFUSION DATA

Phosphine (Control Sample)

2 cm Square Wafer

V_{oc} mV	I_{sc} mA	I_{300} mA
592	140	136
589	140	136
590	137	135
593	138	135
594	136	135
590	139	135
594	137	134
591	139	134
$\bar{x}$ 591.6	138.2	135.0
s_x* 1.92	1.49	0.76

*Unbiased estimate of standard deviation

uniform junctions and efficient solar cells. It was found that if the applied layer is too thick, it may flake during drying. This thickness limitation was less stringent for texturized than polished or semi-polished cells. Better control of the sprayed layer thickness was achieved through dilution of the N-250 by the addition of anhydrous isopropyl alcohol to 30% volume concentration. The applied diffusion source was fired in a nitrogen atmosphere with a 25 minute ramp from 700°C up to 900°C, a ten minute drive at this temperature and a 25 minute ramp back down to 700°C in all cases.

The N-250 diffusion source was found to yield consistently good results with texturized wafers. In attempting to use this diffusion source with non-texturized wafers, the diluted N-250 process discussed earlier was found to give erratic results. Non-diluted N-250 was also investigated, and similarly was found to produce erratic results. Subsequent development work focused on the evaluation of alternative diffusion sources.

In a first experiment, alcohol-based N-250 (diluted) was compared with water-based Phosphorofilm℠ source (both obtained from Emulsitone Co.), and the effects of various atmospheres were investigated. NaOH polished (non-texturized) 2-inch round wafers were used for this experiment. The wafers were cleaned using a hydrogen peroxide/ammonium hydroxide solution which was shown to leave a hydrophilic surface on the cells which allowed uniform wetting. Diffusions were carried out at 850°C for 80 minutes. We also used a variety of atmospheres as depicted in Table 3.6-4. Cell fabrication was completed with printed aluminum backs, chemical cleaning of front oxides and aluminum back and front surface printed silver front contacts, and evaporated anti-reflection coating. The complete process sequence thus reflects the baseline process except for front surface

Table 3.6-4

EFFECT OF DIFFUSION SOURCE
AND ATMOSPHERE ON CELL PERFORMANCE
($T = 850^{o}C$)

DIFFUSION CONDITIONS				NO AR			EVAP. SiO AR		
Atmosphere	Source Sample Size	Sta-tistics	ρ_s Ω/□	V_{oc} mV	I_{sc} mA	I_{500} mA	V_{oc} mV	I_{sc} mA	I_{500} mA
O_2 80 min.	N-250	$\bar{x}$	93.9	587.4	449.6	127.3	587.4	568.2	167.3
	η = 10	σ	11.8	6.3	50.4	41.6	6.3	82.6	43.4
N_2 80 min.	N-250	$\bar{x}$	34.2	578.1	551.4	378.9	586.2	729.4	498.8
	n = 8	σ	3.2	27.2	4.7	116.1	24.4	9.2	148.5
	Phosphorofilm®	$\bar{x}$	57.1	582.3	419.5	159.8	585.5	539.8	194.3
	n = 10	σ	16.4	15.0	59.8	94.2	14.0	90.3	128.0
N_2 70 min.	N-250	$\bar{x}$	33.7	609.4	547.0	540.8	615.3	716.2	538.7
	n = 10	σ	6.05	4.9	1.9	67.9	5.0	12.9	106.9
O_2 10 min.	Phosphorofilm®	$\bar{x}$	51.0	580.0	542.0	330.2	586.8	719.5	445.5
	n = 4	σ	8.7	20.3	9.2	90.4	1[illegible].1	7.6	111.1
87% N_2 + 23% O_2	N-250	$\bar{x}$	39.6	606.1	543.4	277.5	611.5	721.9	329.5
	n = 8	σ	3.7	1.5	5.3	52.0	2.4	12.3	74.3
80 min.	Phosphorofilm®	$\bar{x}$	50.3	540.0	543.7	233.7	551.0	723.3	280.0
	n = 3	σ	5.6	3.7	3.3	37.4	2.2	11.3	46.8

Cell structure:
2.12" round 2 ohm-cm wafers

cleaning and AR coating. The best results for N-250 was diffusion in N_2 for 70 minutes, followed by O_2 for 10 minutes at 850°C. Cells emerging from this treatment yielded open circuit voltages as high as 620 mV and load point current (I_{500}) as high as 600 mA with an evaporated AR coating.

There appeared to be an interaction between the diffusion atmosphere and development of the P+ structure with the N-250 source. High open circuit voltages were obtained with mixed nitrogen-oxygen atmosphere and with nitrogen followed by oxygen. With pure oxygen or pure nitrogen single atmospheres, open circuit voltages were below 590 mV. In the case of the pure oxygen atmosphere, the sheet resistance was high, indicating a shallow junction and probable shunting of the junction by the front metallization. In the case of the nitrogen atmosphere, the resulting diffusion film was poorly removed by hydrofluoric acid, presumably due to the presence of silicon nitride or oxynitride. This may give rise to front contact resistance and/or interface with the P+ formation on the back surface.

The results with the Phosphorofilm® source were quite erratic and inferior as compared to those for the N-250. This may be due to a shallower junction as evidenced by the higher sheet resistance values observed for the Phosphorofilm® source. No satisfactory P+ (as evidenced by V_{oc}) was obtained for any of the Phosphorofilm® diffusions.

In a second experiment, the effect of different surface preparation methods on diffusion from the N-250 source were evaluated. The matrix included: (1) hydrophilic clean, (2) leave as etched after NaOH polish, (3) bake in atmosphere for 15 minutes at 200°C. The only one of the above three methods

showing any sign of dewetting was the bake for 15 minutes at 200°C. This was repeated a second time with identical results. At this time, it appears that it may not be necessary to hydrophilic clean. After diffusing the three groups of cells at 850°C in nitrogen followed by oxygen, it was found that an erratically high sheet resistance occurred with the 'hydrophilic' group. Based on previous experience, it should have been in the same range as the 'as etched' group (see sheet resistance data in Table 3.6-4). Table 3.6-5 shows the sheet resistance variations of each group.

The Phosphorofilm® was compared with concentrated N-250 and Accuspin® PX-10 diffusion sources. Diffusions were carried out at 900°C for various times on 'as etched' surfaces. Cell outputs are presented in Table 3.6-6. The N-250 source showed the better uniformity in this experiment. The PX-10 produced the highest output cell. The Phosphorofilm® once again was very erratic and inferior compared to the other two sources. Preliminary data on the PX-10 appeared very promising.

Time-temperature response surfaces were investigated for both concentrated N-250 and Accuspin® PX-10. Cell fabrication in both cases was completed using printed aluminum backs, chemical cleaning of front diffusion oxide, and aluminum backs, and application of printed silver front contacts. The process sequence reflects the base line process except for the front surface cleaning procedure and the fact that no AR coating was applied.

TABLE 3.6-5

DIFFUSED SHEET RESISTANCE OBTAINED WITH DIFFERENT SURFACE PRETREATMENTS

Wafer Number	Hydrophilic Clean Ω/□	Baked 15 Min.-200^{0}C Ω/□	NaOH Polished As Etched Ω/□
1	98-104	99-130	46-50
2	71-78	100-115	31-33
3	93-101	99-115	33-40
4	101-109	141-150	71-81
5	120-125	127-137	41-50
6	68-99	130-156	22-27
7	99-116	74-84	33-38
8	95-105	72-86	26-29
9	122-125	76-85	29-30
10	140-158	88-135	31-37

Table 3.6-6

COMPARISON OF DIFFUSION FROM N-250 PHOSPHOROFILM® AND ACCUSPIN® PX-10 AT 900°C MEASURED WITHOUT AR COATING

Time and Atmosphere	Source	Defective* %	V_{oc} mV	V_{sc} mA	I_{500} mA
50 min. N_2 10 min. O_2	N-250	0	601	499	453
25 min. N_2 5 min. O_2	N-250	0	599	479	426
50 min. N_2 10 min. O_2	Phosphorofilm	20	553	473	287
25 min. N_2 10 min. O_2	Phosphorofilm	40	505	408	22
25 min. N_2 5 min. O_2	PX-10	20	602	507	424
10 min. N_2 5 min. O_2	PX-10	0	601	530	393

*Fill factor less than 55%

For the initial experiments with concentrated N-250 source, we used NaOH polish-etched (non-textured) 2" round wafers that were hydrophilic cleaned prior to spraying. The diffusion time and temperature was varied. The electrical performance results were very erratic, with the best results being obtained with firing in N_2 only for 50 minutes, followed by O_2 for 10 minutes (Table 3.6-7). These parameters gave open circuit voltages as high as 611 mV and load current (I_{500}) as high as 488 mA without AR coating.

Another matrix using NaOH etched (non-textured) 2-inch round wafers was run. One group was hydrophilic cleaned before spraying. The surfaces of the remaining wafers were left "as is" after NaOH polish etching before spraying on the diffusion source. Diffusion was carried out at 900°C for various times, which are listed in the last three entries of Table 3.6-7. The results of this test indicated that firing for 50 minutes in N_2 only, followed by O_2 for 10 minutes without hydrophilic treatment is capable of producing cells as good as those which underwent the hydrophilic treatment process; however, a higher proportion of defective cells was generated. It appears that there was poor P+ BSF formation in each group as indicated by an erratic V_{oc}. These results suggest that N-250 is not a satisfactory spray-on diffusion source since excessively deep junctions ($\rho_s \cong$ 10-15) are required in order to obtain consistent results. The observed load and short circuit currents for these deep junctions (Table 3.6-7) were deceptively high due to the spectral distribution of the tungsten light source used for the measurements.

The initial results obtained with the PX-10 source were very good. Diffusion was carried out at 900°C for various times as shown in Table 3.6-8. We used NaOH polished etched 2" round

Table 3.6-7

TIME-TEMPERATURE RESPONSE SURFACE FOR DIFFUSION
WITH CONCENTRATED N-250 SOURCE
MEASURED WITHOUT AR COATING

Treatment		Defective* %	Ps Ohms/□	V_{oc} mV	I_{sc} mA	I_{500} mA
NaOH polish etch Hydrophilic treated surface	70 min. N_2 10 min. O_2 850°C	40	12	593	458	315
	70 min. N_2 10 min. O_2 875°C	60	69	589	510	210
	50 min. N_2 10 min. O_2 900°C	0	9.5	603	528	470
	30 min. N_2 10 min. O_2 925°C	0	17	587	462	364
	15 min. N_2 10 min. O_2 950°C	0	16	603	508	416
	50 min. N_2 10 min. O_2 900°C	14.2	13	598	487	420
	30 min. N_2 10 min. O_2 900°C	50	19	596	518	344
NaOH polish etch	15 min. N_2 10 min. O_2 900°C	37.5	40	581	502	329
	50 min. N_2 10 min. O_2 900°C	70	17	498	433	433

*Fill factor less than 55%

Table 3.6-8

TIME-TEMPERATURE RESPONSE SURFACE
FOR DIFFUSION WITH ACCUSPIN® PX-10
MEASURED WITHOUT AR COATING
900°C

Treatment	Defective* %	Ps Ohms/□	V_{oc} mV	I_{sc} mA	I_{500} ma
10 min. N_2 5 min. O_2	10	30-35	607	550	478
15 min. N_2 10 min. O_2	10	25-30	604	530	453
30 min. N_2 10 min. O_2	14	20-22	604	507	438
60 min. N_2 10 min. O_2	11	15-18	600	494	400

*Fill factor less than 55%

wafers with no hydrophilic treatment before spraying on the PX-10 source. Diffused wafers were given a back etch in concentrated HF acid. The best results were obtained with the PX-10 diffused in N_2 only for 10 minutes, followed by O_2 for 5 minutes, for a total diffusion time of 15 minutes. These conditions produced open circuit voltages as high as 608 mV and load point current (I_{500}) as high as 495 mA without an AR coating. The sheet resistance range was 30-35 Ω/□.

Experimental tests were continued in an effort to verify the experimentally observed superior performance of cells sprayed with PX-10, over cells sprayed with N-250.

The first group of cells was fabricated using the baseline processing sequence. NaOH etched 2" round wafers were used to compare the N-250 and PX-10 diffusion sources. The PX-10 cells gave the best results. The average open circuit voltage was 604 mV and the average load point current (I_{500}) was 432 mA for 19 of 20 cells. For the N-250 cells the average open circuit voltage was 602 mV and the average load point current (I_{500}) was 409 mA for 14 of 20 cells.

As a further comparison of the PX-10 and the N-250 diffusion sources, an experiment was run varying the applied thickness of PX-10. In run 4.27.9 a thin spray-on coat of PX-10, a thick coat of PX-10 and a normal coat of N-250 were applied on 2.12 x 2.12 inch square NaOH polished wafers. The cells were processed in accordance with the proposed sequence except that the junctions were cleaned chemically and the wafers were not AR coated.

The electrical performance results of this run indicated efficiencies of 8.6% (equivalent to 11.5% with AR coating), 10.4% (= 13.9% with AR coating) and 8.4% (= 11.1% with AR coating) for the average efficiency of the thin PX-10, thick PX-10 and N-250, respectively (Table 3.6-9). The performance of cells with thinly applied PX-10 may be low due to a non-uniform diffusion which is indicated by the lower shunt resistance, although the sheet resistance of diffused wafers for both the thin and thick PX-10 appeared the same. Some cells produced with the thick spray-on PX-10 source showed areas of source remaining after the HF treatment. These layers may be acting as an antireflective coating in these areas, resulting in increasing the short circuit current and current at load. This is consistent with the visual evidence, that the cells with spotty surfaces generally have higher short circuit currents. Comparison of the two diffusion sources is confused because the performance characteristics of the deeply diffused N-250 group are suspect, the reason being the tungsten light source spectrum used to characterize the cells is not influenced by a deep junction as much as a true AM1 solar spectrum would be.

It was speculated that the method of applying the PX-10 source by air brush may be contributing to the uniformity problem mentioned above. Air brush application may not produce a sufficiently uniform coating. Spinning-on PX-10 appears to give a thin ($\sim$1 mil) uniform layer of source which results in a wafer surface which is easily cleaned with an HF treatment. To compare the effects of different methods of applying PX-10, cells were fabricated by spraying-on and spinning-on the diffusion source to a 3" round wafer with a NaOH polished (non-textured) surface. After the P+ formation and aluminum back contact, a 2" x 2" square wafer was cut out. Cutting the square wafers out, chemically cleaning the front surface, and no AR coating were the only

Table 3.6-9

Run 4.27.9

PX-10 SPRAYING THICKNESS EFFECTS

No AR Coating
2.12" x 2.12" Cells

	AVERAGE			
	V_{oc} (mV)	I_{sc} (mA)	I_{500} (mA)	R_{sh} (Ω)
Thin PX-10	605	681	500	19.4
Thick PX-10	605	708	560	17.8
N-250	599	621	485	11.0

deviations from the baseline process. The spin-on wafers appeared more uniform but were lower in output at load point current I_{500}. The average open circuit voltage was 602 mV with the highest being 604 mV, and the average load point current (I_{500}) was 531 mA with the highest being 575 mA.

At this time PX-10 appeared superior to N-250 because it produced superior performance cells and also required a shorter diffusion time cycle. Additional experiments were then performed to explore the time-temperature response surface for diffusion with the PX-10 diffusion source. The cells were fabricated using the baseline process sequence, with the exception that the wafers were sectioned by laser scribing prior to front metallization and no AR coating was applied. The diffusion source was applied by spinning because of lack of suitable spray equipment.

The baseline diffusion of 10 minutes in N_2 and then 5 minutes in O_2 at 900°C was performed in run 4.30.9. The average efficiency of this run was 10.0 (equivalent to 13.3% with AR coating). A diffusion time of 10 minutes in N_2 and 5 minutes in O_2 was selected in run 4.31.9 while the temperature was varied between 850 and 925°C in 25°C intervals. The average efficiencies for this run were 7.2% (= 9.8% with AR coating), 8.6% (= 11.6% with AR coating), 8.9% (=12.9 with AR coating), 9.3% (= 12.5% with AR coating), for the 850, 875, 900 and 925°C diffusion temperatures, respectively. The control group of 900°C was about 10% lower than run 4.30.9. This drop was traced to the diffusion source being spun-on and dried the night before the diffusion occurred.

Run 4.31.9 was repeated in 4.33.9, and the source was diffused within one hour of source application. The average efficiencies were 9.2% (=12.3% with AR coating), 10.0% (= 13.5% with AR

coating) and 9.9% (= 13.2% with AR coating) for the 850, 875, 900 and 925°C diffusion temperatures, respectively. The control group of 900°C was the same as run 4.20.9. The three temperatures of 875, 900 and 925°C appear to have similar efficiencies, but they do reflect a variation in sheet resistivity and short circuit current as a function of temperature.

As an additional verification of the 875, 900 and 925°C temperature invariance, both the 875 (run 5.44.9) and 925°C (run 5.41.9) were repeated in separate experiments using the 900°C diffusion as a control. In run 5.44.9 the average efficiencies were 9.8% (= 13.1% with AR coating) and 9.7% (= 13.2% with AR coating) for the 875 and 900°C (control) diffusion temperatures, respectively. In run 5.41.9 the average efficiencies were 9.2% (= 12.4% with AR coating) and 9.2% (= 12.3% with AR coating) for the 900 (control) and 925°C diffusion temperatures, respectively. Although the performance does not appear to be strongly temperature dependent in the 900 ± 25°C range, there does appear to be a short circuit current dependence. The temperature dependence of performance at load may be masked by the low shunt resistance in these runs. Results of these experiments are summarized in Table 3.6-10.

In view of the resistance effects, two more experiments were run: 6.48.9 and 6.51.9. Tables 3.6-11 and 3.6-12 show a summarization of the results. Looking at the results of these experiments in contrast to the previous experiments, there are differences among cells diffused at different temperatures. The best cells were obtained from wafers diffused at 925°C. The improved sensitivity of run 6.48.9 as compared to previous experiments is attributed to the improvement in shunt resistance.

Table 3.6-10

JUNCTION FORMATION EXPERIMENTS

Run No.	Temperature	Average Value						Equivalent with AR (%)
		Sheet (Ω/□)	V_{oc} (mV)	I_{sc} (mA)	I_{500} (mA)	R_{sh} (Ω)	η (%)	
4.30.9	900°C	26-31	602.3	635	514	19.5	10.0	13.3
4.31.9	850°C	59-76	591	601	376	6.6	7.2	9.8
4.31.9	875°C	40-49	597	604	448	6.3	8.6	11.6
4.31.9	900°C	27-34	598	594	461	7.1	8.9	12.0
4.31.9	925°C	18-19	598	576	475	8.6	9.2	12.4
4.33.9	850°C	55-65	598	628	474	9.1	9.2	12.3
4.33.9	875°C	39-48	603	633	516	9.3	10.1	13.4
4.33.9	900°C	29-34	602	610	514	11.1	10.0	13.4
4.33.9	925°C	19-21	602	595	510	14.3	9.9	13.2
5.41.9	900°C	31-39	601	648	524	6.5	9.2	12.4
5.41.9	925°C	20-23	603	630	522	7.9	9.2	12.3
5.44.9	875°C	42-48	601	676	556	7.9	9.8	13.1
5.44.9	900°C	33-37	604	664	559	8.8	9.9	13.2

Table 3.6-11

DIFFUSION EXPERIMENT 6-48-9

Group	Diffusion			Measurements (No A/R)				
	Temp. °C	Time (Minutes)		Sheet-R Ω/□	V_{oc} mV	I_{sc} mA	I_{500} mA	R_{sh} Ω
		N_2-Only	O_2-Only					
A*	850	15	5					
B*	850	25	5					
C	875	10	5	43 (38-56)	601 (579-606)	696 (656-721)	450 (162-575)	(45-125)
D*	875	15	5					
E	900	7	3	32	628 (599-628)	700 (685-708	557 (510-594	56 (42-100)
F	900	10	5	24 (23-26)	605 (602-607)	689 (681-697	572 (523-600)	63 (38-179)
G	925	5	2	29 (28-30)	605 (603-607)	698 (689-707)	611 (604-621)	28 (22-36)
H	925	7	3	24 (23-25)	605 (602-606)	687 (682-665)	606 (592-619)	24 (15-42)
I	950	4	1	22 (19-23)	602 (597-604)	666 (659-673)	574 (610-606)	26 (12-83)
J	950	5	2	19 (17-21)	601 (592-627)	660 (632-668)	518 (569-598)	19 (11-167)

*Experiment failed due to operator error at diffusion step.

Table 3.6-12

DIFFUSION EXPERIMENT 6-51-9

Group	Diffusion			Measurements (No A/R)				
	Temp. °C	Time (Minutes)		Sheet-R Ω/□	V_{oc} mV	I_{sc} mA	I_{500} mA	R_{sh} Ω
		N_2-Only	O_2-Only					
A	875	25	5	29 (26-34)	608 (606-611)	683 (664-706)	508 (384-565)	75 (36-119)
B	875	15	5	38 (34-42)	602 (590-607)	690 (666-711)	470 (391-506)	76 (41-113)
C*	875	7	3	35 (34-37)	605 (603-607)	710 (698-719)	544 (510-572)	117 (29-185)
D*	900	7	3	52 (50-55)	602 (601-605)	712 (704-721)	446 (377-496)	86 (63-116)
E	900	5	2	32 (31-34)	604 (601-606)	698 (681-712)	543 (507-563)	102 (45-152)
F	900	4	1	57 (53-60)	600 (597-604)	706 (689-724)	419 (259-478)	87 (22-139)
G	925	5	2	28 (27-29)	604 (602-605)	692 (681-702)	565 (517-590)	84 (43-132)
H	925	4	1	34 (32-35)	602 (600-604)	696 (685-713)	517 (473-546)	63 (39-94)

*It appears like a mix-up between Groups C and D; might have been interchanged.

Immediately following the application of the PX-10 diffusion source, the wafers have been dried in a conventional oven at 150°C for 15 minutes. This drying process is very costly due to slow throughput. In an effort to significantly reduce the processing time expended at this step, an alternative method, infrared drying, was explored.

A group of cells was fabricated using the conventional processing sequence, with the exception that the PX-10 baking step prior to diffusion was performed in an IR belt furnace. The hot zone of the IR furnace, 18" in length, was originally set at 300°C. By varying the belt speeds to 20, 30, 40 and 50 inches per minute, the baking times for these belt speeds were 0.1, 0.6, 0.45 and 0.36 minutes, respectively. The electrical performances of the completed IR baked and conventional baked cells were measured and may be found in Table 3.6-13. The measured photovoltaic parameters (V_{oc}, I_{sc}, I_{500} and R_{sh}) indicated no significant difference in electrical performance between the two groups. The sheet resistance for all tested cells ranged from 30 to 40 Ω/□. The results of this work therefore suggest that the conventional baking process may successfully be replaced by a short-term baking in an IR belt furnace of reasonable length.

Preliminary evaluation of junction formation with an IR furnace was conducted during this contract. High diffusion temperatures were required due to furnace belt speed limitations. This evaluation indicated that the PX-10 diffusion source could be successfully fired in a properly designed IR furnace.

Square shaped (110) single crystals were processed in accordance with our standard process sequence, except the edges were edge etched instead of laser scribed. Before the junction formation

Table 3.6-13

PX-10 IR BAKE

Time (sec.)	# of Cells	V_{oc} (mV)	I_{sc} (mA)	I_{500} (mA)	R_{sh} (Ω)
108	4	600	698	630	56
72	6	598	688	619	68
54	5	600	694	640	74
43	7	599	682	626	65
Conventional Bake 150°C, 15 min.	11	603	702	637	49

step the wafers were divided into three groups. The first group was controls, fired in a tube furnace at 900°C. The second and third groups were fired in an IR furnace at 925°C and 950°C respectively, for two minutes. Table 3.6-14 lists the resultant data of these cells (without AR coating). The sheet resistance of the second group was very high, indicating too short a diffusion time or too low a temperature. The open circuit voltage (V_{oc}), short circuit current (I_{sc}) and current at 500 mv (I_{500}) were much lower than the controls (Group 1). The low output of these cells was due to the shallow junction and the rapid spike firing and quenching of the IR furnace.

The sheet resistance of the third group was in the same range as the control group. The average output of these cells was slightly lower than the controls; the V_{oc} was 7 mv lower, the I_{sc} was 6% lower, and the I_{500} was 10% lower. Considering the adverse conditions of firing at 950°C where bulk lifetime effects degrade the cell and the rapid spike firing and quenching these cells experienced, these results are very encouraging. These results indicated that a properly designed IR furnace may be capable of firing the spin-on PX-10 diffusion source to produce an efficient solar cell.

Spin-on techniques for forming junctions are not as cost effective as spray-on techniques due to low throughput rate and high material usage. In order to render the diffusion process cost effective, Allied Chemical has recommended using the Accuspin® PX-10 diffusion source for spraying. An evaluation of PX-10 as a spray-on source was reevaluated.

Control cells were processed in accordance with the conventional processing sequence using PX-10. The cells under evaluation

Table 3.6-14

GROUP 1 - CONTROL
(σ = 26 - 35 Ω/□)
(No. of cells = 20)

	V_{oc} (mv)	I_{sc} (mA)	I_{500} (mA)	R_{sh} (Ω)
	596	793	689	38.2
	593	798	679	38.2
	598	819	649	68.5
	589	795	692	49.0
	596	797	699	46.3
	596	796	707	51.5
	597	795	709	28.4
	597	814	692	44.3
	596	793	700	32.5
	594	793	700	32.5
	597	800	712	28.3
	600	807	711	25.4
	592	797	688	21.4
	593	803	697	20.0
	596	802	665	11.3
	594	792	685	24.4
	596	797	690	19.3
	594	790	698	58.1
	593	792	696	28.4
	594	784	695	39.7
Average	595.1	797.9	692.7	35.3
σ	2.44	8.13	15.2	14.4

Table 3.6-14 (Cont'd)

GROUP 2 - IR FIRE FOR 2 MIN. AT 925°C
(σ = 50 - 80 Ω/□)
(No. of cells = 12)

	V_{oc} (mv)	I_{sc} (mA)	I_{500} (mA)	R_{sh} (Ω)
	569	657	263	142.9
	571	690	372	142.9
	580	702	467	102.0
	578	703	425	156.3
	582	721	478	135.1
	585	710	478	128.2
	581	651	369	75.8
	558	669	235	147.1
	580	735	511	131.6
	583	715	490	106.4
	565	712	297	151.5
Average	575.6	696.9	398.6	129.1
$\hat{\sigma}$	8.63	27.1	98.0	24.7

Table 3.6-14 (Cont'd)

GROUP 3 - IR FIRE FOR 2 MIN. AT 950°C
(σ = 24 - 38 Ω/□)
(No. of cells = 11)

	V_{oc} (mv)	I_{sc} (mA)	I_{500} (mA)	R_{sh} (Ω)
	584	737	620	66.7
	588	753	636	200.0
	585	732	627	122.0
	583	737	617	172.4
	581	747	617	142.9
	586	756	636	156.3
	585	737	600	172.4
	591	758	642	161.3
	589	772	634	166.7
	584	747	589	185.2
	585	756	627	172.4
Average	588.0	748.4	622.3	156.2
δ	2.28	12.0	16.2	36.1

were processed similarly to the controls except the PX-10 diffusion source was sprayed on with a hand held Paasche airbrush.

The results of this experiment are given in table 3.6-15. All electrical measurements are identical (± one standard deviation). Therefore it can be concluded from this experiment that Allied Chemical Accuspin® PX-10 diffusion source may be used as a spray-on as well as a spin-on source.

Table 3.6-15

SPIN-ON VS. SPRAY-ON DIFFUSION
(No AR Coating)

Properties / Process Type	$\rho \pm \hat{\sigma}$ ($\Omega/\square$)	$V_{oc} \pm \hat{\sigma}$ (mV)	$I_{sc} \pm \hat{\sigma}$ (mA)	$I_{500} \pm \hat{\sigma}$ (mA)	$R_{sh} \pm \hat{\sigma}$ (Ω)
Spray-on	30.2 ± 3.3	611 ± 2	679 ± 10	612 ± 32	17.0 ± 5.0
Spin-on	32.0 ± 2.8	610 ± 1	665 ± 6	595 ± 29	17.4 ± 3.6

3.7 COFIRING N^+ JUNCTION & ALUMINUM P^+ BACK

3.7.1 Recommendations

We were unable to simultaneously fire the front diffusion (N^+) and the aluminum back contact because of excessive reaction of the aluminum with oxygen and silicon. We recommend that this operation be replaced with separate firing cycles which are specifically designed for each process.

3.7.2 Work Performed

In attempting to fire the aluminum during the diffusion cycle, we have discovered that the time required for the diffusion causes excess dissolution of silicon into the aluminum. The reaction appears to involve reaction with oxygen in the furnace atmosphere, with the development of a thick scoriaceous layer on the back of the wafer. This effect precludes firing the aluminum during the diffusion step as had been originally planned. In order to retain a process sequence which does not involve back etching we investigated the possibility of firing the aluminum on phosphorus diffused surfaces.

In order to test this possibility, aluminum paste was printed and fired at 850°C for 30 seconds on one surface of a round, 2 ohm-cm wafer which had been diffused on both sides using a PH_3 gaseous source. In order to provide an adequate test, the junction depth was 0.35 mm, well beyond the depth which will be encountered in actual solar cell fabrication. After dicing into 2 cm squares, cells were completed using standard controlled aerospace cell fabrication processes. AR coating was omitted. Measurements of V_{oc}, I_{sc} and I_{500} were made using AM1 xenon illumination. The results are reported in Table 3.7-1.

Table 3.7-1

PROPERTIES OF SOLAR CELLS WITH ALUMINUM PASTE BACK-FIELD
NO BACK ETCH

V_{oc} mV	I_{sc} mA	I_{500} mA
616	142	137
609	141	135
617	140	135
612	139	134
613	139	134
613	139	134
615	139	134
610	140	134
618	139	133
612	138	133
611	141	133
608	139	133
615	137	133
612	139	133
615	139	132
610	140	132
612	139	132
615	138	132
616	138	131
616	137	131
612	139	131
612	137	131
612	141	131
612	137	131
613	138	130
613	139	130
613	137	129
614	135	129
616	136	129
615	136	128
614	134	128
609	136	127
618	140	127
612	133	127
613	136	127
606	136	127
613	140	126
614	134	126
613	138	125
612	136	125
608	138	124
610	137	124
610	137	124
613	139	124
607	140	122
611	139	122
609	138	114*
612	136	113*
603	138	92.6*
610	142	92.4*
604	137	57.6*
$\bar{x}$ 612.6	138.1	129.8
σ 2.71	1.96	3.79

*Cells treated as outliers, data not included in calculated statistical parameters.

This diffusion cycle for N-250 was tested on four sets of cells with variations in surface preparation and method or dopant application. In all cases the cells were fabricated on 10 ohm-cm silicon wafers with evaporated contacts and P^+ back surface field 2 cm x 2 cm cells were cut from round after completion of all processing. Results are reported in Table 3.7-2, together with the surface treatment and method of application.

The first group of samples was sprayed with a heavy layer of undiluted N-250. Care was necessary in order to prevent flaking upon drying; polished samples had a higher tendency for flaking. A stain layer remained on the surface after a 5% HF etch following the diffusion. The group 2 cells were sprayed with N-250 that had been diluted with 30% IPA. Very thin layers of N-250 were applied and no stain layer remained after the 5% HF etch. These cells also provided very good response, however, I_{sc} is lower than group 1, suggesting that the stain in that group acted as an antireflective coating. N-250 was applied to the third group by means of a contact transfer and produced good cells. Contact transfer of N-250 onto nontextured cells (group 4) also produced good cells with a reduced output resulting from lack of texturing. The high open circuit voltage of these cells is attributable to the P^+ back.

Additional experiments were carried out on 2 ohm-cm wafers. In these the diluted N-250 source was sprayed on and diffused at a lower temperature (850^{o}C for 30 minutes). In one experiment an aluminum back was applied, in the other an evaporated back contact was applied. The results are reported in Table 3.7-3. In both cases good cells were obtained with output at load comparable to cells in the previous experiments. In this experiment the aluminum back did not cause the expected increase in open circuit voltage and short circuit current for some unknown reason.

Table 3.7-2

Output Parameters at AM0 for non-AR coated cells prepared by diffusion from N-250 source with a diffusion cycle of 25 minutes ramp from 700°C to 900°C, 10 minutes at 900°C, 25 minute ramp from 900°C to 700°C.

Experiment	Treatment		V_{oc}	I_{sc}	I_{400}
1.	Surface texturized to a matte finish. Undiluted N-250 applied by spraying. Some diffusion residue was resistant to HF, and acted as an AR coating.		620	141	140
			616	140	138
			617	137	135
			619	141	139
			614	141	137
			619	137	135
			616	139	138
			616	139	137
		$\bar{X}$	517.1	139.4	137.4
		σ	1.90	1.58	1.65
2.	Surface texturized to form sharply defined pyramids. Undiluted N-250 applied by spraying. Diffusion glass removed by HF soak (30 sec. in 5% HF)		613	137	134
			613	132	129
			612	129	128
			614	129	128
			612	138	128
			613	139	130
			614	134	130
			616	135	130
			615	134	132
		$\bar{X}$	613.6	134.1	129.9
		σ	1.26	3.41	1.91
3.	Surface texturized to a matte finish. N-250 applied by contact transfer from Dextilose paper. Diffusion glass removed by HF soak (30 sec in 5% HF)		616	128	126
			612	129	121
			613	127	124
			614	134	126
			614	128	124
			618	137	134
			612	132	131
			612	132	131
			616	130	128
			618	130	129
			618	129	127
			616	129	127
		$\bar{X}$	614.9	130.4	127.3
		σ	2.29	2.75	3.42

Table 3.7-2 (continued)

Experiment	Treatment	V_{oc}	I_{sc}	I_{400}
4.	Surface smooth etched in 30% NaOH. N-250 applied by contact transfer from Dextilose paper. Diffusion glass removed by HF soak (10 sec in 5% HF)	613	107	106
		610	112	108
		604	108	91
		606	106	94
		609	113	99
		610	110	87
		612	106	93
		613	108	92
		602	107	93
		$\bar{X}$ 608.4	108.6	95.9
		σ 3.77	2.40	6.64

Table 3.7-3

Output parameters at AM0 for non-AR coated cells prepared by diffusion from N-250 source with a diffusion cycle of 20 minutes ramp from 700°C to 850°C, 30 minutes at 850°C, 20 minute ramp from 900°C to 700°C.

Experiment	Treatment	V_{oc}	I_{sc}	I_{400}
1.	Texturized surface. Diluted N-250 applied by spraying. Diffusion glass removed by soak in HF (10 sec in 5% HF) Aluminum back contact.	599	133	129
		597	136	129
		602	139	133
		600	130	120
		600	134	128
		$\bar{X}$ 599.6	134.4	127.8
		σ 1.62	3.01	4.26
2.	Texturized surface. Diluted N-250 applied by spraying. Diffusion glass removed by soak in HF (10 sec in 5% HF) Evaporated back contact.	600	144	143
		604	147	138
		599	147	132
		599	146	135
		602	146	134
		549	147	131
		603	145	133
		598	147	125
		601	147	136
		600	145	131
		599	145	132
		603	146	134
		600	146	132
		601	146	129
		603	145	135
		598	146	133
		$\bar{X}$ 600.5	145.9	133.4
		σ 1.85	0.90	3.8

The observed characteristics are substantially those one would expect of a normal P^+ back field cell on this type of material, indicating that the junction was eliminated over substantially all of the back surface. This is particularly evident in the open circuit voltage ($\bar{x}$ = 612 mW) which would be about 600 mV for this material in the absence of a back field. There is no evidence of a badly degraded curve shape; however, further detailed comparison against a control standard is required to be sure that the curve shape is completely unaffected.

3.8 PRINTED ALUMINUM P^+ BACK

3.8.1 Recommendations

The inclusion of a printed aluminum P^+ back contact in the process sequence is recommended. Initial difficulties with low shunt resistance have been overcome by improving processing procedures. These procedure changes included not removing the diffusion oxide prior to the aluminum back contact, and exercising greater caution to eliminate sources of contamination (e.g. tools, fixtures, etc.). The aluminum firing cycle was shown to be compatable for use with printed front contacts. Warpage of the cell due to differences in thermal expansion of silicon and aluminum has been reduced by allowing streets of bare silicon between blocks of aluminum. IR furnace drying and firing printed aluminum back contacts is recommended due to the cost effectiveness and high throughput rate of this technique.

The observed characteristics are substantially those one would expect of a normal P^+ back field cell on this type of material, indicating that the junction was eliminated over substantially all of the back surface. This is particularly evident in the open circuit voltage ($\bar{x}$ = 612 mW) which would be about 600 mV for this material in the absence of a back field. There is no evidence of a badly degraded curve shape; however, further detailed comparison against a control standard is required to be sure that the curve shape is completely unaffected.

3.8.2 Work Performed

Experience has shown that the best P^+ back surface field effects are obtained with aluminum pastes when fired at rather high temperatures for short time periods with steep heating and cooling

temperature ramps. These requirements can be understood by considering the aluminum-silicon phase diagram (Figure 3.8-A). What is desired is to obtain a uniform layer of heavily aluminum doped silicon on the back surface of the wafer.

When the printed wafer is heated to the temperature range 750^{o} - 900^{o}C, the aluminum melts and can dissolve silicon to the extent of about 22 to 34 atomic percent. Upon subsequent cooling, silicon will solidify and be heavily doped (saturated) with aluminum. As the system cools the silicon content of the melt decreases until the eutectic composition and temperature is reached, where an intimate mixture of aluminum and silicon phases forms.

With rapid heating, only the aluminum adjacent to the interface will be saturated. There will be a composition gradient into the aluminum with the silicon concentration decreasing with increasing distance from the interface. Thus, upon cooling, the natural tendency of the silicon to deposit epitaxially on the readily available solid silicon surface at the interface rather than the formation of new silicon nuclei will be reinforced. The concentration gradient will also minimize the formation of liquid layer instability due to depletion of the silicon in the liquid as the interface advances with falling temperature.

The rapid heating will also tend to result in a smoother interface. The (111) surfaces of silicon are thermodynamically favored in contact with molten aluminum. By heating rapidly, the aluminum adjacent to the interface is maintained in a superheated (undersaturated) condition which results in kinetic effects dominating to produce a relatively smoother surface on the (100) oriented wafer surface. This effect will also minimize local excess penetration of the molten aluminum, and subsequently formed P^{+} layer, at localized inhomogeneities or imperfections in the silicon crystal.

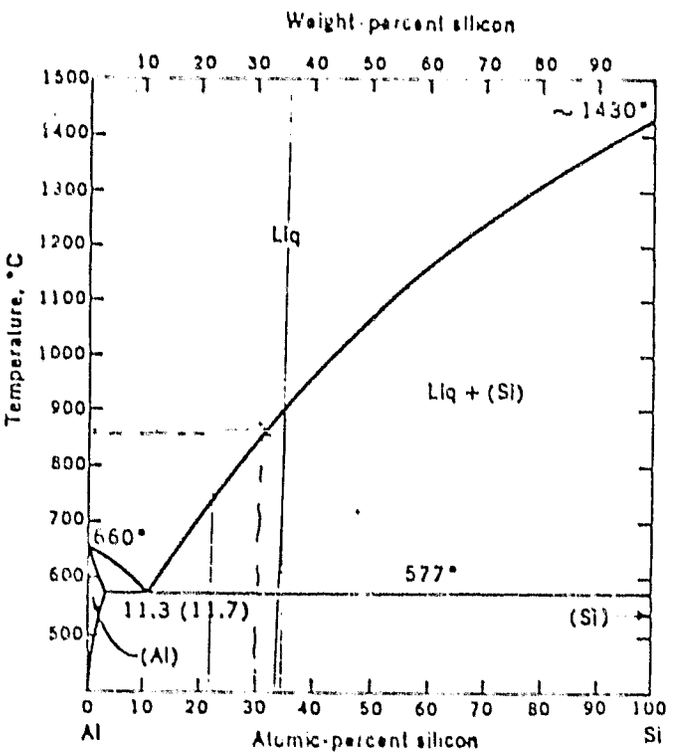

Figure 3.8-A

SILICON-ALUMINUM PHASE DIAGRAM[3]

When printed aluminum paste is fired in a non-oxidizing atmosphere such as nitrogen, satisfactory results are not obtained since the melt which forms tends to puddle up into lenticular clumps resulting in nonuniform alloying. When fired in an oxidizing atmosphere, the outermost particles oxidize and sinter together to form a crust which prevents the puddling action of the underlying molten layer. This sintered crust must be subsequently removed in order to make electrical contact.

An initial series of cell fabrication experiments were carried out in order to demonstrate the effectiveness of an Al back contact metallization, both as a P^+ back surface field and as a means of removing the diffused N^+ layer. These experiments are summarized in Table 3.8-1. In all cases cells were fabricated on 2 inch diameter 10 ohm-cm P-type round wafers. Surfaces were prepared by a damage removal etch in hot 30% sodium hydroxide with no texturizing. Junctions were formed at a depth of 0.3 μm by phosphine diffusion. Front contacts were evaporated with Ti-Pd-Ag after removal of the diffusion oxide by 10 second immersion in 5% HF. Back contact preparation was varied as indicated in Table 3.8-1. Aluminum paste back contacts were printed using an Aramco Products, Inc. Model 3130 Printer. Screens were 200 mesh stainless steel with a 1 mil emulsion, which gave a paste layer approximately 0.7 mil thick after drying. The printed paste was dried for 15 minutes at 200°C in air.

No AR coating was applied. After cell processing was completed 2 x 2 cm cells were sawn from the round disks in order to provide junction cleanup.

The first experiment demonstrates the problem of producing a cell without removing the diffused N^+ layer. When the N^+ layer is removed by back etching, the back contact is able to make ohmic

Table 3.8-1

FORMATION OF P+ BACK CONTACT THROUGH DIFFUSED LAYERS

Exp.	Back Etch	Back Contact	Firing Condition		E_{oc} mV	I_{sc} mA	I_{400} mA
1.	no	Evap.	none		no response		
2.	yes	Evap.	none		542	89	88
					538	88	87
					538	86	85
					538	85	84
					541	89	88
					541	90	89
					536	86	85
					541	89	88
					539	87	86
					538	88	87
				$\bar{X}$	539	87.7	86.7
				σ	1.87	1.55	1.55
3.	yes	Paste Aℓ	10 sec. 900°C		600	94	83
					597	96	96
					596	98	96
					589	95	92
					585	94	93
					588	95	93
					571	94	90
					563	92	89
					592	96	95
					580	93	91
				$\bar{X}$	586	94.7	91.8
				σ	11.2	1.61	3.71
4.	no	Paste Aℓ	10 sec 900°C		604	97	95
					604	96	95
					601	96	95
					600	97	96
					603	95	95
					596	96	95
					605	96	95
					602	97	96
					601	96	95
					605	95	94
					602	97	96
					600	96	96
					604	96	95
					604	96	95
				$\bar{X}$	602	96.1	95.2
				σ	2.40	0.63	0.558

Table 3.8-1 (Cont'd)

Formation of P^+ Back Contact Through Diffused Layers

Exp.	Back Etch	Back Contact	Firing Condition	E_{oc} mV	I_{sc} mA	I_{400} mA
5.	no	Paste Aℓ	15 sec 800°C	589	95	92
				584	94	93
				588	95	93
				571	94	90
				563	92	89
				592	96	95
				563	92	86
				580	93	91
				$\bar{X}$ 579	93.9	91.1
				σ 10.9	1.36	2.61

contact. In experiment 2, the cells had a V_{oc} and I_{sc} characteristic of 10 ohm-cm material without a back field. On firing an Al back contact to produce a P^+ layer (experiment 3), the V_{oc} increased 10% and the I_{sc} increased 5%. The ability of the P^+ layer to remove the N^+ layer during firing is demonstrated in experiment 4. Comparison of the data for this experiment with the preceding one suggests that the back etch process used in experiment 3 somehow contributed to degradation of the cell, possibly by damage to the front surface. Experiment 5 in which the aluminum back was fired at a lower temperature, indicates the sensitivity of the process to the firing cycle.

The firing cycle requirements are believed to be determined by the need for sufficient time to allow the dissolution of silicon into the molten aluminum while avoiding excessive oxidation of the molten aluminum-silicon alloy. In the experimental work performed thus far, we have developed a process using tube furnaces. A small number (1-5) of two inch wafers are placed horizontally on a light quartz rail boat. This is moved rapidly into the heated zone of the tube furnace, allowed to remain for the specified time and then rapidly pulled into the cool portion of the furnace tube. This procedure was used to define a reasonably reproducible firing cycle and to attain the required short firing cycle. No attempt was made to define the exact time-temperature profile seen by the wafers.

The various factors involved are illustrated by the results of a time-temperature matrix experiment for Alcoa 1401 paste on 2.12 inch round cells. Previous experimental work utilized Englehard 3484A aluminum paste. However, considerable difficulties were encountered in cleaning the sintered layer on the Englehard paste and it was subsequently displaced by a formulation prepared by mixing Alcoa #1401 aluminum powder with a vehicle designated as V-13 (Table 3.8-2).

Table 3.8-2

COMPOSITION AND PREPARATION
OF V-13 VEHICLE

	Parts by Weight		
α Terpinol	46 to 45	1/1 ratio	Total = 100 parts by weight
Butyl Carbitol Acetate	46 to 45		
Ethyl Cellulose (N-14)	8 to 10		
Tixatrol ST	1.5		

Procedure

a) To the mixture of α terpinol and butyl carbitol acetate at 70°C add ethyl cellulose. Stir constantly until dissolved.

b) Cool to room temperature

c) Disperse Thixatrol ST in above mixture using a Waring blender. Do not allow temperature of mix during blending to exceed 50°C.

d) Age for 16 hours at room temperature before use.

Sources for the above materials are as follows:

α Terpinol and Butyl Carbitol Acetate	MC/B Manufacturing Chemists 2121 South Leo Street Los Angeles, CA
Ethyl Cellulose (N-14)	Hercules, Incorporated 500 South Lafayette Place Los Angeles, CA
Thixatrol ST	NL Industries, Incorporated Industrial Chemical Division Hightstown, NJ 08520

The cells utilized in the time-temperature matrix experiment for Alcoa 1401 paste were fabricated by the following process sequence:

1) Texture etch wafers
2) Phosphine diffuse to 30 ohms square
3) Back etch with 100% HF
4) Print, dry and fire aluminum paste
5) 10% HF for 2 minutes
6) Sand edge of wafer
7) Remove sintered (unmelted) aluminum
8) Clean wafers in acetic acid and solvents
9) Print, dry and fire silver front paste
10) Test cells

The sixth step of sanding the edge is a very unreliable process. If the edges are not sanded enough, shunting around the edge will persist, and if edges are sanded too much, wafer damage will occur, and will appear in the form of shunting. As one sands the edge of the wafer, the V_{oc}, I_{sc} and I at load will increase to a maximum and then decrease. The results of this experiment are given in Table 3.8-3.

All of the cells that were fired at 900°C, except for the cells fired for 10 seconds, had puddles of thick aluminum on the back, and the sintered (unmelted) aluminum was difficult to remove. The cells fired at 850°C had a good uniform layer of melted aluminum on the back. Cells fired at 750°C and 800°C tended to wet the silicon erratically. The cells exhibited high series resistance which prevented measurement of load point current. These cells failed to develop the open circuit voltage characteristic of a good P^+ layer.

Table 3.8-3

Results of time-temperature firing cycle matrix for aluminum paste made with 70% Alcoa 1401 aluminum powder with 30% V-13 vehicle, 2.12 inch round cells with no AR coating. Tungsten AMI light source.

Firing Time	750°C	800°C	850°C	900°C
		V_{oc} (mV)		
10 Sec.	--	--	607.5	610(1)*
20 Sec.	--	599	609	605(1)
30 Sec.	--	560	607.5	596(1)
40 Sec.	601.5	607.5	607	590(1)
50 Sec.	576.5	604	--	--
60 Sec.	566.0	--	--	--
		I_{sc} (mA/cm^2)		
10 Sec.	--	--	30.3	31.13(1)
20 Sec.	--	31.18	26.68	29.38(1)
30 Sec.	--	35.55	30.87	29.46(1)
40 Sec.	29.24	30.52	30.08	28.98(1)
50 Sec.	30.78	30.41	--	--
60 Sec.	35.6	--	--	--

Table 3.8-3 (Cont'd)

Firing Time	750°C	800°C	850°C	900°C
	I_{500} (mA/cm^2)			
10 Sec.	--	--	25.27	26.87(1)
20 Sec.	--	-0-	26.52	25.38(1)
30 Sec.	--	-0-	25.89	22.17(1)
40 Sec.	23.27	26.94	25.12	21.38
50 Sec.	-0-	8.34(1)	--	--
60 Sec.	-0-	--	--	--

* Data are averages of 2 cells except where indicated otherwise. Complete data are given in Appendix A.

Among the cells with a uniform melted aluminum layer after removal of the sintered aluminum, those fired at 850°C for 20 seconds displayed the highest efficiency.

A more limited time-temperature matrix experiment was carried out with paste made from AMPAL aluminum powder. The Alcoa powder was replaced by AMPAL #631 aluminum powder (Atomized Metal Powder, Inc.) when it was discovered that Alcoa #1401 is no longer available. In both cases the mixture was a 70 wt. percent aluminum powder and 30 wt. percent V-13 vehicle. A second matrix experiment was performed to verify the results and to narrow down the optimum time. For these experiments the processing sequence was modified to provide junction cleaning by saw scribing and breaking:

1) Texture etch
2) Phosphine diffuse wafers
3) HF back of wafers
4) Print, dry and fire aluminum paste (AMPAL 631 aluminum paste)
5) HF wafers
6) Remove unconsolidated aluminum powder and clean wafers
7) Print, dry and fire front silver paste
8) Dice 1.4" squares
9) Test cells

The results of this experiment are reported in Table 3.8-4.

As a result of the experimental work performed to optimize the firing cycle for the aluminum paste, it was determined that the firing cycle should be:

Table 3.8-4

Time-temperature matrix for 1.4 inch square cells made with 70% Ampal #631 aluminum powder in 30% V-13 vehicle. Data reported are average of 5 cells. No AR coating on cells.

	Matrix I		Matrix II	
Firing Time	825°C	850°C	825°C	850°C
	V_{oc} (mV)			
20 Sec.	--	606.8	--	602.0
30 Sec.	608.8	606.4	602.8	601.5
40 Sec.	--	--	604.0	--
50 Sec.	606.8	--	601.3	--
	I_{sc} (mA/cm^2)			
20 Sec.	--	30.83	--	31.08
30 Sec.	32.53	31.16	30.92	31.18
40 Sec.	--	--	31.04	--
50 Sec.	32.28	--	30.84	--

Table 3.8-4 (Cont'd)

	Set I		Set II	
Firing Time	825°C	850°C	825°C	850°C
	I_{500} (mA/cm^2)			
20 Sec.	--	24.33	--	25.46
30 Sec.	25.35	16.37	26.20	25.49
40 Sec.	--	--	26.49	--
50 Sec.	24.42	--	24.79	--
	η_{500} %			
20 Sec.	--	12.2	--	12.7
30 Sec.	12.7	11.7	13.1	12.7
40 Sec.	--	--	13.2	--
50 Sec.	12.2	--	12.4	--

1) 10 seconds at 900°C for Englehard Paste
2) 20 seconds at 850°C for Alcoa #1401
3) 40 seconds at 825°C for AMPAL powder

The optimum firing time and temperature was thus found to be dependent upon the type of aluminum powder utilized in the paste.

The direction of subsequent experimental work was to integrate the printed aluminum P^+ back contact process into the processing sequence shown in Table 3.8-5, using non-texturized Wacker square cells. Preliminary attempts produced cells having very inferior electrical performance characteristics. Some of these early results were undoubtedly influenced by the erratic and inadequate performance of N-250 diffusion source on non-textured surfaces and interactions between the diffusion, front metal and aluminum back processes due to refractory surface films formed during the diffusion process.

A second major source of difficulty has been found to be that a large change in the optimum firing cycle for the printed aluminum back is required in shifting from a 2.12 inch round wafer to a 2.12 inch square wafer. Optimum firing for the former had been previously determined to be 40 seconds at 825°C with AMPAL aluminum powder. We have subsequently determined that with our furnace arrangement, paste made with this aluminum powder has an optimum firing cycle on 2.12 inch square wafers of about 80 seconds at 850°C.

In order to minimize the effects of other process steps (diffusion, printed front contacts) the time-temperature matrix experiment was performed using phosphine diffused wafers, junction cleaning by saw cutting 2cm x 2cm wafers from the aluminum fired 2.12 inch square wafers, and applying evaporated front contacts. Two sets

Table 3.8-5

PROCESS SEQUENCE

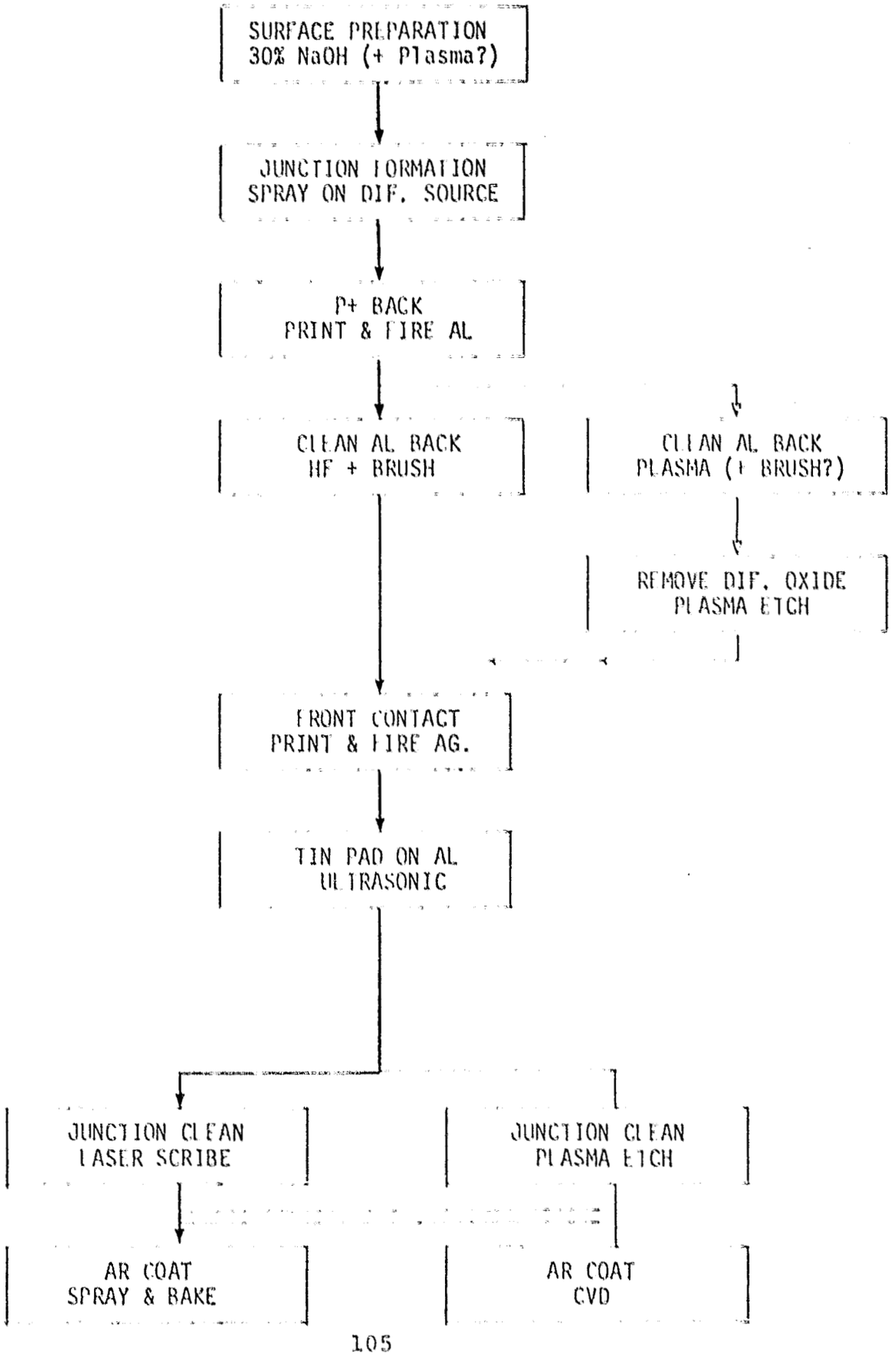

were run, one with an HF back-etch after diffusion to remove oxides, the second with an HF-HNO_3 back-etch to remove both oxides and the diffused layer. The results are reported in Table 3.8-6, wherein the first parameter in each data cell is for the HF back-etch set and the second is for the HF-HNO_3 back etch set. The number of surviving 2 cm x 2 cm cells which were measured is shown in parentheses.

Two sets of 2.12 inch square cells (with HF and HF + HNO_3 back-etch) were fired for 60 seconds at 850^{o}C and fabricated with printed silver front contacts to verify the preceding firing cycle determination. Results are reported in Table 3.8-7. Examination of this table shows that the open circuit voltage is very comparable to that obtained for a firing cycle of 60 seconds at 850^{o}C using evaporated metal (Table 3.8-6), namely 587 and 592 mV vs 587 and 594 mV. The short circuit current is slightly lower (22.7 and 22.9 mA/cm^2 vs 23.8 and 24.1 mA/cm^2). These results indicate that the aluminum firing cycle is suitable for use with the printed front contacts. The load point current is down substantially for the printed front contact cells (14.6 and 16.5 mA/cm^2 vs 22.0 and 21.8 mA/cm^2) indicating other deficiencies in the cells made with printed front contacts.

A portion of this difference in load point current can be attributed to the difference in shunt resistance (315 and 700 ohms/cm^2 vs 1780 and 790 ohms/cm^2). Examination of the shunt resistance data in Table 3.8-8 for evaporated contacts, indicate an erratic behavior of this parameter. This suggests that cell degradation resulting in low shunt resistance is associated with the aluminum back. The most severe shunting resulted from contamination of the front surface by the aluminum. This most commonly occurred by contact of the wafer front surface with another surface which had been contaminated (e.g. tools, fixtures, etc.). In order to

Table 3.8-6

CELL PARAMETERS FOR TIME-TEMPERATURE MATRIX FOR FIRING ALUMINUM BACKS ON 2.12" SQUARE CELLS.

See text for description of cells and processing.
(No AR Coating)

Time	825°C	850°C	875°C
		V_{oc} (mV)	
20 sec.	558 (4)	523 (3)	(0)
	-	583 (4)	586 (2)
40 sec.	580 (4)	593 (3)	585 (2)
	575 (4)	529 (1)	589 (3)
60 sec.	580 (1)	587 (3)	586 (2)
	587 (3)	594 (3)	592 (2)
80 sec.	580 (1)	586 (3)	572 (2)
	542 (3)	594 (3)	-

Table 3.8-6 (Cont'd)

Time	825°C	850°C	875°C
		i_{500} (mA/cm^2)	
20 sec.	14.4 (4)	5.9 (3)	(0)
		20.3 (4)	20.5 (2)
40 sec.	19.5 (4)	20.8 (3)	19.7 (3)
	16.8 (4)	8.8 (1)	24.9 (3)
60 sec.	19.8 (1)	22.0 (3)	21.1 (2)
	20.7 (3)	21.8 (3)	22.0 (1)
80 sec.	20.3 (1)	21.3 (3)	15.8 (2)
	11.3 (3)	23.0 (3)	-

Table 3.8-6 (Cont'd)

Time	825°C	850°C	875°C
		R_{sh} (ohms/c.m^2)	
20 sec.	3050 (4)	364 (3)	(0)
	-	217 (4)	550 (2)
40 sec.	18400 (4)	1190 (3)	1460 (3)
	925 (4)	870 (11)	1560 (3)
60 sec.	2500 (1)	1780 (3)	873 (2)
	3040 (3)	790 (3)	1820 (1)
80 sec.	6670 (1)	4760 (3)	1940 (2)
	1510 (3)	3250 (3)	-

Table 3.8-7

EVALUATION OF 60 SECOND 850°C ALUMINUM BACK FIRING CYCLE WITH PRINTED FRONT CONTACTS

(Sample size = 7, no AR Coating)

Back Etch	R_{sh} Ohms/cm^2	V_{oc} mV	I_{sc} mA	I_{500} mA
HF	315	587	22.7	14.6
HF + HNO_3	700	592	22.9	16.5

Table 3.8-8

CELL PARAMETERS FOR CONTROL LOTS
MADE WITH Ti-Pd-Ag EVAPORATED FRONT
AND Cr-Pd-Ag EVAPORATED BACK CONTACTS
ON PHOSPHINE DIFFUSED WAFER.

(No AR Coating, Sample Size = 3)

R_{sh} Ohms/cm^2	V_{oc} mV	I_{sc} mA	I_{500} mA
66,700	589	20.1	18.1
50,000	587	19.5	17.8

provide as much protection as possible, the diffusion oxide was not removed until after the aluminum back contact process. The thin oxide which formed on the back of the cell did not affect the formation of the back contact.

The P^+ back surface field process with an aluminum back contact as discussed above, was shown to be a viable technique. The voltage was 610 to 620 mV. One potentially serious problem was identified however. The aluminum produces a strain in the cell due to the thermal expansion coefficient difference between silicon and aluminum. The strain causes the wafer to bow, which may create problems with automatic handling equipment. A proposed solution to this bowing problem is to allow streets of bare silicon between blocks of aluminum, Figure 3.8-B. Two questions need to be answered concerning this patterned aluminum back. First, how effective is the pattern in reducing the bowing. Second, does the pattern reduce the effectiveness of the back surface field.

To measure the effect of bowing, 2.12 x 2.12 inch wafers were thinned by etching to 5 mils and printed with both a normal full back contact and the new patterned back contact (run 4.23.9). Both sets of wafers had a radius of curvature of 7.5 cm after firing. The cylinder defined by the curvature was parallel to the support rods of the sintering boat, Figure 3.8-C. After the wafers were dipped in a dilute solution of hydrofluoric acid and the unconsolidated aluminum was removed by brushing, the wafers had a radius of curvature of 16.5 and 79.5 cm for the full back and pattern back, respectively, indicating that the pattern is indeed effective in reducing the bowing effects.

The second experiment, run 5.35.9, was designed to determine the effect of the pattern back on cell electrical performance. The

Figure 3.8-B

Pattern for Aluminum Back
to Reduce Bowing Effects

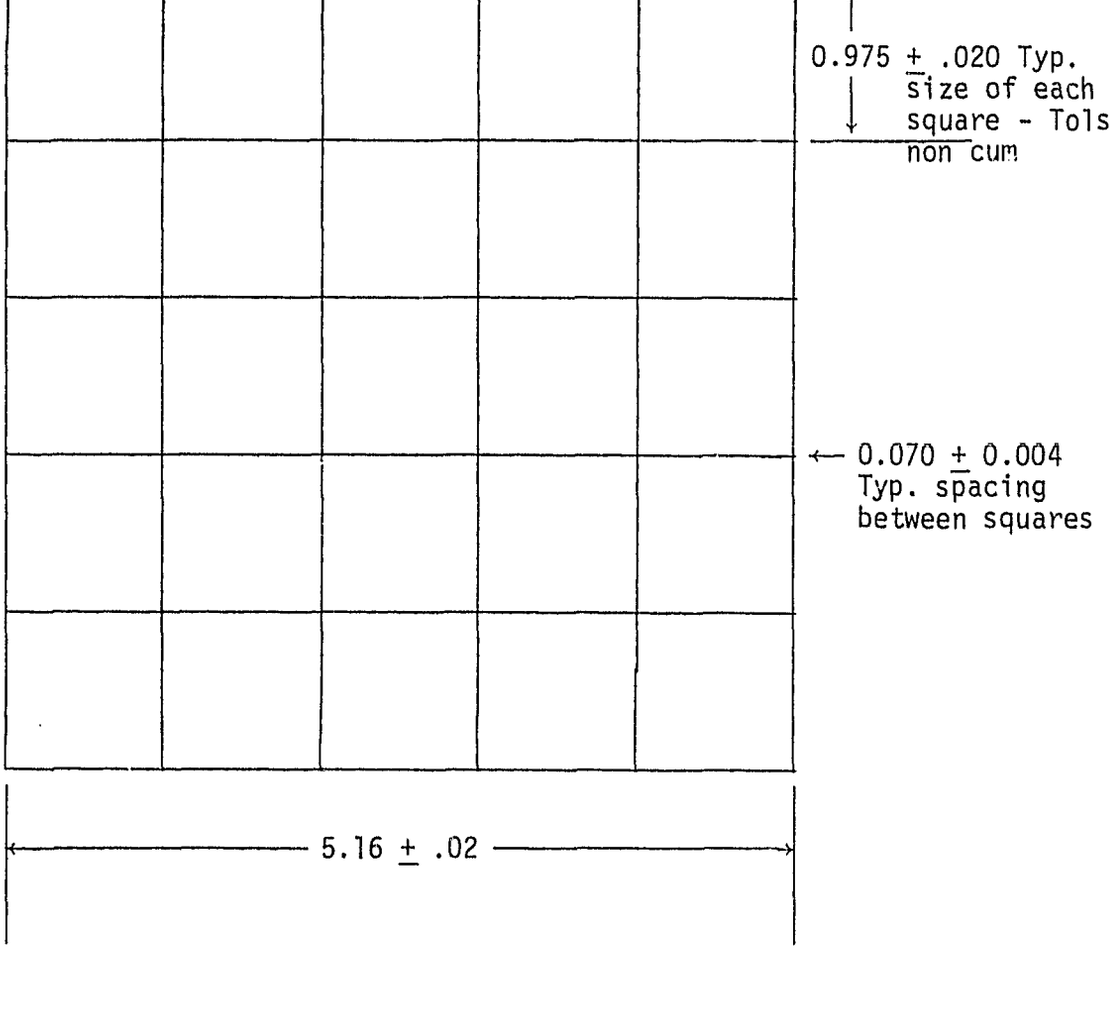

DIMENSIONS ARE IN CENTIMETERS
TOLERANCES: .XXX = ± .02

Back Contact
Pattern P+
(Screen Printing)

PART NO. NM 516-P-070

Note: Squares are areas of open screen

Figure 3.8-C

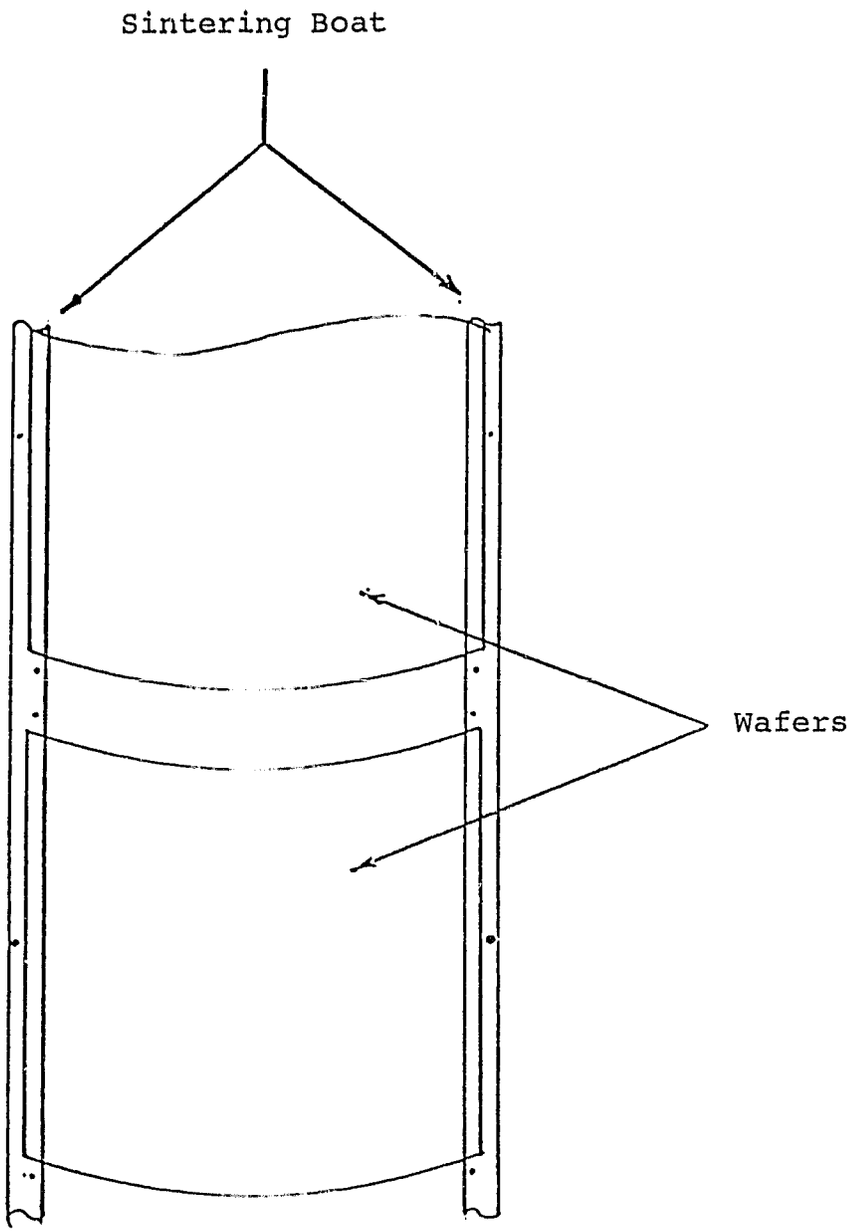

RELATIONSHIP OF CELL BENDING TO
SINTERING BOAT CONFIGURATION

wafers were processed in accordance with the baseline process except the wafers were laser scribed prior to front silver metallization and no AR coating was applied. The open circuit voltage was the same for both back contact patterns, and the efficiencies were 9.0% (= 12.1% with AR coating) and 8.5% (= 11.4% with AR coating) for the pattern back and full back, respectively. Both of these sets of cells had low output due to shunting problems.

In order to obtain a larger data base on the pattern back surface field, three separate runs were processed, 5.43.9A, B, and C, by three different technicians. These runs were processed the same as those of run 5.35.9. The cell characteristics of all three runs were practically the same, very similar to the results of run 5.35.9. The results are summarized in Table 3.8-9.

In comparing the shunt resistance from run 5.46.9, and all other runs, it is evident that the 10 ohm-cm material from Wacker produces cells with superior shunt resistance. This may be due to the low impurity level in this 10 ohm-cm material. A larger data base must be established before an accurate conclusion can be drawn.

Experimental work on printed aluminum P^+ back contacts was concluded with an investigation of a modified firing technique. Preliminary experiments carried out on infrared belt furnace equipment at Radiant Technology Corporation, Cerritos, California, have indicated that this type of equipment can be adapted to achieve the required firing cycle. IR furnace drying and firing is a high throughput, cost effective technique which may be utilized to produce a reliable back surface field and back contact.

Table 3.8-9

BACK SURFACE FIELD

Run #	p+ Back	Sheet ρ (Ω/□)	Average Values V_{oc} (mV)	I_{sc} (mA)	I_{500} (mA)	R_{sh} (Ω)	(%)	Equiv. η with AR (%)
5.25.9	Pattern	32-36	604	650	525	6.4	9.0	12.1
5.35.9	Full	32-40	603	648	498	4.9	8.6	11.5
5.35.9	Full	28-40	604	651	487	5.8	8.5	11.3
5.43.9A	Pattern	33.3	602	659	512	7.3	9.0	12.1
5.43.9B	Pattern	33.6	602	669	505	6.9	8.8	11.9
5.43.9C	Pattern	32.6	603	664	516	4.7	9.1	12.2

An infrared belt furnace was procured and utilized to evaluate aluminum paste firing. Two different lots of silicon were chosen for this experiment, 0.1 to 0.5 Ω-cm TI silicon and 7 to 10 Ω-cm Wacker silicon. To simulate our normal 80 second tube firing of our back contact, the belt speed was held constant at 18 inches/min. and the temperature was varied between 800 and 900°C in 25°C intervals. These wafers were dried in an oven prior to firing. The optimum temperature was between 825 and 850°C, Table 3.8-10. In an attempt to obtain a better understanding of the time-temperature effects, the belt speed was increased to 36 inches/min. (40 sec. firing cycle) and the temperature was varied between 875 and 925°C in 25°C intervals. The optimum temperature was 875°C, Table 3.8-11. Some of the high temperature, long firing cycles caused bumps and unalloyed areas to occur on the aluminum. To determine whether these unalloyed areas were caused by organics remaining in the paste, the wafers were sent through a 400°C drying cycle in zone 1 and 2 prior to firing at 875°C at a belt speed of 18, 24 and 36 inches/min. No improvement occurred with this extra drying step, Table 3.8-12. The bumps and unalloyed areas appear to be caused by firing cycles that are too long and/or too hot.

To determine a suitable drying cycle, wafers processed in accordance with the processing sequence shown in Figure 3.8-D were printed with aluminum paste and dried in the IR furnace for 0.75, 1.0, and 2.0 minutes, by varying the belt speed. The wafers were then removed and sent through the IR firing zone. Table 3.8-13 shows the tabulated raw data and averages. Good results were obtained with both a one and two minute (belt speed 18 and 9 inches per minute) drying cycle.

An attempt was made to dry the aluminum paste at the same belt speed as the firing of the paste. The IR drying zone of the furnace was set at a nominal 400°C. Wafers processed in

Table 3.8-10

IR FIRING OF ALUMINUM BACK SURFACE FIELD
VARIABLE TEMPERATURE AND CONSTANT BELT SPEED
NO AR COATING 2.12 x 2.12 INCH SQUARES

Run 10.73.9
Dried in Oven for 20 min. @ 200°C
Belt Speed 18 inches/min.

Silicon Type	Zone 1	Zone 2	Zone 3	Zone 4	V_{oc} (mV)	I_{sc} (mA)	I_{500} (mA)	R_{sh} (Ω)	Comments
TI	0	0	800	800	581	571	303	2.0	
TI					592	583	402	3.0	
Wacker					595	706	597	43.0	
TI	0	0	825	825	592	593	402	2.4	
Wacker					600	718	615	35.5	
TI	0	0	850	850	578	585	281	1.9	
TI					591	582	408	3.4	
TI					581	572	285	1.7	
TI					590	585	387	2.2	
TI					597	593	473	4.2	
Wacker					601	706	600	34.0	
Wacker					602	698	606	43.0	
Wacker					600	707	612	28.4	
TI	0	0	875	875	598	570	490	7.8	Bumps
Wacker					600	690	599	45.9	Bumps
TI	0	0	900	900	Broken				Bumps
TI					Broken				Bumps
Wacker					585	686	547	20.0	Bumps

Table 3.8-11

IR FIRING OF ALUMINUM BACK SURFACE FIELD
VARIABLE TEMPERATURE AND CONSTANT BELT SPEED
NO AR COATING 2.12 x 2.12 INCH SQUARES

Run 10.73.9
Dried in Oven for 20 min. @ 200°C
Belt Speed 36 inch/min.

Silicon Type	Zone 1	Zone 2	Zone 3	Zone 4	V_{oc} (mV)	I_{sc} (mA)	I_{500} (mA)	R_{sh} (Ω)	Comments
TI	0	0	875	875	596	577	464	5.5	
Wacker					600	704	613	54.3	
TI	0	0	900	900	594	578	461	6.4	
Wacker					598	700	601	56.2	
TI	0	0	925	925	591	584	470	6.6	Bumps
Wacker					582	667	495	70.4	Bumps

Table 3.8-12

IR FIRING OF ALUMINUM BACK SURFACE FIELD
CONSTANT TEMPERATURE AND VARIABLE BELT SPEED
NO AR COATING 2.12 x 2.12 INCH SQUARES

Run 10.73.9
Dried in Oven for 20 min. @ 200°C

Zone 1, Zone 2, Zone 3, Zone 4: 260, 410, 875, 875°C

Silicon Type	Belt Speed (inch/min.)	V_{oc} (mV)	I_{sc} (mA)	I_{500} (mA)	R_{sh} (Ω)	Comments
TI	18	588	584	414	4.3	Bumps
TI		594	577	472	8.1	Bumps
Wacker		597	705	606	49.0	Bumps
TI	24	593	575	451	7.7	
TI		593	586	465	6.0	
Wacker		601	705	614	82.0	
Wacker		598	700	600	119.0	
TI	36	591	577	456	7.1	
TI		595	580	455	4.6	
Wacker		600	693	588	72.5	
Wacker		599	687	586	42.4	

Figure 3.8-D

PROCESS SEQUENCE

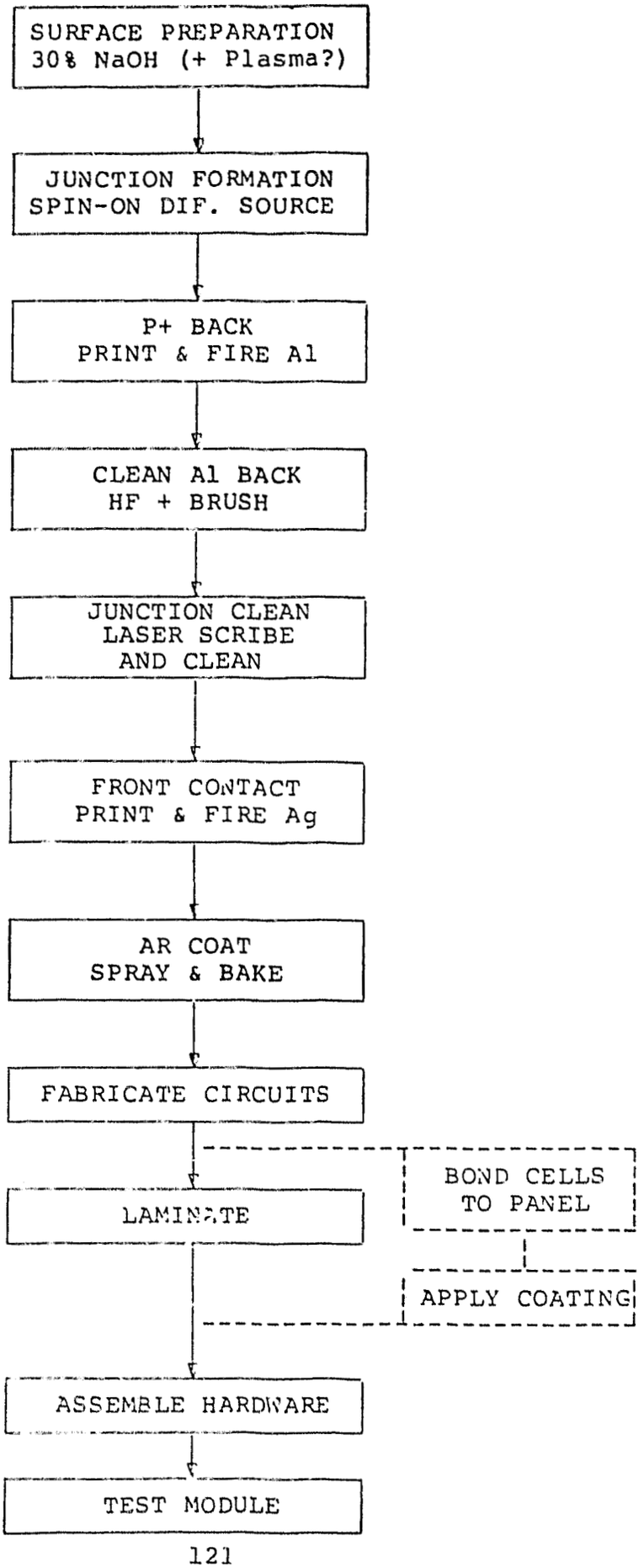

Table 3.8-13

IR DRY OF ALUMINUM P+ BACK

Temperature = 310°C

(No AR Coating)

Drying Conditions \ Properties	ρ (Ω)	V_{oc} (mV)	I_{sc} (mA)	I_{500} (mA)	R_{sh} (Ω)
2 min.	34.1	612	690	622	14.7
	28.2	614	688	623	15.7
	27.5	612	680	616	21.7
	28.6	613	690	632	22.8
	27.6	611	683	606	12.7
	28.3	609	682	571	6.6
	30.1	613	687	625	17.3
	33.1	614	690	543	20.2
Ave.	29.7	612	686	605	16.0
1 min.	29.7	612	680	615	19.5
	29.1	613	676	626	21.8
	29.6	611	681	614	13.2
	31.8	613	686	631	18.5
Ave.	30.1	612	681	622	18.3
0.75 min.	28.2	612	681	620	12.2
	27.0	610	678	599	11.1
	31.6	608	647	539	12.8
	27.4	611	676	592	10.8
	31.3	610	675	512	6.2
	29.3	613	685	611	17.2
	31.9	612	685	596	14.3
	31.1	612	686	560	11.1
Ave.	29.7	611	677	579	12.0

accordance with the processing sequence shown in Figure 3.8-D were drie for 4.0, 2.0, 1.5, and 1.0 minutes, by varying the belt speed. Control wafers were dried in an oven for 15 minutes at 200^{o}C. After drying, the wafers were removed from the belt and then sent through the IR firing zone. Table 3.8-14 lists the average results of this evaluation. The aluminum paste of the first group (4.0 minute drying) peeled in some cases and resulted in poor power output. The other three groups showed comparable results to that of the control group. From this data it is evident that the aluminum P^{+} paste can be sequentially dried and fired in an IR furnace.

Table 3.8-14

IR DRIED ALUMINUM PASTE WAFERS

	# of Cells	Drying Time (min)	Drying Temp °C	V_{oc} (mv)	I_{sc} (mA)	I_{500} (mA)	R_{sh} (Ω)
Average	9	4	400	592	694	391	31.3
$\hat{\sigma}$				1.9	5.3	48.6	7.6
Average	17	2	400	600	615	553	30.4
$\hat{\sigma}$				3.2	10.6	46.7	10.2
Average	17	1.5	400	601	728	581	25.3
$\hat{\sigma}$				1.7	5.5	25.9	13.0
Average	16	1.0	400	603	733	565	28.3
$\hat{\sigma}$				2.0	6.5	45.7	11.6
CONTROL OVEN DRIED WAFERS							
Average	13	15	200	601	723	555	31.2
$\hat{\sigma}$				2.8	4.1	50.5	9.6

3.9 CLEANING PRIOR TO FRONT METALLIZATION

3.9.1 Recommendations

Cleaning wafer surfaces prior to front metallization with HCl and/or HF treatment is recommended to remove excess aluminum particles as well as the oxide on the front surface. This chemical cleaning process was found to be beneficial to cell performance.

3.9.2 Work Performed

Major shunt resistance problems have plagued Spectrolab's cell fabrication for some time. The problem has been traced to the front surface contamination metallization and/or application.

Surface condition prior to front metallization appears to be an important factor in cell performance. It was observed that processed wafers which have had a long period of storage prior to front metallization have lower shunt resistance. This observation led to an experiment in which wafers were prepared in accordance with our baseline process with the exception that the junction was chemically cleaned. These wafers were etched in a 10% solution of hydrofluoric acid for 30 seconds immediately prior to front metallization, and they were not AR coated (Run 6.47.9). The shunt resistance was 3 times as high and the efficiency was 9.6% (= 12.8% with AR coating), 1.3% higher than the wafers not treated with HF. These results indicate that an HF surface treatment prior to front metallization is beneficial. The HF surface treatment is probably removing excess aluminum particles as well as the oxide on the front surface. If this treatment is removing excess aluminum particles, HCl will work just as well.

In run 6.59.9 the surface was treated with HF and/or HCl for a total time of 30, 60 and 120 seconds, Table 3.9-1. The most consistent results were from the group which had an HCl and HF treatment. The group treated with HF gave favorable results also. These results support the hypothesis that aluminum particles remain on the front surface after the back cleaning step. They should be removed with HCl and/or HF.

The original surface cleaning step prior to front metallization, outlined in Table 3.9-2, was intended to remove any AlF_3 and $AlCl_3$ material remaining after the HCl and/or HF surface treatment. In run 6.52.9 wafers were cleaned to various stages of this cleaning step in an attempt to determine the beneficial and detrimental stages and also to reduce the number of stages. The average values for V_{oc}, I_{sc}, I_{load} (500 mV) and shunt resistance are tabulated in Table 3.9-3.

The acetic acid and acetone were beneficial to cell performance. The first hot D.I. water rinse appears detrimental. The alcohol and second hot D.I. water soak may not be necessary.

The cleaning procedure used in our process included both the HCl and HF dip and all seven cleaning steps. This cleaning procedure was not optimized under this contract, and no effort was undertaken to reduce the number of sets in the process.

Table 3.9-1

Run 6.49.9

Acid Treatment After Aluminum Brushing
and Before Printing Front Contact

Treatment	V_{oc}	I_{sc}	I_{500}	R_{sh}
HCl 30 Sec.	598	617	469	12.6
HCl 60 Sec.	602	621	510	18.7
HCl 120 Sec.	606	655	580	33.4
HF 30 Sec.	604	639	551	32.7
HF 60 Sec.	603	626	535	34.7
HF 120 Sec.	605	650	576	49.0
HCl 15 Sec. HF 15 Sec.	606	650	582	49.5
HCl 30 Sec. HF 30 Sec.	604	642	564	22.7
HCl 60 Sec. HF 60 Sec.	606	661	590	44.8

Table 3.9-2

CLEANING STEP

Cleaning Treatment Prior to Printing Front Metal

Influence on Cell Performance		
Beneficial	1)	50% Acetic Acid, 1 minute (RT)
Detrimental	2)	Rinse in hot D.I. water, 30 sec. (75-90%)
Beneficial	3)	Rinse in acetone, 30 sec. (RT)
Beneficial	4)	Soak in acetone, 2 min. (RT)
Unknown	5)	Soak in alcohol, 2 min. (RT)
Unknown	6)	Soak in hot D.I. water, 2 min (75-90^{o}C)
	7)	Rinse in cold D.I. water and spin dry

Table 3.9-3

PERFORMANCE OF CELLS WITH VARIOUS CLEANING TREATMENT PRIOR TO PRINTING FRONT METAL

Run 6.52.9

Stages Included in Cleaning Step	V_{oc}	I_{sc}	I_{500}	R_{sh}
7	603	676	409	7.8
1 + 7	609	694	510	17.6
1 + 2 + 7	606	698	419	10.4
1 + 2 + 3 + 7	608	694	485	13.5
1 + 2 + 3 + 4 + 7	611	702	553	25.6
1 + 2 + 3 + 4 + 5 + 7	610	701	542	26.0
1 + 2 + 3 + 4 + 5 + 6 + 7	610	702	555	24.9

* Defined in Table 3.9-2

3.10 ISOLATION DIELECTRIC

3.10.1 Recommendations

We concluded that the technology of electrical isolation dielectrics is not at a suitable stage of technology readiness for application to isolate wraparound contacts. We recommend that this design feature and the associated process steps be dropped from consideration at the present time. The concept of wraparound contacts is attractive and should be considered for further development.

3.10.2 Work Performed

An isolation dielectric was proposed to prepare a wraparound cell. The dielectric would insulate the back surface and edges at the point of wraparound. This should not be confused with a diffusion masking dielectric which has the purpose of protecting the edge of the cell from diffusion which would cause shunting.

The following specific criteria were established in searching for a suitable printable dielectric:

1) Maturation temperature between 550 and 650°C
2) Thermal expansion coefficient between 3.9 and 4.6 $\times 10^{-6}/^{\circ}C$.
3) Freedom from bubbles and pinholes

Four families of glasses were explored for this application. These included (1) phosphate glasses (Series 4I), (2) germania/tantalum and silica/tantalum glasses (Series 6I), (3) baria/magnesia borosilicate glasses (Series 7I) and (4) modifie titania precipitated glasses (Series 9I). Details of the exploratory

Table 3.10-1

COMPOSITION OF SERIES 6I-2-2
ISOLATION DIELECTRIC GLASS

Oxides	Equivalents	Alcohol Percent
Li_2O	0.605	8.30
ZnO	0.395	5.42
Al_2O_3	0.186	2.55
B_2O_3	4.608	63.25
Ta_2O_5	0.096	1.32
SiO_2	1.395	19.15
P_2O_5	---	---

investigation are described in Appendix C. One of the silica/tantalum glasses designated 6I-2-2 having the composition given in Table 3.10-1 was selected as most promising.

To test the effectiveness and proper sintering procedure, 18 wafers with aluminum contacts were screen printed with 6I-2-2 and dried for 15 minutes at 150°C. The dielectrics were then sintered for 5 to 15 minutes at 600 to 700°C in a tube furnace. Four silver contact areas were brushed on, dried and sintered. The resistance between the aluminum and silver was measured, and the adherence of the dielectric and silver was determined by applying and peeling #600 Scotch tape. Results are reported in Table 3.10-2.

All wafers had sufficiently high resistance, but all wafers except the ones fired for 15 minutes at 700°C had an adherence problem between the dielectric and silver. Closer observation of these two wafers revealed cracking of the dielectric. Further experiments showed that the dielectric over the aluminum cracked on cooling if completely fired due to the mismatch between the expansion coefficient of the aluminum and that of the dielectric. The presence of these cracks resulted in some shunting of the cell, which would undoubtedly worsen with humidity. The cracking could be avoided by underfiring the dielectric, however, this did not turn out to be a viable solution because the incompletely fired dielectric reacted with the silver paste to form an interface with poor adhesion.

Table 3.10-2

PROPERTIES OF CONTACTS TO
6I-2-2 ISOLATION DIELECTRIC

Temp.		5 min.	10 min.	15 min.
600°C	Resistance (10^3 ohm)	∞	∞	∞
	No. of Peeled Contacts	8	8	8
650°C	Resistance (10^3 ohm)	∞	∞	∞
	No. of Peeled Contacts	8	8	8
700°C	Resistance (10^3 ohm)	∞	450	90
	No. of Peeled Contacts	8	3	0.0

3.11 PRINTED FRONT CONTACTS

3.11.1 Recommendations

Printed silver front contacts have been found to be suitable for fabrication of solar cells. The inclusion of this low cost processing technique in the processing sequence is recommended. Initial results with infrared drying and firing of screen printed silver paste contacts indicate possibilities of producing high efficiency, four inch square cells at the rate of 350 per hour. Replacement of the more expensive Ag paste with air firable Ni paste with 20% frit from Thick Film Systems, Inc., was hindered primarily by high series resistance. It is recommended that additional work should be pursued in an effort to reduce the series resistance of screen printed nickel contacts.

3.11.2 Work Performed

The firing of a fritted metallization contact paste on a silicon solar cell surface is accompanied by a number of complex interactions. As an example, the possibility of deleterious contamination in the vicinity of the shallow junction is always a matter of concern. The assessment of this possibility is complicated by such considerations as whether any paste borne contaminants migrate into the silicon, given the time and temperature conditions available.

On the basis of our experience with fritted paste contact metallization we believe that while likely sources of problems such as contamination and contact resistance may be significant, the situation is usually dominated by oxidative attack of the silicon by the frit. Contact adherence of a paste formulation is primarily achieved by oxide formation and solution processes at the

silicon surfaces. Thus the firing step is commonly carried out in an oxidizing atmosphere. The SiO_2 layer which acts as a rate limiting membrane on the silicon surface is unable to perform this function under the metallization paste because it is dissolved by the frit. Oxidation and solution can proceed rapidly, with shunting of the junction or even complete shorting, depending on the depth of the junction and extent of the attack.

Preliminary screening tests have been run on a number of commercially available silver metallization pastes. These tests consisted of fabricating solar cells using the firing time and temperature matrix given in Table 3.11-1. The firing procedure consisted of rapidly pushing a light quartz rail boat on which the waters were horizontally mounted, into the heated zone of a tube furnace. A shallower than normal junction depth (.18 - .2 μm) was used in order to increase sensitivity of the test to the oxidation attack described above. This also tended to make the results somewhat more erratic. Paste firing was carried out in a flowing gas atmosphere consisting of 1500 cc/min. N_2 and 1500 cc/min. O_2 to further increase the sensitivity.

Output curves obtained on cells fabricated with two different pastes with 650°C firing temperatures are shown in Figures 3.11-A and 3.11-B. The development of these curve sequences can be understood in terms of the oxidative attack outlined above. For very short firing times there is a very high contact resistance giving rise to a high cell series resistance. With increasing firing time the contact resistance will decrease as shown schematically in Figure 3.11-C. However, with longer firing times the cell shunt resistance, which is high for short firing times, will begin to decrease. At the time at which degradation of shunt resistance becomes significant for a given frit composition, the firing temperature will depend on the junction depth. Thus, the

Table 3.11-1

TIME-TEMPERATURE MATRIX
USED FOR PASTE EVALUATION

	650°C	700°C	750°C
15 Sec.	void	X	X
30 Sec.	X	X	X
45 Sec.	X	X	X
60 Sec.	X	X	X
75 Sec.	void	X	X
90 Sec.	X	X	X
120 Sec.	X	void	void
180 Sec.	X	void	void

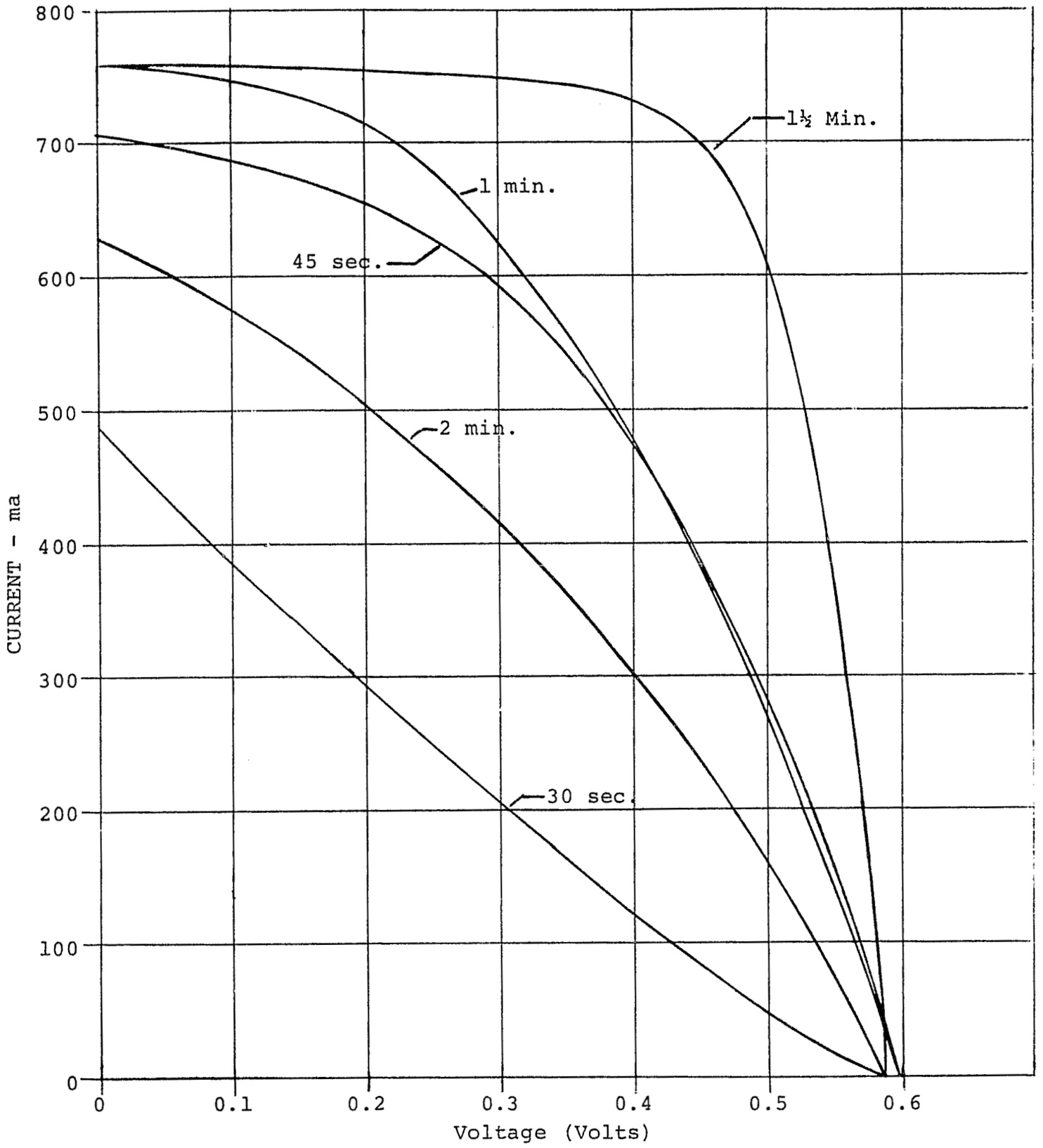

Figure 3.11-A EFFECT OF FIRING TIME AT 650°C ON CURVE SHAPE, PASTE A

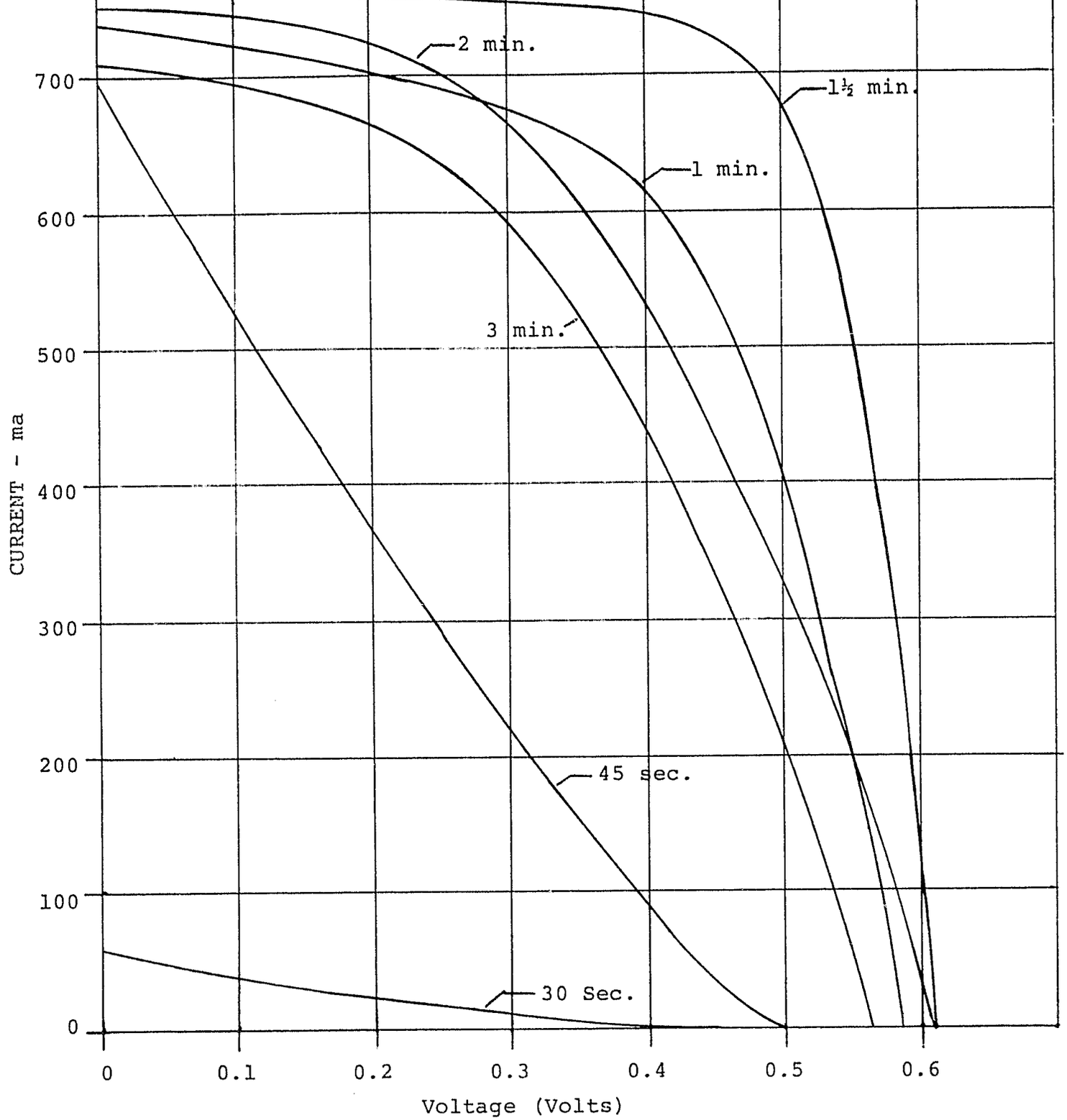

Figure 3.11-B EFFECT OF FIRING TIME AT 650°C ON CURVE SHAPE, PASTE B

Figure 3.11-C

EFFECT OF PASTE FIRING TIME ON
ON SOLAR CELL MODEL PARAMETERS
SCHEMATIC

SPECTROLAB
a subsidiary of Hughes Aircraft Co.

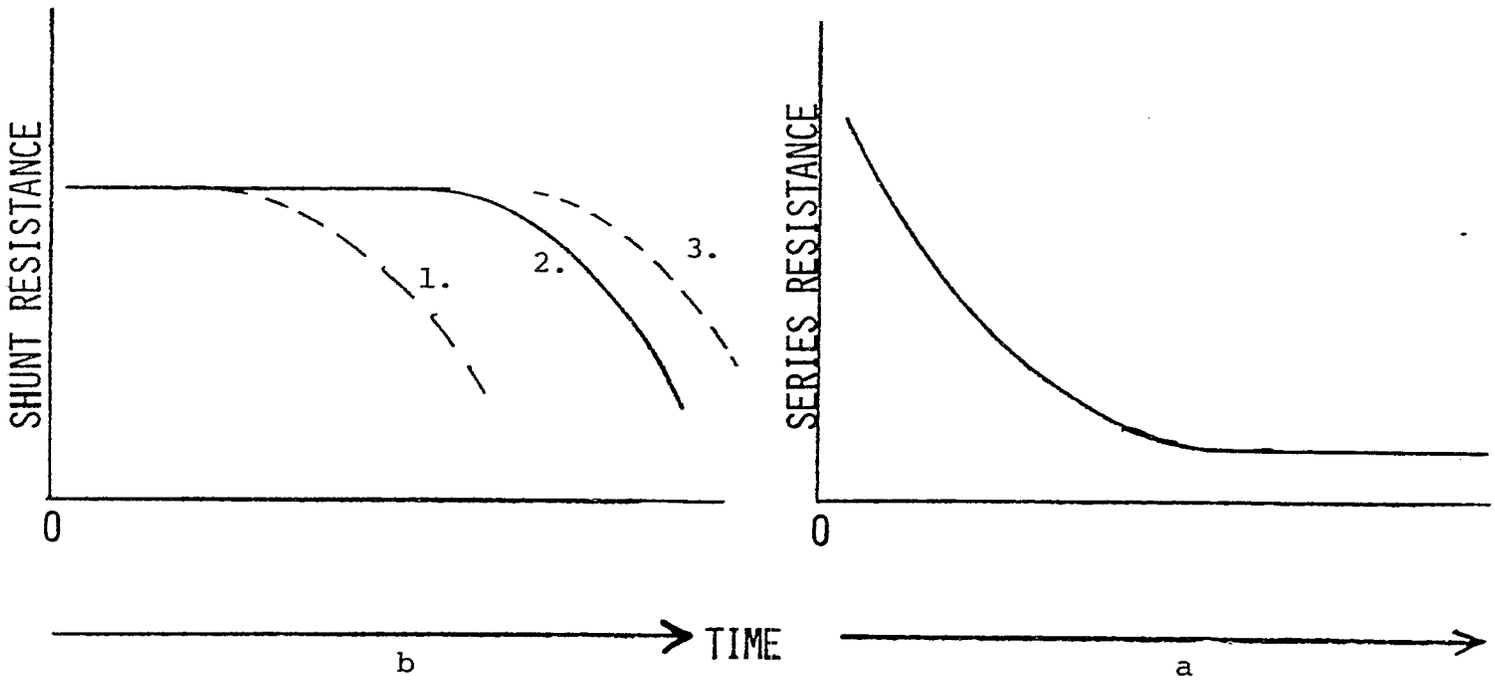

curves in Figure 3.11-C(b) represent successively deeper junction in the progression from 1 through 3. The expected consequences of these resistance effects on the I_{sc}, V_{oc} and fill factor parameters of the output curves are shown schematically in Figure 3.11-D.

Guided by the hypothesis of oxidative attack of the silicon accompanied by solution of the SiO_2 in the frit during the firing process, the effects of varying the amount of frit in the paste and additions of N type diffusion sources were investigated. In general, both of these led to improved performance.

The optimum frit content is usually less than that normally present in commercial pastes and appears to be about 5%. The effect of reducing the frit content of Cermalloy 4450 silver paste by the addition of Thick Film Systems A-250 fritless silver paste is shown in Figure 3.11-E.

Emulsitone 233 (Sb) and Transene N-Diffusol have been found to be useful additives in the amounts of about 2% by weight. The effect of adding Emulsitone 233 (Sb) to Electro-Science Laboratories 590 silver paste is shown in Figure 3.11-F. These diffusion source additives frequently have the effect of reducing the sensitivity of the time-temperature firing cycle.

In order to further investigate the silver paste-silicon interaction, solar cells were produced with four silver pastes. The silver in the paste does not melt during the sintering treatment, but the glass frit does melt. The major interaction with the silicon will be with the frit, not the silver. In order to investigate this interaction, the silver was removed, after measurement of I-V curves, with a dilute solution of hydrogen peroxide.

Figure 3.11-D

EFFECT OF PASTE FIRING TIME ON I-E CURVE
SCHEMATIC

SPECTROLAB
a subsidiary of Hughes Aircraft Co.

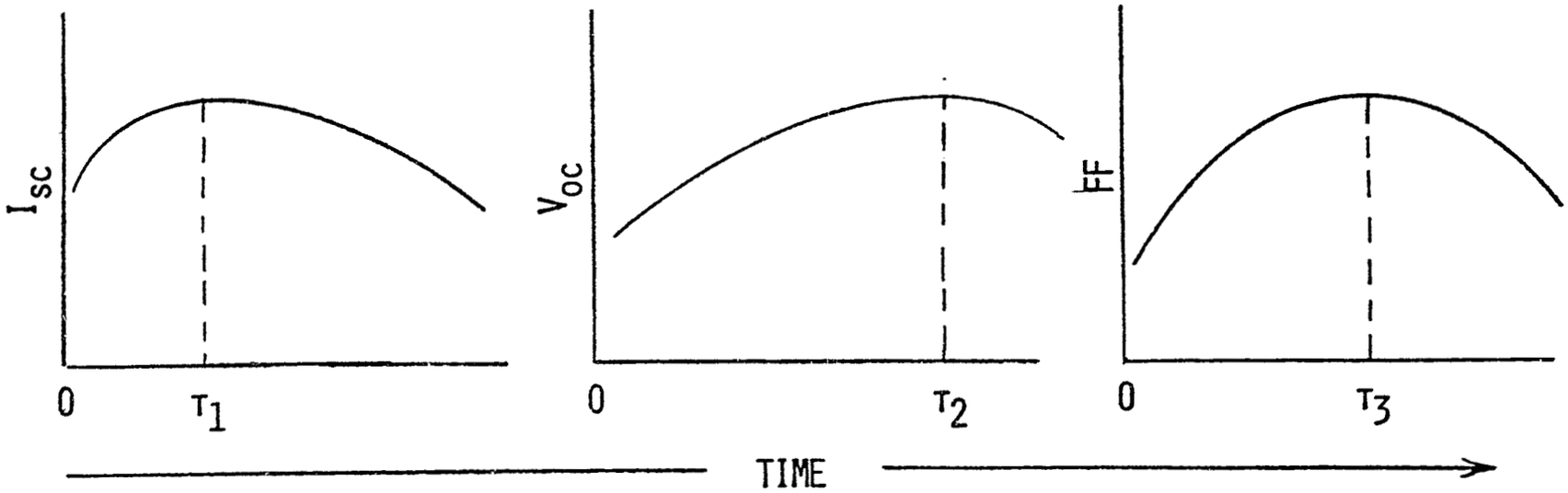

Figure 3.11-E

IMPROVEMENT OF CURVE SHAPE
BY REDUCING FRIT CONTENT OF PASTE

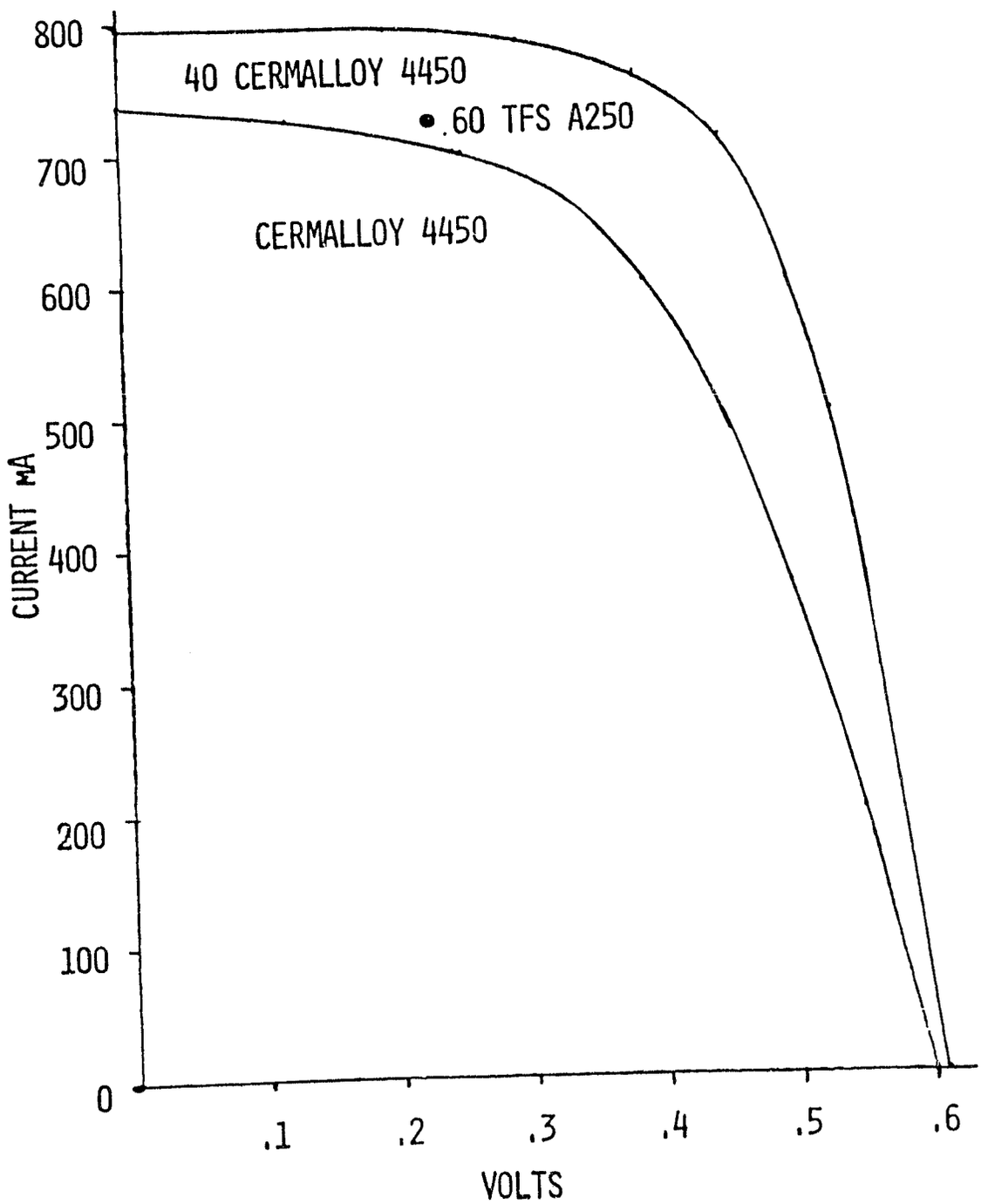

Figure 3.11-F

EFFECT OF N-TYPE DIFFUSION SOURCE
ADDITION TO COMMERCIAL SILVER PASTE ON
SOLAR CELL PERFORMANCE

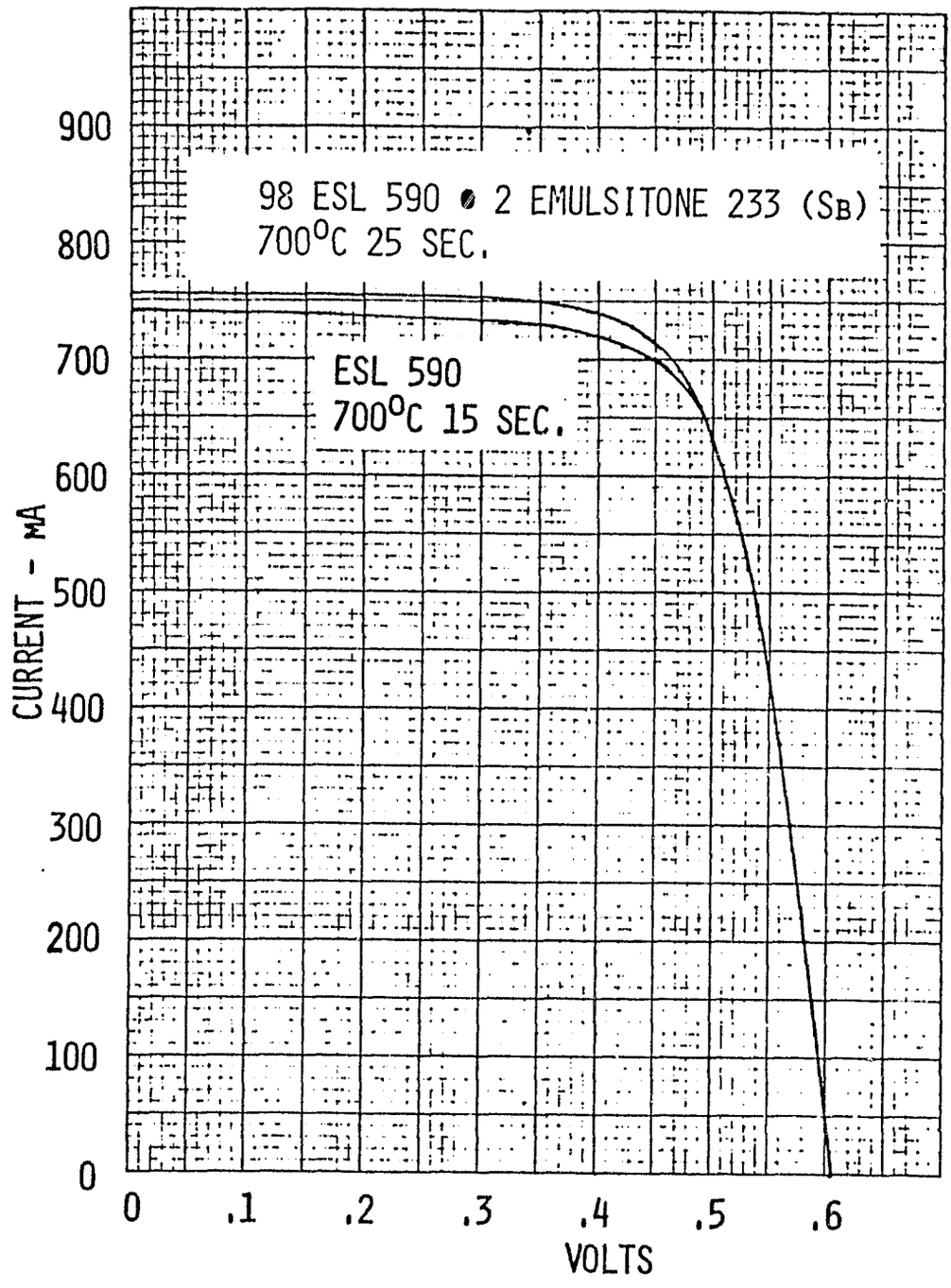

Fluorescent analysis with a SEM revealed the basic composition of the glass frit that remained after etching. The elements and intensities of the fluorescent radiation observed in the four types of paste are given in Table 3.11-2; light elements (boron and lithium) which might be in these pastes cannot be detected by this method. I-V curves for best cells produced from these pastes are shown in Figures 3.11-G through 3.11-J. The metallization firing conditions and paste identification are given on the curves. The pastes having a larger percentage of aluminum appear to have more shunting. The pastes that did not have any aluminum gave the best I-V curve but did not have the adherence necessary for good metallization.

SEM micrographs of the glass frit on the silicon's surface appear to be very similar for all pastes. The glass frit flows during the sintering process forming structural networks across the texture surface. The DuPont 7095 conductive silver paste flows very well at 700^{o}C and forms a continuous layer of frit under the silver grid contacts (Figure 3.11-K). There does not appear to be any degradation of the textured surface. The Electroscience 590 and Electroscience 590 with 2% Emulsitone #733 (Sb dopant) does not flow as well as the DuPont 7095. The frit forms networks across pyramids with areas free of frit. The pyramids appear to have spots growing on their sides, possibly frit (Figures 3.11-L and 3.11-M). There does not appear to be any degradation of the textured surface. The EMCA Ag 92 appears to be the lowest melting frit forming the heaviest layer of frit on the textured surface (Figure 3.11-N). The frit appears to have flowed beyond the area of the silver grid contact and coated the adjacent textured surface with a thin layer of frit. The frit does not appear to have any detrimental effect on the silicon.

Table 3.11-2

RELATIVE FLUORESCENCE INTENSITIES OF ELEMENTS PRESENT IN FRITS OF SILVER CONDUCTIVE PASTES

Elements and Emission Lines	Dupont 7095	Electroscience Type 590	Electroscience 590 + 2% Emulsitone 733	EMCA Ag 92
Pb M_{α}(2)	10	10	10	10
Al K_{α}	43	19	9	-0-
P K_{α}	-0-	41	41	-0-
K K_{α}	-0-	55	34	-0-
Si K_{α}(2)	47	95	77	111
Na K_{α}(2)	-0-	5	2	5
Ag L_{β}	20	22	20	22
Sb L_{α}	-0-	-0-	-0-	-0-

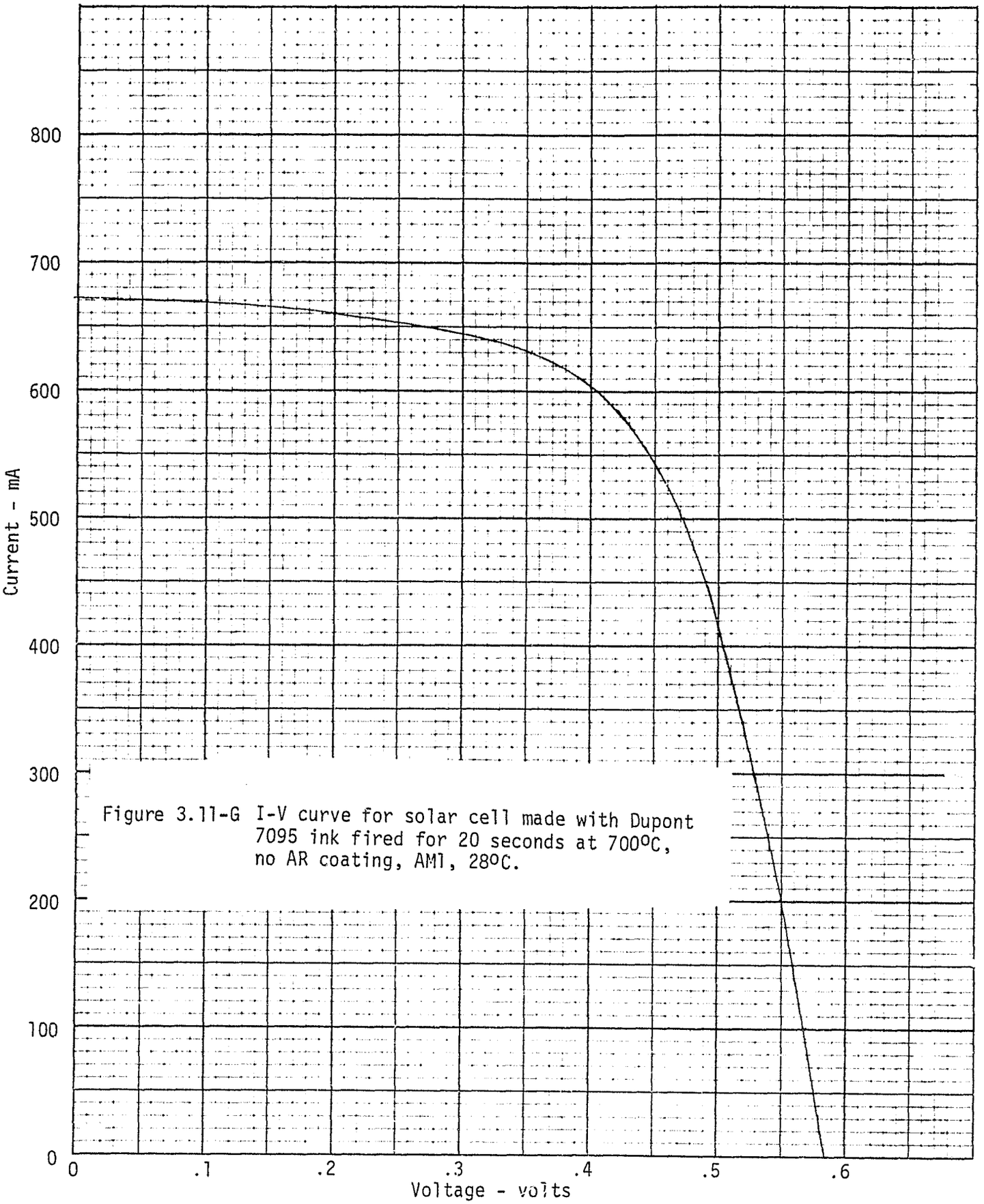

Figure 3.11-G I-V curve for solar cell made with Dupont 7095 ink fired for 20 seconds at 700°C, no AR coating, AM1, 28°C.

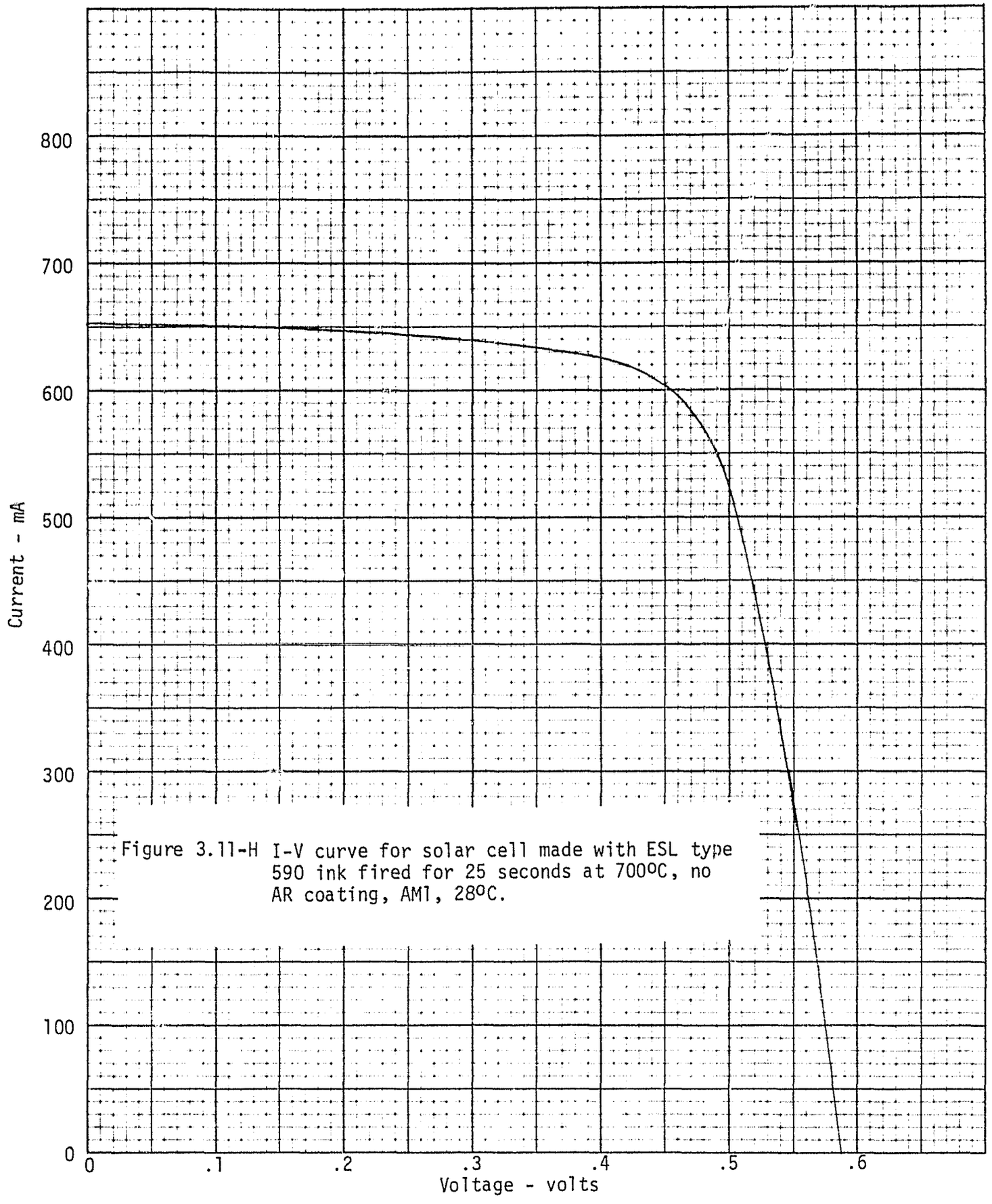

Figure 3.11-H I-V curve for solar cell made with ESL type 590 ink fired for 25 seconds at 700°C, no AR coating, AM1, 28°C.

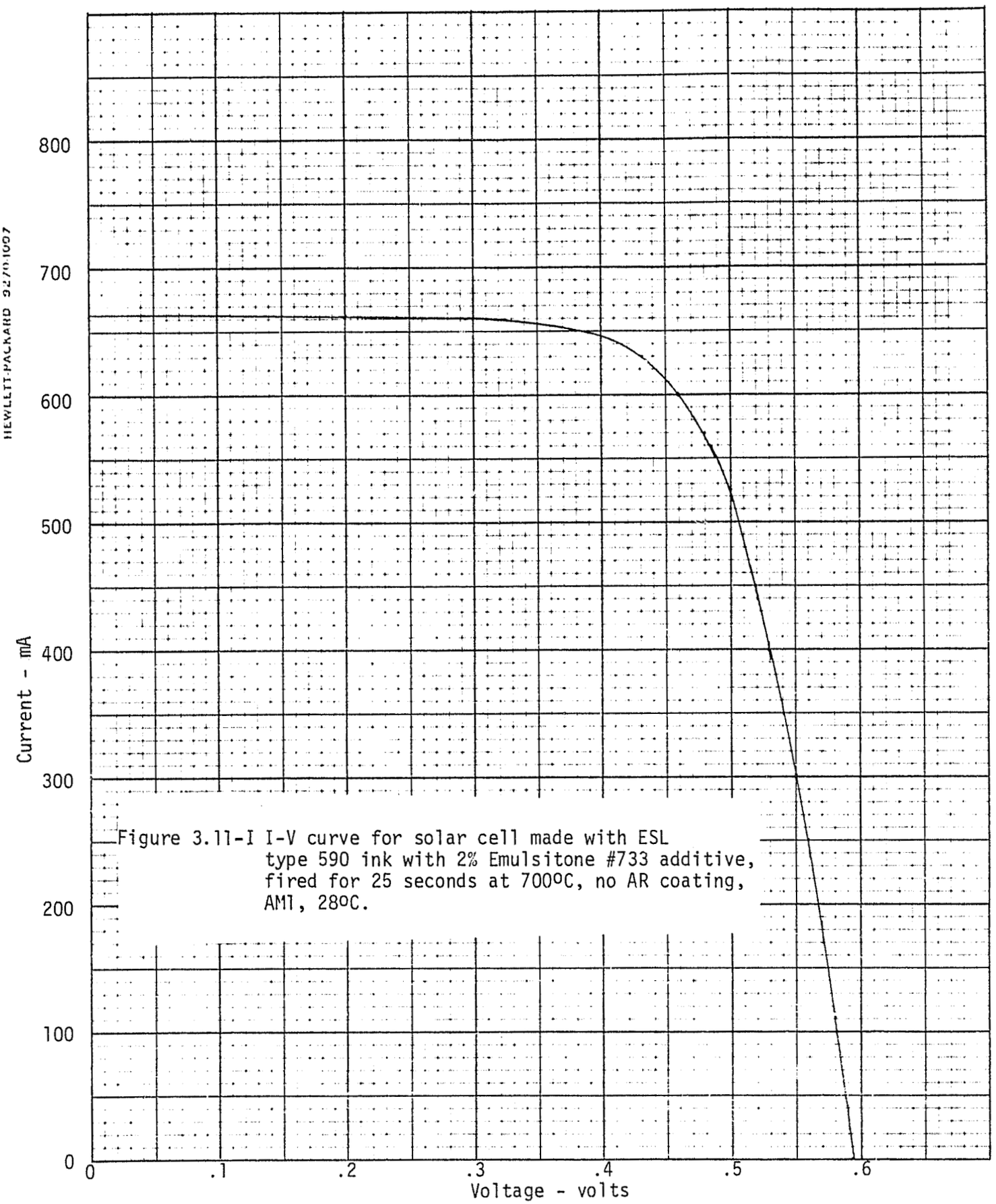

Figure 3.11-I I-V curve for solar cell made with ESL type 590 ink with 2% Emulsitone #733 additive, fired for 25 seconds at 700°C, no AR coating, AM1, 28°C.

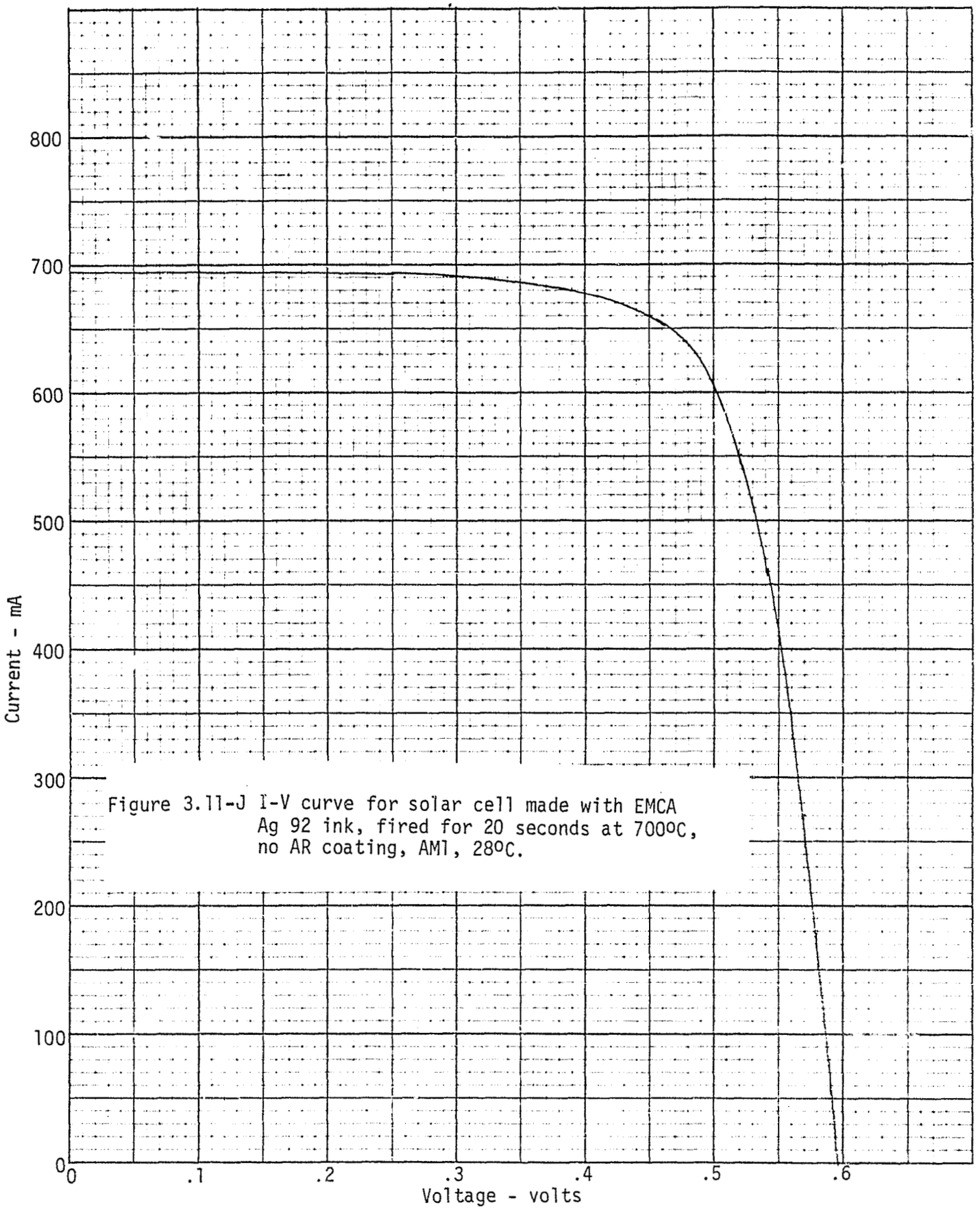

Figure 3.11-J I-V curve for solar cell made with EMCA Ag 92 ink, fired for 20 seconds at 700°C, no AR coating, AM1, 28°C.

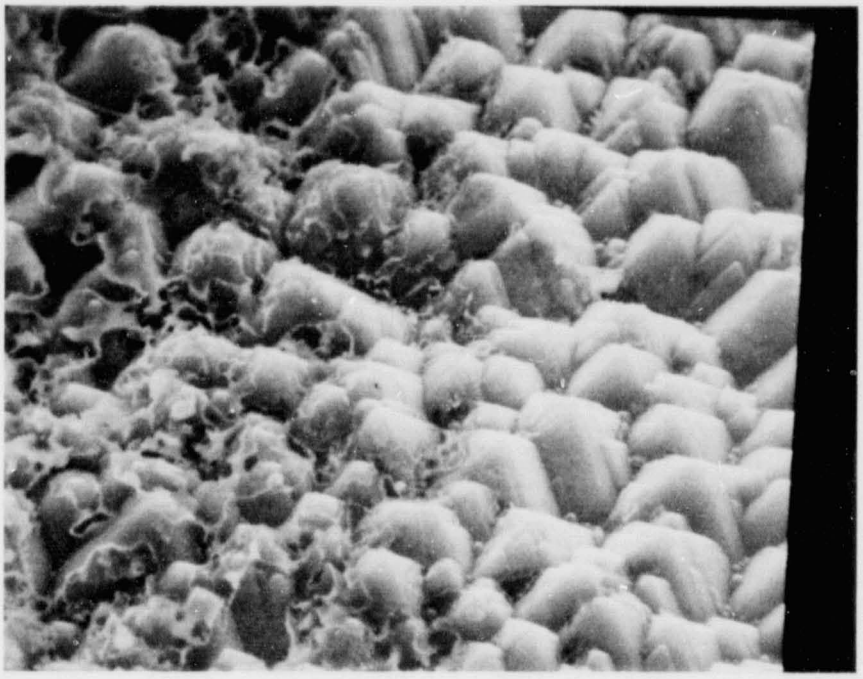

Figure 3.11-Ka 2000X

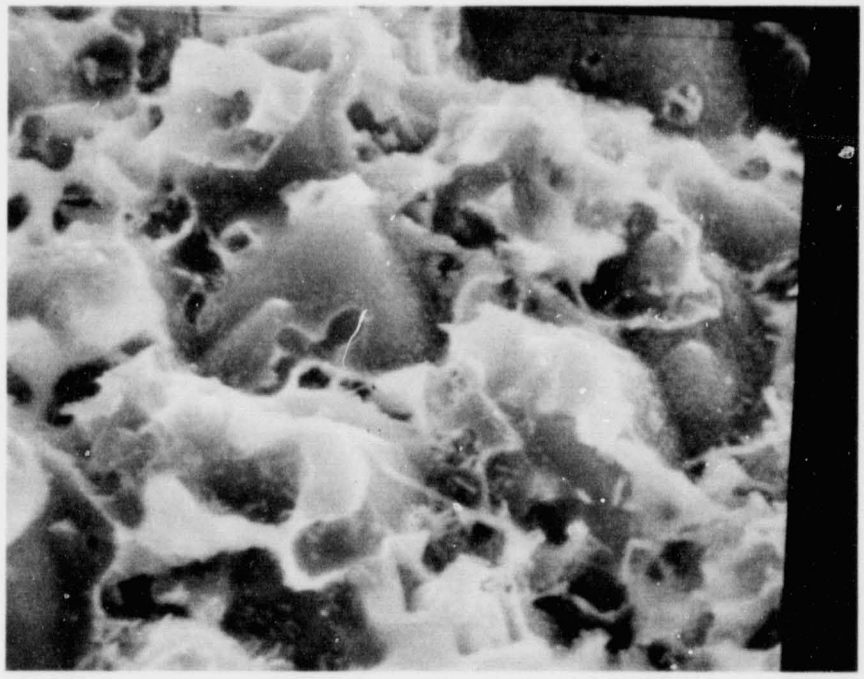

Figure 3.11-Kb 5000X

Figure 3.11-K SEM of silver metallization contract area after removal of silver by dilute hydrogen peroxide. Dupont 7095 silver ink.

Figure 3.11-La 2000X

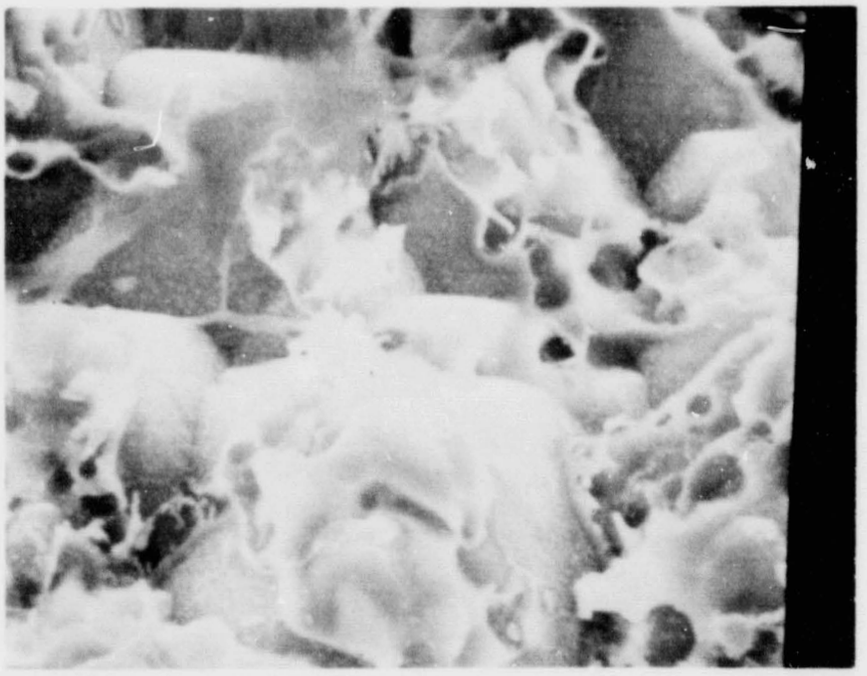

Figure 3.11-Lb 5000X

Figure 3.11-L SEM of silver metallization contact area after removal of silver by dilute hydrogen peroxide. Electroscience 590 silver ink.

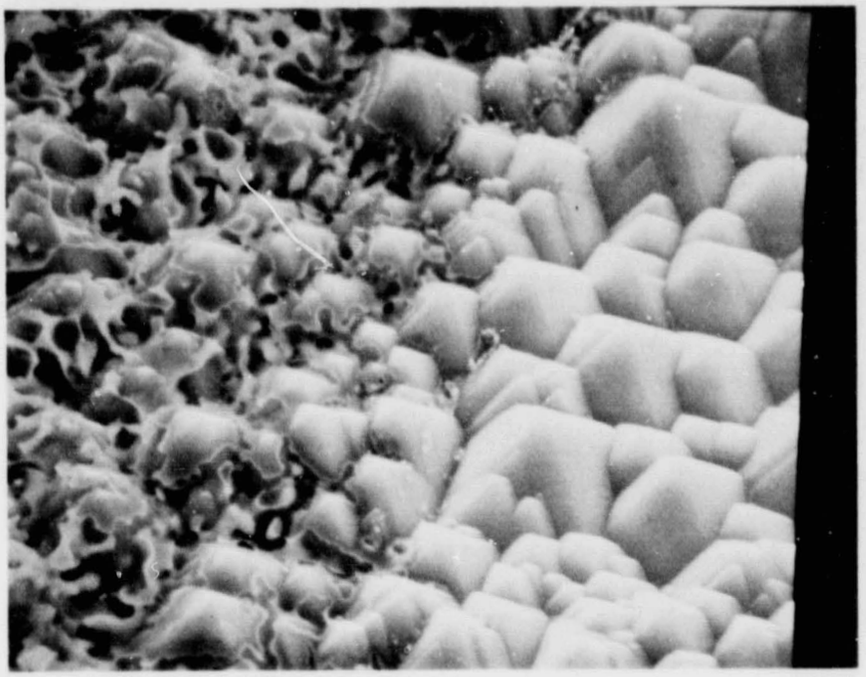

Figure 3.11-Ma 2000X

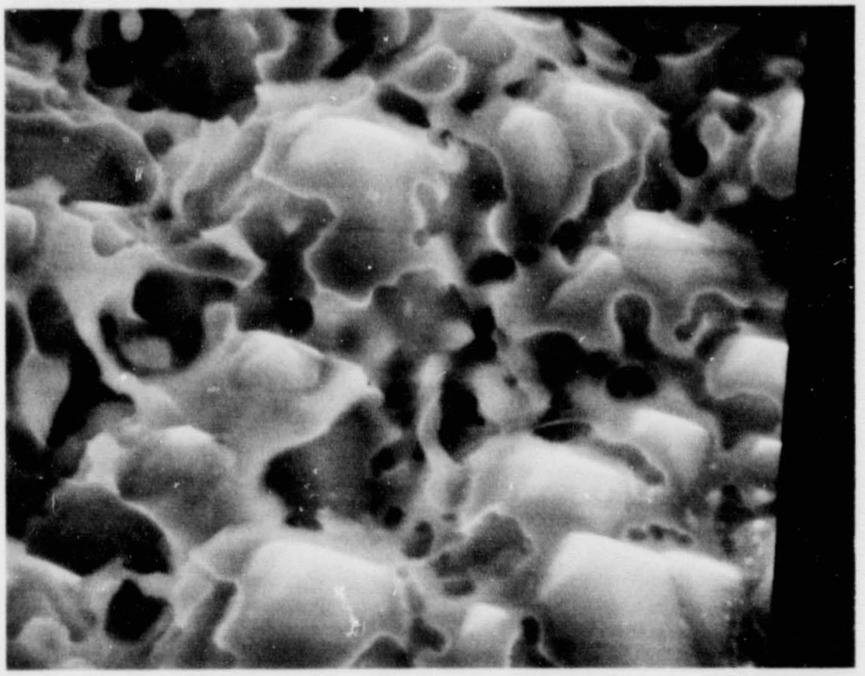

Figure 3.11-Mb 5000X

Figure 3.11-M SEM of silver metallization contact area after removal of silver by dilute hydrogen peroxide. Electroscience 590 silver ink + 2% Emulsitone 733 (Ag).

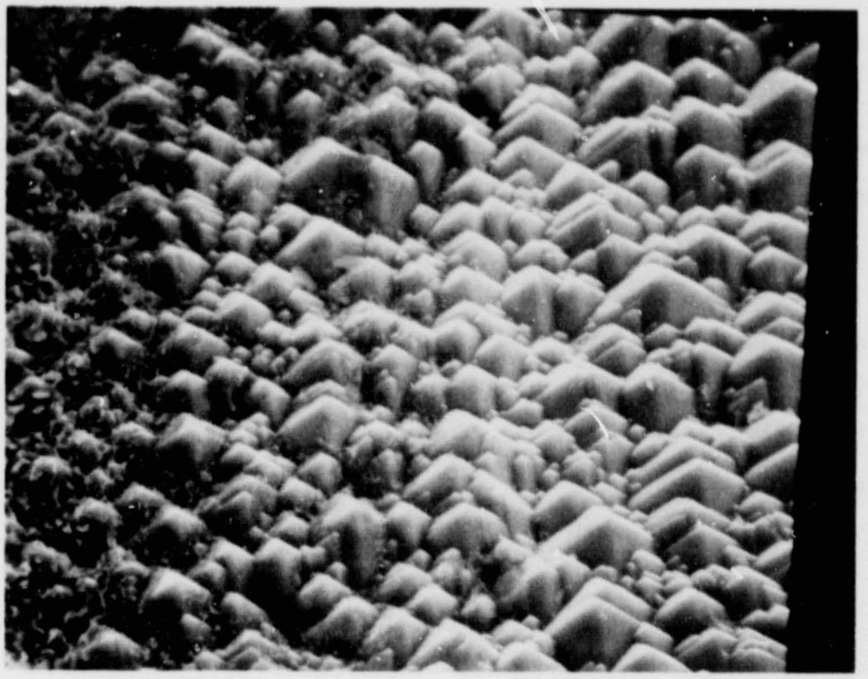

A B C

Figure 3.11-Na 2000X

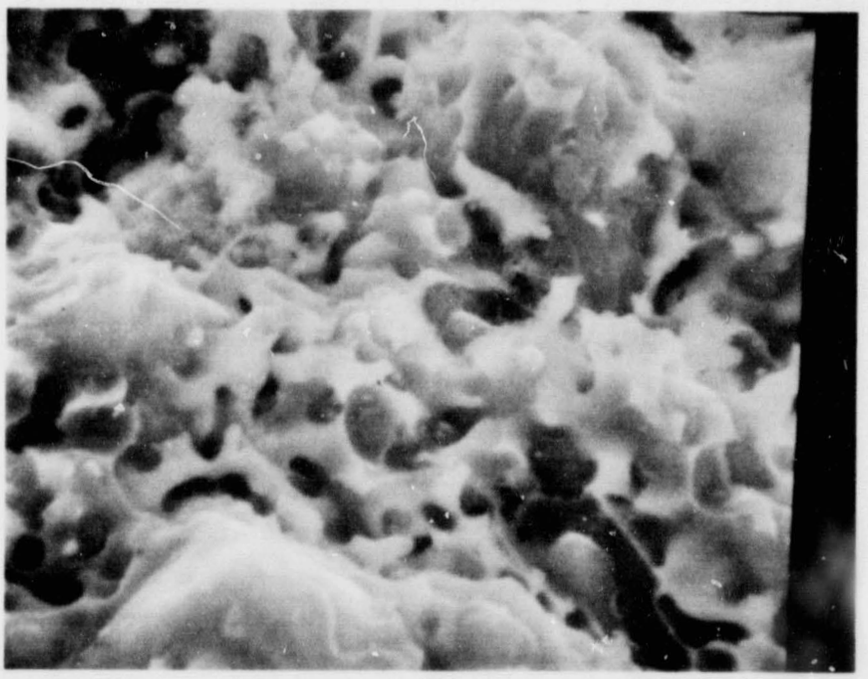

Figure 3.11-Nb 5000X

Figure 3.11-N SEM of silver metallization contact area after removal of silver by dilute hydrogen peroxide. EMCA Ag 92 silver ink.

If one compares the I-V curves for the various commercial fritted silver pastes tested and the fluorescent analysis of these pastes, it appears that aluminum is a detrimental element. To determine whether aluminum-free frits produce high efficiency solar cells, three types of low melting frits were prepared (Table 3.11-3). Two percent by weight of these frits was added to a fritless silver paste. Figure 3.11-O shows characteristic curves for cells made with paste based on Frit #2. All of these pastes produced very good cells and passed a tape pull test with Scotch Brand 600 tape; but when these pastes were soldered, the interconnect absorbed the silver on the contact, and the interconnections pulled off at a low load of 200 grams.

These frits developed at Spectrolab appear to satisfy the requirements for high efficiency solar cells, but they lack adherence after soldering. Additional development of these frits needs to be conducted in order to produce a silver paste that is adherent after soldering and produces a high efficiency solar cell. The commercial silver pastes listed in Table 3.11-4 were evaluated with respect to output of cells fabricated with various firing cycles. Those pastes indicated by asterisks are those giving better results. The Thick Film Systems A256 with the addition of 2% N-Diffusol was selected as the baseline material for subsequent work. The A256 designation was later changed to 3347 by Thick Film Systems.

The series resistance of the current cell design fabricated with screen printed front metal was evaluated. The front collector pattern was found to be a major contributor to the series resistance. The measured series resistance was in the range of 80 to 100 mΩ. The series resistance was calculated to be 90 mΩ as summarized in Table 3.11-5. The detailed series resistance

Table 3.11-3

COMPOSITION OF ALUMINUM-FREE GLASS FRITS

	Weight Percent of Oxides			
Frit No.	PbO	B_2O_3	P_2O_5	SiO_2
1.	93.81	4.65	--	1.54
2.	91.97	4.36	1.46	2.20
3.	95.56	4.44	2.68	--

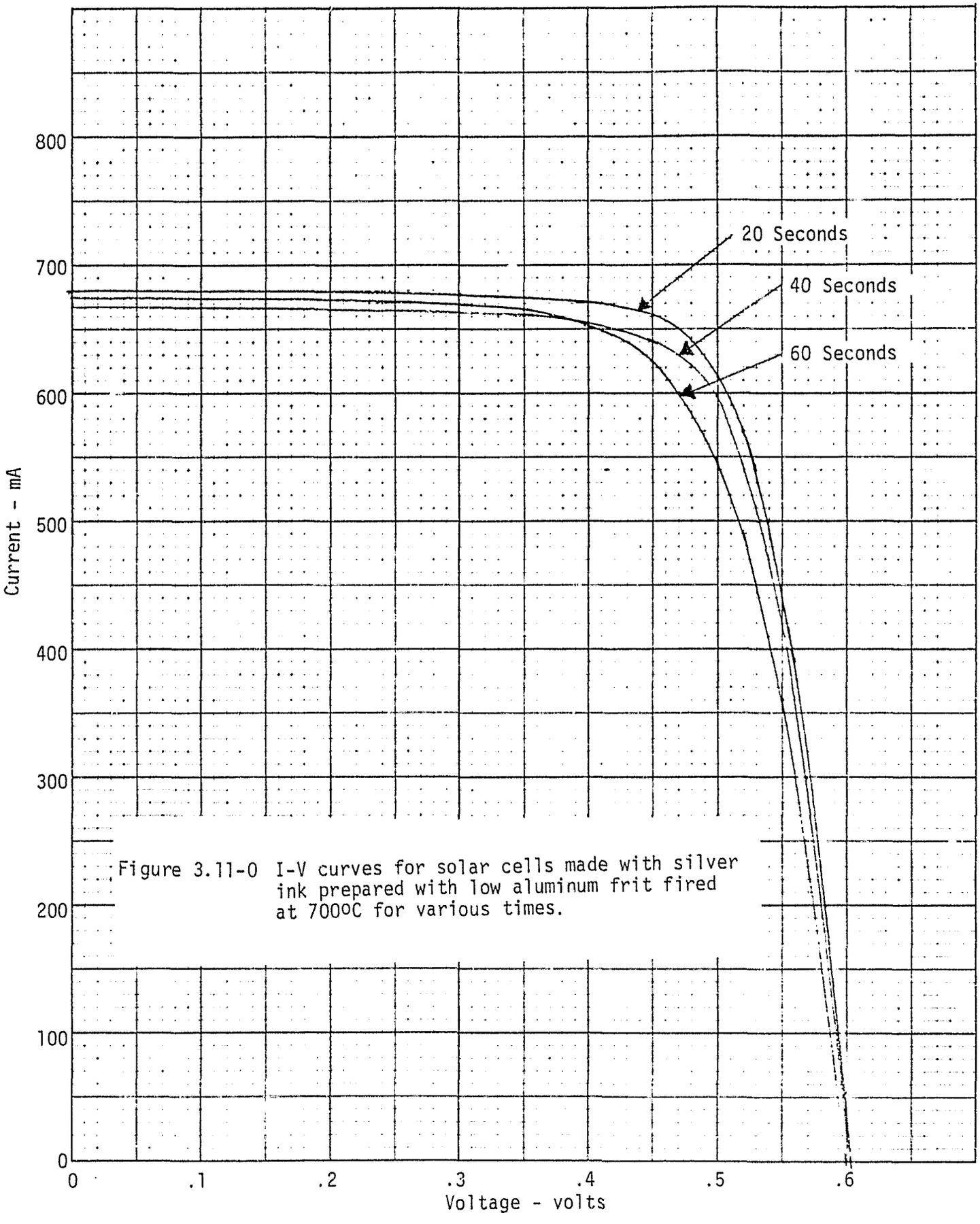

Figure 3.11-0 I-V curves for solar cells made with silver ink prepared with low aluminum frit fired at 700°C for various times.

Table 3.11-4

COMMERCIAL AG PASTES
EVALUATED FOR USE AS COLLECTOR METALLIZATION

AVX	6080
Cermaloy	4450
DuPont	7095*
	7713
	8032
Electromaterials	AG-6058-1
	AG-92*
Electroscience Lab	590*
Englehard	E-439-A/B*/C
	A2735
	A2921 (Mod. 025)*
	A3233
Methode Dev. Co.	3521
	3522
Plessey	L15-1260-T1
Thick Film Systems	A250 (Fritless)
	A256* (3347)
	A268
	A3330
Transene	100
	200

*Pastes giving better results as received from vendor.

Table 3.11-5

Calculated Contributions to Cell
Series Resistance

Component	Resistance
Base Region	3.4 mΩ
Diffused Layer	14.9 mΩ
Gridlines	7.0 mΩ
Collector Bar	64.8 mΩ
Total	90.1 mΩ

Table 3.11-6

EXPERIMENT 6.51.9

AVERAGE VALUES

Effect of Solder Coating Ohmic Collector Bar
on Cell Performance

BEFORE SOLDER ON OHMIC			AFTER SOLDER ON OHMIC		
V_{oc} mV	I_{sc} mA	I_{500} mA	V_{oc} mV	I_{sc} mA	I_{500} mA
604	702	507	604	706	565
(599-611)	(688-719)	(339-590)	(600-610)	(669-727)	(388-638)

calculation is given in Appendix 1. The major contribution to the series resistance is that of the ohmic collector bar. In order to verify these results, the center ohmic collector of a cell was coated with solder. The change in the I-V characteristics (Figure 3.11-P) indicated a 25 mΩ reduction in series resistance. Experiment 6.51.9 (Table 3.11-6) further verified these results. It was thus concluded that the front ohmic collector could be redesigned to be more effective.

As a part of this evaluation, the conductivity of the front contact metal was also examined. Test patterns were screened onto 50 ohm-cm 2" silicon wafers to provide suitable lines on which to perform measurements (see Figure 3.11-Q). The effective line length of the pattern was 72.90 cm and the width and height varied with the type of paste used. Widths were measured by Talysurf and optical methods. The resistance of the printed contact line was measured with a General Radio Digi-Bridge meter which has a resolution of 1 milli-ohm. The resistance of each half of the pattern was measured in addition to the entire pattern to guard against isolated gaps or pinched down regions. Measurements of all lines in one pattern revealed a maximum of 4% variation in fourteen 1.95 cm long lines which is indicative of uniformity within a pattern.

Three different silver conductive thick film pastes were tested including the previously used Thick Film Systems 3347 + 2% Transene N-Diffusol. The resistance, half pattern resistance, and line width are measured values which were used to calculate the resistivity and line thickness. These values are presented in Table 3.11-7. The cross-sectional area necessary for the resistivity calculation was determined by gravimetric integration of the Talysurf curves for each paste. The effective line thickness was then calculated from the line length, based on resistivity.

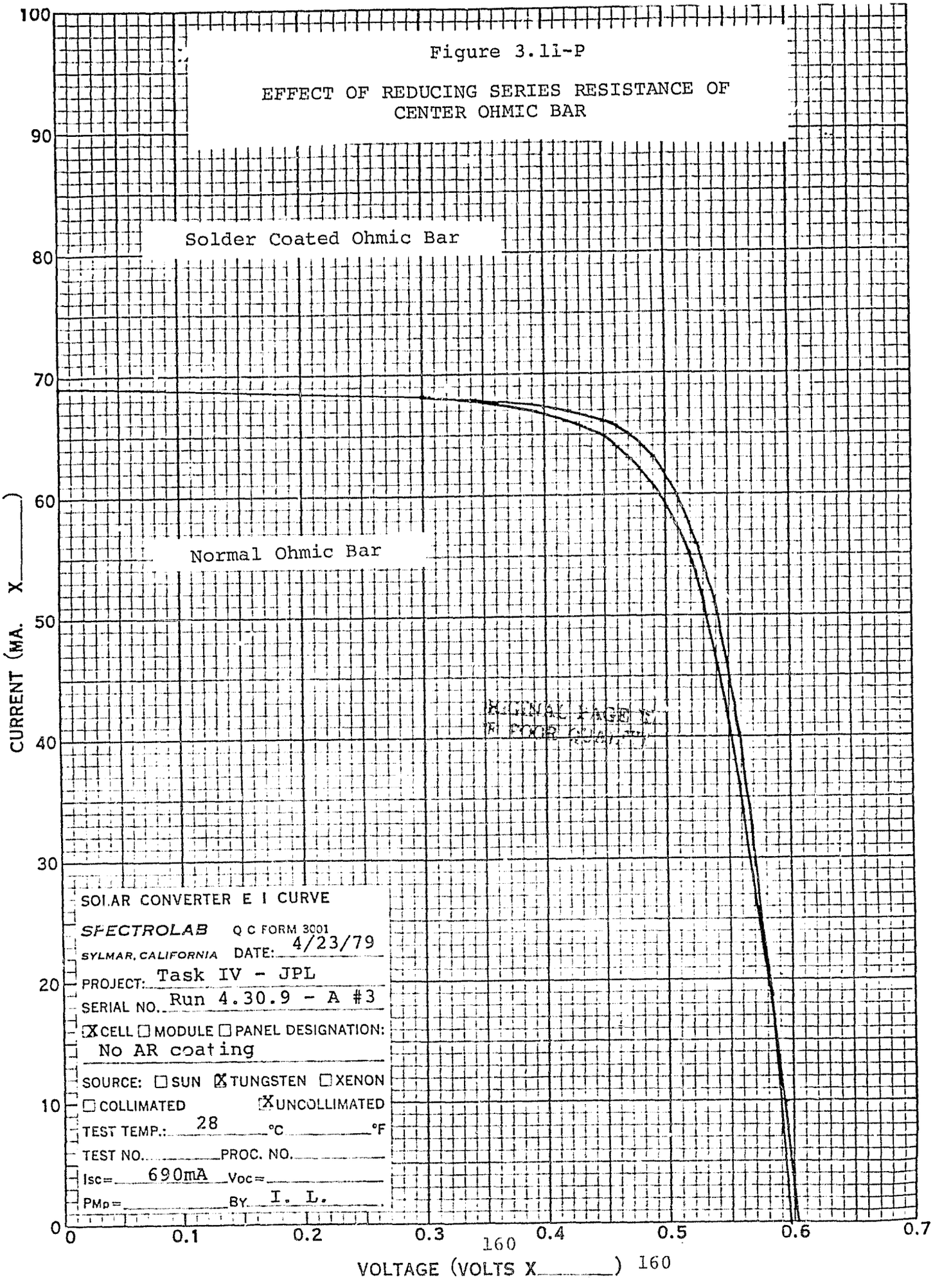
Figure 3.11-P
EFFECT OF REDUCING SERIES RESISTANCE OF CENTER OHMIC BAR
Solder Coated Ohmic Bar
Normal Ohmic Bar
ORIGINAL PAGE IS
OF POOR QUALITY
SOLAR CONVERTER E I CURVE
SPECTROLAB Q C FORM 3001
SYLMAR, CALIFORNIA DATE: 4/23/79
PROJECT: Task IV - JPL
SERIAL NO.: Run 4.30.9 - A #3
X CELL ☐ MODULE ☐ PANEL DESIGNATION:
No AR coating
SOURCE: ☐ SUN X TUNGSTEN ☐ XENON
☐ COLLIMATED X UNCOLLIMATED
TEST TEMP.: 28 °C °F
TEST NO. PROC. NO.
Isc= 690mA Voc=
PMp= BY I. L.
CURRENT (MA. X)
VOLTAGE (VOLTS X) 160
100
90
80
70
60
50
40
30
20
10
0
0
0.1
0.2
0.3
0.4
0.5
0.6
0.7
160

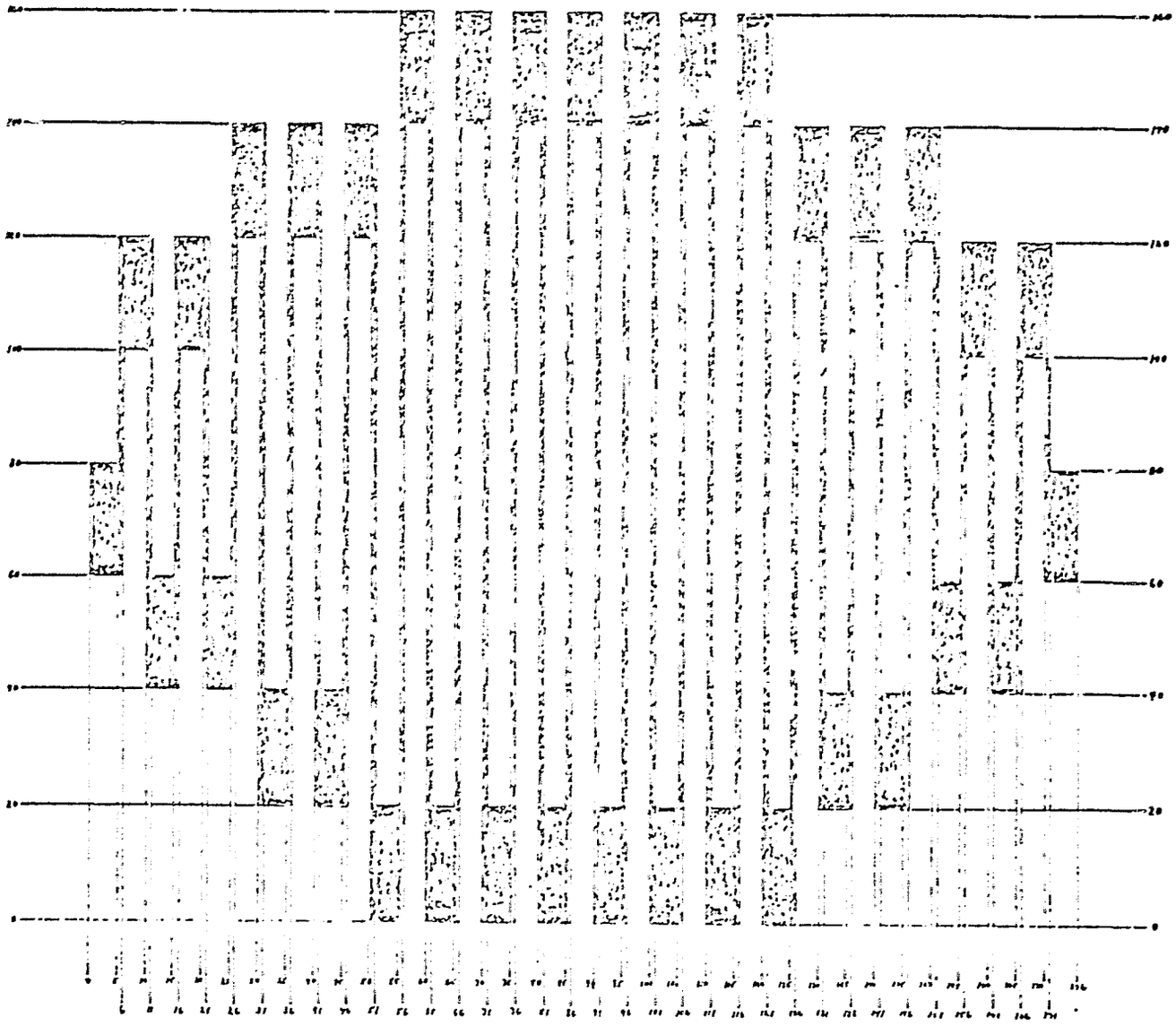

Spectrolab, Inc.

X-Y Diagram

Test Pattern TP-1

Scale: 1 Div. =
0.25 mm

JWT
8-28-75

Figure 3.11-Q

Test Pattern for Determining Resistivity of Contact Metallization

Table 3.11-7

RESISTIVITY OF COMMERCIAL SILVER PASTES

Thick Film Paste	Resistance		Line Width (mil)	Resistivity ($\mu\Omega$-cm)	Cross-Sectional Area (mil^2)	Line Thickness (mil)	$\frac{\rho}{\rho_{Ag}}$ $\rho_{Ag}=1.6\,\mu\Omega$-cm
	Full Pattern (Ω)	Half Pattern (Ω)					
Dupont	9.48	4.83/4.77	14.0	2.90	3.46	.25	1.8
Electro Science Lab Ag590	7.935	4.00/4.06	10.1	5.07	7.23	.71	3.2
Thick Film Systems 3347+2% N-Diffusol							
Sample 1	5.96	3.03/3.03	10.0	4.20	7.96	.80	2.6
Sample 2	7.48	3.86/3.73	10.0	4.62	6.97	.70	2.9

All samples fired at 700°C for 40 seconds in 20% O_2, 80% N_2

The resistance of the TFS-3347 + 2% N-Diffusol paste was the lowest, even though the resistivity (ρ_{TFS} = 2.75ρ bulk silver) is higher than the DuPont 7095. The DuPont paste had the lowest resistivity (ρDuPont = 1.8ρ bulk silver), however, less material was deposited and it flowed more, resulting in thinner, wider gridlines of smaller cross-sectional area. The ESL AG590 paste had a slightly higher resistance and resistivity than the TFS paste.

To reduce the series resistance, a screen with a 2 mil emulsion was procured and evaluated. This screen indeed reduced the series resistance from about 90 to 60 milli-ohms for the 1 and 2 mil emulsion screen, respectively. However, the screen with 2 mil emulsion has a greater tendency to clog the 6 mil gridlines. This results in broken printed gridlines and higher series resistance. An improved method for producing cells with low series resistance would be to apply the gridlines and center ohmic collector in two separate operations, with the introduction of a cost penalty for the additional screen printing operation.

The Radiation Technology Infrared Furnace was investigated for possible use in the cell process sequence discussed earlier. The IR furnace consists of four controlled zones of IR lamps. Cells that pass through the furnace are carried under the lamps on a nine inch wide metal wire belt with a variable speed between ten and seventy inches/min. The first two zones were designed for drying and paste contact at a temperature between 0 and 400^{o}C. The combined length of these two zones is thirty-six inches. The second two zones were designed for the firing of either the aluminum P^{+} contact or the printed silver front contact at a temperature between 300 and 1100^{o}C. The combined length of these two zones is twenty-four inches.

In order to test the performance of the furnace, wafers were processed in accordance with our standard process sequence, except chat the wafers were laser scribed prior to front surface metallization. In our initial experiment (8.61.9) with the IR furnace, the wafers were dried in an oven at 125°C prior to IR firing. The front contacts were fired in the IR furnace with IR zones 3 and 4 set at 700°C. The belt speed was varied between 20 and 50 inches/min. The optimum belt speed was about 40 in./min., Table 3.11-8. The control wafers fired in a tube furnace were processed in parallel with the IR fired wafers, Table 3.11-9. These wafers were fired for 30 seconds at 700°C and had a higher output than the IR wafers processed on the 50 in./min. belt. The control wafers were compared with the 50 in./min. belt, because throughput is a major consideration. The IR fired wafer with a 50 in./min. belt speed remained in the 24 in. firing bank for 29 seconds and had a very low output. The 40 in./min. belt speed had a much better output. This indicated that the 700°C firing bank was too low for proper silver firing and throughput.

A second experiment (9.65.9) was run with the belt speed held constant at 50 in./min. (29 sec. in the firing zone) and the temperature of the last two firing zones was varied. The third zone was varied between 750 and 800°C, and the fourth zone was varied between 725 and 800°C. All of the wafers were dried in an oven at 125°C. Nine additional wafers were fired under these conditions as shown in Table 3.11-10.

In a third experiment, an attempt was made to simulate the oven drying by turning on the first two zones. The wafers were dried in zones 1 and 2 and were fired in zones 3 and 4. A drying temperature of 260°C and 410°C in zones 1 and 2, respectively,

Table 3.11-8

IR Firing of Silver Front Contacts
Constant Temperature and Variable Belt Speed
AR Coated 2.12x2.12 inch squares
Run 8.61.9

Zone Settings: Zone 1, Zone 2, Zone 3, Zone 4: 0, 0, 700, 700 (^{o}C)

Belt speed Inch/min	V_{oc} (mv)	I_{sc} (ma)	I_{500} (ma)	R_{sh}
50	611	843	407	106
"	568	820	475	29.6
40	610	854	719	15.7
"	612	836	713	24.5
"	610	809	693	21.4
"	611	825	698	19.2
"	608	791	652	14.1
"	610	809	669	13.9
"	609	829	697	7.30
Average	610	822	692	16.6
30	607	796	646	27.6
"	609	824	675	18.3
"	608	811	665	24.0
"	606	793	643	20.3
Average	608	806	657	22.6
20	602	766	546	23.0
"	605	799	546	40.3

Table 3.11-9

Control Cells, Tube Fired Silver Front Contacts

AR Coated 2.12x2.12 inch squares

Run 8.61.9

Tube Fired at 700°C for 30 sec.

	V_{oc} (mv)	I_{sc} (ma)	I_{500} (ma)	R_{sh} (Ω)
	607	803	675	19.9
	607	787	675	22.4
	608	796	702	23.1
	610	804	715	22.1
	608	782	692	21.7
Average	608	794	692	21.8

Table 3.11-10

IR Firing of Silver Front Contacts
Variable Temperature and Constant Belt Speed
No AR Coating 2.12 x 2.12 Inch Squares
Run 9.65.9
Belt Speed 50 inch/min

Zone 1 Temp (^{o}C)	Zone 2 Temp (^{o}C)	Zone 3 Temp (^{o}C)	Zone 4 Temp (^{o}C)	V_{oc} (mv)	I_{sc} (ma)	I_{500} (ma)	R_{sh} (Ω)
0	0	800	800	593	663	574	44.3
				594	637	549	23.0
0	0	775	775	596	716	608	19.1
				599	657	570	27.5
0	0	800	750	600	663	585	45.5
				598	641	564	37.6
0	0	750	750	601	676	596	38.2
				599	654	572	29.8
0	0	775	725	601	688	601	43.9
				600	668	557	23.0
				601	674	562	55.0
				*602	663	393	34.5
				599	680	571	43.1
				599	677	530	32.9
				*600	674	524	42.4
				*600	684	401	31.9
				596	702	488	42.0
				600	699	584	47.6
				600	668	583	61.0
		Average		600	682	560	43.6

* Broken grid lines not taken into average.

was judged to be the optimum setting. Seven additional samples were fired under these optimum drying conditions when zone 3 was set at 750°C and zone 4 was set at 700°C, Table 3.11-11. The output of these cells was slightly lower than the control group which was fired in a tube furnace, Table 3.11-12.

Reexamination of the data of run 9.65.9 indicated that the setting of 260, 410, 750 and 750°C for zones 1, 2, 3, and 4, respectively, may be optimum. In run 9.66.9 four different (110) oriented lots of silicon were processed with half of each lot used as controls and half dried and fired under the optimum IR setting, Table 3.11-13, 3.11-14, 3.11-15, and 3.11-16. In all lots, the IR firing was better than the tube firing. The first two lots of wafers from Wacker were superior to those from the second two lots purchased from Texas Instruments.

These initial results of the infrared drying and firing of screen printed silver paste contacts indicate possibilities of producing high efficiency, four inch square cells at the rate of 350 per hour.

The remaining work performed in this task emphasized the replacement of the more expensive Ag paste by certain base metal pastes. Our choice for the replacement was air firable Ni paste with 20% frit from Thick Film Systems, Inc.

We were concerned with three problems: 1) electrical behavior, 2) adherent nature of the air fired Ni contact, and 3) the solderability of the air fired Ni contact with conventional solder (Pb-Sn).

Table 3.11-11

IR Drying and Firing of Silver Front Contacts
Variable Temperature and Constant Belt Speed
No AR Coating 2.12 x 2.12 Inch Squares
Belt Speed 50 inch/min.
Run 9.65.9

Zone 1 Temp (°C)	Zone 2 Temp (°C)	Zone 3 Temp (°C)	Zone 4 Temp (°C)	V_{oc} (mv)	I_{sc} (ma)	I_{500} (ma)	R_{sh} (Ω)
310	430	750	750	599	664	578	24.2
				598	652	553	25.6
225	360	750	750	599	661	585	15.8
				600	665	597	27.0
260	410	775	725	598	661	573	28.7
				598	664	577	41.0
260	410	750	750	598	703	600	23.6
				600	695	595	24.5
260	410	750	700	596	681	540	13.6
				601	670	559	50.5
				601	680	581	60.2
				601	684	476	25.0
				599	746	598	41.0
				601	671	557	58.9
				601	681	530	33.1
		Average		600	688	549	35.3

Table 3.11-12

Control Cells, Tube Fired Silver Front Contacts
No AR Coating 2.12 x 2.12 inch squares
Run 9.65.9
Tube Fired at 700°C for 30 sec.

	V_{oc} (mv)	I_{sc} (ma)	I_{500} (ma)	R_{sh} (Ω)
	598	699	585	22.6
	600	669	583	40.3
	601	687	599	84.8
	602	690	602	70.4
	602	683	600	38.5
	601	669	578	46.3
	601	680	588	26.5
	601	677	590	46.7
Average	601	682	591	47.0

Table 3.11-13

IR Vs Tube Fired Front Silver Contacts
No AR Coating 2.12 x 2.12 Inch Squares
Run 9.66.9
Silicon Type: (110) (637A) Wacker (10.0 Ω-cm)
IR Fired Silver front contacts
Belt Speed 50 inch/min

Zone 1, Zone 2, Zone 3, Zone 4: 260, 410, 750, 750 (^{o}C)

	V_{oc} (mv)	I_{sc} (ma)	I_{500} (ma(	R_{sh} (Ω)
	601	750	604	48.1
	600	747	601	64.1
	600	754	610	76.9
	602	751	607	55.0
	601	755	610	82.0
Average	601	751	606	65.2

Tube Fired at 700^{o}C for 30 sec.

	600	727	576	29.6
	596	665	517	64.1
	598	700	558	96.1
	698	694	559	65.8
	602	756	610	31.9
Average	599	708	564	57.5

Table 3.11-14

IR Vs Tube Fired Front Silver Contacts
No AR Coating 2.12 x 2.12 Inch Squares
Run 9.66.9
Silicon Type: (110) (512) Wacker (2.0 Ω-cm)
IR Fired Silver Front Contacts
Belt Speed: 50 inch/min

Zone 1, Zone 2, Zone 3, Zone 4: 260, 410, 750, 750 (^{o}C)

	V_{oc} (mv)	I_{sc} (ma)	I_{500} (ma)	R_{sh} (Ω)
	598	747	593	45.9
	600	745	614	125.0
	604	718	609	30.9
	604	713	605	31.9
	596	757	605	75.8
Average	600	736	605	61.9
	Tube Fired at 700^{o}C for 30 sec.			
	602	702	576	17.7
	603	701	583	25.3
	596	702	557	82.0
	596	686	544	90.9
Average	599	698	565	54.0

Table 3.11-15

IR Vs Tube Fired Front Silver Contacts
No AR Coating 2.12 x 2.12 Inch Squares
Run 9.66.9

Silicon Type: (110) (4950-1) Texas Instrument (0.4 Ω-cm)

IR Fired Silver Front Contacts
Belt Speed 50 inch/min

Zone 1, Zone 2, Zone 3, Zone 4: 260, 410, 750, 750 (^{o}C)

	V_{oc} (mv)	I_{sc} (ma)	I_{500} (ma)	R_{sh} (Ω)
	604	638	526	9.75
	603	615	529	14.0
	602	620	519	13.9
	603	620	532	20.9
	603	608	520	14.9
	603	616	528	18.0
Average	603	620	526	15.2
	Tube Fired at 700^{o}C for 30 sec.			
	600	598	482	20.1
	601	617	502	17.2
	599	602	479	14.2
	603	628	512	16.0
	604	636	536	12.6
	599	595	478	23.6
Average	601	613	498	17.3

Table 3.11-16

IR Vs Tube Fired Front Silver Contacts
No AR Coating 2.12 x 2.12 Inch Squares
Run 9.66.9
Silicon Type: (110) (4950-2) Texas Instrument (0.4 Ω-cm)
IR Fired Silver Front Contacts
Belt Speed 50 inch/min

Zone 1, Zone 2, Zone 3, Zone 4: 260, 410, 750, 750 (^{o}C)

	V_{oc} (mv)	I_{sc} (ma)	I_{500} (ma)	R_{sh} (Ω)
	596	584	431	7.80
	599	599	490	9.24
	595	567	463	8.58
	600	604	475	6.54
	599	614	485	6.00
	599	617	498	7.49
	599	604	440	5.64
	598	609	465	4.21
Average	598	600	472	7.90
	Tube Fired at 700^{o}C for 30 sec.			
	593	573	390	8.59
	600	616	491	13.2
	596	576	425	10.5
	591	568	394	10.0
	598	613	477	10.9
	599	615	466	10.3
	589	542	348	7.07
Average	595	586	427	10.1

C-3

Ni paste was first screen printed onto cells and then oven dried. Various temperatures (650°C to 750°C) and times (30 to 120 sec.) were explored to determine an optimum air firing schedule for the Ni thick film contact. Electrical performance results indicated that series resistance was the major problem. Nickel paste-silicon junction interaction appeared to be minimal.

One sample from each sintering condition was etched in a 5% NH_4OH solution for 10 seconds to remove possible "oxide layers" on the contact surfaces and to prepare the surfaces for soldering. Samples before and after etching were electrically tested, and the results are listed in Table 3.11-17. In general, etching seemed to improve the electrical performances of the cells, however, this treatment did destroy the adherence between the contacts and the silicon substrates.

A few "as air fired" samples were dip-soldered, (Sn-Pb-Ag solder and organic acid flux) and their electrical performance measurements before and after soldering are shown in Table 3.11-18. Significant improvements in electrical performance after soldering were observed. Microscopic examinations of the two soldered samples revealed substantial layers of solder on the Ni contacts.

Cells printed with Ni paste of high frit (20%) content, and fired at various temperatures and times in an N_2 gas atmosphere were not able to be soldered. However, resintering of these specimens in air seemed to enhance their solderability. Electrical performance data of some selected specimens before and after resintering and soldering are presented in Table 3.11-19.

Table 3.11-17

Sintering Temp (°C)	Sintering Time (Sec.)	V_{oc}	I_{sc}	I_{500}	R_{sh} at 500	Etching 5% NH_4OH	V_{oc}	I_{sc}	I_{500}	R_{sh} at 500
650	30	566	129	30	1250	10 sec.	565	125	0	1000
650	60	545	199	30	52	10 Sec.	546	192	0	64
650	120	126	103	0	3	10 Sec.	153	111	0	4
700	30	148	106	0	3	10 Sec.	152	105	0	4
700	60	0	0	0	∞	10 Sec.	0	35	0	∞
700	120	0	24	0	∞	10 Sec.	0	0	0	∞
750	10	516	253	17	47	10 Sec.	512	239	0	53
750	30	0	42	0	∞	10 Sec.	0	42	0	∞
750	60	0	29	0	∞	10 Sec.	0	32	0	∞
750	120	0	22	0	∞	10 Sec.	0	36	0	∞

Table 3.11-18

Sintering Temp. (^{o}C)	Sintering Time (Sec.)	V_{oc}	I_{sc}	I_{500}	R_{sh}	Dip Soldering	V_{oc}	I_{sc}	I_{500}	R_{sh}	Adherence
650	30	569	148	35	41	Sn-Pb-Ag with Organic Acid Flux	586	291	88	132	Good
650	60	513	205	12	23		551	352	58	40	Good

Table 3.11-19

Sintering N_2 650°C	V_{oc}	I_{sc}	I_{500}	R_{sh}	Re-Sintering Air 650°C	V_{oc}	I_{sc}	I_{500}	Dip-Soldering Pb-Sn-Ag	V_{oc}	I_{sc}	I_{500}	R_{sh}
60 Sec.	586	259	65	238	60 Sec.	581	221	0	Org. Acid Flux	591	550	166	116
60 Sec.	576	289	65	122	60 Sec.	567	317	0	"	591	811	328	40
60 Sec.	414	313	0	5	60 Sec.	284	263	0	"	376	404	0	3
60 Sec.	395	270	0	5	60 Sec.	294	237	0	"	387	462	0	3

Similar studies were performed on cells screen printed with air firable Cu paste. Extremely high series resistances and low shunt resistances were measured. These types of degradation modes are believed to be due to insufficient sintering of the contacts and excess penetration of Cu into the junctions during sintering. Consequently, work on copper screen printed cells was discontinued.

3.12 BACK CONTACT PADS

3.12.1 Recommendations

The original process sequence envisioned the use of a screen printed silver contact pad on the aluminum back to which the interconnects could be subsequently soldered. This was found to be susceptible to anodic corrosion. A tin-10% zinc alloy solder pad applied by ultrasonic techniques to the aluminum back was found to be acceptable for soldering tabs directly to the aluminum back and is recommended.

3.12.2 Work Performed

A fritted and a frit-free silver paste were printed on top of the aluminum metallization. Samples were exposed to 100% humidity at 65°C for 7 days. Both materials exhibited corrosion products and peeled to some degree, with the frit-free material showing poorer adherence. Zinc and indium additives to the aluminum were tested. This modification did not improve the corrosion resistance of the aluminum-silver couple in humidity testing. The use of a precious metal paste (TRS 3402 Pd-Ag) offered no adherence advantage over less expensive materials such as DuPont 7095. The use of a high frit paste such as TFS 3303 (∿ 15% frit) resulted in improved humidity tolerance with an unfortunate concurrent loss in solderability.

Tin and 90% tin-10% zinc solder pads were applied to the aluminum back contact metallization by ultrasonic soldering techniques. Interconnects of tin and lead-tin plated copper mesh were soldered to cells with these solder pads. These interconnects were pre-pulled at 90° to approximately 1000 grams, Table 3.12-1. The cells with interconnect that did not fail during the pre-pull test were subjected to 100% humidity at 70°C for 168 hours. The cell interconnects were then re-pulled to failure (Table 3.12-1). These combinations demonstrated good adherence and tolerance to humidity. The tin-zinc pads experienced a small degree of corrosion whereas the tin did not change during the exposure.

Table 3.12-1

BACK CONTACT METALLIZATION
SOLDER TO ALUMIMUM P^+
by Ultrasonic Soldering Pad

Cell No.	Pad	Solder	Flux	Pre-Pull Test (grams)	Pull Test After Humid. (grams)
1	Sn	Pb-Sn	α-611	1550	1375
23	"	"	"	1050*	-
24	"	"	"	1060	1600
25	"	"	"	1110	1275
26	"	"	"	1060	1200
3	Sn	Sn	organic	1150*	-
4	"	"	"	750*	-
5	"	"	"	850*	-
17	"	"	"	980	1100
18	"	"	"	1130	1250
19	"	"	"	960	1180
20	"	"	"	1030	425
6	Sn-.1Zn	Pb-Sn	α-611	1040	1025
32	"	"	"	1110	675
33	"	"	"	1030	775
34	"	"	"	1100	775
35	"	"	"	960	700
36	"	"	"	1050	800
37	"	"	"	1140	700
8	Sn-.1Zn	Pb-Sn	organic	800	-
9	"	"	"	1220	1100
10	"	"	"	1000	-
27	"	"	"	1040	1200
28	"	"	"	925	800
29	"	"	"	960	1050

*Failure by cell breakage

3.13 PLASMA ETCHING

3.13.1 Recommendations

Plasma etching metallized silicon solar cells with SF_6 after removal of the diffusion oxide was found to result in improved solar cell electrical performances. Consequently, inclusion of this processing technique into the overall processing sequence is recommended.

3.13.2 Work Performed

Experimental work performed on plasma etching focused on:

(1) Removal of the diffusion oxide

(2) Plasma etching non-metallized cells

(3) Plasma etching completed cells

The work performed in each of these areas is discussed below.

Diffusion oxide removal experiments were set up to etch wafers from 30 seconds to 7 minutes with Freon 23 at a chamber pressure or approximately 500 mtorr. Etch temperatures varied from 25°C to 200°C. Little or no removal of diffusion oxides was seen at short (.5 to 3.5 min.) etch times. Several samples showed oxide removal in and near the center indicating possible non-uniformities in diffusion oxide thickness. A 3-7 minute Freon 23 plasma etch resulted in a flaky residue which rinsed clean after treatment with alcohol and water. Cells fabricated from these wafers could not be tested because printed front metallization would not adhere.

A comparison of etching characteristics was made of sulfur hexafluoride and Freon 14 + 8% oxygen by plasma etching non-metallized silicon solar cells after removal of the diffusion oxide. An

excessively slow etch rate prohibited examination of Freon 14 without O_2. Three groups of wafers were fabricated for the experiment. The first group was P type, 1-3 ohm-cm material that had only been given the standard 30% NaOH surface etch. These wafers were kept as the controls. The second group of wafers was also P type, 1-3 ohm-cm material that had only been given the standard 30% NaOH surface etch. These wafers were kept as the controls. The second group of wafers was also P type, 1-3 ohm-cm material that had been given the standard surface etch, but these wafers were plasma etched for five and ten minutes in both Freon 14 + 8% O_2 and SF_6. The third group of wafers was chemically etched P type, 1-3 ohm-cm material that had been diffused with phosphorus. These wafers were also etched for five and ten minutes in both Freon 14 + 8% O_2 and SF_6. These samples were examined with a scanning electron microscope and photos were taken (Figures 3.13-A - 3.13-E). The brightly colored spots appearing on all samples were shown to contain iron by EDAX measurements. This residue is a suspected corrosion product of the plasma etch platen. Careful examination of all samples showed the iron compound to be nonuniformly distributed over the samples. This explains the absence of contaminants on some photos.

Comparison of both diffused and non-diffused samples plasma etched with SF_6 or Freon 14 + 8% reveal dramatic differences. Most notable are the large pits on Freon 14 + 8% O_2 etched samples which do not appear on the relatively smooth post SF_6 etched wafer surface. This confirms suspicions of pitting raised from previous experiments. Phosphorus diffused samples etched with Freon 14 + 8% O_2 and contacted, displayed shunt resistance readings 50% lower than those measured from SF_6 etched or control samples.

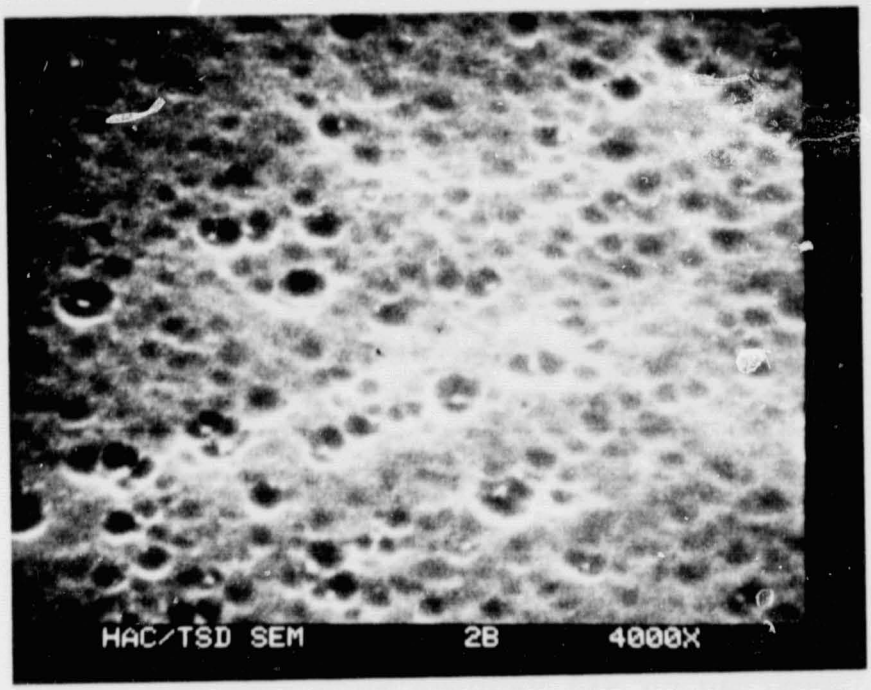

Figure 3.13-A
Phosphorus diffusion on boron doped base etched 10 min. with Freon 14 + 8% O_2 at 26°C. Mag. 4000X

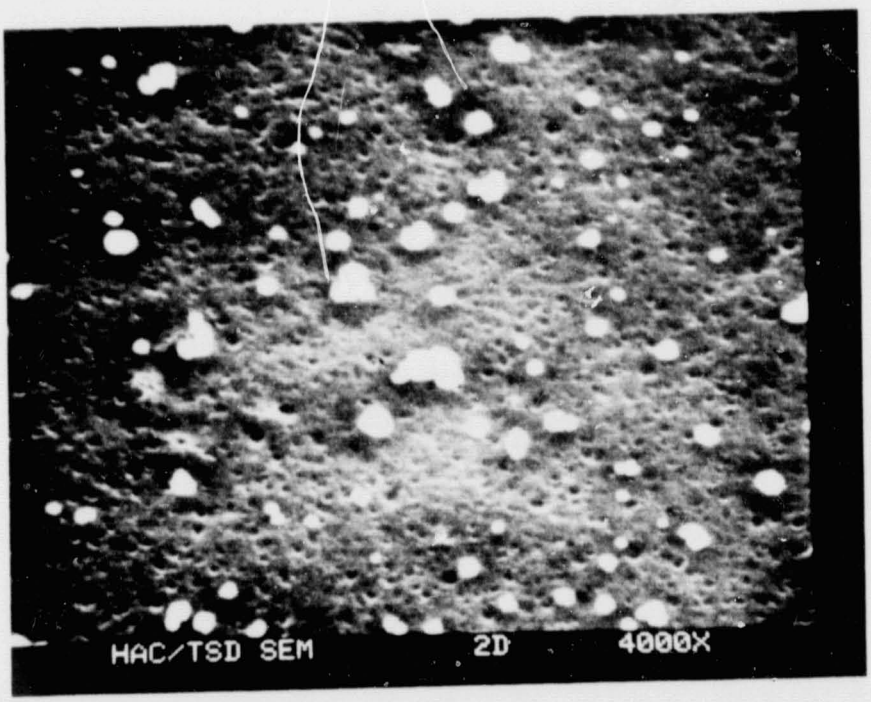

Figure 3.13-B
Boron doped base material etched 10 min. with Freon 14 + 8% O_2 at 26°C. Mag. 4000X

Figure 3.13-C
Control sample standard boron doped base given 30% NaOH surface etch.
Mag. 4500X

Figure 3.13-D
Phosphorus diffusion on boron doped base etched 10 min. with SF_6 at 26°C.
Mag. 4000X

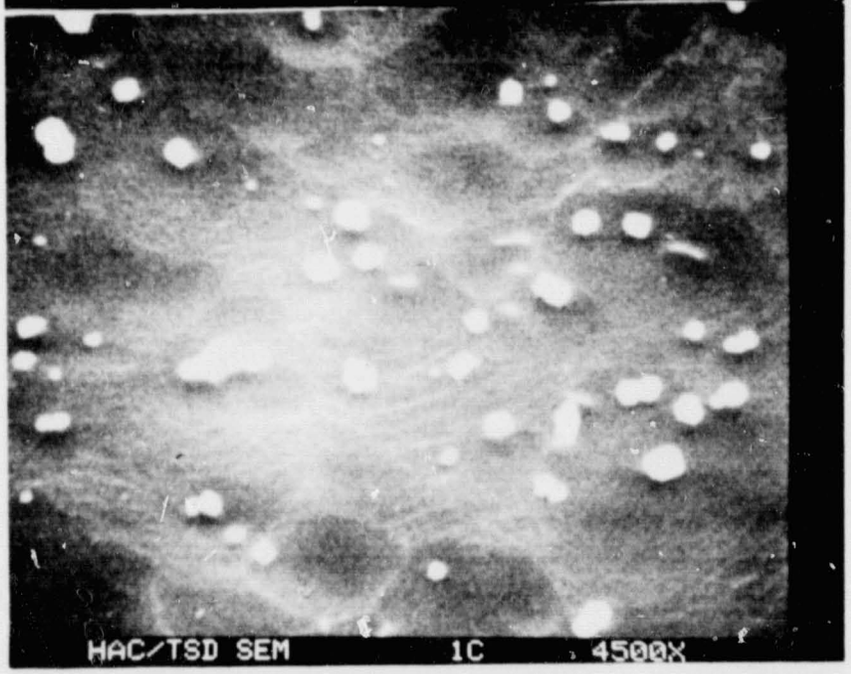

Figure 3.13-E
Boron doped base material etched 10 min. with SF_6 at 26°C.
Mag. 4500X

Phosphorus diffused samples etched with Freon 14 + 8% O_2 appear to have larger pits than non-diffused wafers (Figure 3.13-A). Surface damage and near surface phosphorus precipitates formed during diffusion may enhance plasma etch pitting action. Precipitates removed during etching leave voids which may broaden and deepen with further etching.

Further experimental evaluation was performed in order to determine the effect of plasma etching completed cells in SF_6 or Freon 14 + 8% O_2. A series of 12 finished cells were etched in SF_6 for 6 to 90 seconds. Short circuit current and load point current (500 mV) measurements were taken before and after each run. The results showed maximum cell performance improvement (approximately 12%) after a 60 second etch (Figure 3.13-F). The SF_6 plasma etch rate of (100) orientation silicon is 900-100 Å/min. This rate was determined by step etching and step measurement with a Talysurf profiliometer. When this experiment was repeated with Freon 14 + 8% oxygen, improved solar cell performance was again achieved.

Several mechanisms would account for the improved solar cell performance attained by plasma etching completed cells in SF_6 or Freon 14 + 8% oxygen. These mechanisms include removal of lattice damage and phosphorus precipitates (the so-called dead layer) in the first 300-500 Å, junction depth shallowing, and plasma induced surface pitting. Removal of the dead layer is an unlikely explanation for cell improvement, because dead layer recombination processes are likely to be replaced by surface recombination processes after 500 Å of silicon removal. Moreover, the cells that showed the greatest improvement had over 1000 Å of material removed from the front surface. Plasma induced surface pitting was also an inadequate explanation for the I_{sc} increases in the SF_6 experiment because SF_6 does not pit the surface of the wafer. Junction depth shallowing is a more likely explanation, because greater than 1000 Å

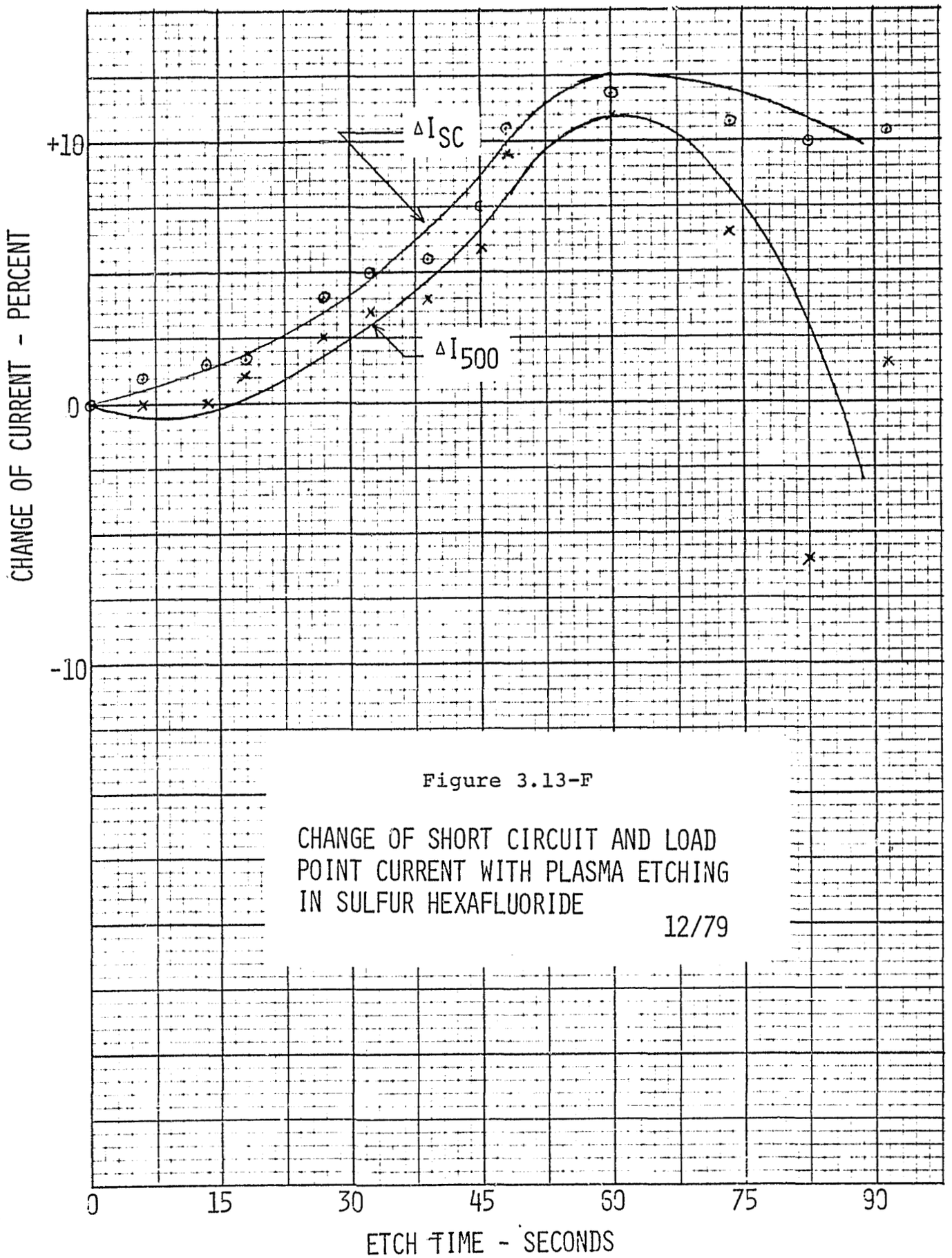

Figure 3.13-F

CHANGE OF SHORT CIRCUIT AND LOAD POINT CURRENT WITH PLASMA ETCHING IN SULFUR HEXAFLUORIDE

12/79

of material was removed from the front surface after plasma etching. Spectral response measurements performed before and after plasma etching support this hypothesis. The largest increase in the short circuit current response is seen at the short wavelengths (Figure 3.13-G). Data scatter at longer wavelengths requires further spectral response measurements in order to obtain an unambiguous result.

The performance increases observed with sulphur hexafluoride support previous conclusions about a Freon 14 + 8% oxygen etching atmosphere. Earlier it had been determined that about fifty percent of the cell improvement after etching with Freon 14 + 8% oxygen was attributable to AR effects. This was verified by etching 500 Å off the front surface of the silicon solar cell with both Freon 14 + 8% oxygen and sulphur hexafluoride. A fifteen percent and six percent improvement was seen with Freon 14 + 8% oxygen and sulphur hexaflouride, respectively. About nine percent of the improvement seen with Freon 14 + 8% oxygen was attributed to the antireflective effects of pitting. The pitting was not noticed with sulphur hexaflouride.

Figure 3.13-G

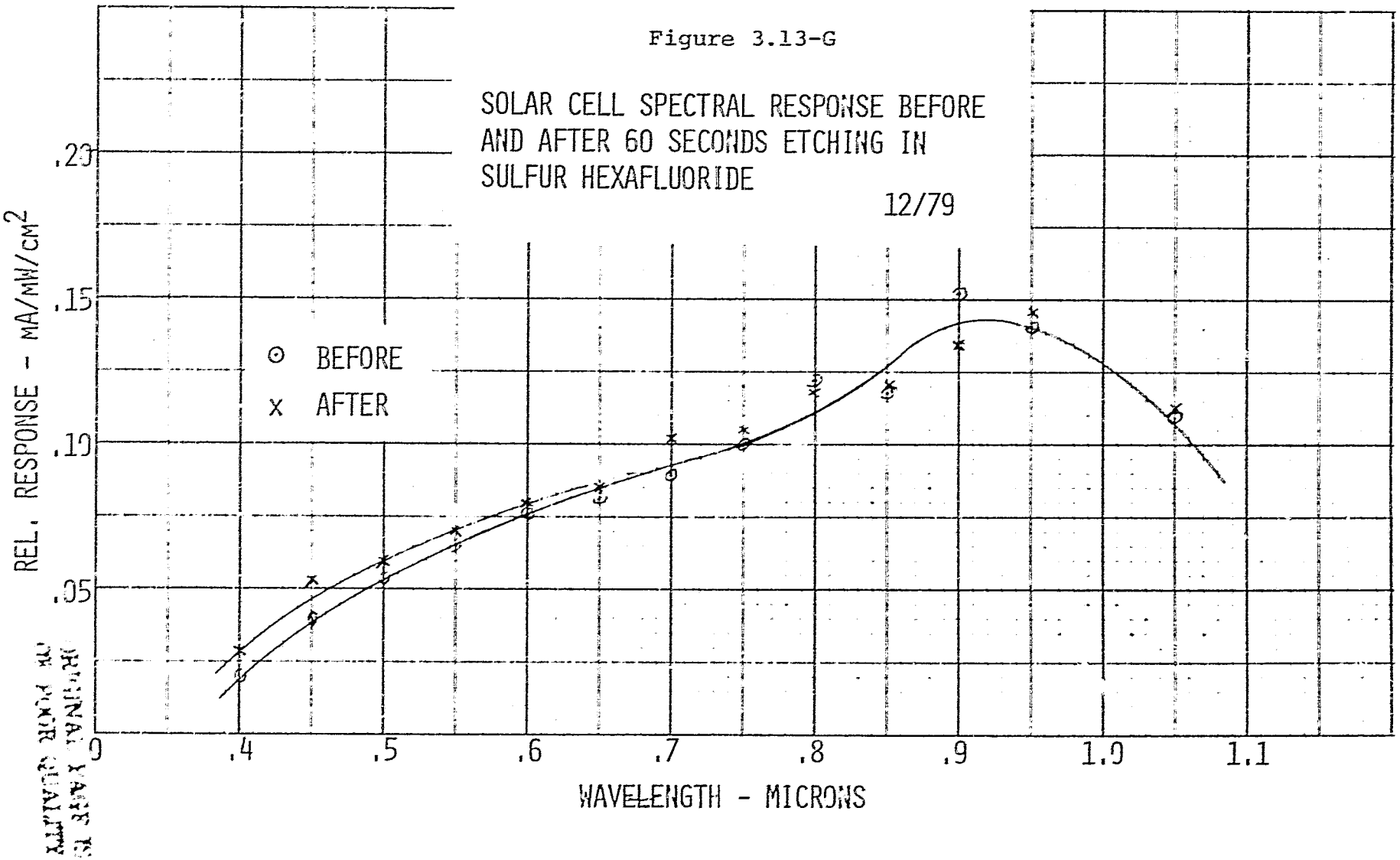
SOLAR CELL SPECTRAL RESPONSE BEFORE AND AFTER 60 SECONDS ETCHING IN SULFUR HEXAFLUORIDE
12/79
⊙ BEFORE
X AFTER
REL. RESPONSE - MA/MW/CM2
.20
.15
.10
.05
0
.4
.5
.6
.7
.8
.9
1.0
1.1
WAVELENGTH - MICRONS

3.14 JUNCTION ISOLATION

3.14.1 Recommendations

Junction isolation by laser scribing the front surface of finished, non-AR coated solar cells was demonstrated to be a viable process. It is therefore recommended that this process step be incorporated into the overall processing sequence. We recommend scribe lines 6-7 mils deep and 1½ mils wide.

3.14.2 Work Performed

The Spectrolab baseline process includes laser scribe for junction cleanup. This may be accomplished by scribing the back side then breaking or scribing through the junction from the front side.

To determine the effects of laser scribing on the cell's characteristics, wafers were processed in accordance with our standard process, except the wafers were divided into two groups prior to junction cleaning. The first group was saw cut and chemically etched and the second was laser scribed from the back and breaking the edge, run 4.29.9. The results of these two groups, Table 3.14-1, were very similar indicating that laser scribing is an effective method of junction removal.

To confirm the results of run 4.29.9, we ran a similar group of wafers, run 4.32.9, Table 3.14-2. (Eight cells were saw cut and chemically etched as a control and the remaining 25 cells were laser scribed.) The results were very encouraging; the saw cut and chemically etched cells had an average efficiency of 9.2% (12.4% with AR coating) for 6 out of 9 cells. Laser scribed cells had an average efficiency of 9.7% (12.9% with AR coating) for 25 out of 25 cells. The laser scribed cells probably had a larger yield due to decreased cell handling.

Table 3.14-1

Run 4.29.9

Preliminary Comparison of Saw Cutting
with Chemical Etch and Laser Scribing

No AR Coating (2.0 x 2.0")

	Averages of 8			
	V_{oc} (mV)	I_{sc} (mA)	I_{500} (mA)	R_s (ohm)
Saw Cut	601	674	491	7.65
Laser Scribe	601	644	491	5.72

Table 3.14-2

Run 4.32.9

COMPARISON OF SAW CUTTING AND CHEMICAL ETCH AND LASER SCRIBING

No AR Coating

(2.1" x 2.1")

	V_{oc} (mV)	I_{sc} (mA)	I_{500} (mA)	R_{sh} (Ω)
Saw Cut Average	602	644	498	13.1
Laser Scribe Average	603	670	551	11.7

These initial findings suggest that junction clean-up through laser scribing and breaking is equal to or better than saw cutting and edge etch treatment. However, there are some problems associated with this process. If we begin with square wafers, laser scribing through the Al (p+) layer produces silicon waste. A minimum of 50 mils may be successfully cleaved from each edge. Starting with a 4" x 4" wafer, a minimum 5% loss of material is realized in laser scribing and cleaving. Junction isolation, by scribing a shallow street along the front edge of a finished cell, would eliminate damage and waste. The shallow street may be laser scribed as close as 10 mils to the edge of the cell, thus decreasing the active area of a 4" x 4" cell by only 1%.

Junction isolation by laser scribing from the front required development. It was believed that a low power output (1-5 watts), laser beam is needed to scribe a shallow street that is free of the silicon remelt material which may cause current leakage. In the present resonator mode, TEM_{01}, 10-15 watts average power are delivered in a hollow cylindrically-shaped beam. Looked at in a cross section the beam strikes the substrate at two points of greatest intensity. Depending upon laser pulse frequency, chuck speed, and laser current input, silicon remelt material may build up. These variables control laser drilled hole overlap, laser kerf width, and laser scribe depth. The interaction of these variables can be described by the Q-factor. The Q-factor is equal to the product of kerf width (mils) and pulse frequency (KHZ) divided by chuck speed (IPS). It has been stated by the laser scribe manufacturer, Quantronix Corporation, that material is ejected from the kerf at an angle of 45^{o} to the substrate surface with little or no residue remaining in the kerf at a Q-factor of 3. At Q-factors greater than 3, material is ejected at increasingly lower angles to the substrate surface and some material is trapped as a slag residue. At Q-factors less than 3, laser drilled holes

overlap insufficiently to form a continuous kerf. At a Q-factor of 3 in the TEM_{01} mode, junction damage may result from the high power. In the TEM_{00} resonator mode a solid cylindrical line beam strikes the substrate at 1-5 watts. A low power, point focused beam may allow complete evacuation of material with no junction damage.

As part of an initial evaluation of the suitability of front side laser scribing for junction isolation, twenty 2.1 x 2.1" cells were fabricated. Shunt resistance measurements and I-V curves were taken prior to laser scribing. Chuck speed varied from 8 to 10 inches per second, laser current input was set at 34 amps and pulse frequency was set to ensure a Q-factor of 3 using TEM_{01}. The cells were then laser scribed and all measurements retaken.

Short circuit current (I_{sc}) measurements did not decrease, and open circuit voltage measurements decreased slightly. Microscopic inspection of the laser scribed grooves showed significant remelt material. Cell degradation was evident from the shapes of the I-V curves (Figure 3.14-A). This degradation appears to be associated with a decreased shunt resistance. The shunt resistance measured by dark current techniques did not change. This would be consistent with shunting at the laser scribe line which would be masked in the dark current measurement by spreading resistance between the grid fingers and scribe lines.

The work performed thus far indicated that junction isolation by scribing from the front in the TEM_{01} resonator mode is unsuitable in agreement with a Quantronix analysis. At a Q-factor of 3, significant remelt material was seen in the laser scribed channels. This, and the high power laser beam, may have contributed to cell power loss as seen from the I-V curves.

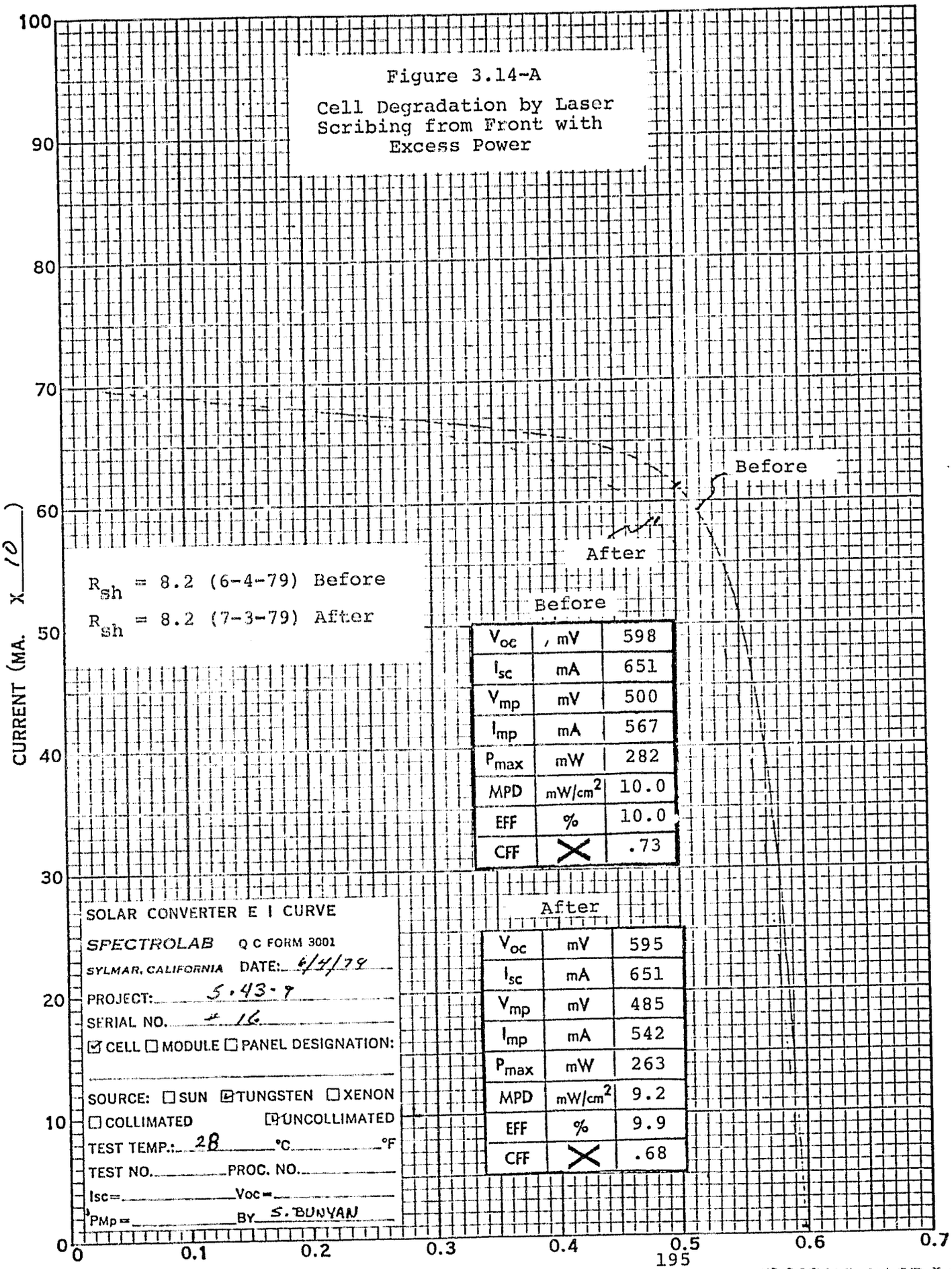

Before

V_{oc}	mV	598
I_{sc}	mA	651
V_{mp}	mV	500
I_{mp}	mA	567
P_{max}	mW	282
MPD	mW/cm^2	10.0
EFF	%	10.0
CFF	X	.73

After

V_{oc}	mV	595
I_{sc}	mA	651
V_{mp}	mV	485
I_{mp}	mA	542
P_{max}	mW	263
MPD	mW/cm^2	9.2
EFF	%	9.9
CFF	X	.68

The laser scriber at Spectrolab was converted to the TEM_{00} mode for evaluation. Laser output was varied between 3 and 7 watts/cm^2 and the Q-factor was varied between 3000 and 9000 pulses/inch. A laser cut was made between 5 and 10 mils from each edge on the front side of the cell. Control cells were laser scribed through the Al(P+) back and cleaved. Current at 500 mV (I_{500}) and shunt resistance (R_{sh}) were plotted as a function of Q-factor. A family of curves were produced representing laser power output levels of 3, 5, and 7 watts/cm^2 (Figure 3.14-B). The best I_{500} and R_{sh} were achieved at a laser output 7 watts/cm^2 level of and a Q-factor of 3000 pulses/inch. This represents a non-AR coated cell efficiency of 10.4% which was equivalent to non-AR coated control cells. A maximum deviation of 10% from the mean was seen in I_{500} values. R_{sh} values varied by as much as 20% from the mean. Five samples each were measured to generate each data point. Machine limitations prevented the examination of lower Q-factors and higher power levels.

Laser cut integrity was examined with a scanning electron microscope as a function of Q-factor and laser output. A clean continuous cut was achieved at a Q-factor of 3 over a range of 3 to 7 watts/cm^2 laser output (Figure 3.14-C). However, a change from a Q-factor of 3000 to 7000 pulses/inch at 7 watts/cm^2 laser output to current leakage (Figure 3.14-D). A low laser output of 3 watts/cm^2 and a high Q-factor of 7000 pulses/inch also produced non-optimized groove characteristics (Figure 3.14-E).

Many factors contribute to laser cut integrity and process reliability. Laser pulse fluctuations, laser beam size and shape, and the orientation of the cell surface with respect to the laser beam have been identified. Machinery designed for precise control of these parameters will improve process reproducibility.

Figure 3.14-B
VARIATION OF SHUNT RESISTANCE AND
CURRENT AT 500 mV WITH Q-FACTOR

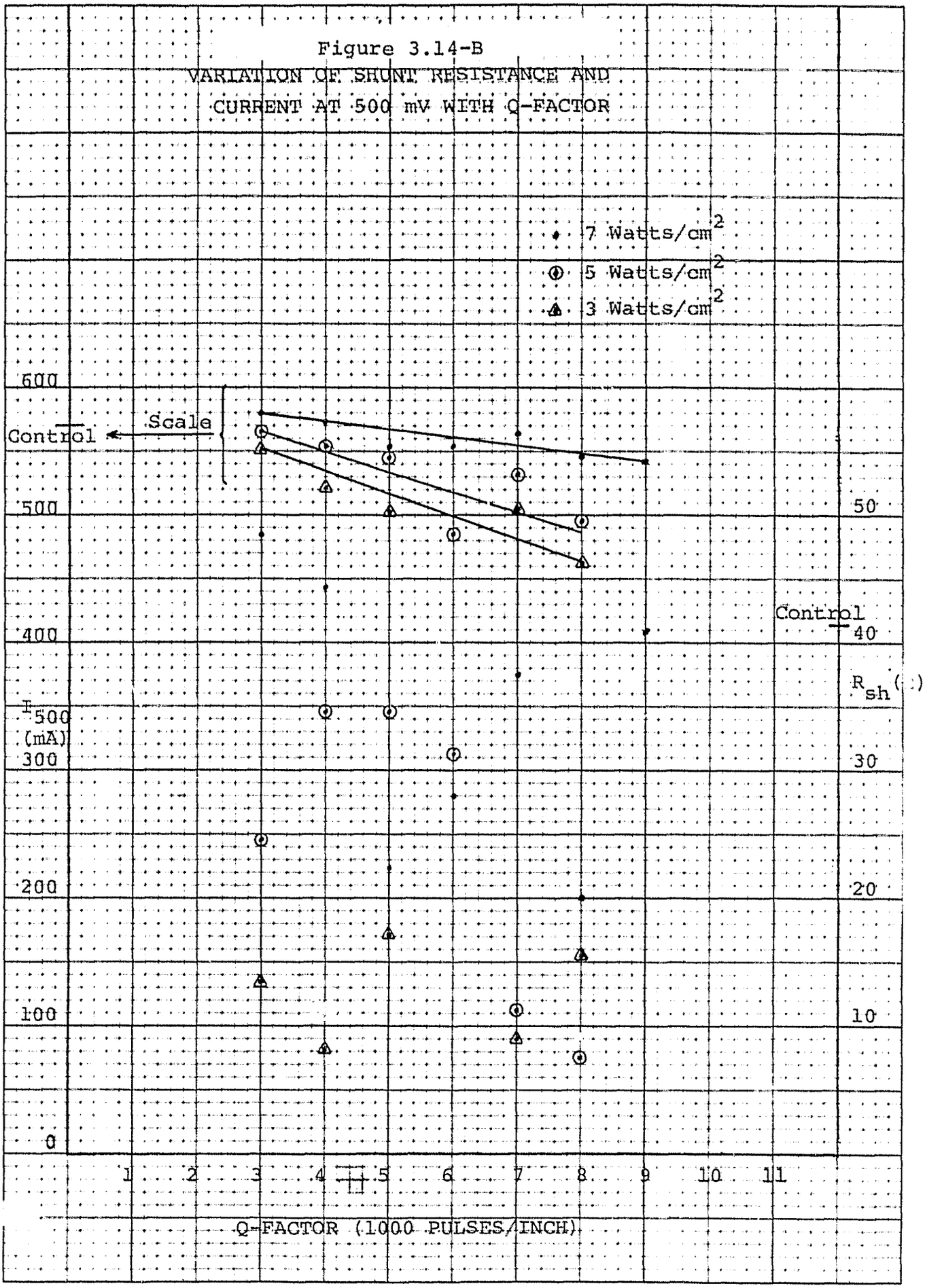

Figure 3.14-C

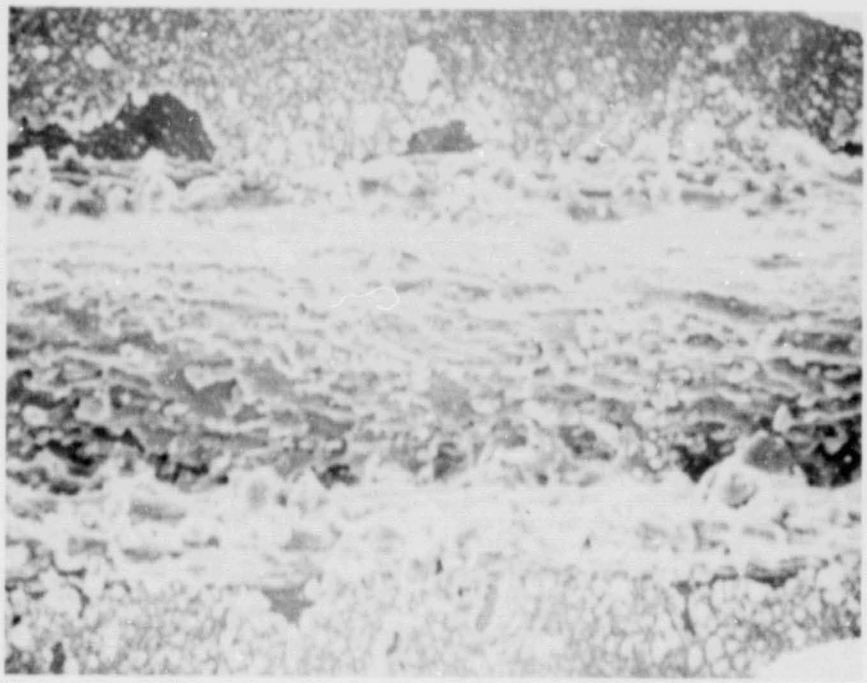

3 watts/cm^2 Qf = 3 1000X

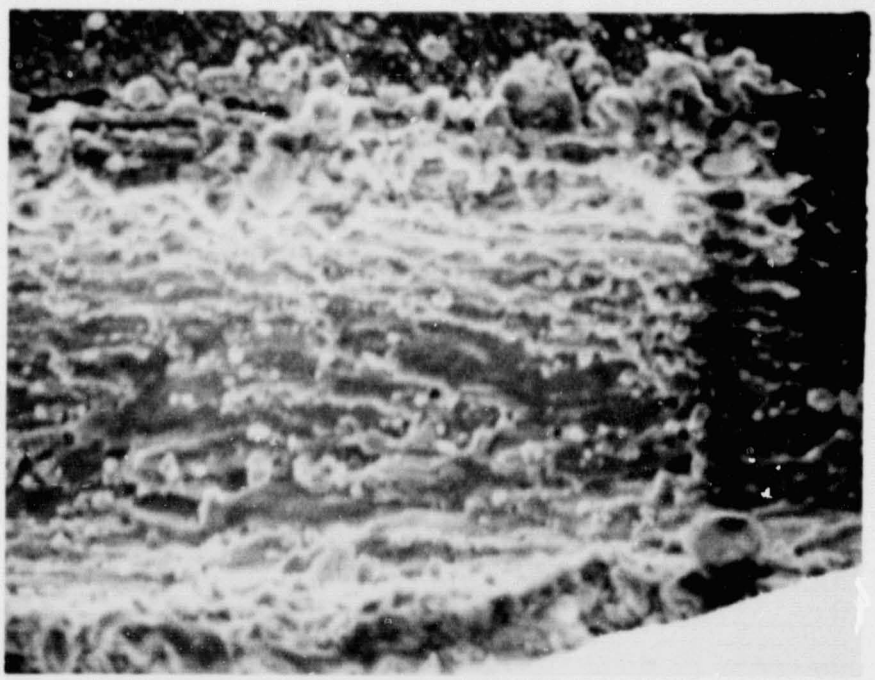

7 watts/cm^2 Qf = 3 1000X

Figure 3.14-D

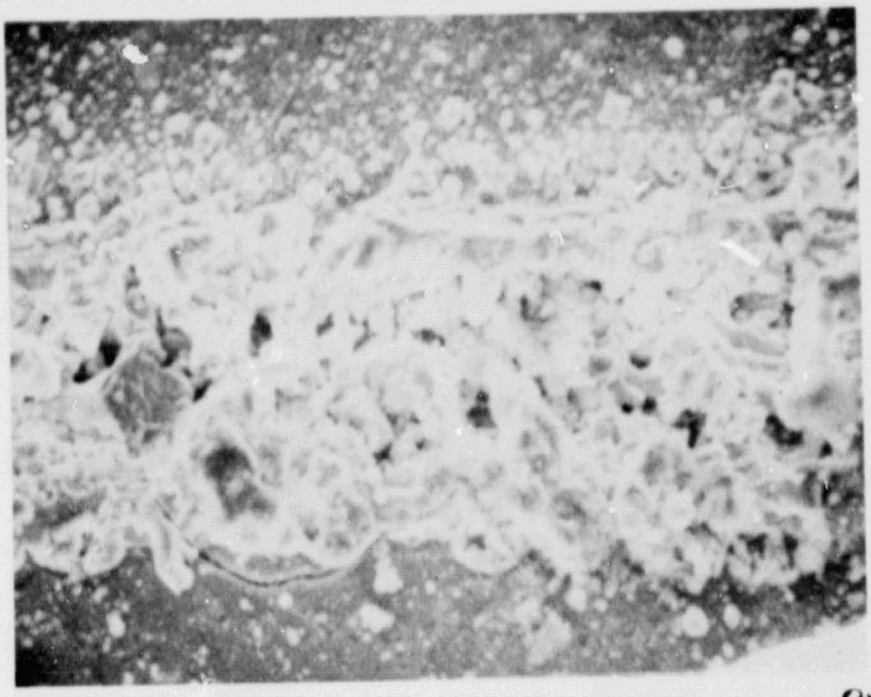

7 watts/cm^2 Qf = 5 1000X

7 watts/cm^2 Qf = 7 1000X

Figure 3.14-E

3 watts/cm^2 Qf = 7 1000X

A beam monitor device is available which will enable precise adjustment of laser pulse amplitude to within 5% deviation. Other undesirable beam characteristics may be detected and eliminated with this device.

A second harmonic generator is also available which converts the wavelength of the laser emission from 1.06 μ to 0.53 μ. The Si absorption coefficient (α Si) at 0.53 μ is 100 times that of 1.06 μ light. Therefore, a far greater portion of 0.53 light is absorbed in the near surface region than that 1.06 μ. Use of a 0.53 laser should give rise to complete evacuation of silicon from the laser scribe groove which would minimize current leakage paths and improve process reliability.

A number of cells were sent to Quantronix in an attempt to laser scribe cells through the front junction using the second harmonic of the neodymium yag laser (0.53 μm). The results of this experiment, Table 3.14-3, indicate that this technique is acceptable for junction isolation. It was believed that using the neodimium yag laser scriber in the second harmonic (0.53 μm) to scribe the front junction would be a low cost process of isolating the junction.

To verify that laser scribing through the front junction is an acceptable process, additional cells were shipped to Quantronix. Control cells were processed in accordance with our standard process sequence except no AR coating was applied, results given in Table 3.14-4. The cells under investigation were laser scribed into squares prior to surface preparation and were processed similar to the controls except for the laser scribing process, results given in Table 3.14-5. It can easily be seen from this data that the cells which were sent to Quantronix have a serious shunting problem, which is directly associated with laser scribing from the front surface through the junction. Although the laser

Table 3.14-3

LASER SCRIBED THROUGH FRONT JUNCTION
(No AR Coating)

Specimen	V_{oc} (mV)	I_{sc} (mA)	I_{500} (mA)	R_{sh} (Ω)
1	609	686	621	86
2	610	716	639	59
3	611	703	592	71
4	609	710	642	74
Average	609	703	623	51

Table 3.14-4

LASER SCRIBED CELLS

Controls - Laser Scribed from Back of Cell and Cleaved

	V_{oc} (mV)	I_{sc} (mA)	I_{500} (mA)	R_{sh} (Ω)
	600	690	601	10.9
	602	676	624	28.7
	603	675	620	33.8
	604	682	626	64.1
	603	691	632	51.0
	601	670	602	17.3
	604	686	637	42.0
	602	700	639	38.5
	600	669	607	30.0
	602	683	633	50.0
	600	673	608	27.5
	600	678	627	40.0
	601	681	627	45.5
	602	689	644	92.6
	602	687	640	58.1
	603	687	637	65.0
	602	691	647	64.1
	603	692	645	50.5
	602	695	644	42.2
	603	695	639	30.1
Average	601.9	684.5	628.9	44.09
$\hat{\sigma}$	1.3	8.8	14.6	18.9

Table 3.14-5

LASER SCRIBED CELLS

Laser Scribed through Front Junction

	V_{oc} (mV)	I_{sc} (mA)	I_{500} (mA)	R_{sh} (Ω)
	599	717	566	9.0
	601	718	616	11.4
	600	711	603	9.9
	602	713	610	8.9
	604	721	622	10.1
	598	716	611	9.5
	599	718	604	8.7
	603	719	632	12.5
	603	713	581	11.1
	601	718	624	12.2
	600	715	613	11.1
	601	718	614	8.5
	602	715	610	9.2
	601	715	619	10.4
	600	712	613	10.0
	601	721	615	9.2
	601	709	612	11.0
	601	707	565	7.1
	600	702	618	16.7
	599	701	600	11.3
	602	709	626	18.8
	602	709	632	21.2
	601	714	632	20.6
	602	712	594	20.2
	601	709	629	19.1
	* 593	681	266	8.0
	600	704	592	14.9
	602	717	625	11.9
	603	706	622	14.7
	603	711	630	14.8
	602	709	617	14.9
Average/$\hat{\sigma}$	601.1/1.4	712.6/5.4	611.6/17.6	12.6/4.0

*Cell Not taken into average

scribing degradation was only 2%, additional investigations need to be conducted in order to identify the proper method of laser scribing from the front to isolate the junction.

3.15 AR COATING

3.15.1 Recommendations

Experimental investigations were performed to determine the suitability of the titanium isopropoxide AR coating solution developed by RCA on 30% NaOH etched, "pillowed" wafer surfaces. Due to spray-on equipment contamination problems encountered at Sensor Technology, Inc., experimental work was unable to reach completion. It is recommended that work in this area should continue when in-house spray-on equipment is available at Spectrolab, Inc.

3.15.2 Work Performed

Spray-on and spin-on AR coating methods were investigated with titanium Silica Film "C"® obtained from Emulsitone Corporation. A hand-held Paasche Airbrush proved impractical, necessitating the use of an automatic spray system. Gridline shadowing effects prevented uniform spin application to finished cells, but TiSi Film "C" was able to be homogenously spun-on to wafers with a 30% NaOH surface preparation prior to gridline printing. This suggested possible spin-dry-print-dry-cofire process sequence for screen printed metallization and AR coat.

Five drops of TiSi Film "C" were spun at 3000 RPM onto wafers which had been etched in 30% NaOH. The sample was separated into two lots which were dried at 150°C and 200°C for 15 minutes. A front contact was then screen-printed and dried at 125°C for 15 minutes. Each lot was separated into four groups, and the AR coat and metallization were cofired at 700°C for 30 sec., 45 sec., 60 sec., and 75 sec. Conclusions were difficult to draw due to the wide scattering of data (Table 3.15-1).

Table 3.15-1

EVALUATION OF SPIN-ON SUITABILITY OF TITANIUM SILICAFILM "C"

Run 5.37.9

	V_{oc} (mV)	I_{sc} (mA)	I_{500} (mA)	R_{sh} (Ω)
Control				
Average	603	489	439	22.8
150°C Bake				
30 Sec. Sinter	607	618	331	33.8
	607	614	356	16.0
	608	618	392	80.7
	613	614	450	43.9
	611	629	383	46.3
45	606	623	413	22.1
	606	606	335	12.5
60	605	622	378	18.4
	604	621	399	21.6
75	600	613	179	17.4
	598	606	220	18.0
200°C Bake				
30 Sec. Sinter	609	623	409	29.6
	611	607	441	62.5
	606	611	393	22.3
	601	609	397	10.4
	609	620	478	25.8
45	603	623	315	14.2
	598	611	21[illegible]	14.4
60	607	628	518	34.3
	604	632	352	19.5
75	606	626	494	23.4
	600	591	286	36.0

A second experiment was devised which involved varying the drying time at a constant temperature and also the spin velocities around values used in the previous experiment. The firing schedule was 30 seconds at 700°C. The short circuit current (I_{sc}) increased with decreasing spin velocity, peaking at the slowest spin velocity. Cell characteristics did not vary with drying time. Results are summarized in Table 3.15-2. This process configuration is not acceptable because of the high series resistance.

Spin-on difficulties prompted the investigation of spray-on AR sources with an Advanced Concepts spray system using equipment at Sensor Technology, Inc. The Advanced Concepts spray system consists of a spray chamber followed by a convection heating oven and infrared furnace. A reciprocating spray head moving back and forth across the sample deposits an atomized mist. Spray parameters include conveyor velocity, reciprocator velocity, atomization pressure and the flow rate of the liquid material being applied.

Attention was also shifted to a titanium isopropoxide AR coating solution developed by RCA, shown by them to have the capability of 35% efficiency enhancement (slightly better than they observed with TiSi film "C"). After much experimentation a uniform blue-violet AR coat was applied to wafers etched with 30% NaOH.

Square cells oriented with gridlines parallel to, and center ohmic perpendicular to, the reciprocator motion were coated and dried with the results summarized in Table 3.15-3. The surface appeared speckled with light colored strips 1/16" wide running the length of the trailing edge of each gridline.

Several JPL contractors have reported that they were successful in applying spray-on AR coatings to polished silicon wafer

Table 3.15-2

Effect of Drying Time and Spin Rate of AR Coating Application - Cofiring of AR Coat and Front Metal Contact

	V_{oc} (mV)	I_{sc} (mA)	I_{500} (mA)	R_{sh} (Ω)	R_{ser} (mΩ)
Control	608	535	479	19.1	95
1A	612	629	408	17.3	277
1B	614	631	432	27.2	242
1C	615	618	502	21.0	161
1D	614	607	437	25.0	242
1E	614	602	469	22.9	193
2A	612	634	418	14.5	222
2B	616	630	508	17.2	147
2C	616	622	576	23.7	132
2D	612	606	435	21.5	101
2E	615	601	503	35.7	89
3A	614	629	455	21.1	233
3B	615	624	482	15.0	147
3C	614	617	497	18.8	147
3D	611	601	471	16.8	161
3E	614	601	502	11.6	112

1 - 200°, 10 min. dry
2 - 200°, 20 min. dry
3 - 200°, 50 min. dry
A - 2000 RPM spin
B - 2500 RPM spin
C - 3000 RPM spin
D - 3500 RPM spin
E - 4000 RPM spin

Table 3.15-3

INITIAL EVALUATION OF EFFICACY OF
SPRAYED ON TITANIUM ISO-PROPOXIDE AR COATING

	V_{oc}	I_{sc}	I_{500}	
Average Before AR	603	670	492	(2.1" x 2.1" sq. cells)
Average After AR	609	846	689	

Average Increase: I_{sc} 26%, high of 31%

Average Increase: I_{500} 25%, high of 31%

Spray parameters were as follows:

--source flow rate	10 mil/min.
--atomization pressure	30-35 psi
--reciprocator velocity	90 CPM
--conveyor velocity	2 ft./min.
--reciprocator height from substrate	6 in.
--orifice size	12 mil

surfaces. Work was initiated to determine the suitability of using a spray-on AR coating in conjunction with 30% NaOH etched, "pillowed," wafer surfaces. Experiments were again performed with Advanced Concepts spray equipment at Sensor Technology, Inc. Coating uniformity was optimized by properly adjusting spray parameters. After extensive experimentation, spray parameters were fixed as follows:

Source flow rate	10 cc/min.
Atomization pressure	40 psi
Reciprocation velocity	90 CPM
Conveyor velocity	2 ft./min.
Nozzle height from substrate	6 in.
Nozzle orifice size	10 mils

Average electrical performances of cells spray coated at these parameter values were as follows:

	V_{oc}	I_{sc}	I_{500}	
Before	591.6	707.8	597.0	(Average of 5 samples)
After	592.0	910.0	710.0	
Δ%	+0.06	+28.6	+19.0	

These wafers were processed in an IR furnace peaking 250°C followed by a 60-90 second 200°C hot plate bake-out, a two-step bake-out of 70°, for 10 seconds and 200°C for 3 minutes. A spray-coated cell viewed through an optical microscope was characterized by pinholes. The spray coverage was susceptible to pinholes because the AR source most likely flows between pillows, exposing the highest surfaces. Proper source atomization must be maintained to ensure uniform coverage and prevent source flow. Inspection of the spray system by an Advanced Concepts engineer revealed problems in the nozzle head apparatus which prevented proper AR source atomization.

Further experimental investigations were unable to continue due to ongoing contamination problems with the spray system at Sensor Technology, Inc.

3.16 SUPERSTRATE

3.16.1 Recommendations

We recommend the use of a glass superstrate structure on the basis of current knowledge regarding weatherability of polymeric materials. Although there are some possible substrate materials such as particle board available at lower cost than glass, the substrate structure puts a thin layer of polymeric encapsulant in the position of most severe exposure to weathering.

Based on recent cost quotations for large volume purchases of glass the use of water clear (low iron content) glass such as A5G Industries SUNADEX® having low absorption coefficient is cost effective when average costs are greater than $1.09/watt (1975).

Spectrolab believes that the currently available technology for AR coating glass (selective etching by fluosilicic acid and formation of SiO_2 from sodium silicate) is not sufficiently well developed at the present time for inclusion in a low cost, high volume production process sequence. The benefits to be gained (in increased module conversion efficiency) are sufficiently large that further effort to develop these processes or some other process such as CVD is warranted.

3.16.2 Work Performed

A 16 cell laminated module was adapted for evaluation of light transmission properties. The material to be tested is placed on the glass faceplate of the laminated module. Cyclohexane (index of refraction = 1.42662) is used as an optical coupling agent to minimize reflections at the interface between the test material and the glass module face. The current-voltage curve is measured in a solar simulator with and without the test specimen in position. The combined effect of test material absorption and difference in the reflection between the test absorption and difference in the reflection between the test material and glass module surface can be inferred from the observed short circuit current.

Samples of double strength (0.125 inch) low iron content sheet glass (LO-IRON®) and water clear (SUNADEX®) glass obtained from ASG Industries Inc. were tested in this equipment. These glasses are specified by the manufacturer to have nominal iron contents of 0.05% and 0.01% respectively. Observed values of short circuit current and current at a test voltage of 7.2 volts are reported in Table 3.16-1. Since in this case the test samples are glass, the difference in reflection will be zero to a first approximation. The observed effects are therefore all attributable to absorption. Although not measured in this experiment, we have observed that ordinary float glass (iron content 0.12%) causes a reduction in output of the test module of 6 to 12 percent. We have received quotes for large quantities of SUNADEX® and LO-IRON® and float glass from ASG Industries which are given in Table 3.16-2. Using this cost data and the transmission data from Table 3.16-1 one can estimate the relative cost effectiveness of these two glasses. Assuming a module efficiency of 12% with the use of LO-IRON® glass, the 2% increase in output (at load) with SUNADEX® glass would result in module power increasing from 11.15 watts per square foot to 11.37 watts per square foot. The increase of 0.22 watts would cost $1.09 per watt ($0.69-0.45) ÷ 0.22). Thus under the assumed conditions, use of SUNADEX® glass would be cost effective only if the baseline module cost exceeds $1.09 per watt.

After this evaluation was completed the LO-IRON® glass became unavailable. Assuming the loss due to absorption in float glass to be 6% one can estimate the baseline module cost above which the SUNADEX® type glass would be cost effective. In this case the power differential per module would be 0.62 watts per square foot (11.37 x (.060-.0052)). The cost associated with this differential would be $0.353 (($0.69-$0.47) ÷ .62) for 1/8 inch thick glass. Thus for this combination the use of SUNADEX® glass would be cost effective if the baseline module cost exceeds $0.353 per square foot.

Table 3.16-1

Transmission Measurements of 1/8" thick SUNADEX© glass and LO-IRON® sheet glass using 16 cell solar circuit test panels.

	I_{sc} (mA)	$I_{7.2}$ (mA)	V_{oc} (V)	I_{sc} (mA)	$I_{7.2}$ (mA)	V_{oc} (V)
Test Panel	649	580	9.32	-	-	-
LO IRON ©	627	565	9.31	-3.39	-2.58	-0.11
SUNADEX ©	642	577	9.30	-1.08	-0.52	-0.21

Table 3.16-2

Glass prices for large quantity purchases of standard sizes furnished in standard cases. Minimum of 20 cases of one type of glass. Source: ASG Industries, Kingsport, Tennessee.

Thickness inch	Std. Size inch	Price $ per sq. ft. SUNADEX	LO IRON sheet	STARLUX float
1/8	34 x 76	.69	.45	.47
5/32	34 x 76	.80	.53	NA
	34 x 96	.80	NA	NA
3/16	46 x 76	.91	.61	.51
7/16	46 x 96	1.03	NA	NA

Standard Case Weight & Footage

	SUNADEX	LOW IRON	STARLUX
*1/8	2000# 1200'	2000# 1200'	3000# 1200'
5/32	2000# 1000'	2000# 1000'	NA
3/16	2000# 900'	2000# 900'	2700# 1000'
7/16	2000# 700'	NA	NA

*Shipping cost .12 per sq. ft.

An evaluation was made of the acid etch process for forming an antireflective coating on glass. This process uses a supersaturated solution of silica in fluosilicid acid to selectively dissolve the metal components in the glass.[4] The result is a thin layer of skeletonized pure SiO_2. Due to its porous nature this layer has a low refractive index and can act as an AR film. The selective etching properties of the acid solution depend critically on the silica supersaturation, an essentially unstable condition. We do not believe this process will be an effective, controllable production process because of the solution instability.

Another process for forming antireflective coatings on glass is the development of an SiO_2 layer by acid hardening of a film of sodium silicate (water glass) in aqueous solution. This process has been investigated by Motorola.[5] In their work the sodium silicate solution was applied by photoresist spinning techniques. The films produced were less effective than acid etched films, with peak transmission losses of approximately 1% per side.

We have evaluated coatings formed from water glass films applied by dipping into the solution and, in general, verified the Motorola observations regarding transmission. Effectiveness of the coatings is strongly dependent on uniformity. We have concluded that the process is not adequately developed to handle large panels of glass, moreover the effectiveness leaves something to be desired.

Because of these considerations, we recommend deletion of this step in the process sequence for the present, however, we considered that the potential improvement in module efficiency is so great that further efforts should be made to develop a suitable process. Reflective losses from glass cover panels amount to about 4%. Assuming a module price of $0.50 per watt and a module efficiency of 12%, elimination of this loss would be worth about $2.40 per square meter.

Chemically vapor deposited (CVD) coatings of silicon dioxide and stannic oxide were applied to glass panels by Watkins and Johnson Company. Nominal coating thicknesses were 800, 1000 and 1200 Å. Spectral light transmission in the 300 Å to 10,000 Å wavelength range were measured on each specimen and on an uncoated glass control using a Beckman DK-2A spectrophotometer.

The results showed essentially the same pattern for all the silicon dioxide coated specimens. Comparison to the control indicated approximately a 3% increase in transmission at 10,000 Å decreasing to less than 1% at 5000 Å and on out into the ultraviolet.

The stannic oxide coated specimens showed transmission peaks at about 7750 Å for the 1200 Å coating, 5750 Å for 1000 Å, and 5300 Å for 800 Å. These probably constitute quarter wavelength antireflection peaks. However, the three stannic oxide-coated specimens all showed generally poorer transmission than the control due to the unfavorable index of refraction. The 1200 Å coating showed about a one percent improvement over the control in the immediate region of its peak, but all other regions were significantly below the control. Transmission of the other stannic oxide coatings did not exceed that of the control sample anywhere in the measured region.

3.17 CELL BONDING METHOD OF ENCAPSULATION

3.17.1 Recommendations

No suitable adhesive for bonding cells to the glass superstrate was found except silicones. The high cost of these materials renders them unattractive for use in low cost modules. This is reinforced by the fact that the rise of a silicone adhesive would make application of polymeric back coatings other than silicones difficult, if not impossible. Because of these cost problems we recommend that the bonding and coating process sequence for module assembly be set aside and laminating techniques using polyvinyl butyral or ethylene vinyl acetate be substituted.

Various candidate materials for the protective back coating have been considered. We recommend that further work in this method of encapsulation be discontinued.

3.17.2 Work Performed

A variety of materials was considered for cell bonding. Products which were procured and evaluated are listed in Table 3.17-1.

Bonding Method

Preliminary cell bonding experiments showed some problem areas in this operation. These included relative displacement between cells and superstrate because of sliding at the glue line before the adhesive set, creeping of adhesive around the edge of cells onto unbonded back surfaces, and bubble entrapment in the glue line.

The cell-glass displacement problem reflects the difficulty in holding individual cells in place during assembly and cure operations. This is expected to be less of a problem in an automated system which could be designed with individual cell holding devices.

Table 3.17-1

STATUS OF CANDIDATE ADHESIVE MATERIALS

MANUFACTURER	IDENTIFICATION	TYPE	COMMENTS
Retained for further consideration:			
General Electric	RTV 615	Silicone RTV	
Dow Corning	96-083	Silicone Adhesive	
General Electric	RTV 2144-131	Silicone RTV	
Springborn Labs	EVA	Ethylene Vinyl Acetate Sheet Compounded from DuPont Elvax 150	
Eliminated:			
Dow Corning	Q1-2577 (mica)	Silicone B Stage	Poor light transmission
Dennison	Densil tape	Double Backed	Bubbles and unbonded areas
Loctite	Loctite 524/525	Acrylic/accelerator	Poor light transmission
Hughson	Versilock 506/4	Acrylic/accelerator	Poor light transmission
Hughson	Versilock 521/4	Acrylic/accelerator	Poor light transmission
Franklin	Rexite P2/SB	Acrylic/accelerator	Poor light transmission
Hysol	EA9446/AB	Acrylic/accelerator	Poor light transmission
Ciba-Geigy	DA-560-4	Acrylic UV Cure	Poor temperature resistance
Rhom and Haas	Acryloid B-7	Acrylic, Thermo-plastic	Bubbles and unbonded areas, poo temperature resistance
Dow Corning	X3-6558	Silicone gel	Poor adhesion and permanently soft, tacky surface
Loctite	353	Acrylic UV cure	Loss of transmission λ<1000m μ after UV exposure
Loctite	524	Acrylic heat cure	Loss of transmission λ<700m μ after UV exposure
Shell	Epon 828/Versamid 125	Epoxy	Loss of transmission λ<550m μ after UV exposure

Adhesive creeping around onto cell back surfaces appeared to be mainly the result of capillary action. The use of a flat pressure plate to hold the cells down against the glass resulted in the two surfaces, glass and pressure plate, so close together that any adhesive squeezed from the glass-cell bond line filled the space around the cell periphery and was drawn into the cell-pressure plate interface by capillary action. Therefore, assembly procedures providing greater glass to pressure plate separation appear desirable.

The bubble problem resulted primarily from air entrapment when two precoated surfaces were joined. Therefore, testing was directed toward development of an assembly procedure in which precoating is not used, and the adhesive is applied so that it spreads over the bonding surfaces as they are brought together. This minimizes bubbles by driving air out ahead of the advancing glue line.

In connection with these cell bonding experiments, attention was also directed toward the need for methods which have potential for development into automated procedures. These considerations led to the conceptual design described in Section 3.19.2 for automated cell bonding.

Tooling to simulate this design was fabricated for adhesively mounting cells on a 2 ft. by 4 ft. superstrate. It was used successfully to position and bond two 10 x 20 cell arrays, one each of 2" round cells and 2.12" square cells. The positioning fixture was designed to place the 2.12" square cells in an array with a nominal spacing of .050" between cells. A vacuum is used to hold the cells retracted against a foamed plastic pressure pad. After applying adhesive to the cells and lowering the glass superstrate onto the array, the vacuum is released so that the pressure pads press the cells against the superstrate forcing the adhesive to spread. A clamping mechanism applied to the superstrate prevents its being lifted by a few cells which might allow others to shift laterally.

The initial positioning and vacuum hold-down prior to bonding cells to superstrate appeared to be perfectly satisfactory. However the clamping mechanism to maintain the cell array configuration during bonding allowed some of the cells to experience a small initial displacement when the vacuum was released. It was found that by reaching under the fixture with a stiff wire, manual repositioning was possible before the bonding material cured. On the panel assembled with square cells there were eleven cases of displacement which required such repositioning to correct cell-to-cell spacing. At this point no further cell drift occurred, and a satisfactory bonded array was obtained.

Positioning tolerances are less critical with two inch round cells. Therefore, larger displacements can be tolerated, and all cell-to-cell spacings on this panel fell well within acceptable limits. The release of the hold-down vacuum also resulted in entrapment of some bubbles in the bond between cells and superstrate. The sudden release of the cells causes them to be pressed too quickly against the superstrate. This does not allow sufficient time for uniform spreading of the bonding material out from the center of the cell. Therefore encirclement and entrapment of air occur causing the bubble formation. This interpretation is substantiated by the fact that another fixture without the vacuum holding feature was previously used at Spectrolab, and bubble formation was insignificant by comparison. However that fixture was much less accurate in positioning and holding the cell array configuration.

Another factor which may affect bubble formation is the time required to apply the bonding material to all the cells of the array. This results in much more spreading on the first cells compared to the last to which the adhesive was applied. These cells have a greater likelihood of forming bubbles when contacted by the glass.

We believe that the deficiencies in this design could be easily eliminated in a production design.

Thermal Stresses in Bonded Solar Cell Panels

Stresses are induced in bonded silicon solar cells when there is a mismatch of thermal expansion between superstrate and silicon cell. A service temperature range of $-40^{\circ}C$ to $+90^{\circ}C$ results in differential of plus or minus $65^{\circ}C$ if cell adhesive is cured at $25^{\circ}C$. From an engineering point of view, selecting a panel material of matching thermal expansion coefficient is the logical solution, however, those materials which have suitable matched coefficients are considerably more expensive than can be justified. Considerably cheaper panel materials may be used if resilient adhesives are used to limit the stresses caused by differential thermal expansion.

A simple stress analysis shows that the stress in silicon is a maximum at the center of the cell, and the maximum stress can be expressed as:

$$S_{silicon} = \frac{0.125\ G(\alpha_{panel} - \alpha_{silicon})\Delta T\ L^2}{(t_{adhesive})\ (t_{silicon})} \qquad (1)$$

Where:
- G is the shear modulus of the adhesive (lbs/in^2)
- α_{panel} is coefficient of linear thermal expansion of the panel ($in/in/^{\circ}C$)
- $\alpha_{silicon}$ is coefficient of linear thermal expansion of silicon ($in/in/^{\circ}C$)
- $t_{adhesive}$ is the thickness of the adhesive (in.)
- $t_{silicon}$ is the thickness of the silicon (in.)
- Δ_T is the temperature differential from the adhesive cure temperature

and
- L is the lateral dimension of the silicon (in.).

Equation (1) shows that the stress introduced in the silicon is directly proportional to the shear modulus of the adhesive; therefore a low-modulus adhesive is helpful in reducing stresses. Stress is also directly proportional to the mismatch of coefficients; therefore the more expansive panel materials will require compensation in other parameters. Stress is inversely proportional to the thickness of the adhesive; therefore a greater thickness of adhesive may be required for more expansive panels. Stress is inversely proportional to the thickness of the silicon; therefore economizing with thinner cells must be accompanied by compensation in other parameters. Finally, the stress level increases as the square of the cell width, requiring appropriate adjustments as cell size increases. Since the expansion coefficient of silicon is smaller than that of any practical panel materials, the silicon stress will be compression for temperatures below the adhesive cure temperature and tension for temperatures above the adhesive cure temperature. Elevated cure temperatures can therefore be used to limit the development of tensile stresses.

Stresses can be limited by using a low-modulus, resilient adhesive to bond cells to glass, however, differences in length produced by temperature change must be accommodated by shear strain in the adhesive. The shear strain in the adhesive will be a maximum at the edge of the cell (Figure 3.17-A), where it will be

$$\gamma = \delta / t_{adhesive}$$

$$= \frac{L(\alpha_{panel} - \alpha_{silicon})\Delta T}{2\, t_{adhesive}} \qquad (2)$$

The variation of adhesive shear strain with cell dimensions and glue line thickness is shown in Figure 3.17-B for cells bonded to sodalime glass with a $65^{o}C$ ΔT.

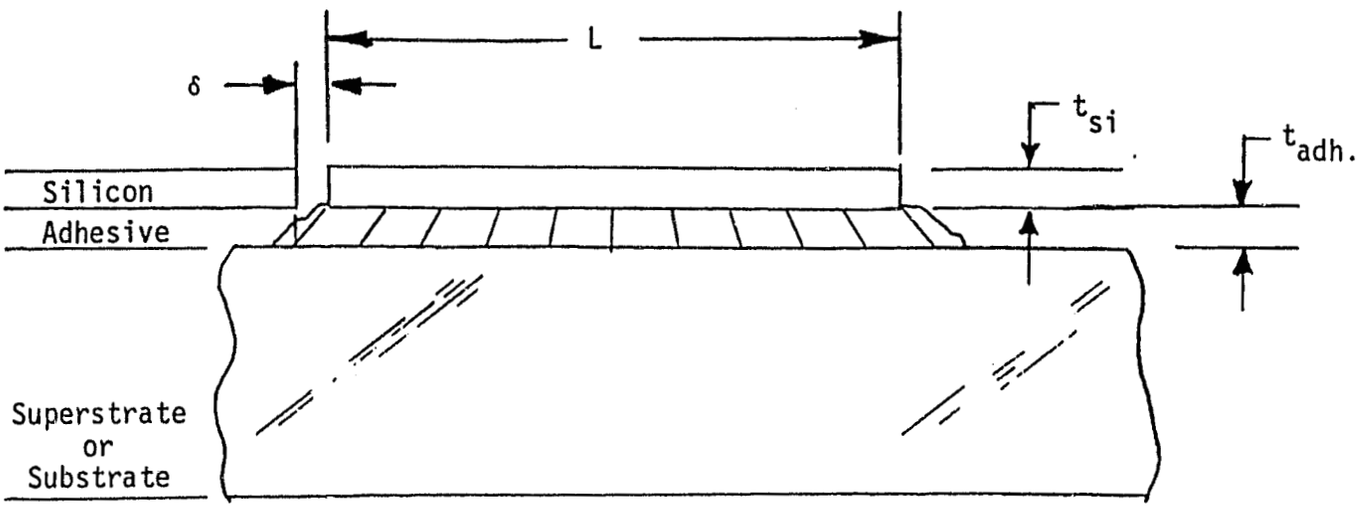

Figure 3.17-A Shear strain in adhesive between silicon solar cell and panel

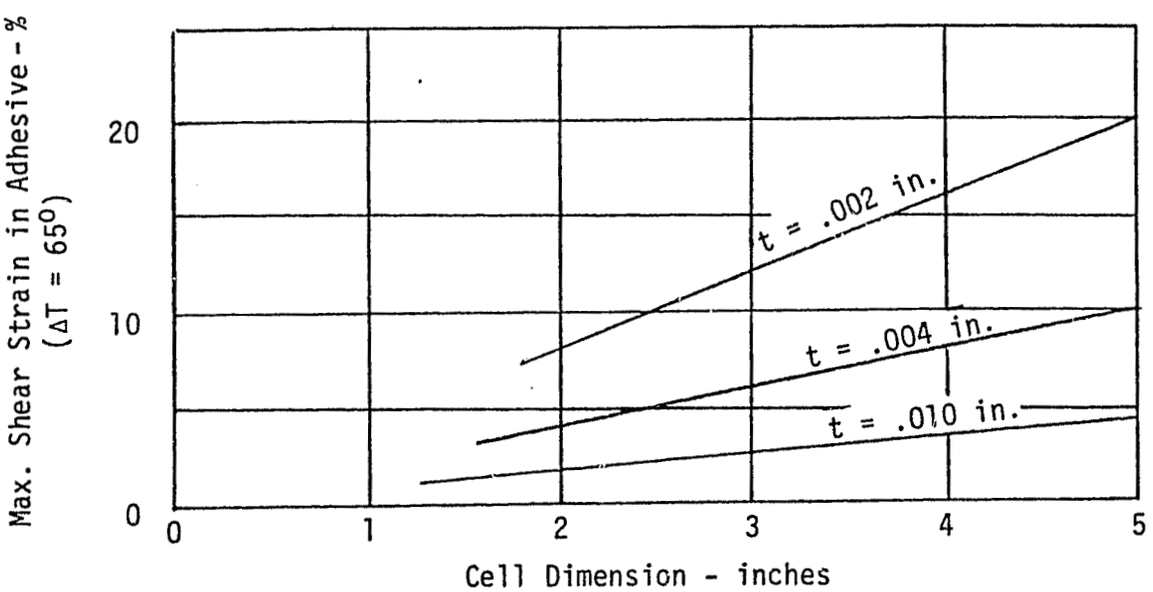

Figure 3.17-B Effect of cell size and glue line thickness on adhesive shear strain, solar cells bonded to soda-lime glass with silicone RTV.

For General Electric RTV 615, ultimate uniaxial shear strain can be approximated at 90%. (Shear deformation data are not available. GE lists 925 psi as the tensile strength and 150% as the elongation. GE technical personnel offered that shear properties might be approximately 60% of tensile.) In view of the biaxial nature of the stress, the allowable shear strain should be much lower, perhaps 20-25%. For this adhesive Figure 3.17-B suggests that the minumum glue line thickness should be about 0.004 inches for cells having lateral dimensions of 4-5 inches. If an elevated cure temperature (150^{o}C) is used and subzero environmental temperatures are expected, the minimum glue line thickness should be increased to .008 or .009 inches in order to accommodate the larger ΔT to the low end of the temperature cycle.

Thermal stress was investigated by subjecting test specimens to cycling from 100^{o}C to progressively lower temperatures to determine the temperature at which differential thermal expansion reached a damaging level. Test specimens consisted of two interconnected 3" solar cells bonded to a glass panel. Bonding materials used include RTV 615 Silicone, 96-083 silicone, and Epon 828/Versamid 125. The same cure temperature, 150^{o}C, was used for all specimens. Specimens were examined for any evidence of damage after each successive low temperature exposure, and also solar cell electrical output measurements were made before and after each cycle.

The low temperature extreme tested -80^{o}C. At this point electrical output has been virtually unaffected, and no detectable mechanical damage has occurred. The one detectable effect was a slight yellowing of the Epon 828/Versamid 125 adhesive.

Bond Strength, Environmental Effects

Adhesive bond strengths as determined by lap-shear tests were measured with and without exposure to thermal cycle and 95% relative humidity. Results for a number of candidate adhesives are

reported in Table 3.17-2. Specimens consisted of appropriate sized cell fragments prebonded to a backing plate and then bonded with the test material to a microscope slide. The microscope slide provides a convenient 1" wide glass member and the bond can be made with a measured overlap in the configuration of a standard lap shear specimen. Most materials also required a metal backing bonded to the glass in order to provide strength enough to insure fracture at the test joint. In fact the bending moment at the joint was such that stronger adhesives caused the brittle glass and cell material to crack in a fragmented pattern which tended to reduce apparent bond strength by reducing effective areas of bond.

The effect of a swelling solvent on coated specimens is the basis of another test to evaluate the resistance of interfacial bonds to permeating species. In order to evaluate the method, several different silicone primer systems were used in the application of RTV 615 silicone coatings to solar cell surfaces. These specimens were then immersed in xylene to swell the silicone coating, and the time required for any visible wrinkling or lifting was observed. A similar test was made using Sylgard 184 silicone. The results in Table 3.17-3 show the times of exposure required for the onset of visible evidence of delamination. The significance of this relative to real time weatherability of the coatings is not immediately evident, however, it does very quickly show distinct differences and should be effective at least as a screening test for distinguishing between materials.

The candidate materials for the protective back coating and their status as of the end of the period are listed in Table 3.17-4.

The primary test used for screening coating materials was adhesive bond strength before and after environmental exposure was measured

Table 3.17-2

ADHESIVE BOND STRENGTH/ENVIRON

LAP SHEAR STRENGTHS LBS/IN^2

(AVERAGE OF APPROX. 10 SPECIMENS)

MATERIAL	AS BONDED, CONTROL			THERMAL CYCLE -40°C to 90°C			HUMIDITY @ 70°C		
	CELL TO CELL	CELL TO GLASS	GLASS TO GLASS	CELL TO CELL	CELL TO GLASS	GLASS TO GLASS	CELL TO CELL	CELL TO GLASS	GLASS TO GLASS
RTV 615	145		173	86		191	250		218
RTV 615/4120 Prim	325		406	345		327	386		315
RTV 615/4155 Prim			205			234			266
RTV 615/1204 Prim		56.5			121			57.0	.
RTV 615/Sylgard Prim		290			473			420	
X3-6558	7.5		123	8.5		125	12.3		161
Loctite 524	812		448	566		428	369		280
Epon 828/Vers 125	744	740	284	272	764	273	436		278
Loctite 353 U.V.		527	572		766	591	468		453
96-083	474		279.5	540		384.6	423		417.2
GE 2144-131	79.4		37.8	77.4		66.8	100.4		72.4
GE 144-131/4120	107.8		52.8	122.4		86.8	145.4		120.6
EVA			105*						
EVA/Z 6020 Primer			249*						

*Less than 10 specimens

Table 3.17-3

RESISTANCE OF SILICONE ELASTOMERS TO SWELLING IN XYLENE

PRIMER COUPLING TESTS

	1st Detectable Lifting	
Primer	RTV 615	Sylgard 184
SS 4155	10 min.	30 min.
SS 4120		2 min.
Q3-6060	10 min.	10 min.
1204	2 min.	2 min.
Sylgard	2 min.	2 min.
Piccotex	1 min.	1 min.

Table 3.17-4

STATUS OF CANDIDATE PROTECTIVE COATING MATERIALS

MANUFACTURER	IDENTIFICATION	TYPE	COMMENTS
Retained for further consideration:			
Dow Corning	Q1-2577	Silicone Coating	
Dow Corning	X3-5063	Silicone Emulsion	
Contour Chec. Co.	XB-1786	Silicone Coating	
Product Techniques	PT 469 Clear	Modified Acrylic	
Bostic Finch	MIL-C-83286	Polyurethane	
Rustoleum	C-1500 white	Alkyd	(Primer needs to be identified)
DuPont	Elvax 150	Ethylene Vinyl Acetate	
Advanced	Urafilm 1-1c-5	Polyurethane	
Eliminated:			
General Electric	RTV 615	Silicone	Poor adhesion
Rohm & Haas/Mobay	QR-568/ Desmodure N75	Oxazolidine Acrylic Polyurethane	Delamination during thermal cycle
Rohm & Haas	Acryloid B-7	Acrylic	Poor adhesion
Dow Corning	R-4-3117	Silicone Coating	Poor adhesion
Photo Chem Prod.	Perma Resin	Epoxy-Acrylic	Poor adhesion after humidity exposure
Deft Chem. Coat.	MIL-L-81352	Acrylic	Poor adhesion

by peel strength. One lb/in. was arbitrarily set as the lower limit for peel strength. Any exposure test resulting in strengths below this level was considered cause for elimination of that candidate material. The data and also supplemental experience from handling the test specimens indicate that several of the materials may continue to cure during exposure, especially during thermal cycle, and exhibit improved properties compared to control specimens. The specimen consisted of a 1 inch wide specimen with a fiberglass tape embedded in the coating material. Force was applied by means of a Hunter Spring RM Tester equipped with a pull test fixture.

Peel strength results are summarized in Table 3.17-5. Peel strength entries shown as >2 represent coating materials with peel strengths too high to be measured by this method. This includes any material with properties such that its peel strength is greater than the apparent strength of the fiberglass cloth tape used to apply the peeling stress to the coating, however, this apparent strength of the fiberglass varies over a wide range. The lower part of the range appears to result from stiffening of the fiberglass cloth by impregnation with the coating materials. With the higher modulus coatings this causes flectural fracture at loads very much below those for normal tensile failures of unstiffened fiberglass. Therefore the method tends to be invalid for the higher modulus coating materials. The >2 reported for these peel strengths is somewhat arbitrary, but on the basis of supplemental observation, scraping, tape pull tests, etc., 2 lbs/in. appears to be a reasonable minimum for the materials involved.

Table 3.17-5

COATING MATERIALS EXPOSURE/ADHESION TESTS

	Peel Strength Tests (pound/inch) (Average Approx. 10 Specimens)					
			Thermal Cycle -40° to 100°C		Humidity 95% 70°C	
Material	Cell	Glass	Cell	Glass	Cell	Glass
Q1-2577	0.6	0.2	0.6	0.2	0.2	0.1
R4-3117	1.3	0.1	1.1	0.1	1.2	0.1
X3-5035	1.7	1.8	1.9	1.9	1.1	1.0
MIL-C-83286	3.64	1.84	3.38	1.02	1.62	1.69
MIL-L-81352	.645	.08	1.06	.009	.52	.37
XB-1786	0.60	0.81	0.61	0.89	0.60	0.93
XB-1786 (w/primer)	0.74	0.96	0.68	0.91	0.66	0.62
C-1590 white	0.95	0.54	0.66	0.39	0.82	0.90
PT469 clear	>2	>2	>2	>2	>2	>2
PT469 white	>2	>2	>2	>2	>2	>2
Perma Resin	>2	>2	>2	>2	>2	.49
MIL-C-83268 with AP-131 Primer	>2	2.5	>2	2.4	>2	>2
Elvax 150	3.2	2.7	1.36	.57	1.16	1.0
Elvax 150/Z6020 Silane Primer	2.5	2.8	.52	2.1	.54	3.1
Elvax 150/Piccotex-Z6020 Primer	1.7	2.5	.62	1.5	.58	2.0
Ultrafilm 1-1c-5	>2		>2		>2	

3.18 LAMINATION METHOD OF ENCAPSULATION

3.18.1 Recommendations

We recommend the use of Ethylene Vinyl Acetate as the material for encapsulation using a vacuum lamination technique.

3.18.2 Experimental

Ethylene Vinyl Acetate (EVA)

The EVA formulations used in this research have been prepared by Springborn Laboratories (Enfield, CT). The clear formulation is #A-9918, and the pigmented version is A-9930. These materials are based on Elvax 150 EVA with cross linking agents, UV screening compounds, anti-oxidants, and pigments added. The final product is an extruded sheet $\sim$ 16 mils thick. More detailed formulation may be obtained by contacting Springborn Laboratories.

These formulations are well suited to the solar cell encapsulation application. When heated, the material passes through a thermoplastic stage at which time gas removal is easily achieved. At a higher temperature the peroxides in the formulation decompose and cause thermosetting through cross-linking of the saturated backbone of the polymer.

Double Vacuum Bag Technique

A double vacuum bag laminating technique was developed when initial experimentation with a single vacuum bag technique was found to be unsuccessful. The use of the second bag duplicates conditions in a true double vacuum chamber. The design of the

fixture utilized in this technique is shown in Figure 3.18-A. Briefly, the tooling consists of a flexible silicon heater and second chamber above the module containing chamber.

The lamination procedure commences by placing the module in the bottom vacuum bag chamber. A 0.010 Teflon FEP sheet is used as a release sheet. A 1/8" silicone face sheet over the teflon completes this chamber. Nylon sheeting is used as the vacuum bagging material. The second chamber contains a 1/8" aluminum sheet and scrim cloth to ensure easy evacuation. A laminating sequence consists of first evacuating both chambers and heating the module, then releasing the top vacuum and heating further. Figure 3.18-B shows the thermal cycle used during lamination. Initially the module sees the pressure through the 1/8" aluminum sheet. This sheet effectively bridges the pressure across the intercell spaces which allows gases to migrate to the edges and be removed. The 1/8" silicone sheet cushions any high points on the cells which might lead to breakage. After a suitable time period, atmospheric pressure is allowed to enter the top compartment. Pressure is now felt by the module through the silicone and Teflon sheets only; thus the EVA is molded into the intercell spaces as well as to the cell backs. Thermosetting of the EVA is complete in this mode when more heat is applied.

To test the viability of the double vacuum bag technique discussed above, two 2' x 4' modules were laminated. The following list represents the recommended layup order of materials:

a) 1/8" tempered glass
b) 5 mil Crane-Glas 230
c) Clear EVA
d) Cell circuit
e) 5 mil Crane-Glas 230
f) White EVA
g) 5 mil Crane-Glas 230
h) 1 mil Al/Polyester film

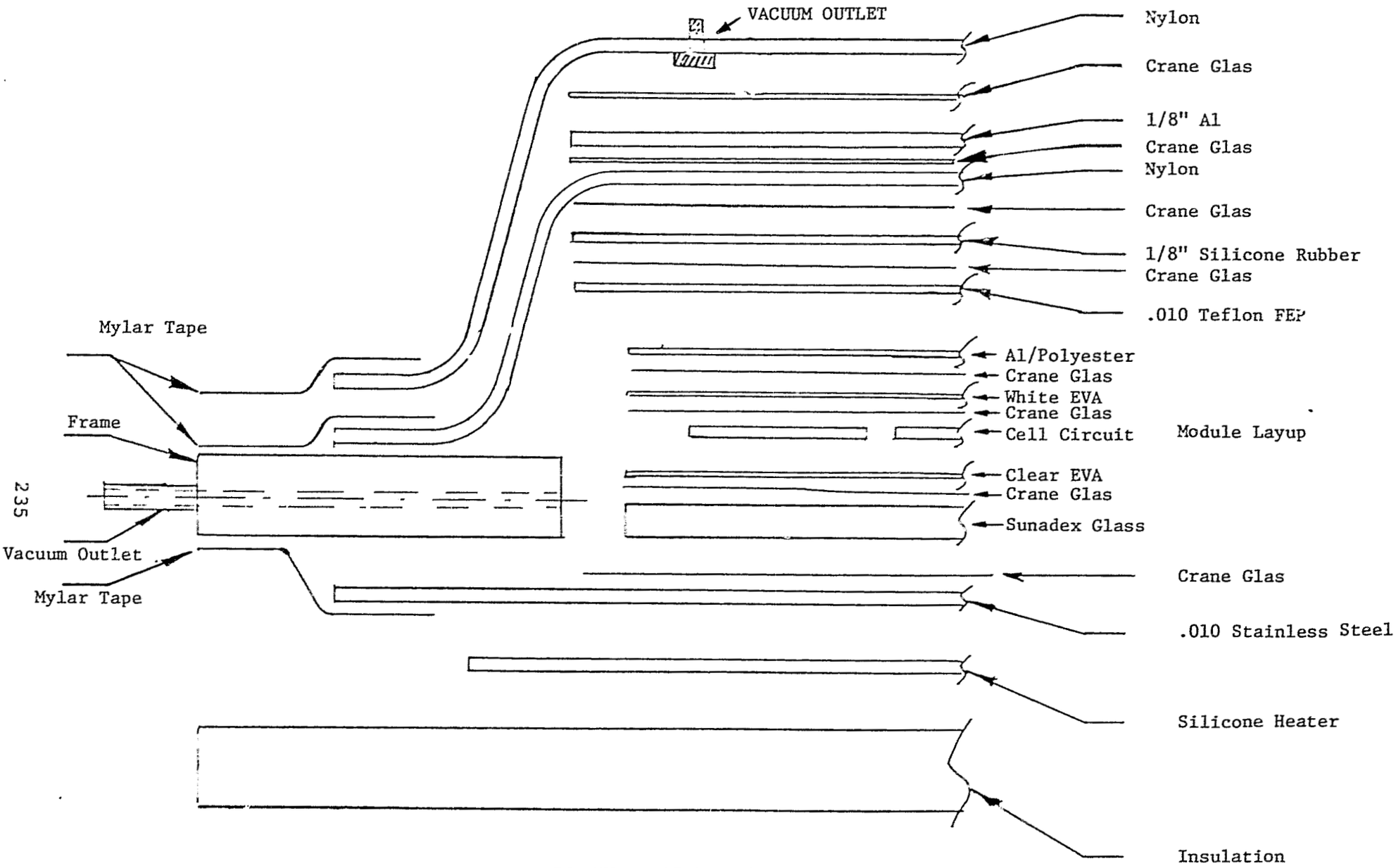

LAMINATING FIXTURE

Figure 3.18-A

AG 7/24/80

Figure 3.18-B

TIME/TEMPERATURE/PRESSURE
CYCLE - SOLAR MODULES
(Double Vacuum Bag Technique)

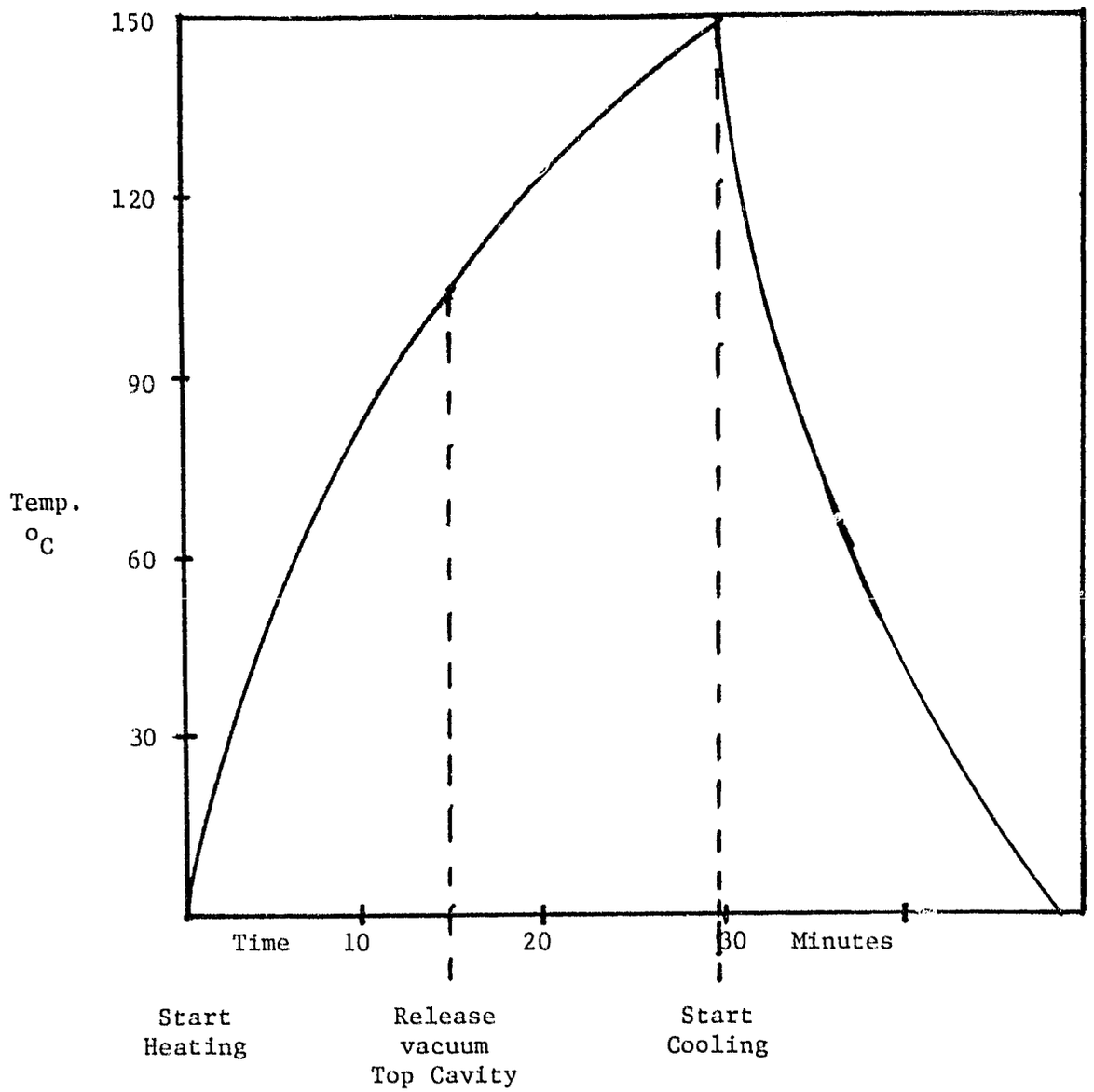

1. Assemble module, load into double vacuum bag.
2. Evacuate both cavities for 20 minutes, start heating.
3. Release top cavity vacuum at 100°C point.
4. Raise temperature to 150°C.
5. Cool, remove module.

There was no evidence of transmittance loss by utilizing 5 mil Crane-Glas in front of the cells. The lamination cycle was 28 minutes long with release of the upper vacuum bag vacuum when the module temperature reached 105°C. Work done on another JPL contract has indicated that the use of Crane-Glas in front of the cells leads to less than 1% transmittance loss. Figures 3.18-C and 3.18-D show the IV curves for the two verification modules constructed. See Section 3.21 for cell verification data.

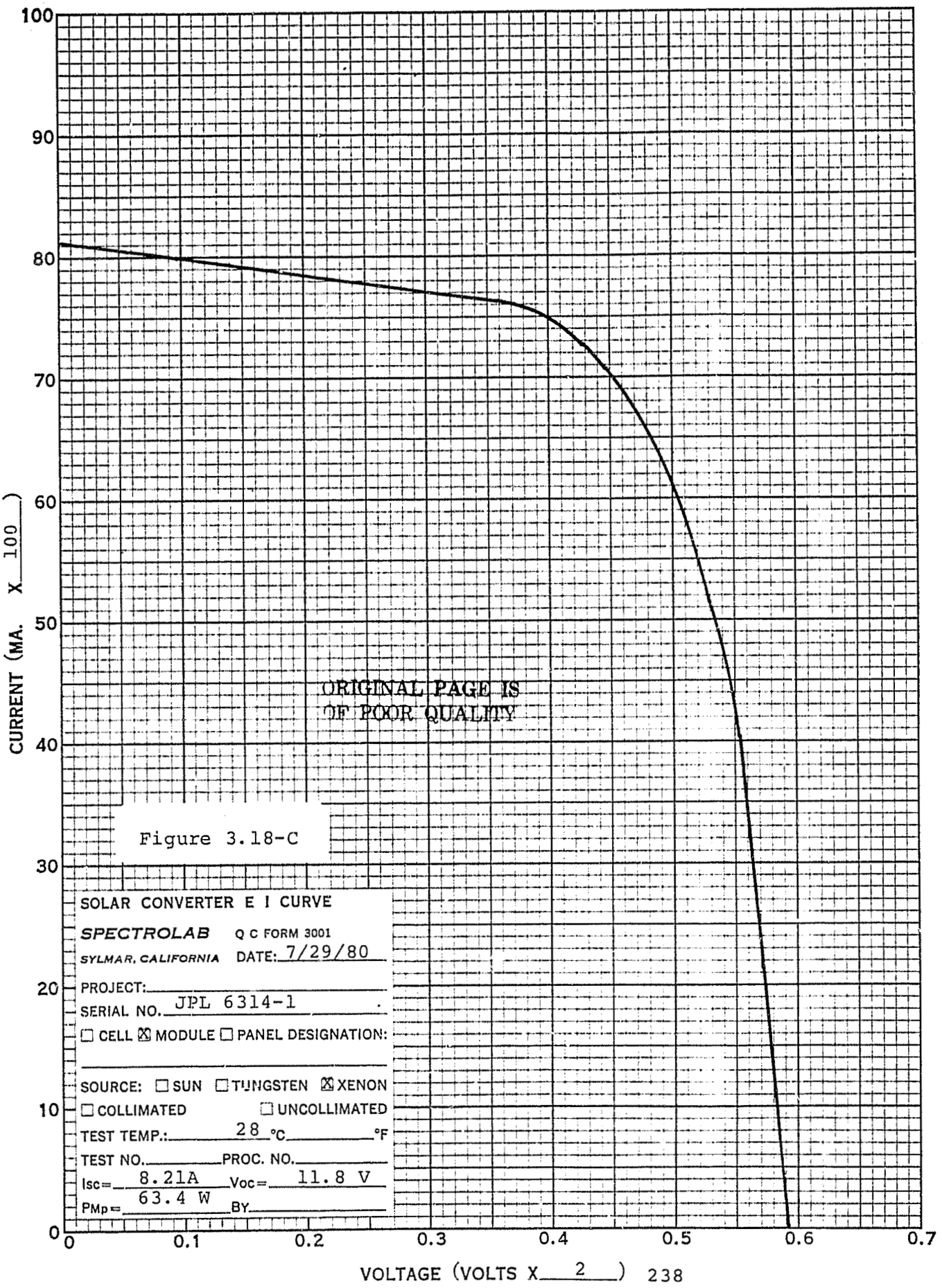
100
90
80
70
60
50
40
30
20
10
0
CURRENT (MA. X 100)
0
0.1
0.2
0.3
0.4
0.5
0.6
0.7
VOLTAGE (VOLTS X 2)
ORIGINAL PAGE IS
OF POOR QUALITY
SOLAR CONVERTER E I CURVE
SPECTROLAB Q C FORM 3001
SYLMAR, CALIFORNIA DATE: 7/29/80
PROJECT:
SERIAL NO. JPL 6314-1
☐ CELL ☒ MODULE ☐ PANEL DESIGNATION:
SOURCE: ☐ SUN ☐ TUNGSTEN ☒ XENON
☐ COLLIMATED ☐ UNCOLLIMATED
TEST TEMP.: 28 °C °F
TEST NO. PROC. NO.
Isc= 8.21A Voc= 11.8 V
PMp= 63.4 W BY

Figure 3.18-C

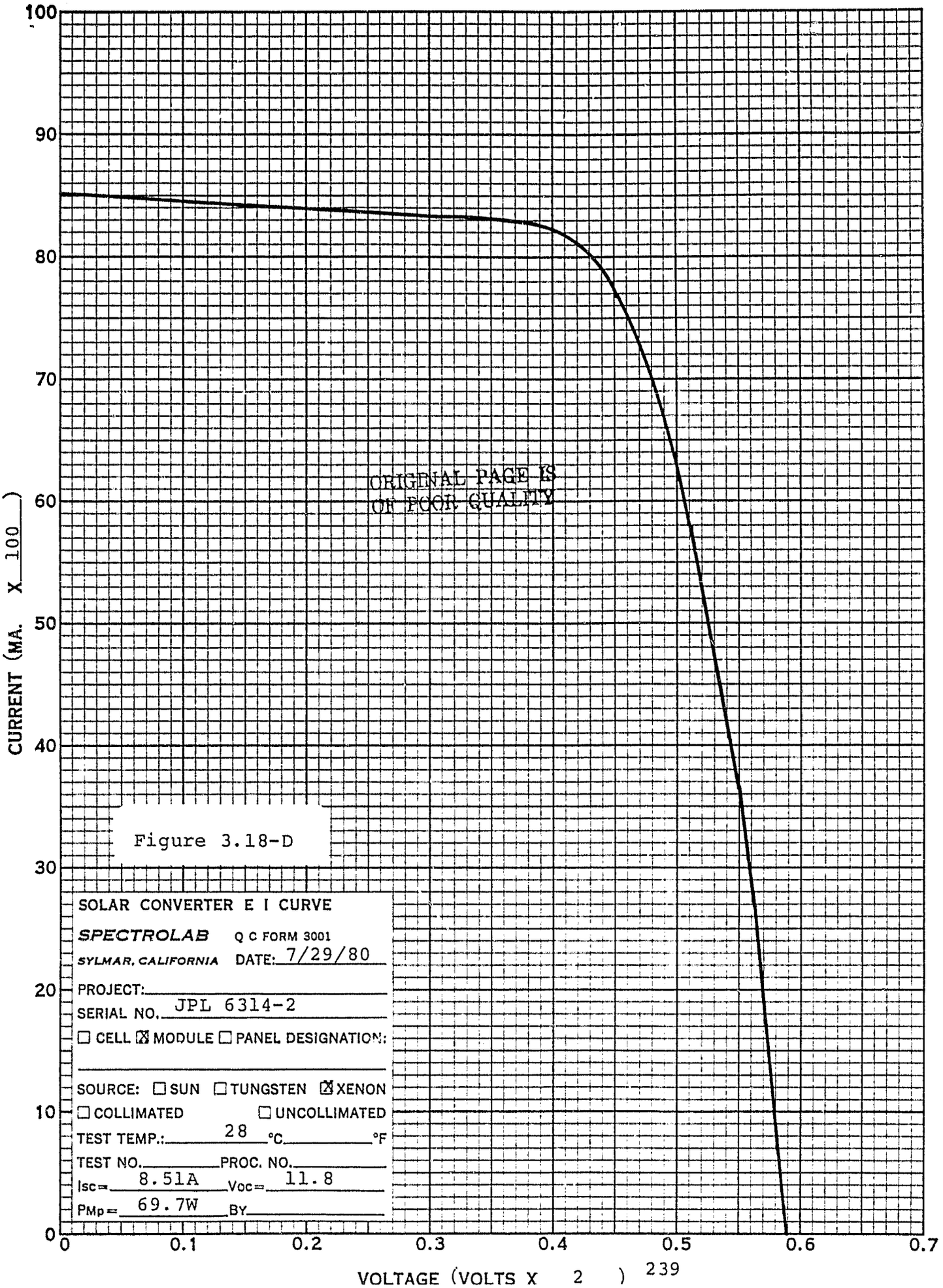
100
90
80
70
60
50
40
30
20
10
0
CURRENT (MA. X 100)
0
0.1
0.2
0.3
0.4
0.5
0.6
0.7
VOLTAGE (VOLTS X 2)
ORIGINAL PAGE IS
OF POOR QUALITY
SOLAR CONVERTER E I CURVE
SPECTROLAB Q C FORM 3001
SYLMAR, CALIFORNIA DATE: 7/29/80
PROJECT:
SERIAL NO. JPL 6314-2
☐ CELL ☒ MODULE ☐ PANEL DESIGNATION:
SOURCE: ☐ SUN ☐ TUNGSTEN ☒ XENON
☐ COLLIMATED ☐ UNCOLLIMATED
TEST TEMP.: 28 °C °F
TEST NO. PROC. NO.
Isc= 8.51A Voc= 11.8
PMp= 69.7W BY

Figure 3.18-D

3.19 MODULE DESIGN AND SOLAR CELL CIRCUIT

3.19.1 Recommendations

For purposes of verification testing of the cell and module process sequences we recommend a module design comprised of a 24 by 48 inch tempered glass superstrate to which is laminated a solar circuit encapsulated in ethylene vinyl acetate (EVA), the whole being mounted in an extruded aluminum frame. The solar cell circuit for the verification testing is to be comprised of 200 square cells having a nominal dimension of 2.12 inches on a side disposed in a 10 x 20 cell layout. Cells will be interconnected by means of solder coated copper ribbons into a circuit with 10 cells in parallel and twenty cells in series. For the 1986 module we recommend a similar configuration with larger size superstrate and cells as might be appropriate at that time.

The laminated structure and use of EVA as encapsulant recommended here is a departure from the original proposal of cells adhesively bonded to the superstrate with a subsequently applied protective coating material. This departure is the consequence of inability to find a suitable adhesive other than silicones as described in a another section.

3.19.2 Work Performed

Square cells cut from 3 inch diameter Czochralski crystals have been decided on as test vehicles for process verification in anticipation of larger square or rectangular sheet materials becoming available. The crystals will be shaped into prisms with square cross sections prior to sawing wafers. The nominal wafer dimension will be 5.3 cm (2.1 inches) on the side. A tentative module design (Figure 3.19-A) has been prepared comprised of a 10 x 20

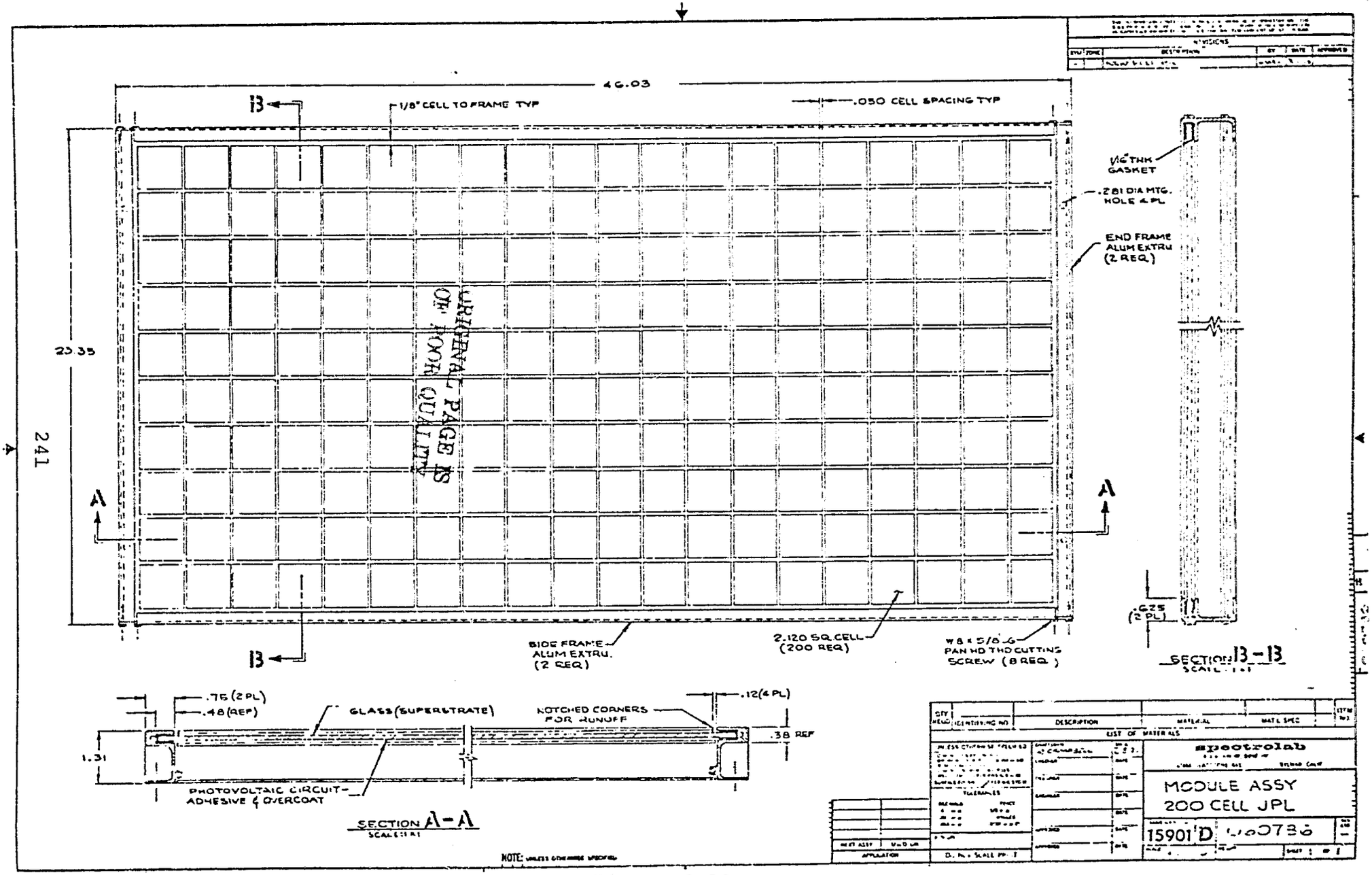
46.03
1/8" CELL TO FRAME TYP
.050 CELL SPACING TYP
23.35
B
A
ORIGINAL PAGE IS OF POOR QUALITY
1/16" THK GASKET
.281 DIA MTG. HOLE 4 PL
END FRAME ALUM EXTRU (2 REQ.)
.625 (2 PL)
SECTION B-B
SCALE 1:1
SIDE FRAME ALUM EXTRU. (2 REQ)
2.120 SQ CELL (200 REQ)
#8 x 5/8 PAN HD THD CUTTING SCREW (8 REQ)
.76 (2 PL)
.48 (REF)
GLASS (SUPERSTRATE)
NOTCHED CORNERS FOR RUNOFF
.12 (4 PL)
.38 REF
1.31
PHOTOVOLTAIC CIRCUIT ADHESIVE & OVERCOAT
SECTION A-A
SCALE 1:1
NOTE:
LIST OF MATERIALS
DESCRIPTION
MATERIAL
MATL SPEC
spectrolab
MODULE ASSY
200 CELL JPL
15901 D
100736

Figure 3.19-A

cell layout. Cells will be interconnected into a circuit with ten cells in parallel and twenty cells in series. Figure 3.19-B shows the superstrate design for this circuit. These circuits are expected to have a peak power of 84 watts at 28°C and either 9.4 or 18.8 volts respectively based on an assumed 15% cell efficiency. The corresponding module efficiency is

$$\frac{(2.10)^2 \times 200 \text{ (cell area)}}{46.03 \times 23.34 \text{ (module area)}} \times 14.5\% = 11.9\%$$

This is before encapsulation and interconnect losses are taken into account.

Cell-to-cell interconnects will be 1" lengths of 2 mil x 0.10 inch copper ribbon. The ribbon is OFHC copper with 1/2 mil solder plating that has been fused. Bus bar material is 3 mil x 0.40 inch copper ribbon, OFHC, 1/2 mil plate, fused. Using the wider ribbon as a bus bar at both ends of the panel (connected to ten 20-cell strings) with termination at the center, the power due to resistance loss in interconnects is approximately 0.3 watts. See Appendix E for calculations. These calculations are extremely conservative, using resistance at 75°C, power at room temperature and not including any conductance for the solder plate.

Cell Bonding Method Assembly Sequence

A design concept for the superstrate assembly is shown in Figure 3.19-C. At the adhesive application station, the cells for an entire superstrate are accurately located in a grid array. Cells are presented face up for automatic application of adhesive by mechanized dispensing heads. By applying a controlled amount of adhesive at the centers of the cells, bubble free adhesive joints will be obtained when the superstrate glass is lowered onto the adhesive mounds which then spread due to the weight of the glass.

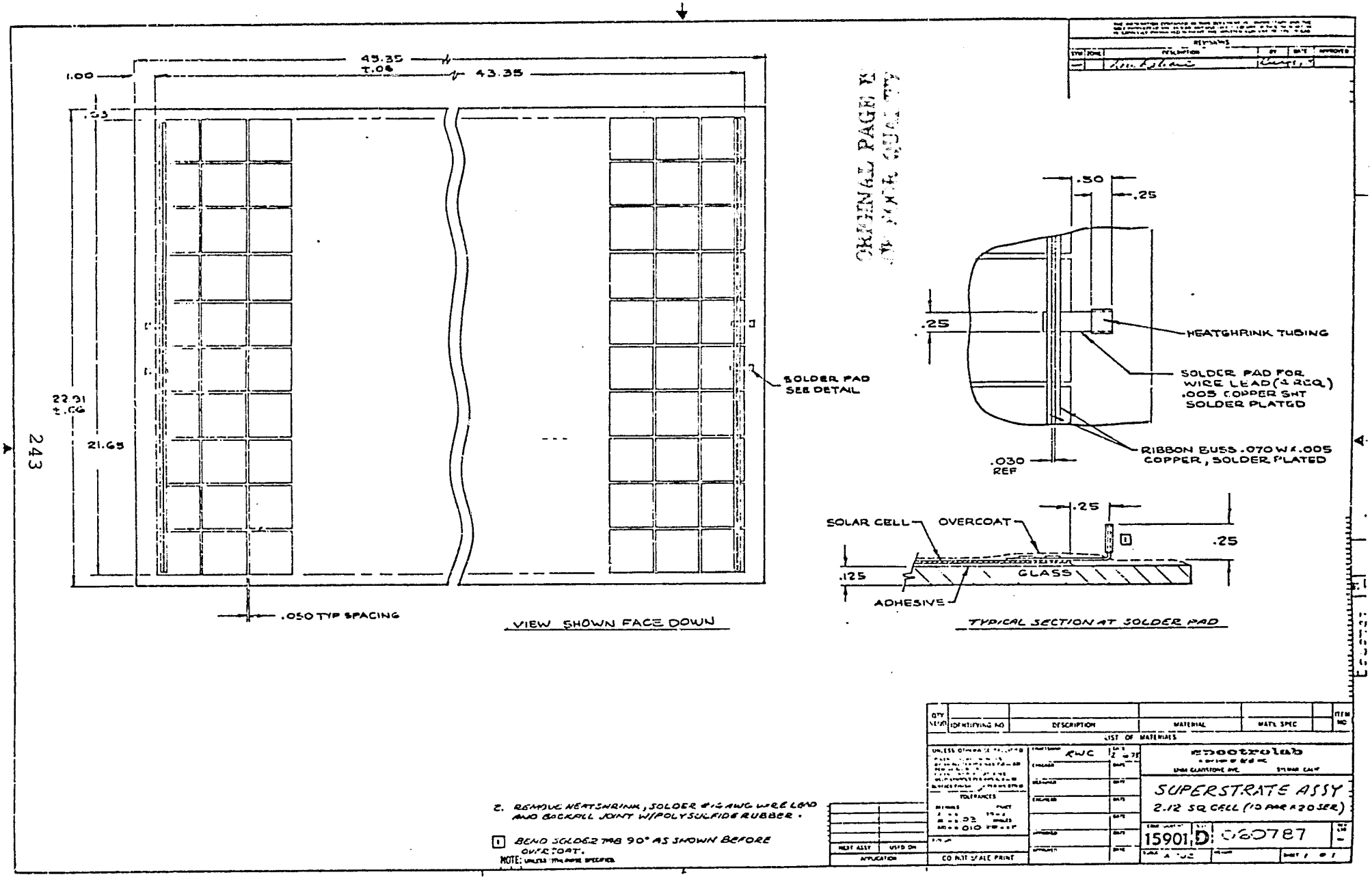
43.35
1.00
43.35
1.00
.05
22.31
21.65
.050 TYP SPACING
SOLDER PAD
SEE DETAIL
VIEW SHOWN FACE DOWN
.50
.25
.25
HEATSHRINK TUBING
SOLDER PAD FOR
WIRE LEAD (4 REQ)
.005 COPPER SHT
SOLDER PLATED
RIBBON BUSS .070 W x .005
COPPER, SOLDER PLATED
.030
REF
SOLAR CELL
OVERCOAT
.25
.25
.125
GLASS
ADHESIVE
TYPICAL SECTION AT SOLDER PAD
2. REMOVE HEATSHRINK, SOLDER #12 AWG WIRE LEAD AND BACKFILL JOINT W/POLYSULFIDE RUBBER.
1 BEND SOLDER TAB 90° AS SHOWN BEFORE OVERCOAT.
NOTE: UNLESS OTHERWISE SPECIFIED
LIST OF MATERIALS
QTY
IDENTIFYING NO
DESCRIPTION
MATERIAL
MATL SPEC
ITEM NO
UNLESS OTHERWISE SPECIFIED
TOLERANCES
RWC
SUPERSTRATE ASSY
2.12 SQ CELL (10 PAR x 20 SER)
15901, D
060787
NEXT ASSY
USED ON
APPLICATION
DO NOT SCALE PRINT

Figure 3.19-B

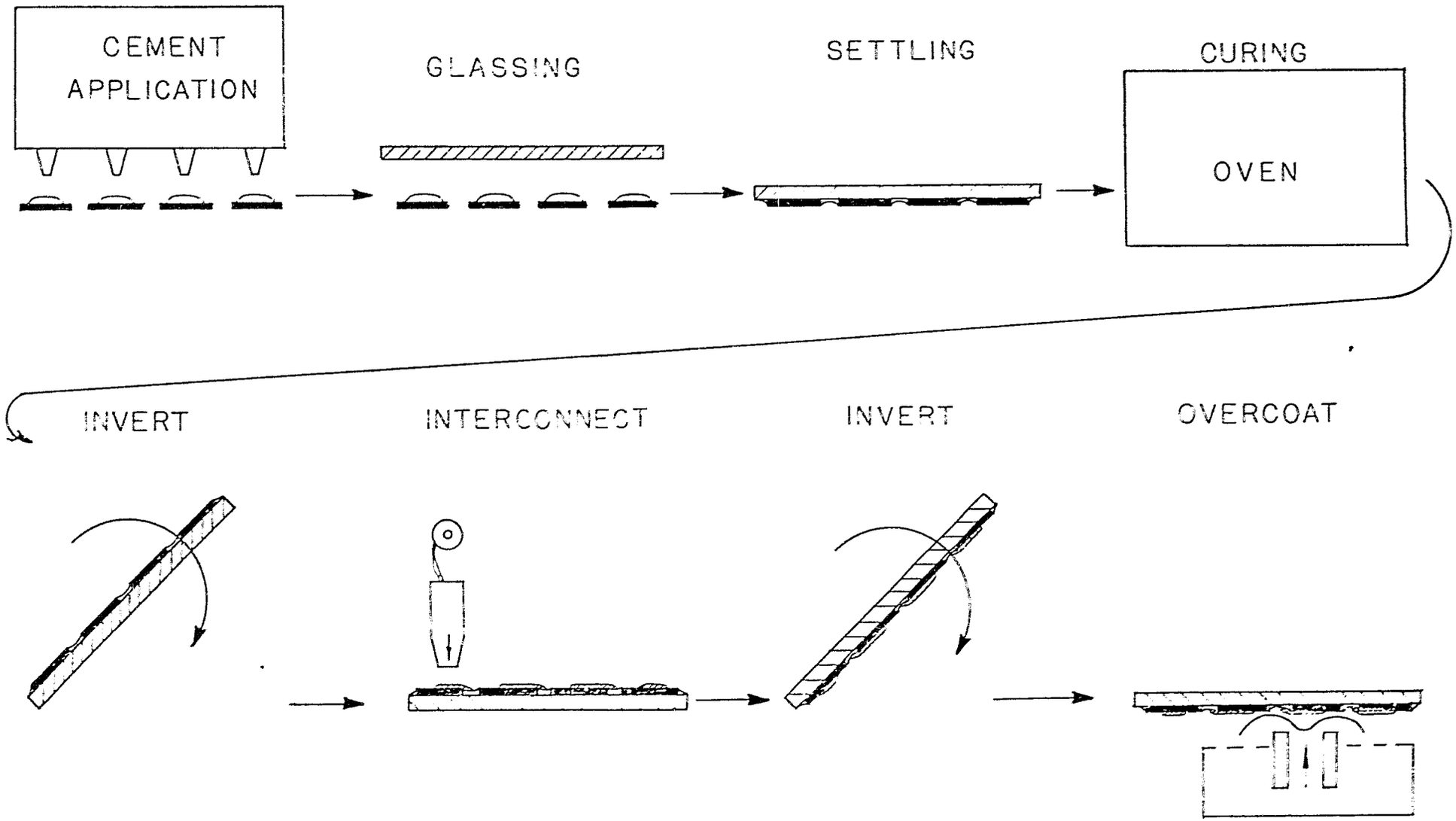

CONCEPTUAL DESIGN OF AUTOMATED SUPERSTRATE ASSEMBLY

Figure 3.19-C

After adhesive application, the grid of cells is advanced to the glassing station. At this station the superstrated glass is transferred by vacuum pick-up arms and accurately positioned on the cell array. The assembly is then moved to another station where time is provided for the adhesive to flow to the edges of the cell. After inspection, the assembly advances into an oven where the adhesive is cured.

The superstrate is then inverted to display the back sides of the cells for interconnection. This is projected to be an automatic reflow soldering process using copper braid interconnect conductors.

A second inversion presents the interconnected solar cell circuit on the lower side of the glass. In this position the superstrate moves continuously through a solvent spray flux removal tank and through an overcoating station. This might be a wave coating process as shown or alternatively could be a spray coating, curtain coating or other suitable process.

Lamination Method Assembly Sequence

Table 3.19-1 lists detailed steps for the lamination assembly sequence. Interconnects are attached to the front contacts of the cell using a solder press which consists of a heated block on a weighted lever with timed controls. Optimum soldering is achieved when the block is at 350° and left on the solder joint for 4 seconds. Flux is used in the process but no additional solder is added, there is sufficient solder in the interconnects plating.

A fixture was built to connect cells into strings. Cells which have been front tabbed are used. The fixture consists of a 3" x 3" heating block with vacuum hold-down attached to a non-heated block

Table 3.19-1

LAMINATION METHOD ASSEMBLY SEQUENCE

1) Cut interconnect
2) Solder interconnect to front ohmic
3) Remove flux
4) Ultrasonically solder interconnected cells to make string
5) Assemble circuit front strings
6) Prime glass and Al/polester film
7) Place Crane Glas on glass
8) Place clear EVA on glass
9) Clean circuit
10) Transfer circuit to EVA
11) Add EVA and Crane Glas on bus bars
12) Place additional Crane Glas over circuit
13) Place white EVA over Crane Glas
14) Place additional Crane Glas over EVA
15) Place Al/polyester film on top
16) Complete layup
17) Laminate
18) Apply frame
19) Prepare terminal box
20) Attach terminal box
21) Seal box
22) Test

3" x 24" through a thin Teflon block. The Teflon block is machined such that there is a .050" spacing between a cell on the heated and unheated block. The small block is heated to 150°C. An ultrasonic soldering iron is used to first put a tin/zinc solder pad on the cell back. This constitutes a shift of this process step from the cell processing sequence to the module assembly sequence. Next, the interconnect (from the adjacent cell positioned on the unheated block) is ultrasonically soldered to the pad. This creates a two-cell string which is slid to one side so another cell may be attached. Longer strings are thus created with great accuracy of intercell spacing.

Pull tests have been completed on cells interconnected in this manner. Back interconnect strengths are shown in Table 3.19-2. 90° pull test failures all exceeded 700 grams; and 45° pull test failure strengths were greater than 1400 grams, the maximum load our test fixtures can apply. Failures that occurred below 1000 grams were all due to silicon fracture. Front interconnects were tested with the 90° pull test (Table 3.19-3). A correlation of the strength of the joint with the amount of time between HF etch and front contact printing was found. If the cells are printed 24 hours, pull strengths greater than 650 grams are found. As the amount of time between HF etch and printing is increased, the pull strengths lessen. If the time is two weeks, the front contact shows no adhesion to the cell. In all front contact pull tests the failure mode is the silver contact separating from the silicon.

After a string of 20 cells was made it was transferred by hand to a sheet of glass where the circuit was assembled. The circuit consists of 200 cells: 10 parallel strings, 2 series blocks, and 10 cells per substring. While our verification module has no diodes we would recommend 1 diode per module to guard against back biasing. The addition of a diode to one of the terminal boxes and the lamination of a ribbon connection for it would not change the assembly sequence appreciably.

Table 3.19-2

BACK INTERCONNECT PULL RESULTS

90^{o} Pull

Cell #	Load at Failure (Grams)	Failure Mode
1	1000	Peel
2	1100	Peel
3	700	Cell Fracture
4	750	Cell Fracture
5	1150	Cell Fracture
6	1400	Cell Fracture
7	>1400	None
8	750	Cell Fracture
9	1000	Peel

45^{o} Pull

Cell #	Load at Failure (Grams)	Failure Mode
1	>1400	None
2	>1400	None
3	>1400	None
4	>1400	None
5	>1400	None
6	>1400	None
7	>1400	None
8	>1400	None
9	>1400	None

Table 3.19-3

FRONT INTERCONNECT PULL RESULTS

90^{o} pull, solder press used

Cell #	Failure Load	
1	710g	
2	680	Printed 24 hours
3	870	after HF etch
4	800	
5	590	
6	1030	Printed 1 week
7	570	after HF etch
8	460	
9	5	
10	5	Printed 3 weeks
11	5	after HF etch
12	5	

Two 2' x 4' verification modules were laminated as described in Section 3.18. The lamination step in a fully mechanical line would be accomplished by a double vacuum chamber capable of handling 12 modules per hour.

After lamination the modules would be framed and terminal boxes would be attached. A final test would complete the sequence.

3.20 EFFECT OF CELL PROCESSING ON CRYSTAL PERFECTION

3.20.1 Recommendations

No evidence was found of gross imperfections such as precipitate particles or dislocations attributable to the screen printing metallization when wafers were examined by x-ray topography. Contrast in the topographs between the regions under the metallization and those not under the metallization suggests a condition of uniform local strain in the silicon immediately adjacent to both silver and aluminum printed and fired contacts. Additional investigation was extended to include transmission and analytical electron microscopy of the wafers subjected to various process treatments.

3.20.2 Work Performed

X-ray topographs were made of the following:

- The etched Si wafer surface to assess the inherent perfection of the starting wafers
- The front contact surface after thermal processing of the Ag-glass frit front metallization paste
- The back Al contact surface after thermal processing
- The Si surface after application and thermal processing of the diffusion masking dielectric

The topographic studies involve Lang reflection x-ray topography. The technique is illustrated in Figure 3.20-A. An x-ray beam from a small source is incident on the Si wafer through a narrow slit. The beam impinges the crystal at an angle adjusted to satisfy the Bragg conditions. A variable width diffracted beam slit is used to prevent extraneous reflections and incoherent radiation from

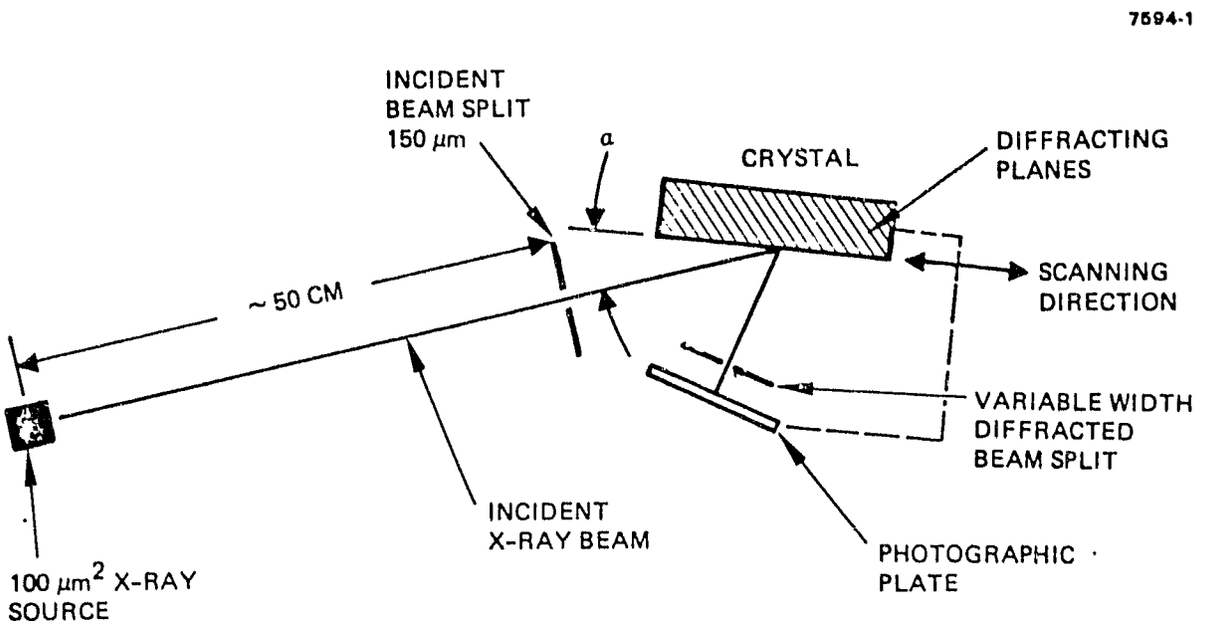

Figure 3.20-A

X-RAY CAMERA GEOMETRY

reaching the photographic plate. The crystal and the photographic plate are then scanned together to produce a reflection topograph of the entire crystal face. If crystal imperfections are present, changes in contrast occur and the type of defect can be identified. The penetration depth of the 40 kV x-rays from a Ni target is of the order of 10 μm. Such penetration depth represents the region of interest in determining the effects of wafer surface treatment, thermal cycles and ohmic contacting.

Starting Wafers

The degree of crystal perfection for wafers having no adjacent ohmic contact or insulator is shown in the x-ray topograph of Figure 3.20-B. The circular wafer, 2 inches in diameter, was cleaved in half and had a crack resulting from the cleaving. The topograph shows no gross imperfections such as inclusions, low angle grain boundaries, slip or large-scale dislocation networks.

Front Contact Area

The front contact area of the solar cell examined by x-ray topography is shown in Figure 3.20-C. The fritted silver paste was applied to a wafer and fired for 20 seconds in air at 700°C. The grid was removed with 1:1 concentrated nitric acid:water after the grid had been fired for 20 seconds at 700°C in air. The x-ray topograph Figure 3.20-D shows a residual pattern of the contact grid, probably caused by uniform local strain resulting from diffusion of constituents of the grid material during firing. It should be noted, however, that the application procedures and the firing cycle did not produce crystal dislocations or slip. The wafer also shows no evidence of warping. The dark horizontal lines are x-ray scanning artifacts, not a property of the wafer.

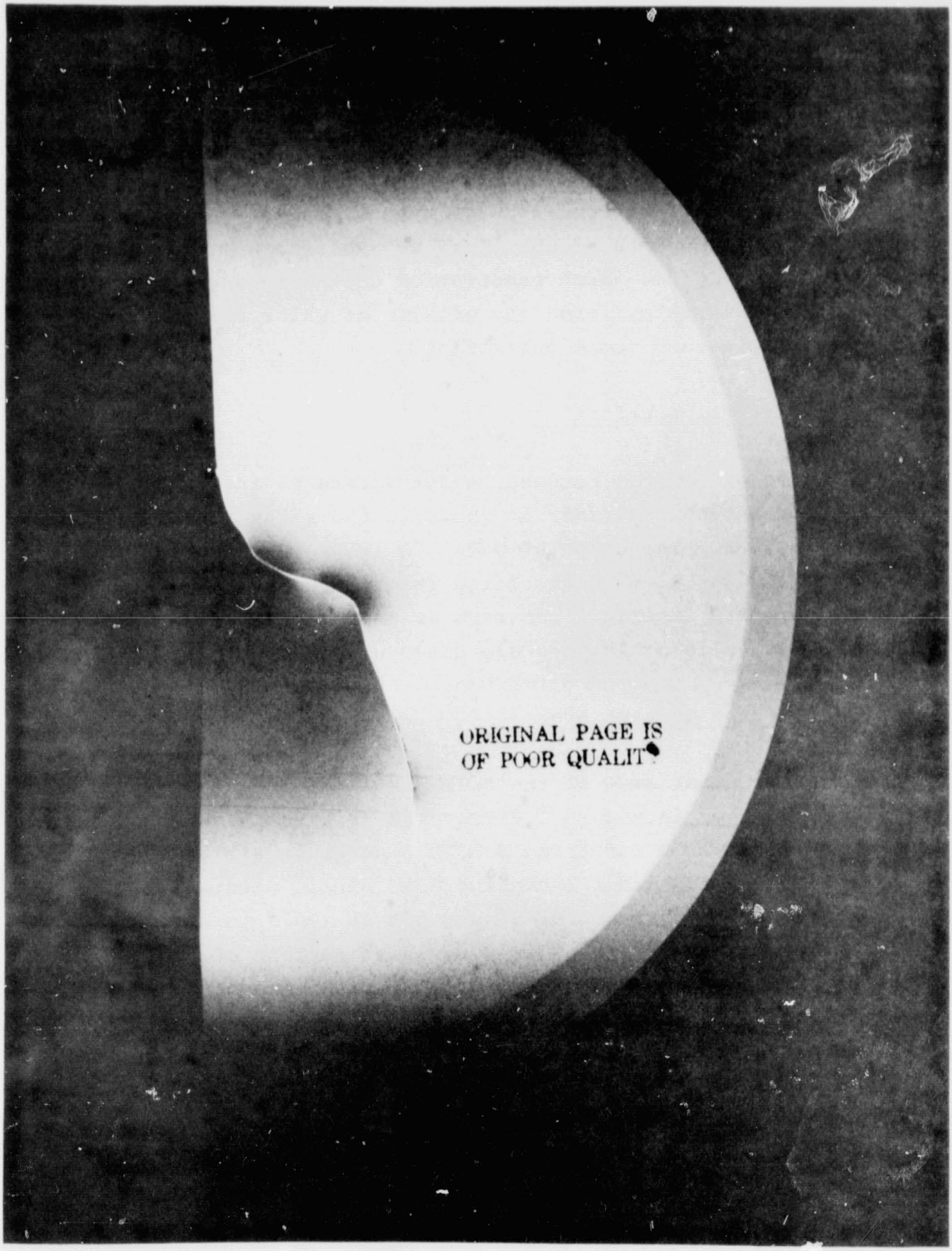

Figure 3.20-B. X-Ray Topograph of Si Wafer with No Contacts

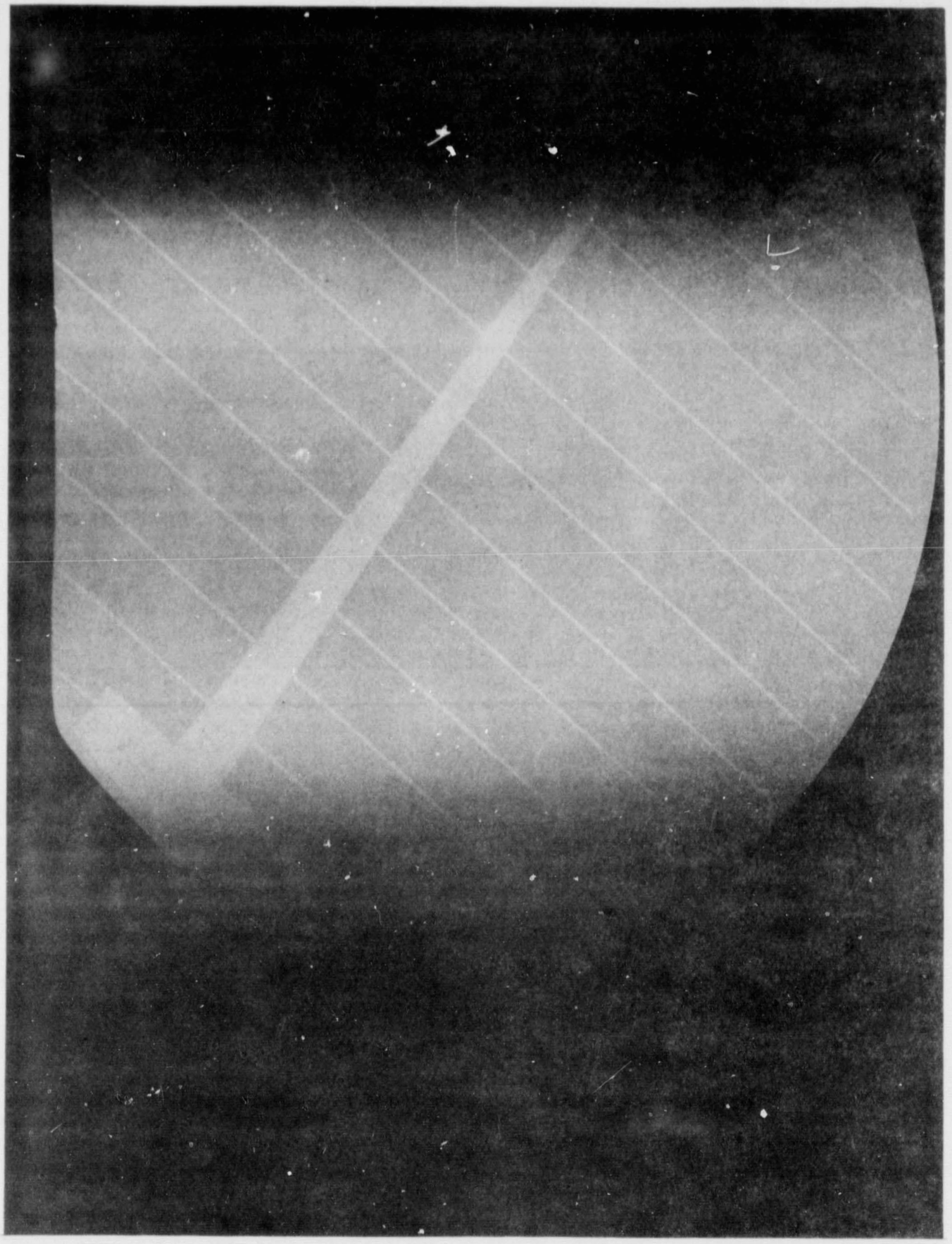

Figure 3.20-C. X-Ray Topograph of Front Contact Area, Si Solar Cell

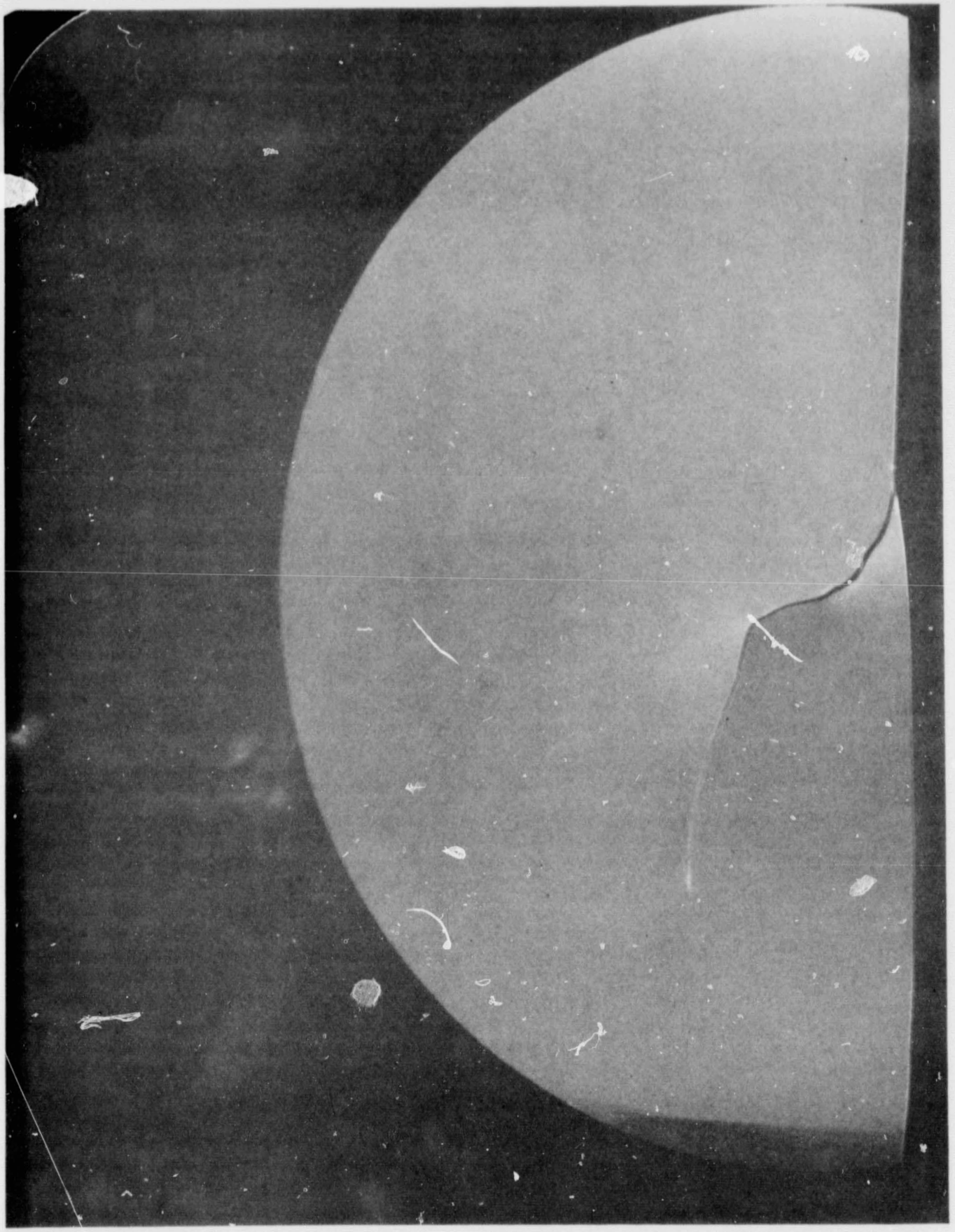

Figure 3.20-D. X-Ray Topograph of Back Contact Area, Si Solar Cell

Back Contact Area

The back contact area of a solar cell was examined by x-ray topography. The Al contact material was applied uniformly to the wafer with the exception of an annular region around the periphery. The wafer was fired using three thermal cycles:

10 seconds at 900°C in air
15 seconds at 600°C in air
20 seconds at 700°C in air

This sequence was selected to simulate thermal cycles included in the process sequence after firing the aluminum. After firing, the aluminum was removed by etching in HCl at 60°C and the x-ray topograph of Figure 3.20-D obtained. This topograph is of the opposite side of the wafer from that shown in Figure 3.20-B. In the region of Al alloying, there is evidence of regrowth regions when the wafer is examined by eye, but the x-ray topograph shows little structure in the Al alloying region with the exception of small circular regions sparsely distributed in the area. In the annular region where there was no Al deposited, these features do not occur. The small circular regions were found to be regions having a thin regrowth layer associated with shallow penetrations by the molten aluminum.

Diffusion Mask

A glassy insulation film for diffusion masking of the phosphorus diffusion was subjected to x-ray topography. In order to determine possible crystal damage from thermal processing of the deposited film on Si, a wafer with a bar pattern of masking film deposited on its surface was subjected to the following firing cycle:

30 minutes at 850°C in N_2
10 seconds at 900°C in air
15 seconds at 600°C in air
20 seconds at 700°C in air

The film was then removed with HF and the x-ray topograph of Figure 3.20-E made. There is no evidence of damage induced in the wafer by the masking film bar pattern which was deposited in the central portion of the wafer (three bars each 25 mm in length and 3 mm, 2 mm and 1 mm width were deposited). The wafer does show extensive slip damage which is especially severe at the edge of the wafer. From experience with other Si device structures, it is not likely that the slip is caused by the deposited diffusion resist pattern or by handling. It should be pointed out that slip of this extent might be deleterious to the electrical terminal characteristics of the solar cells. The observed slip pattern resembles that sometimes found as a result of thermal stresses during crystal growth and may have been present in the original wafer.

From the x-ray characterization it is concluded that:

- The crystal perfection of the wafers is good
- Front ohmic contact procedures do not produce significant crystal damage
- Back contact processing does not produce extensive crystal damage, but there are small circular defects associated with localized regions which are not dissolved into the molten aluminum.
- The firing of the diffusion mask film does not introduce noticeable crystal damage.
- Extensive slip was observed in one wafer believed to be from the crystal growing process.

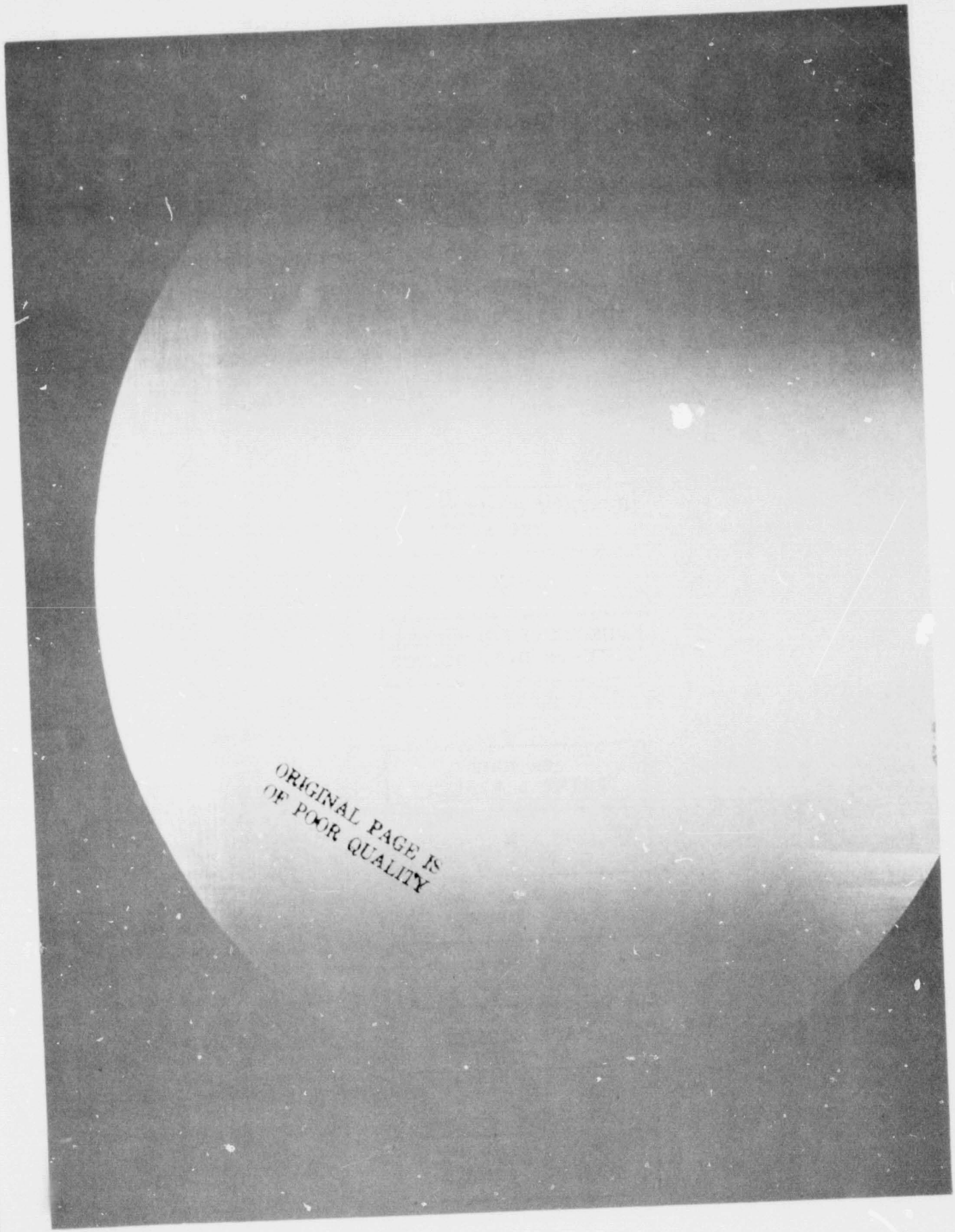

Figure 3.20-E. X-Ray Topograph of Wafer used in Diffusion Mask Experiment

Transmission and Analytical Electron Microscopy of Cell Processing:

This investigation was undertaken to examine the microstructures of ten (10) ID sawed wafers of Si single crystals from Smiel, all oriented (100), which had been subjected to various processing treatments listed below. The samples, numbered 1 through 10, were processed as described in the text. This numerology has been retained throughout the investigation and in this report.

PROCESSING TREATMENT

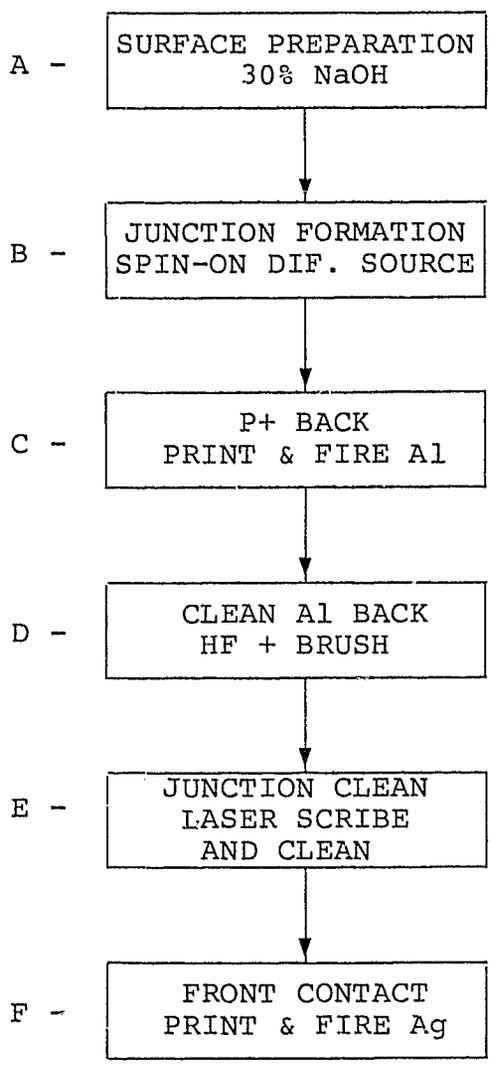

Conventional TEM was done at UCLA using a JEOL model JEM-200 transmission electron microscope operating at 200 KeV. Because of the (100) orientation of the single crystals, most of the photographs were taken under diffracting conditions such that (022) was the strongly diffracting plane; this is the lowest order diffraction vector in the <100> zone. Several samples were also examined in a JEOL model 100 CX TEMSCAN transmission electron microscope operating at 100 KeV. This instrument is an analytical electron microscope (AEM) equipped with a Kevex solid state x-ray detector. This enables one to detect the characteristic x-rays emitted by the various elements contained in the sample. The principle is the same as that employed in an electron microbeam probe, but the spatial resolution is superior by nearly two orders of magnitude.

In what follows, the features observed in each sample will be discussed in turn. It happens that nearly all the photographs were taken at the same magnitude (13,200X); this magnification is indicated in Figure 3.20-1-F. In subsequent photographs the magnification will be indicated only if it differs from that in Figure 3.20-1-F.

SAMPLE 1

Processing treatment A, polished etched to 5 mils from one side sectioned and thinned from the same side to allow electron transmission. Sample prepared as a control.

The specimen examined was chemically polished.

Figure 3.20-1-F shows a linear type defect (A) typical of others seen in this sample, and others as well. This type of defect has no particular crystallographic preference. It is presumed to be debris resulting from cutting of the wafer which was not removed by subsequent polishing of the wafer.

Figure 3.20-1-G is a sequence of photos taken from two adjacent regions of the sample (a) and its corresponding diffraction pattern (b). Figure 3.20-1-G(a) illustrates a curved defect (B), the origin is probably partially etched saw damage since its diffraction pattern contains no extra reflections.

Figure 3.20-1-H shows a region of the sample which appears to contain precipitates (C and D). The diffraction pattern from this region (b) contains additional spots, indicative of a precipitate phase. It is now believed that the extra spots originated from the blotchy "particle" (c), which is probably due to surface contamination.

Figure 3.20-1-I is a sequence from two adjacent regions containing cigar shaped features similar to D in Figure 3.20-1-H. Ordinarily these would be suspected to be precipitates. However, it is noteworthy that they share no common crystallographic orientation. This point will be returned to later in discussion of similar features observed in other samples.

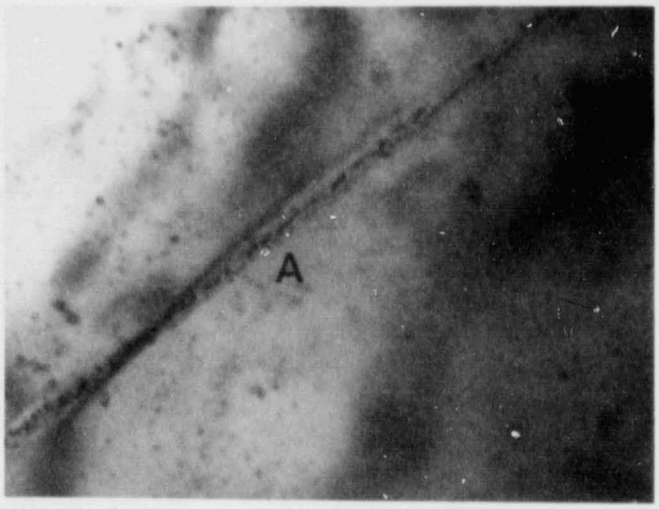

3.20-1-F

1.0μm

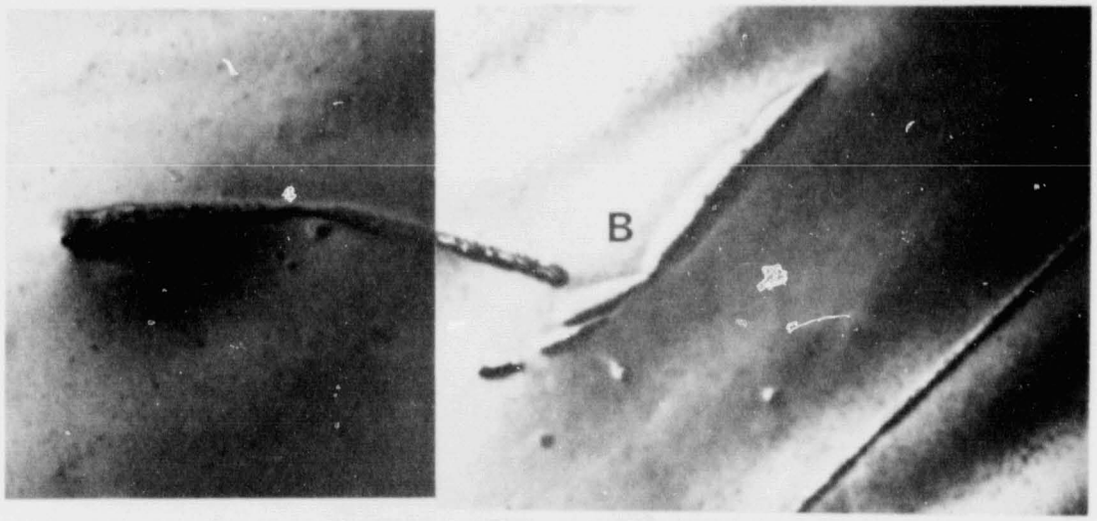

3.20-1-G(a)

3.20-1-G(b)

NaOh Etched Surface

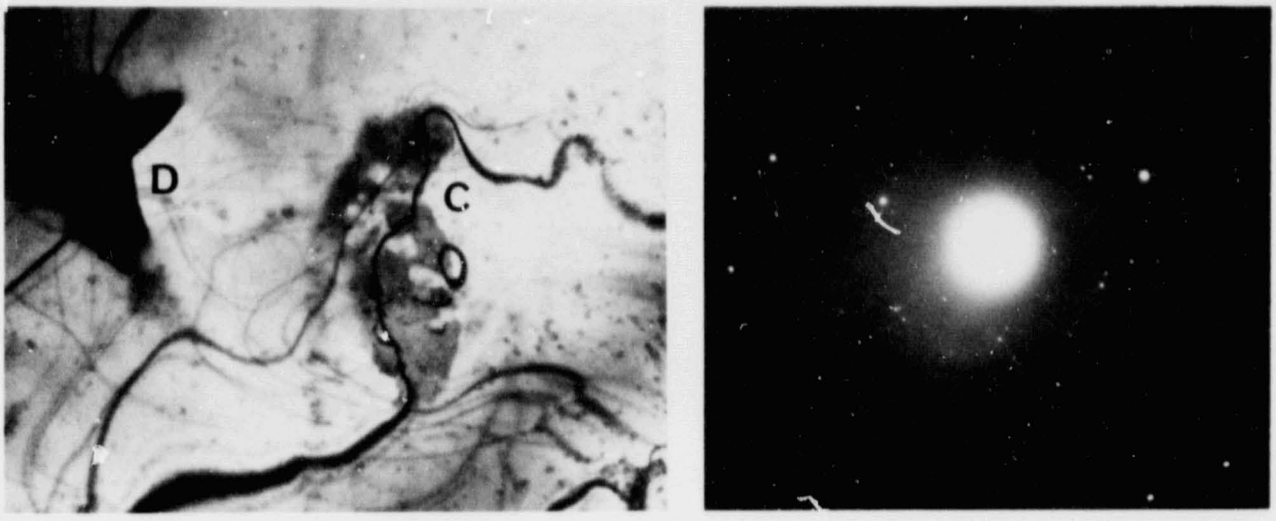

a

3.20-1-H

b

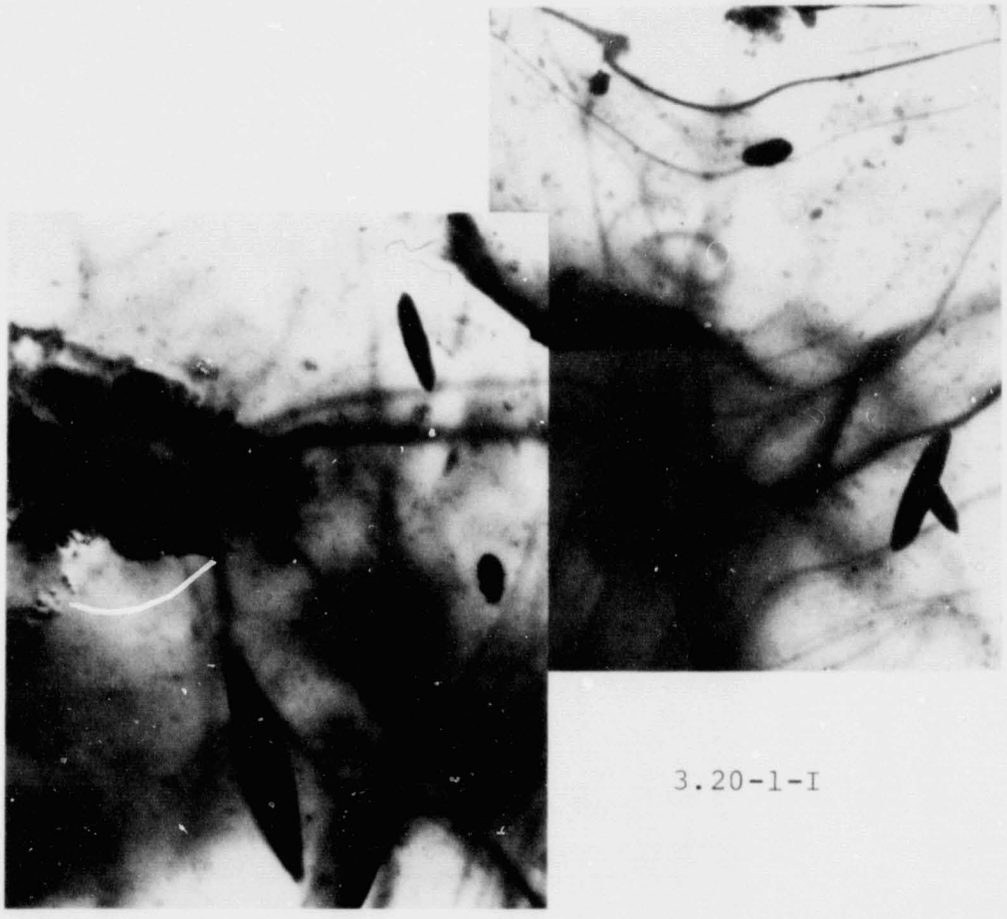

3.20-1-I

SAMPLE 2

Processing treatments A, B, polished etched to 5 mils from the non-diffused side, sectioned and thinned from the non-diffused side to allow electron transmission. Sample prepared to identify any damage or precipitates associated with diffusion.

The specimen examined was jet-thinned.

Figure 3.20-2-J shows a defect (a) which resembles those seen in Figures 3.20-1-F and 3.20-1-G. The diffraction pattern (b) contains only Si reflections.

Figure 3.20-2-K is a sequence of two photographs in which a parallel pair of linear debris-type defects is visible.

The ellipsoidal cigar shaped "precipitates" seen in Figure 3.20-1-I were not observed in this sample, nor were other precipitates.

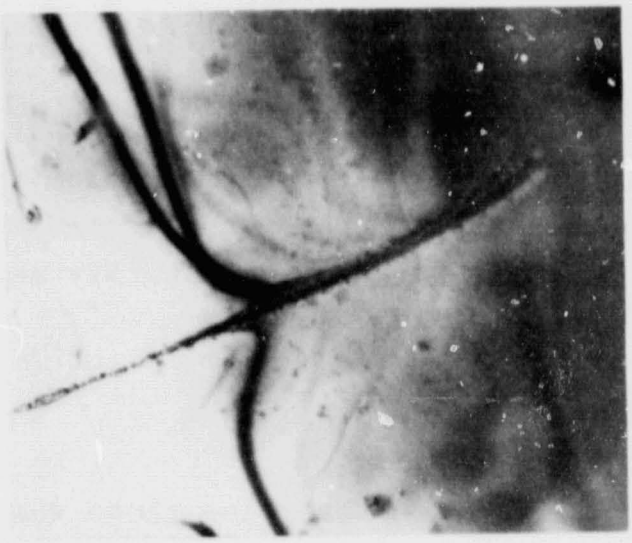

a

b

3.20-2-J

Diffused Surface

3.20-2-K

SAMPLE 3

Processing treatments A, B, plasma etched to approximately 100 Ω/□, polish etched to 5 mils from the non-plasma etched side sectioned and thinned from the non-plasma etched side to allow electron transmission. Sample prepared to identify any local damage associated with plasma etching.

The sample was chemically polished.

Figure 3.20-3-L is a sequence of five photographs (a) illustrating the contrast at a planar or volumetric defect inside the thin foil. The diffraction pattern is shown in (b).

Figure 3.20-3-M is a sequence of three photographs (a) of the same defect seen in Figure 3.20-3-L, taken under different diffracting conditions (b) (two different (022) reflections were used).

The contrast observed at the defect seen in Figures 3.20-3-L(a) and 3.20-3-M(a) is clearly different, and could be due to interface dislocations associated with a large precipitate. However, no extra reflections were observed in the diffraction patterns, so that this conclusion should be regarded as tentative. This sample was also examined in the AEM, but this defect (or similar ones) could not be found.

Figure 3.20-3-N shows a cigar shaped feature not unlike those seen in sample 1. Features of this type were also seen in the AEM, but the x-ray spectra from several of them showed nothing but Si. The nature of these defects is thus difficult to determine, but they do not appear to be particles of a second phase, unless they contain boron and/or oxygen, which cannot be detected.

Diffused and Plasma Etched Surface

3.20-3-L

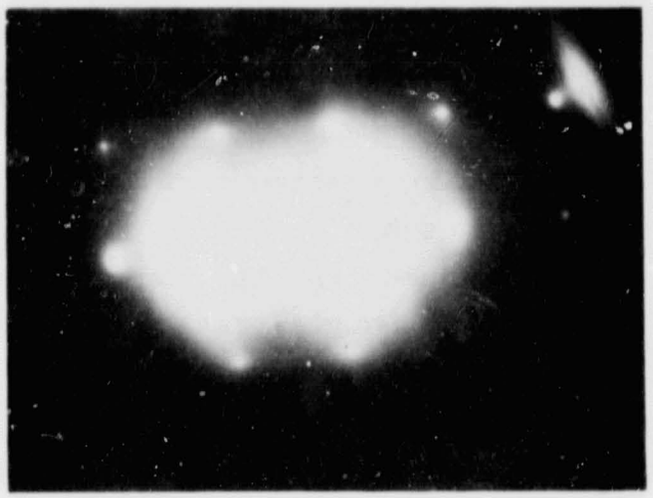

b

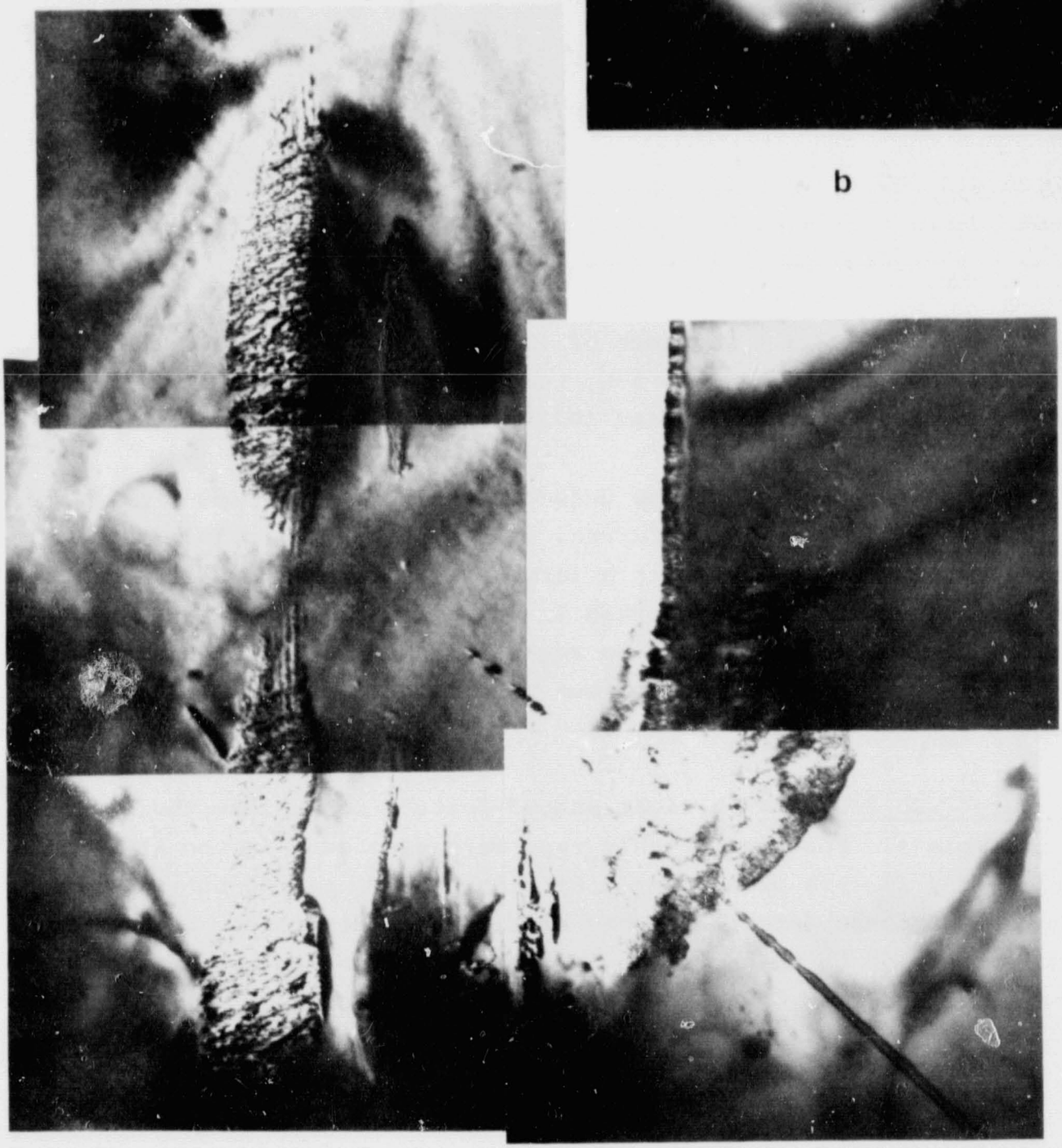

a

3.20-3-M

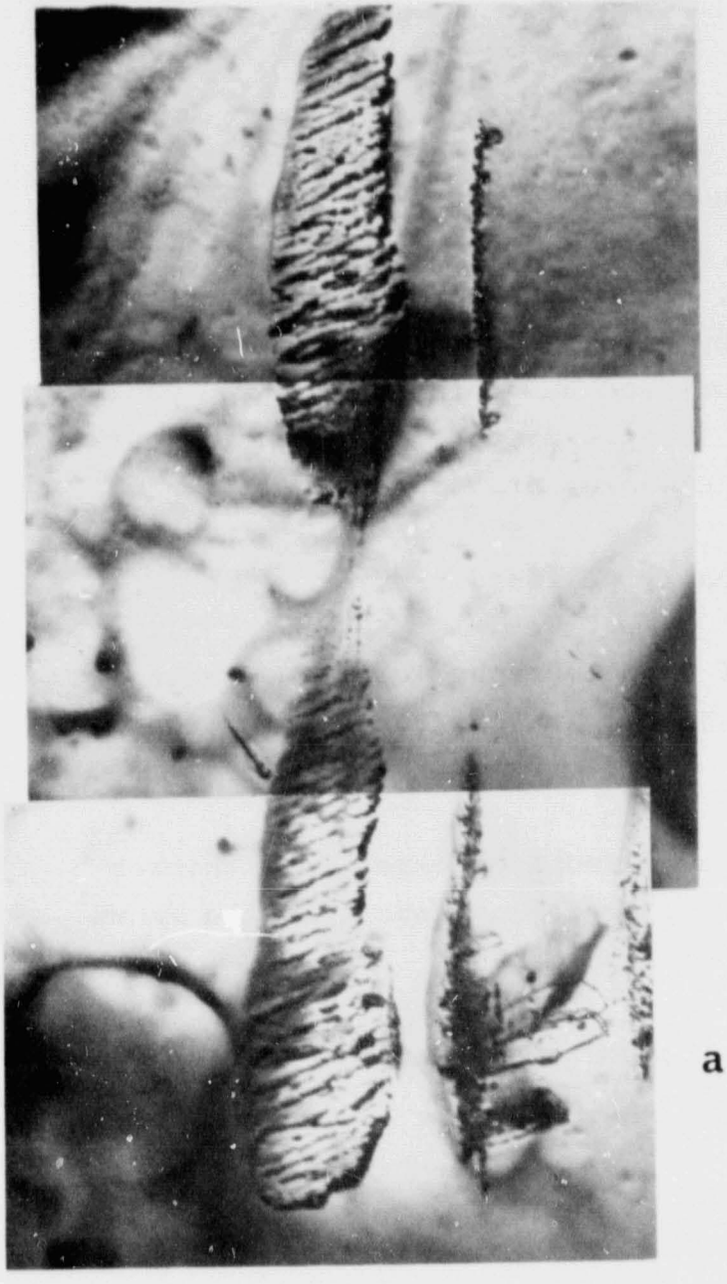

a

b

3.20-3-N

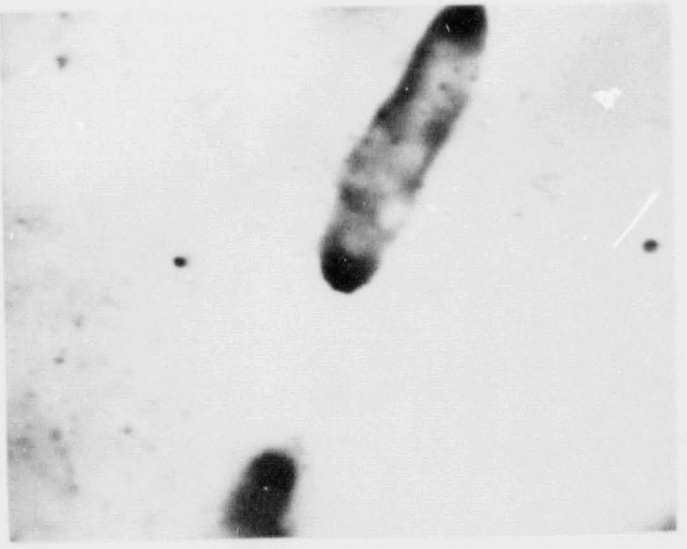

SAMPLE 4

Processing treatment A, B, C, D, etched in hydrochloric to remove aluminum back contact followed by a polish etch to thin the wafer to 5 mils from the back side sectioned and thinned from the back to allow electron transmission. Sample prepared to identify surface damage associated with the cleaning process.

The specimen examined was chemically polished.

Figure 3.20-4-P is a sequence of 5 photographs (a) illustrating a defect resulting from cutting debris. Its diffraction pattern is shown in (b).

Figures 3.20-4-P and 3.20-4-Q show defects observed in a thicker part of the foil. Their origin may be due to damage to the front surface during the brushing of the aluminum.

This sample did not contain the cigar shaped features seen in samples 1 and 3.

3.20-4-O

Diffused Surface After
P+ Formation

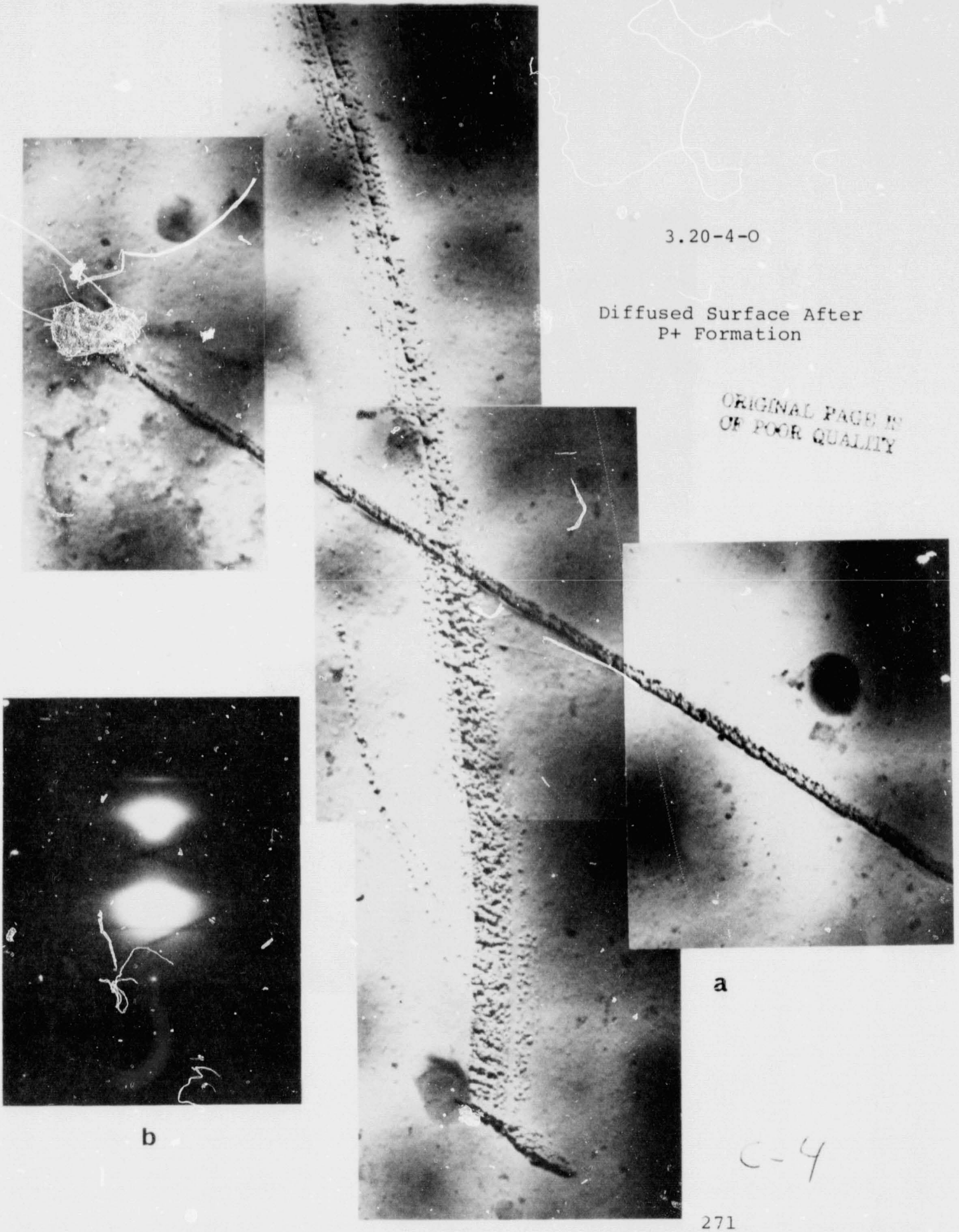

a

b

C-4

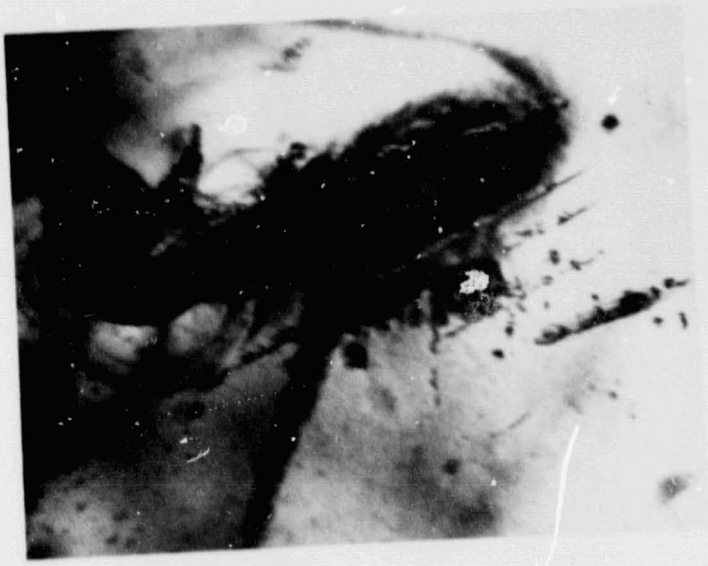

3.20-4-P

3.20-4-Q

SAMPLE 5

Processing treatment A, B, C, D, E, F, etched in hydrochloric to remove aluminum, etched in nitric acid to remove silver, and etched in hydrofluoric acid to remove frit under silver contact. The wafer was then polish etched from the back to 5 mils, sectioned and thinned from the back to allow electron transmission. Sample was prepared from a good quality cell to identify diffused surface damage associated with the standard processing treatment.

The sample examined was jet-thinned.

Figures 3.20-5-R, 3.20-5-S, 3.20-5-U and 3.20-5-V show debris-type damage, although 3.20-5-V also contains some small cigar-shaped features (at A and B) that could be similar to those observed in samples 1 and 3. The diffraction pattern (Figure 3.20-5-R(b) contains extra reflections which are most likely due to surface contamination.

Figure 3.20-5-T illustrates some localized defects which differ in appearance from debris damage. These defects bear some resemblance to those near the defect labelled B in Figure 3.20-G(a).

Some of the damage observed in these illustrations does appear to be due to the process handling, although the efficiency of the cell was high.

Diffused Surface After
Screening Front Contact

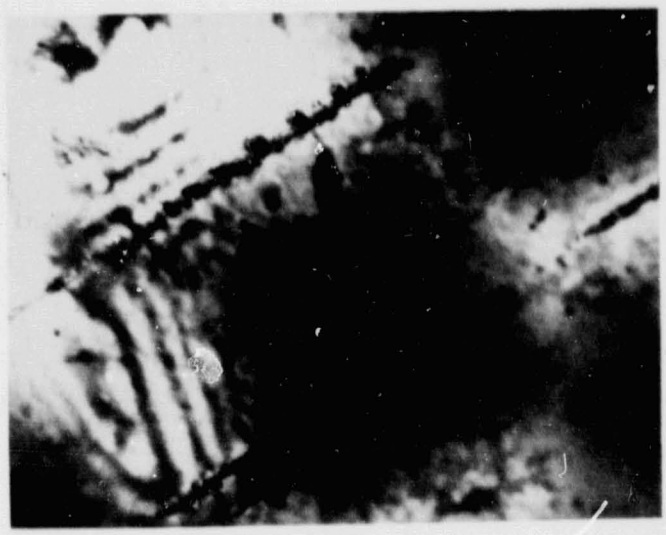

a

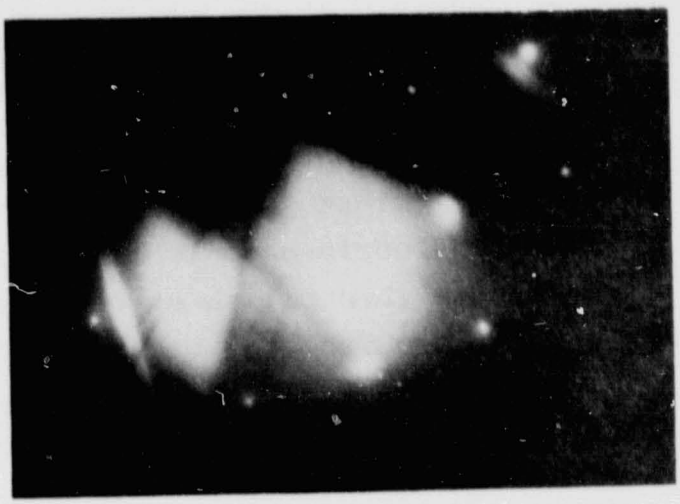

b

3.20-5-R

3.20-5-S

3.20-5-T

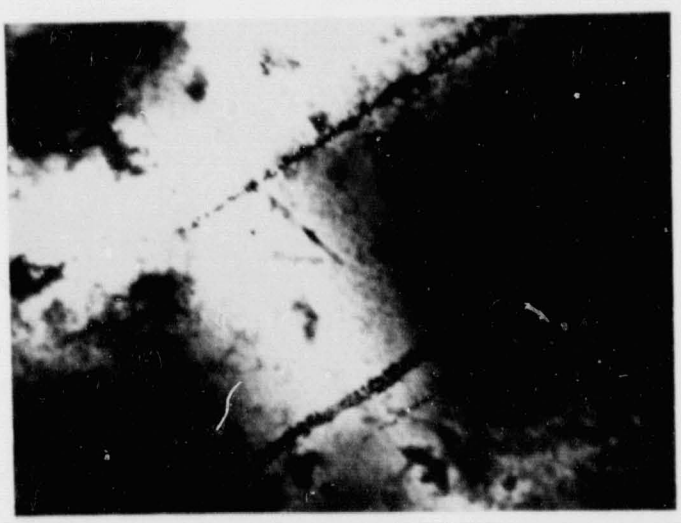

3.20-5-U

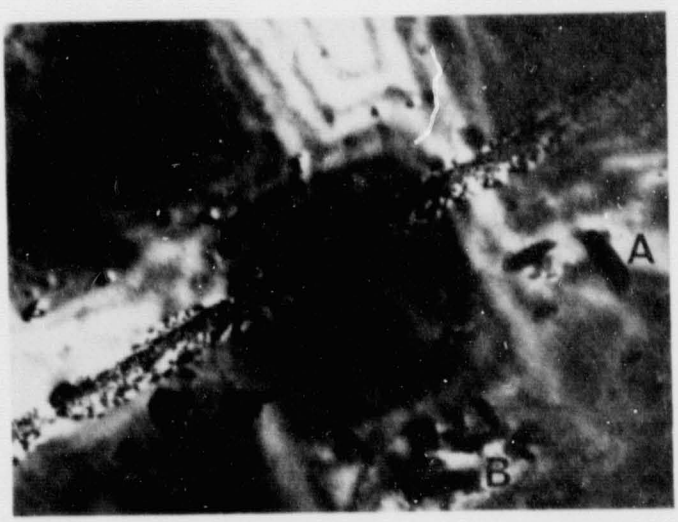

3.20-5-V

SAMPLE 6

Processing treatment A, B, C, D, E, etched in hydrochloric to remove aluminum and polish etched from the front to 5 mils. The sample was then sectioned in the area of a laser scribe line and thinned in that area to allow electron transmission. Sample was prepared to determine damage associated with laser scribing.

The sample examined was jet-thinned.

Figure 3.20-6-W shows a blocky type of "particle" (at A in Figure 3.20-6-W(a)) which was commonly observed in this sample. Surface contamination was also evident. The diffraction pattern (b) contains only Si reflections.

Figure 3.20-6-X illustrates what is unquestionably a precipitate (at B) (possibly an aluminum precipitate) contained within the sample. The extra reflections in the diffraction pattern (b) confirm this hypothesis. Examination of a large area of this sample did not show the presence of similar precipitates, and it is thus suspected that the particle seen in Figure 3.20-6-X(a) is not a representative feature of the microstructure.

Figure 3.20-6-Y shows the same region of the sample under slightly different diffracting conditions. Note that the contrast of the matrix changes drastically, while the feature at C appears the same in (a) and (b). This is typical of surface contamination.

Figure 3.20-6-Z shows a defect resembling that B in Figure 3.20-1-G.

This sample was examined in the AEM. The particle in Figure 3.20-6-X(a) could not be found. The x-ray spectra from blocky particles such as that at A in Figure 3.20-6-W showed only the presence of Si.

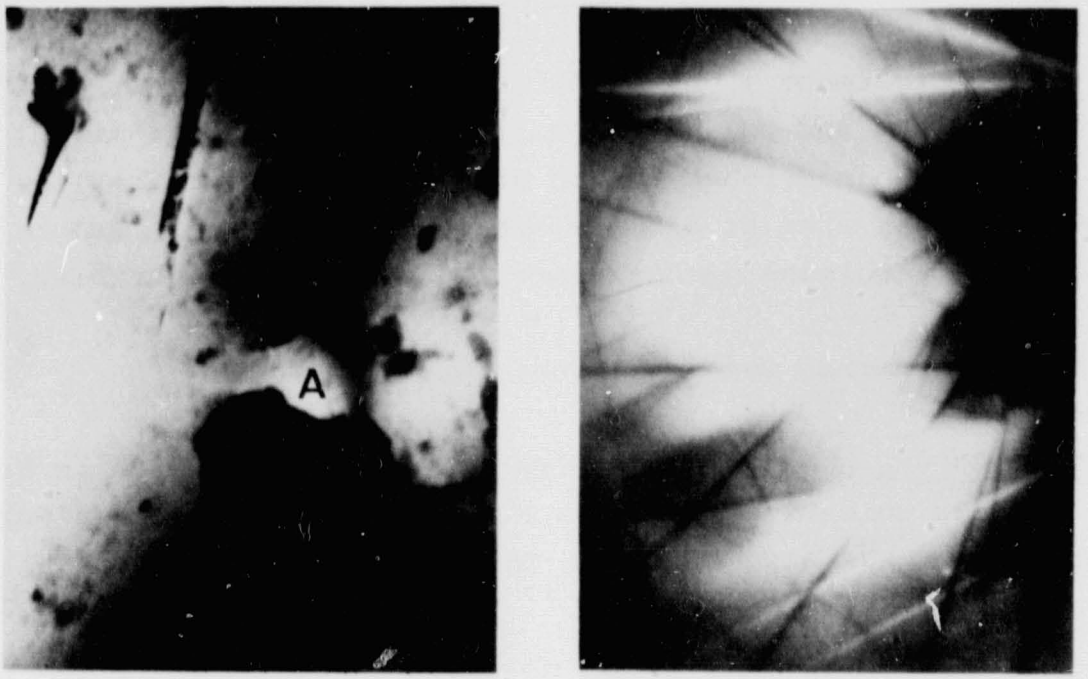

a 3.20-6-W b

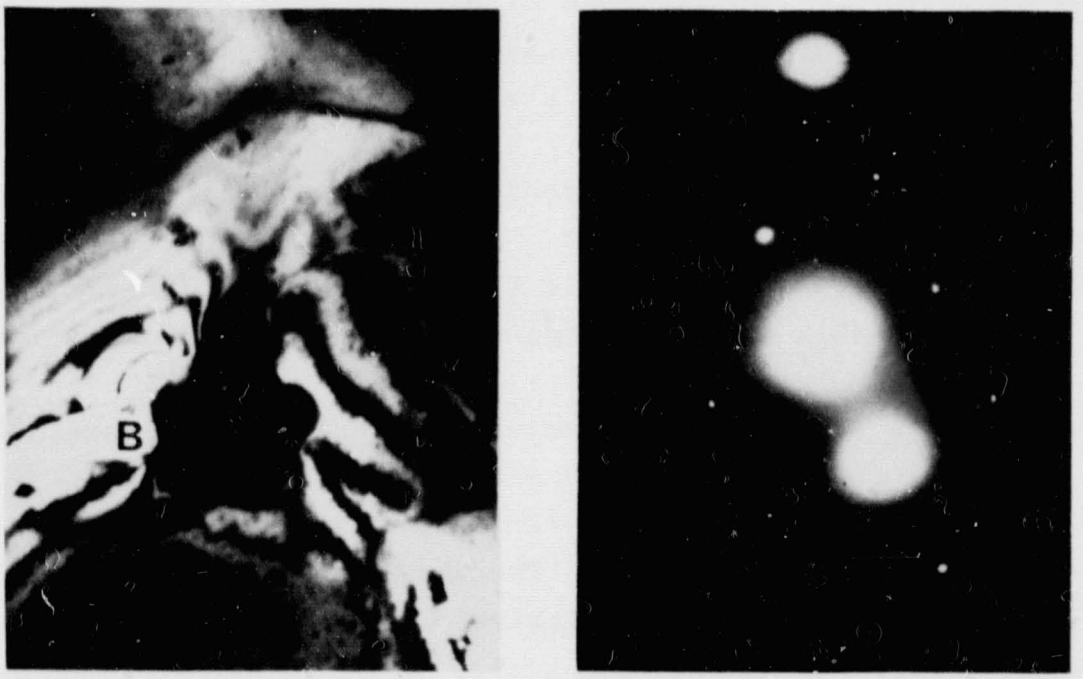

a 3.20-6-X b

Laser Scribed Area

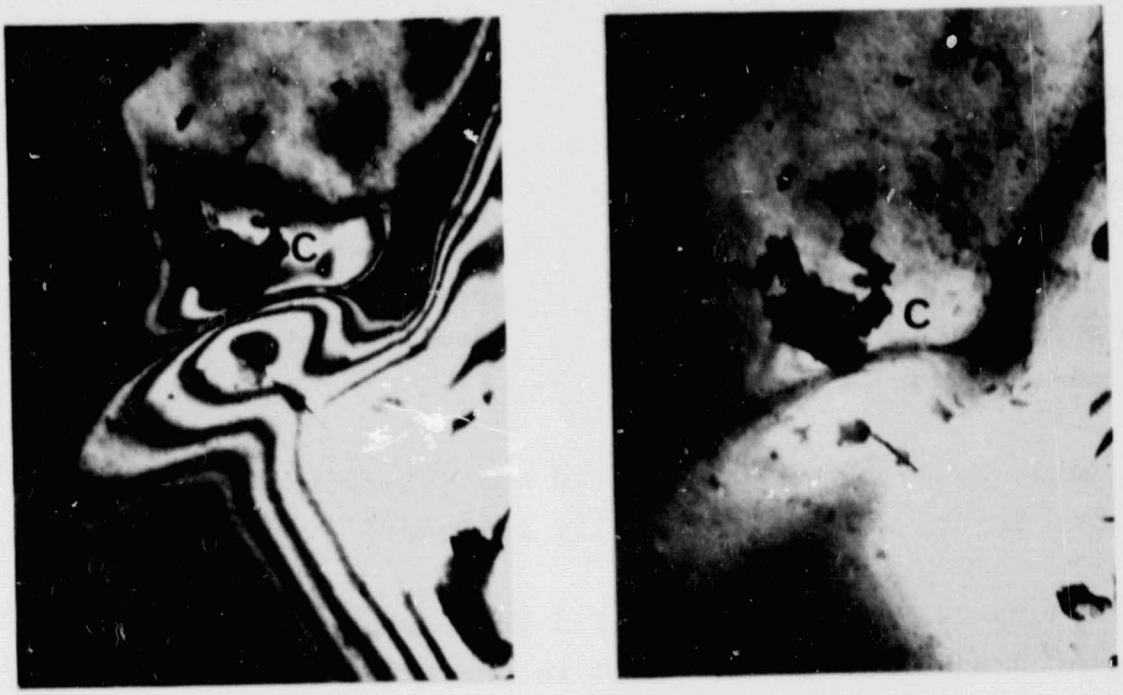

a

3.20-6-Y

b

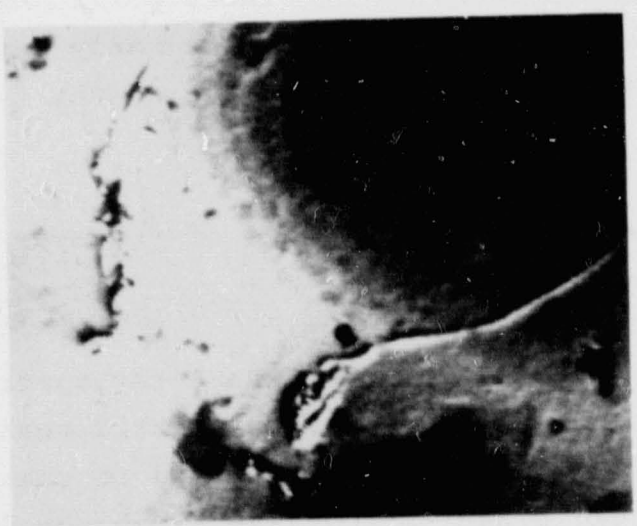

3.20-6-Z

SAMPLE 7

Processing treatment A, B, C, D, E, F, etched in hydrochloric to remove aluminum, etched in nitric acid to remove silver, etched in hydrofluoric acid to remove frit, and polish etched from the back to 5 mils. The sample was then sectioned in the area of the ohmic bar and thinned from the back to allow electron transmission. Sample prepared to identify damage associated with diffused silicon surface--frit or silver interaction.

The sample examined in the JEM-200 was jet-thinned, while that examined in the AEM was chemically polished.

Figure 3.20-7-A is a sequence of 3 photographs (a) of a region containing a defect intermediate in character to those seen in Figures 3.20-1-G(a), 3.20-5-T and 3.20-6-Z. Its origin is unknown, but it may be an example of cutting debris relatively far from the cut surface. No extra reflections were observed in the diffraction pattern (b).

Figure 3.20-7-B shows examples of blocky particles (at A and B in Figure 3.20-7-B(a)) which were not commonly seen in this sample. No extra reflections were observed in the diffraction pattern (b).

Figure 3.20-7-C shows another example of the type of defect seen in Figure 3.20-7-A.

Figures 3.20-7-D and 3.20-7-E show the x-ray spectra (b) taken from two blocky particles (a). The characteristic peaks are labelled. The particle in Figure 3.20-7-D(a) appears to contain S and K, while that in Figure 3.20-7-E contains S but not K. The Cu peaks (Kα and Kβ) in Figures 3.20-7-D(b) and 3.20-7-E(b) do not originate within the sample. The origin of the S and K peaks is not clear.

The analysis of similar particles in Sample 8 suggests that these elements are not confined to the particles, but are present in the matrix as well. This suggests that S and K were introduced as surface contaminants, perhaps in preparation of the specimens or as a component of the vehicle in the silver paste.

3.20-7-A

Diffused and Screen
Printed Silver Area

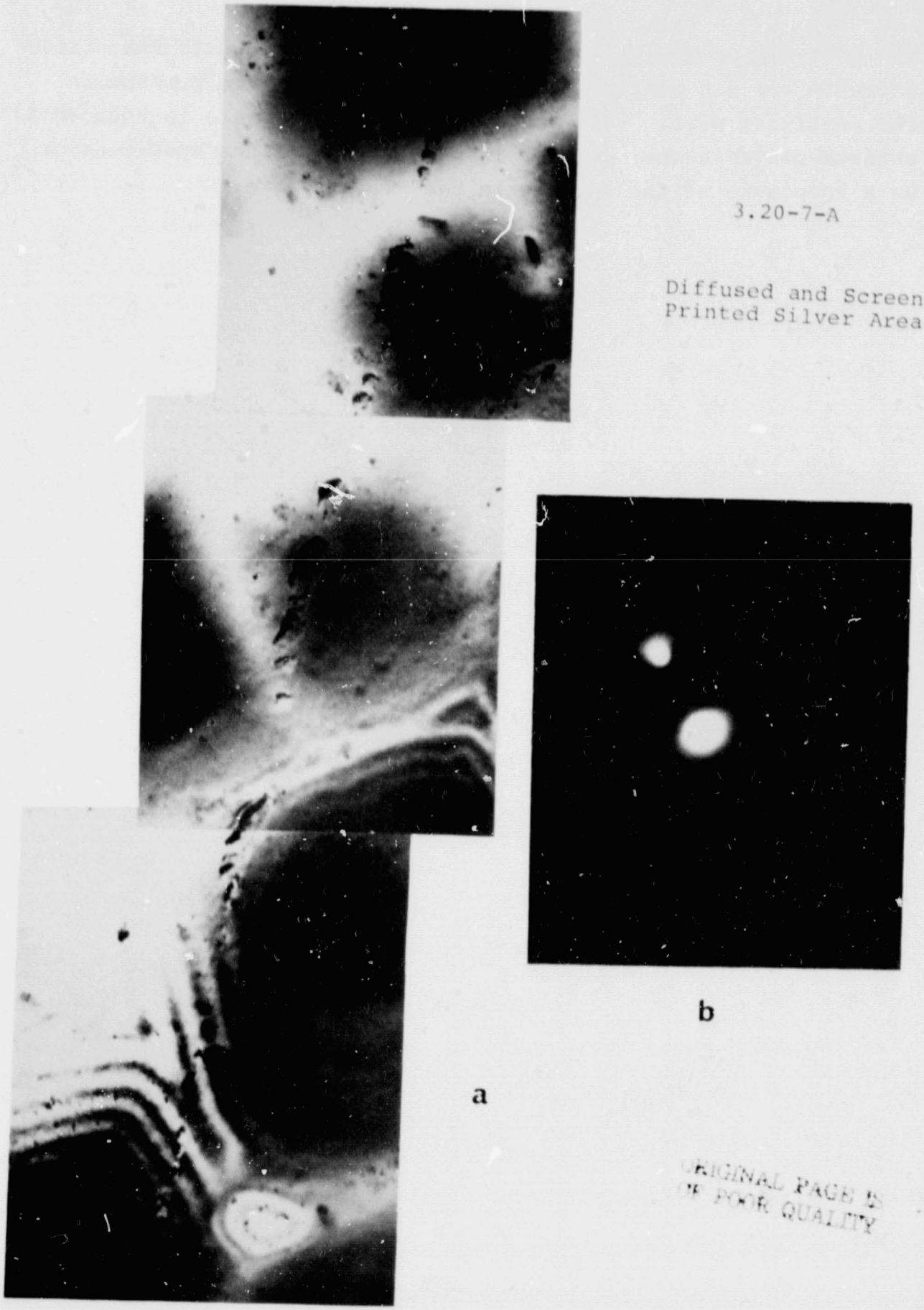

a

b

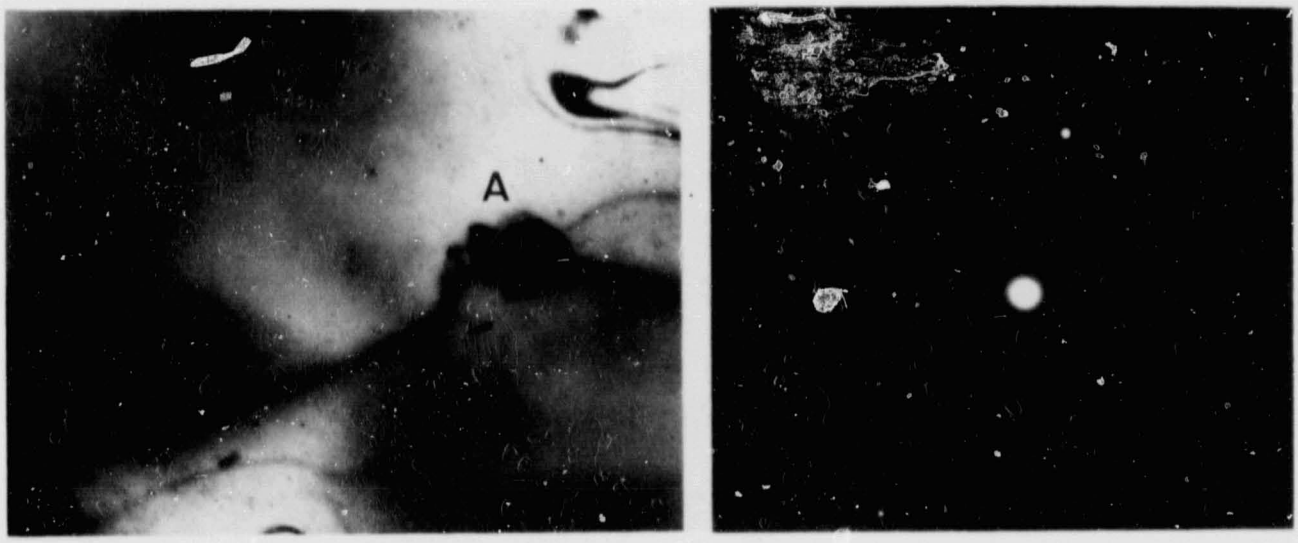

a

3.20-7-B

b

3.20-7-C

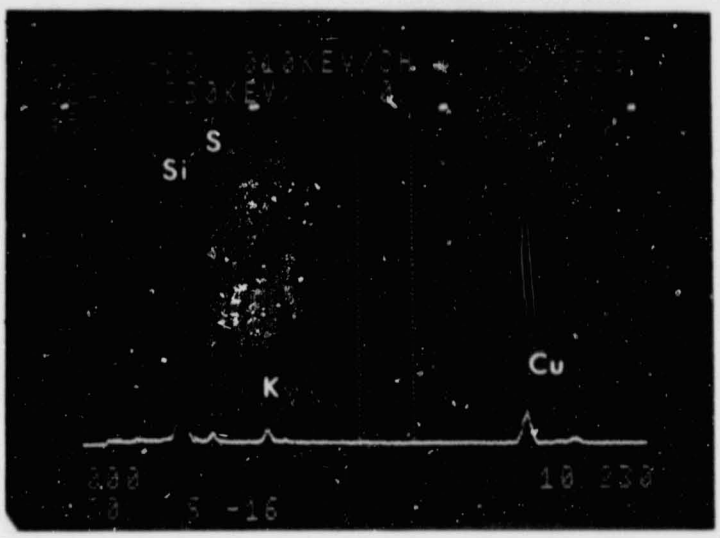

a b

3.20-7-D

1.0μm

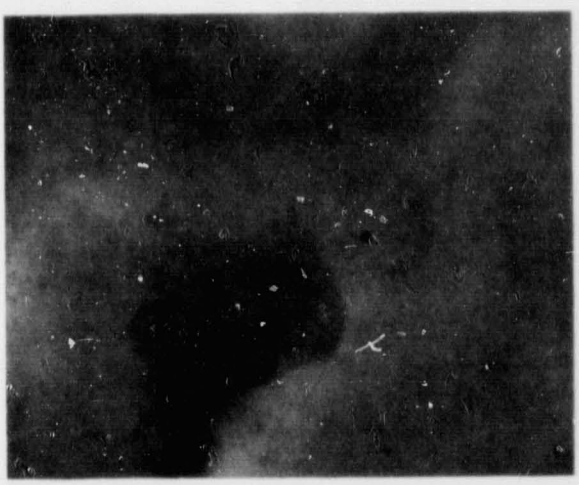

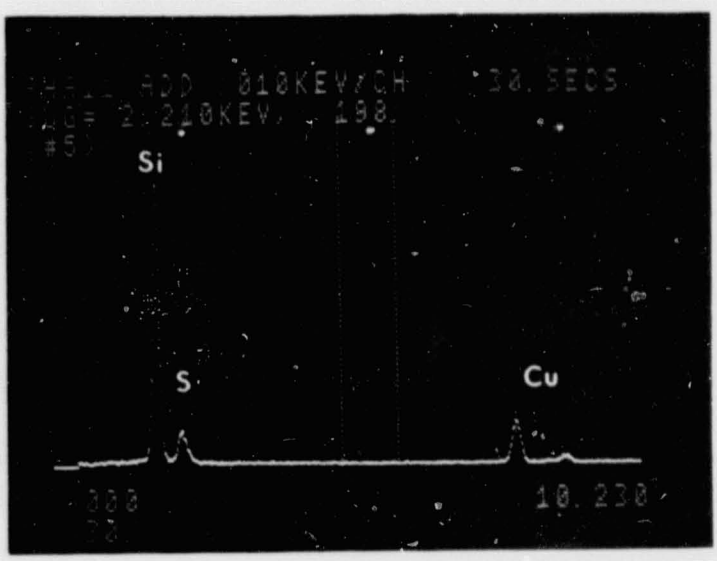

a b

3.20-7-E

SAMPLE 8

Processing treatment A, F, etched in nitric acid to remove silver, etched in hydrofluoric acid to remove frit and polish etched from the back to 5 mils. The sample was then sectioned in the area of the ohmic bar and thinned from the back to allow electron transmission. Sample prepared as a control for sample #7.

A jet-thinned sample was examined in both the JEM-200 and 100 CX TEMSCAN electron microscopes. A chemically thinned sample was also examined in the latter machine.

Figure 3.20-8-F is a sequence of 2 photographs illustrating debris damage.

Figures 3.20-8-G to 3.20-8-K show examples of precipitate like features which resemble the cigar shaped particles seen in Figures 3.20-1-I and 3.20-3-N, though they are more rounded in shape. They were quite widespread in this jet-thinned sample. The diffraction patterns in Figures 3.20-8-J(b) and 3.20-8-K(b) contain faint extra reflections, suggesting that the particles may be true precipitates.

Figure 3.20-8-L is a sequence of 3 photographs taken on the 100 CX TEMSCAN. The sample was chemically polished and the region examined was unperforated (i.e., it had not been polished long enough to produce a small hole). Only debris damage was observed; this sample contained no precipitates in its electron-transparent region. The suspicion here is that the precipitates seen in Figures 3.20-8-G to 3.20-8-K may, in fact, be surface particles somehow produced during specimen preparation. This may be true of many of the particles observed in other samples.

Figure 3.20-8-M shows the result of AEM of the jet-thinned sample containing the apparent precipitates. Arrows point from each spectrum to the region of the sample from which it was obtained. The two uppermost spectra were taken from a "particle" and the matrix adjacent to it. These spectra are virtually identical with both S and Ca in evidence. The lower spectrum, taken from a blocky particle, shows no Ca and perhaps a minute trace of S. Si is the only other element present in all cases. It is the absence of other, more likely, elements, plus the presence of similar unexpected elements both inside and outside the particles, that suggests the apparent microchemistry may be an artifact of the specimen preparation routine. It may be due to rinsing, or to dissolution of the protective lacquers used, followed by washing. Any of these steps could leave residual films on the surface, even when considerable care is taken.

Note that there is no particular crystallographic orientation relationship between the particles and the matrix. This can be construed as additional evidence that they are artifacts resulting from specimen preparation.

3.20-8-F

Non-Diffused and Screen
Printed Silver Area

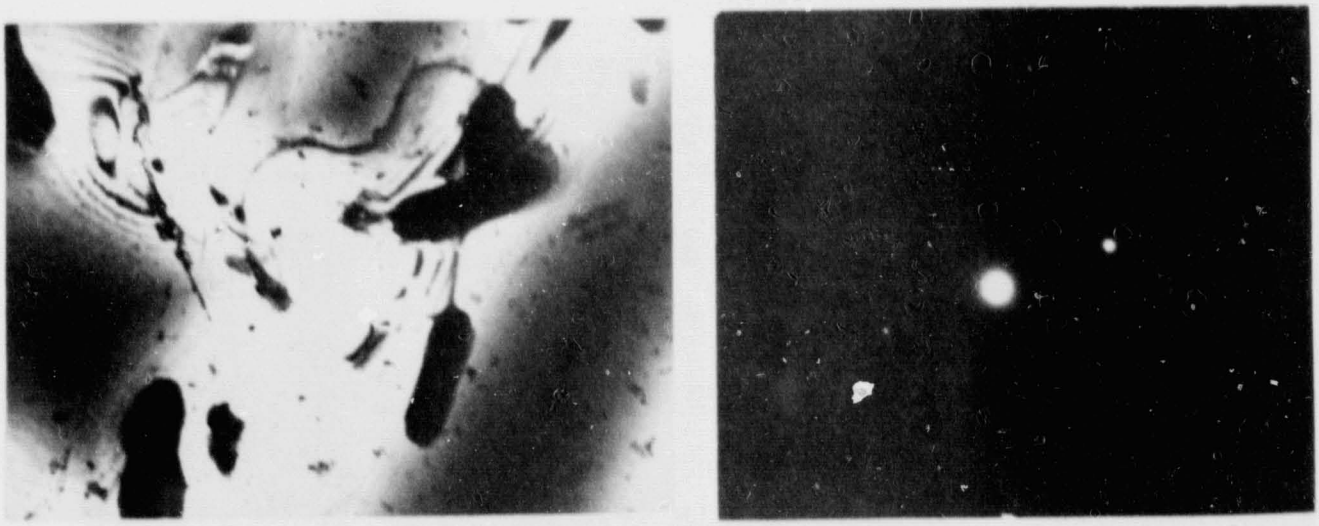

a b

3.20-8-G

3.20-8-H

3.20-8-I

a

3.20-8-J

b

a

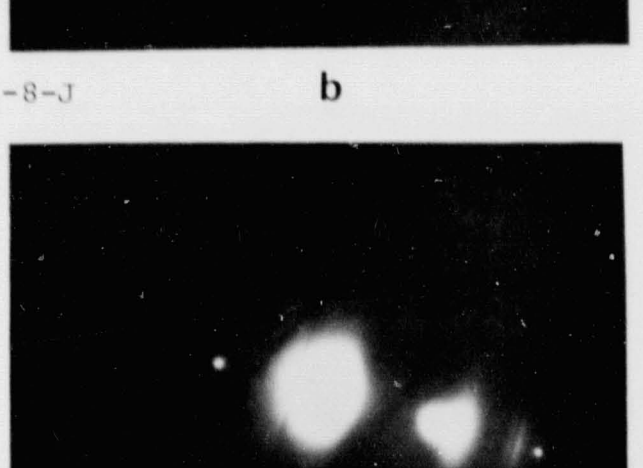

3.20-8-K

b

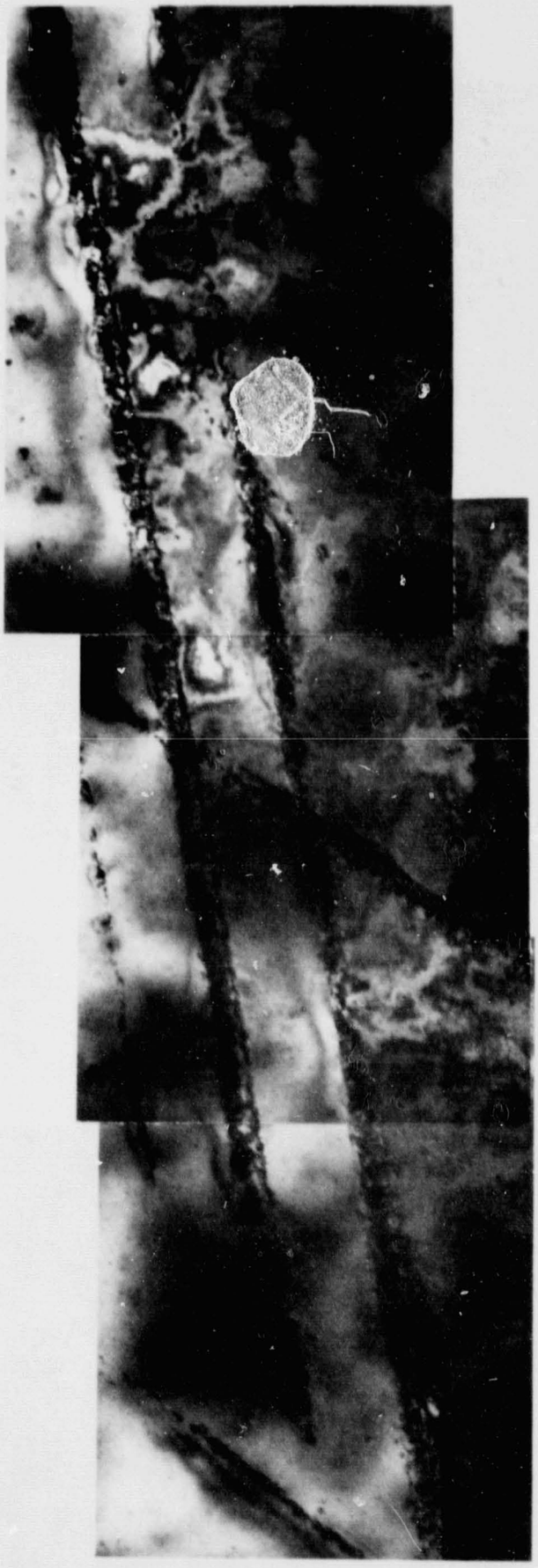

3.20-8-L

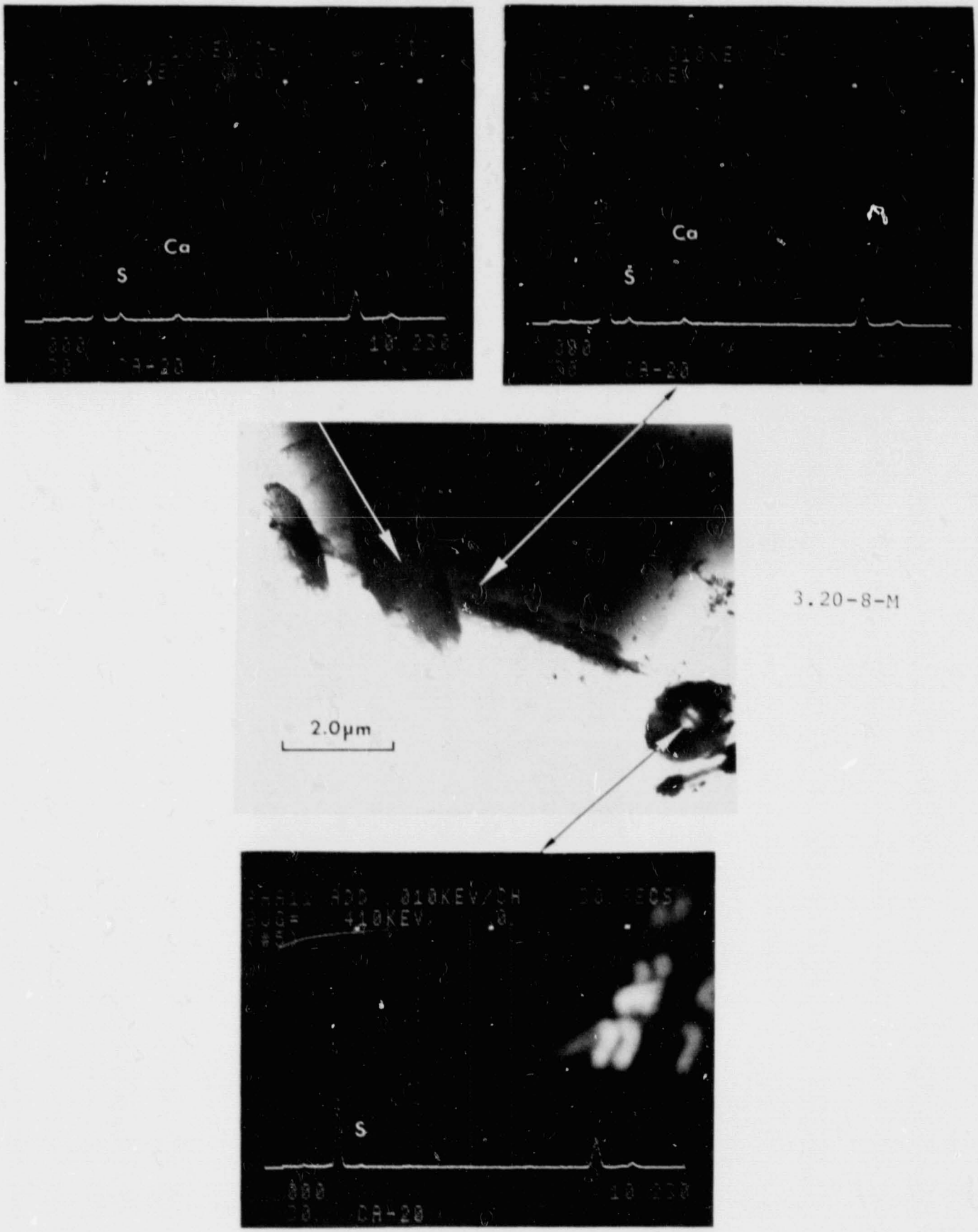

3.20-8-M

SAMPLE 9

Processing treatment A, B, C, D, etched in hydrofluoric acid to remove the aluminum and polish etched from the front to 5 mils. The sample was then sectioned and thinned from the back about 10 μm and then thinned from the front to allow electron transmission. Sample prepared to allow examination of the $P-P^+$ interface.

The sample examined was jet-thinned.

Figure 3.20-9-N shows a region containing what is undoubtedly surface contamination (at A in Figure 3.20-9-N(a)). The diffraction pattern (b) contains faint extra reflections.

Figure 3.20-9-O is representative of many regions of this sample which contained large areas consisting almost entirely of surface contamination. The diffraction pattern (b) contains many extra reflections which are fairly prominent.

Figure 3.20-9-P is a sequence of two photographs taken from a nearly contamination-free region. The rapid variation of the foil thickness is apparent from the numerous thickness extinction contours.

Figure 3.20-9-Q shows the x-ray spectrum (b) from a contamination-rich region (a). A small amount of Fe is present. This iron is due to the impurities in the aluminum paste.

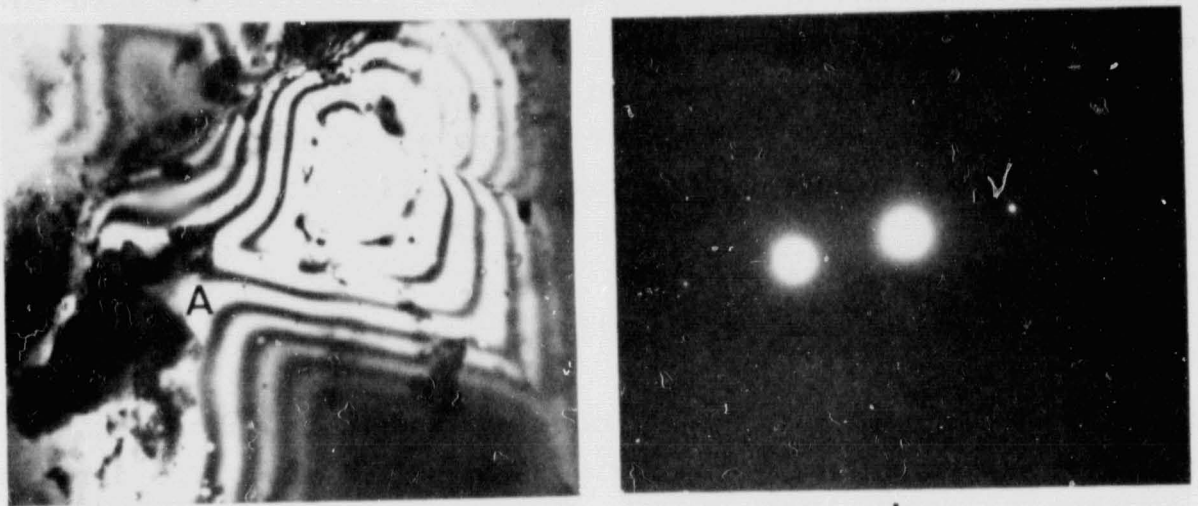

a b

3.20-9-N

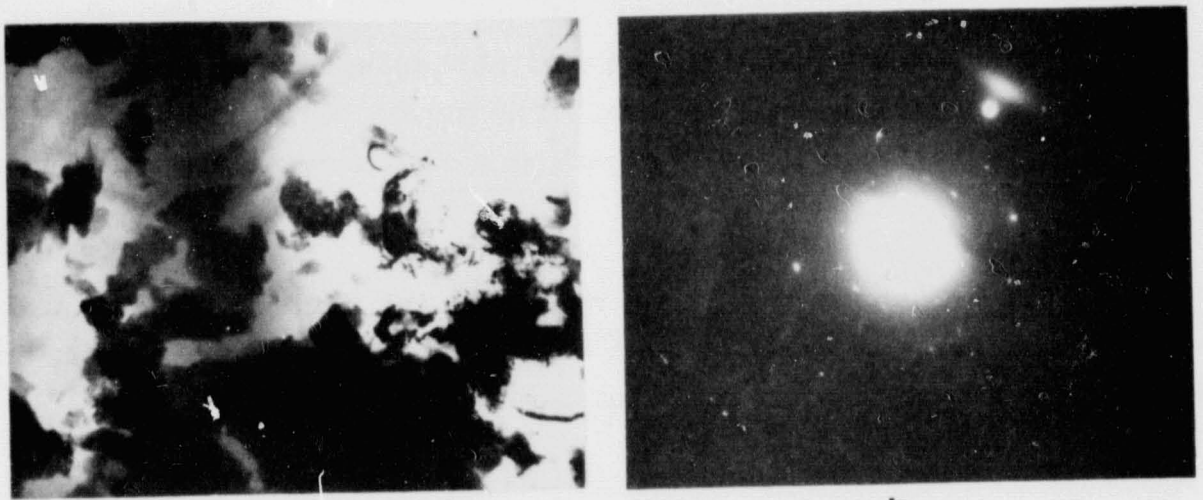

a b

3.20-9-O

Back $P-P^+$ Junction Area

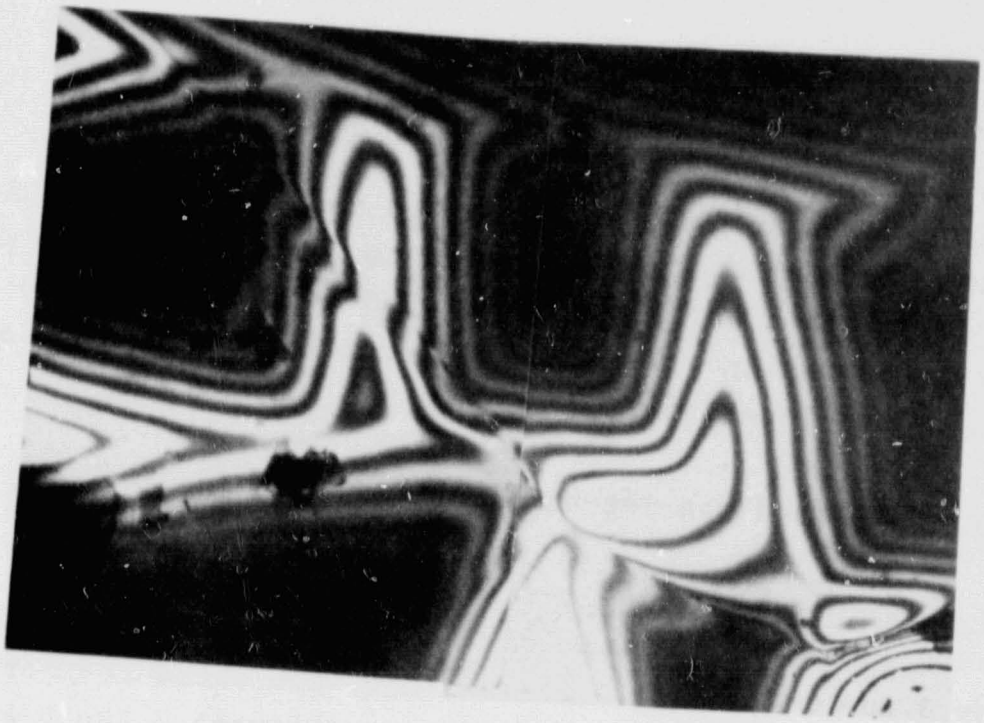

3.20-9-P

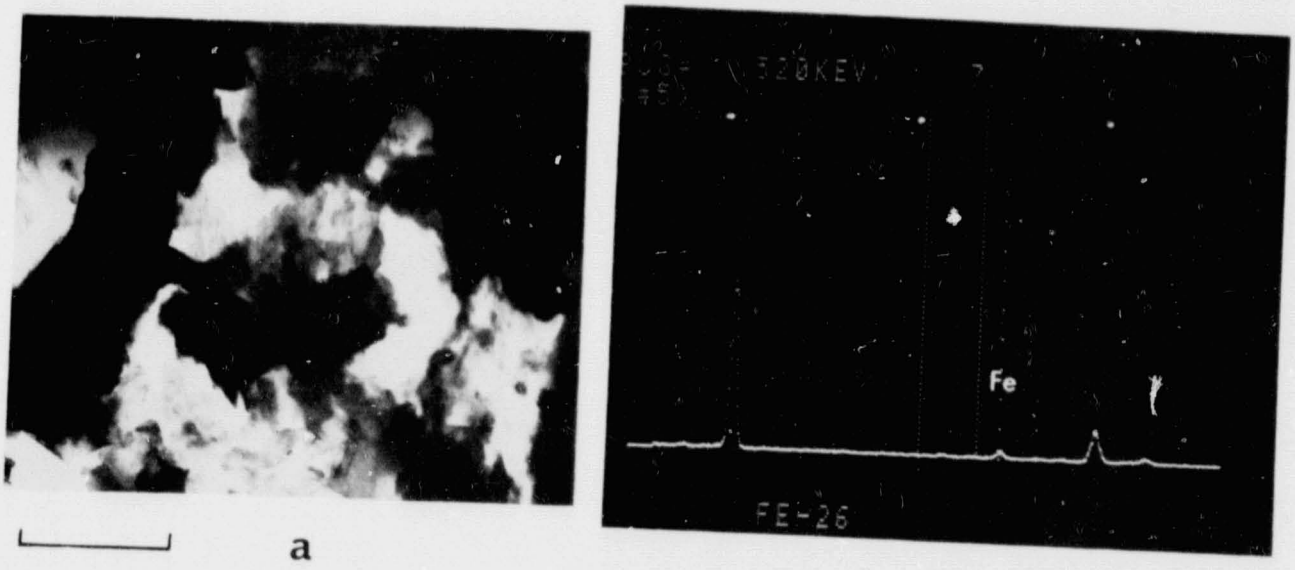

a

b

3.20-9-Q

SAMPLE 10

Processing treatment A, B, C, D, etched in hydrofluoric acid to remove the aluminum and polish etched to 5 mils from the front. The sample was then sectioned and etched from the front to allow electron transmission. Sample prepared to allow examination of the P^+ aluminum interface.

The sample examined was jet-thinned.

Figures 3.20-10-R and 3.20-10-S are representative of what was observed. Surface contamination is evident in the micrographs (Figures 3.20-10-R(a) and 3.20-10-S(a)), and extra reflections are visible in the diffraction patterns (Figures 3.20-10-R(b) and 3.20-10-S(b)). Large contamination-free areas were not observed since the back surface was not etched.

a

b

3.20-10-R

a

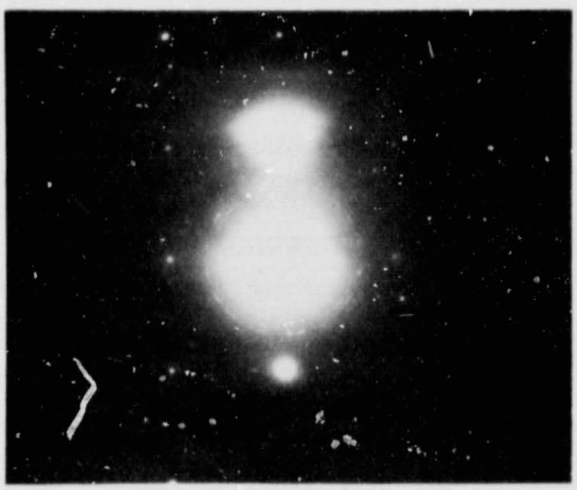

b

3.20-10-S

Back Aluminum - P^+
Silicon Surface

3.21 CELL PROCESS VERIFICATION

A number of wafers were processed according to the fabrication sequence depicted in Table 3.21-1. These 1-3 Ω-cm wafers were diffused to 25 to 35 Ω/□, in a tube furnace at 900°C; the aluminum paste was applied to the cell back and dried in an oven and sintered in an IR furnace; the junction was isolated by laser scribing from the back and breaking; and the silver paste was dried and fired in an IR furnace. The resultant data for two separate runs are shown in Table 3.21-2. The first set of data is the average of the first run, which consisted of 25 wafers purchased from Smiel. The remaining data comprise the results of the second run, which consisted of wafers purchased from Smiel, NBG Corporation (Dymet) and Texas Instruments. Experimental results show that the first run has a slightly greater electrical performance than the second despite the fact that it has a slightly lower shunt resistance. The second run gave identical results with all types of wafers used. All runs produced cells which had efficiencies greater than, or equal to, 10.8% without an AR coating, which implies that these cells would be over 14% with an AR coating.

In the second verification run the wafer lots were diffused at a variety of temperatures and AR coated with evaporated SiO_x. Table 3.21-3 is the average and standard deviation of these lots. These lots were processed using 850, 875, 900 and 925°C as the diffusion drive in temperature. There appears to be a slight degradation in V_{oc} as the temperature is increased from 850 to 925°C, but there does not appear to be any significant loss of current at load (500 mV). Histograms of the best lot at each diffusion temperature are given in Figures 3.21-A, B, C, and D, and the I-V characteristics of cells from each lot are given in Figures 3.21-E, F, G and H.

Table 3.21-1

PROCESS SEQUENCE

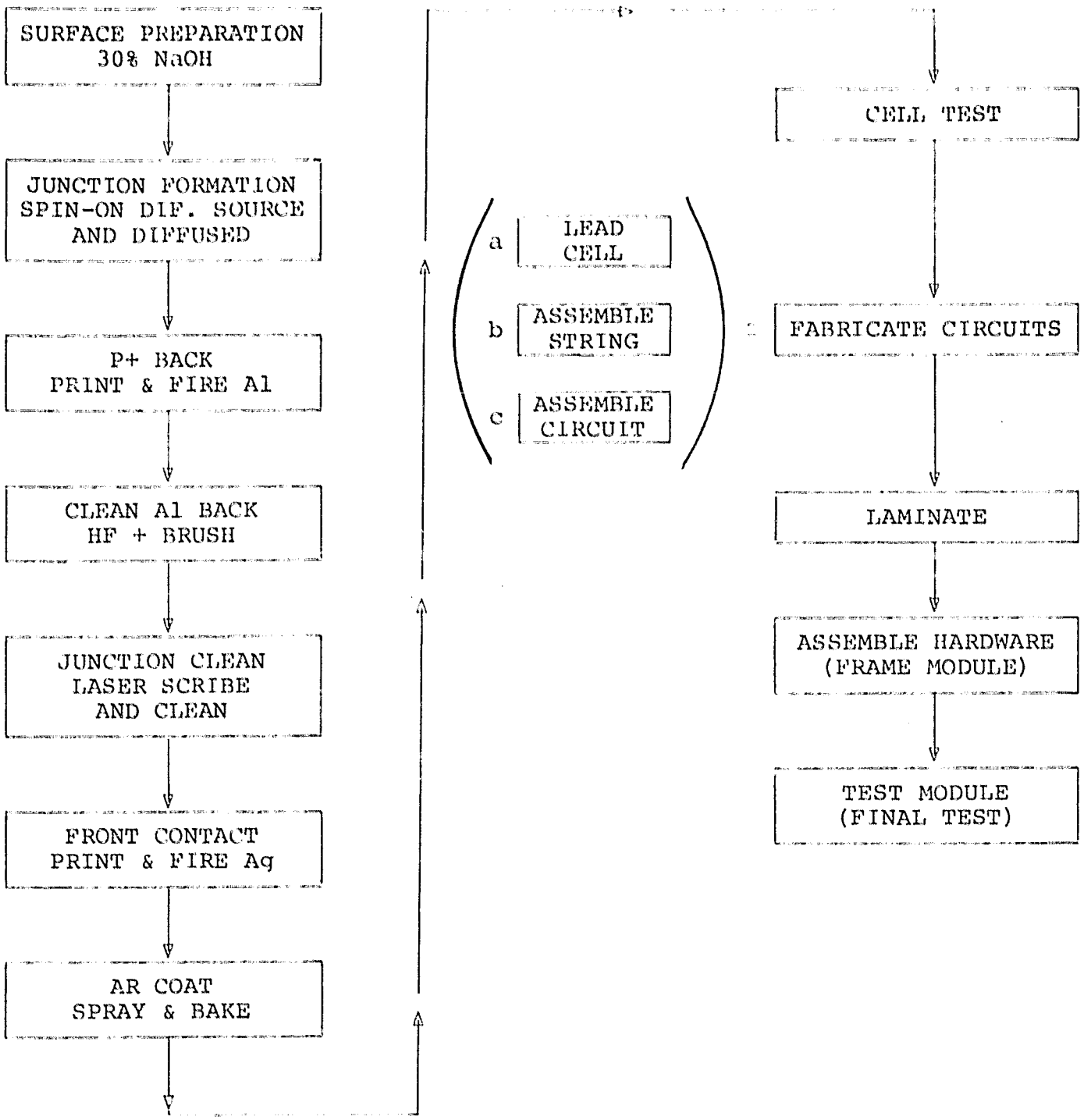

Table 3.21-2

SMALL LOT PROCESS VERIFICATION

Cell Type	# of Cells in Lot	ρ (Ω-cm)	$V_{oc} \pm \hat{\sigma}$ (mV)	$I_{sc} \pm \hat{\sigma}$ (mA)	$I_{500} \pm \hat{\sigma}$ (mA)	$R_{sh} \pm \hat{\sigma}$ (Ω)	$\eta^* \pm \hat{\sigma}$ (%)
Smeil	25	0.5 - 1	611 ± 1	677 ± 13	629 ± 21	17.2 ± 9.5	11.05 ± 0.36
Smeil	21	0.5 - 1	606 ± 2	682 ± 6	614 ± 11	20.5 ± 5.1	10.8 ± 0.2
Dymat	11	1 - 3	605 ± 2	689 ± 9	615 ± 19	24.4 ± 5.1	10.8 ± 0.3
TI	18	0.5 - 1	606 ± 3	676 ± 6	614 ± 14	27.6 ± 9.7	10.8 ± 0.2

*No AR Coating

Table 3.21-3

DIFFUSION TEMPERATURE VERIFICATION

Finished Cell / Start Wafers	Diffusion Time/Temp min/°C	Sheet ρ (Ω/□)	No AR Coating V_{oc} (mv)	No AR Coating I_{sc} (mA)	No AR Coating I_{500} (mA)	No AR Coating R_{sh} (Ω)	AR Coated V_{oc} (mv)	AR Coated I_{sc} (mA)	AR Coated I_{500} (mA)
39/45	80/850	35	608.2	738.5	606.8	149.9			
$\hat{\sigma}$			(1.8)	(8.3)	(30.1)	(65.6)			
37/40	95/850	29	604.4	685.5	633.9	129.4	611.3	934.2	855.4
$\hat{\sigma}$			(1.14)	(4.68)	(15.2)	(47.0)	(1.19)	(14.9)	(25.9)
45/50	30/875	30	606	725	534.1	130.1			
$\hat{\sigma}$			(1.44)	(98.9)	(94.9)	(54.8)			
34/40	25/875	34	602.5	688.2	618.6	67.8			
$\hat{\sigma}$			(1.1)	(4.7)	(31.8)	(25.7)			
35/4	13/900	29	603.1	615.7	660	98.0	609.4	938.4	859.0
$\hat{\sigma}$			(3.0	(12.7)	(16.1)	(153.8)	(3.4)	(15.1)	(51.8)
37/40	11/900	32	589.4	682.4	537.8	85.4			
$\hat{\sigma}$			(5.2)	(18.3)	(54.7)	(30.9)			
39/41	6/925	25	601.2	679.1	623.4	59.2			
$\hat{\sigma}$			(2.4)	(9.6)	(11.7)	(19.3)			
37/40	4/925	33	572.2	710.2	462.9	177.3			
$\hat{\sigma}$			(4.1)	(32.5)	(80.7)	(82.3)			

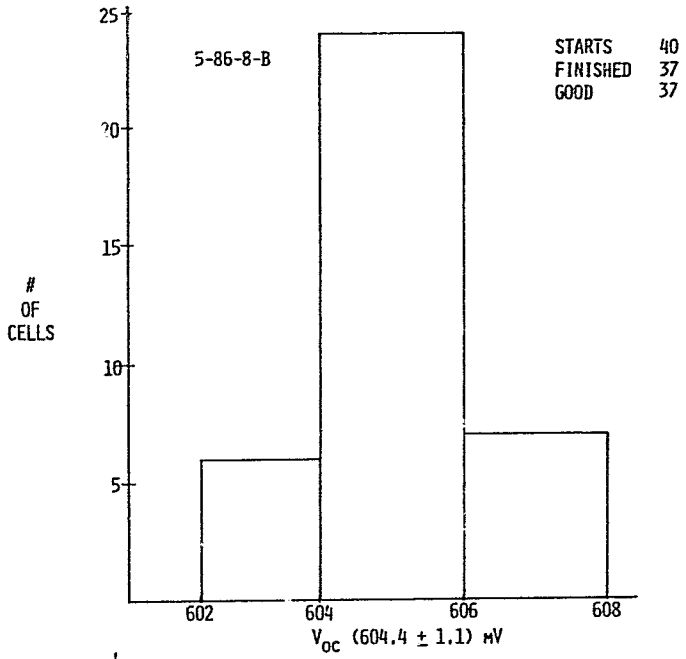

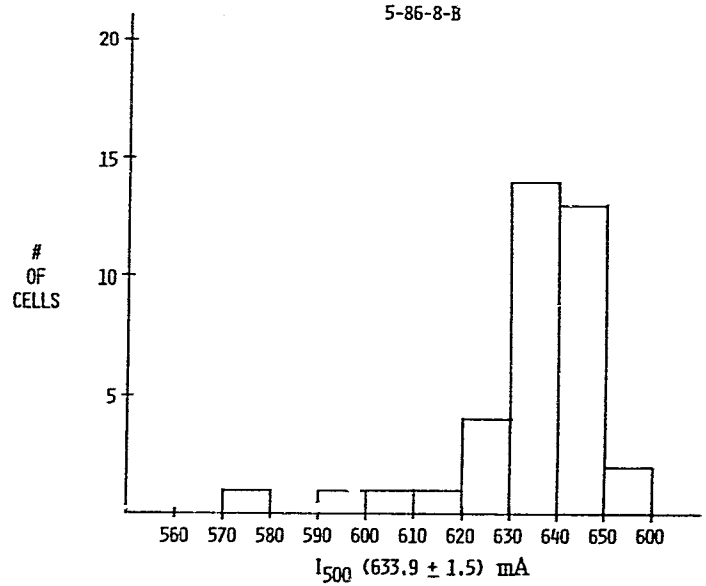

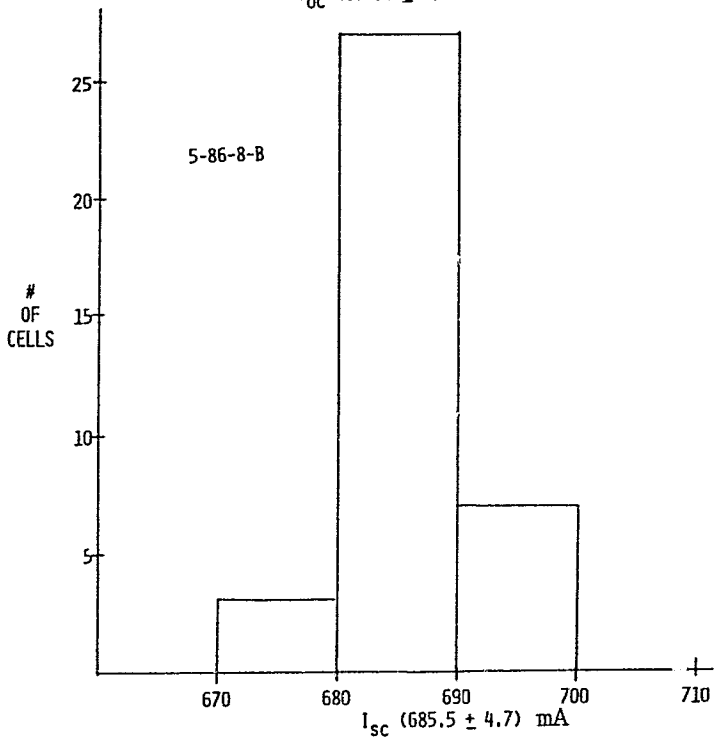

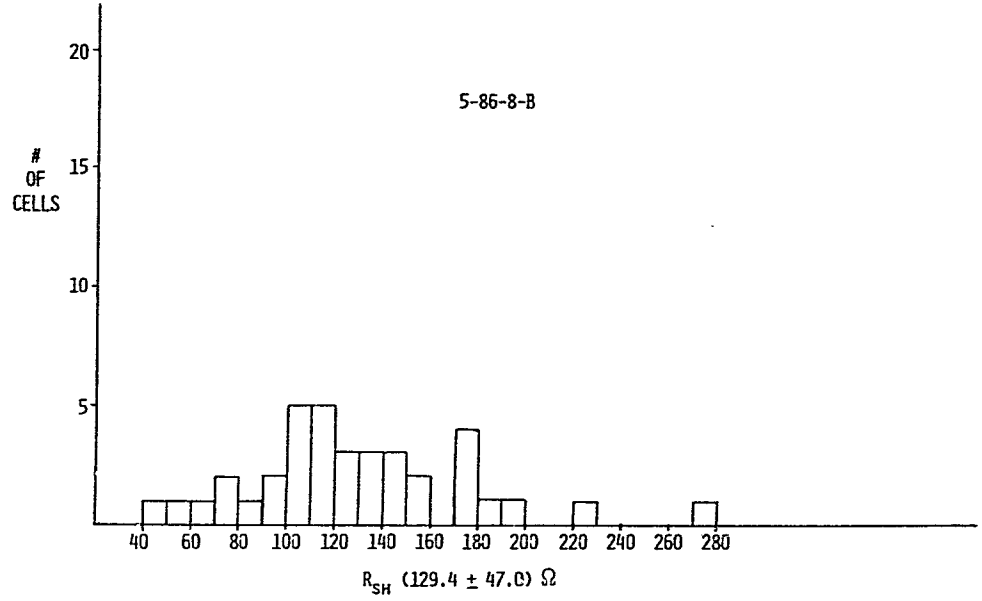

Figure 3.21-A. HISTOGRAM OF CELLS DIFFUSED FOR 95 MINUTES AT 850°C

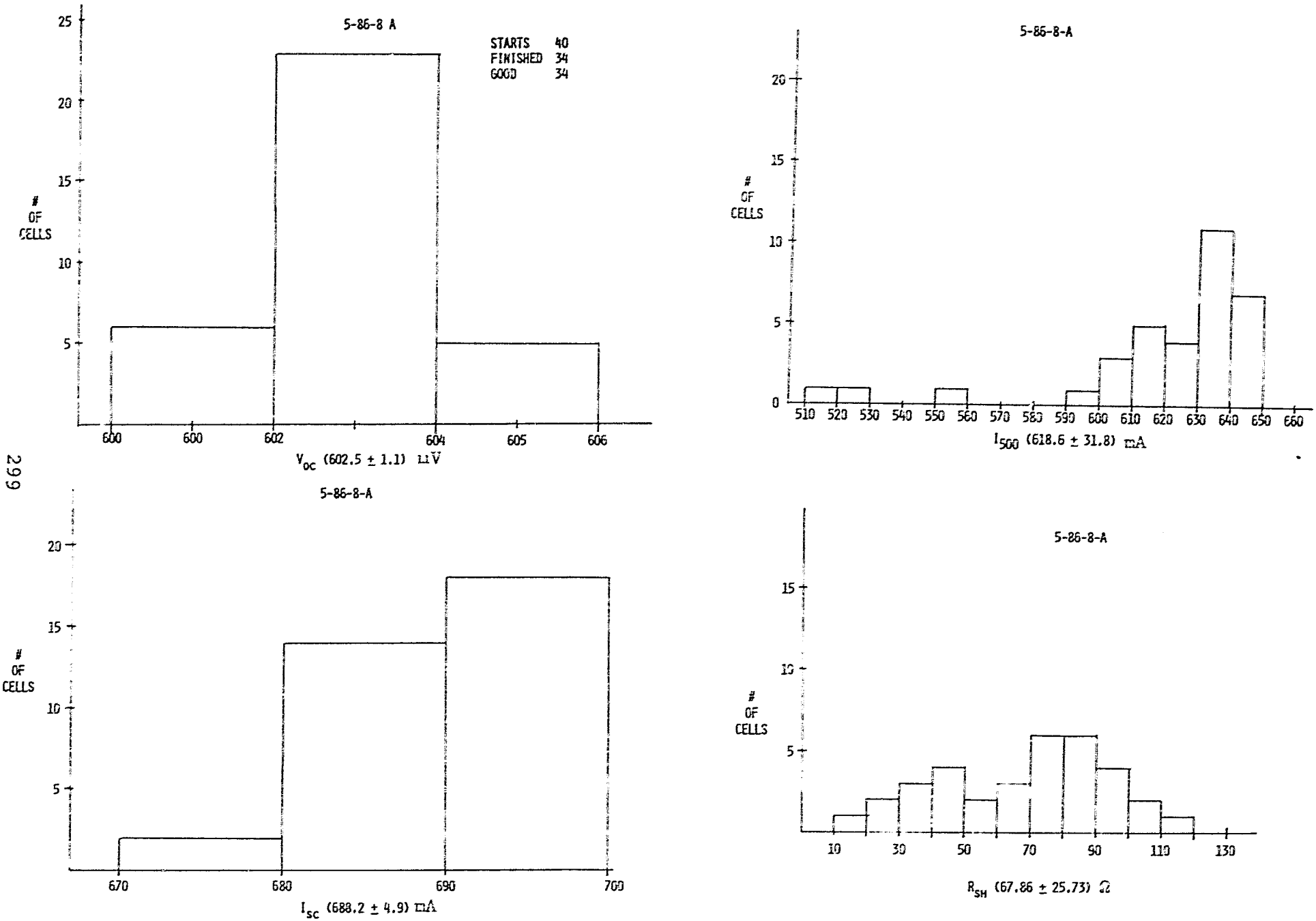

Figure 3.21-B. HISTOGRAM OF CELLS DIFFUSED FOR 25 MINUTES AT 875°C

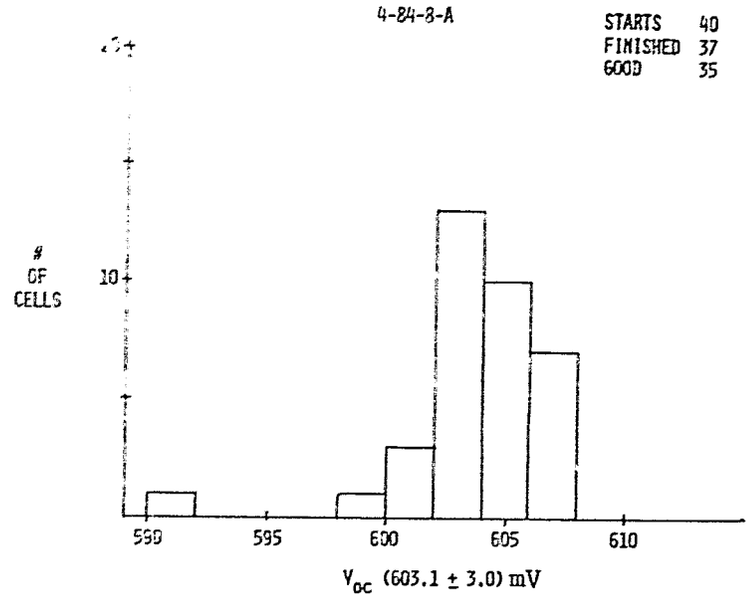

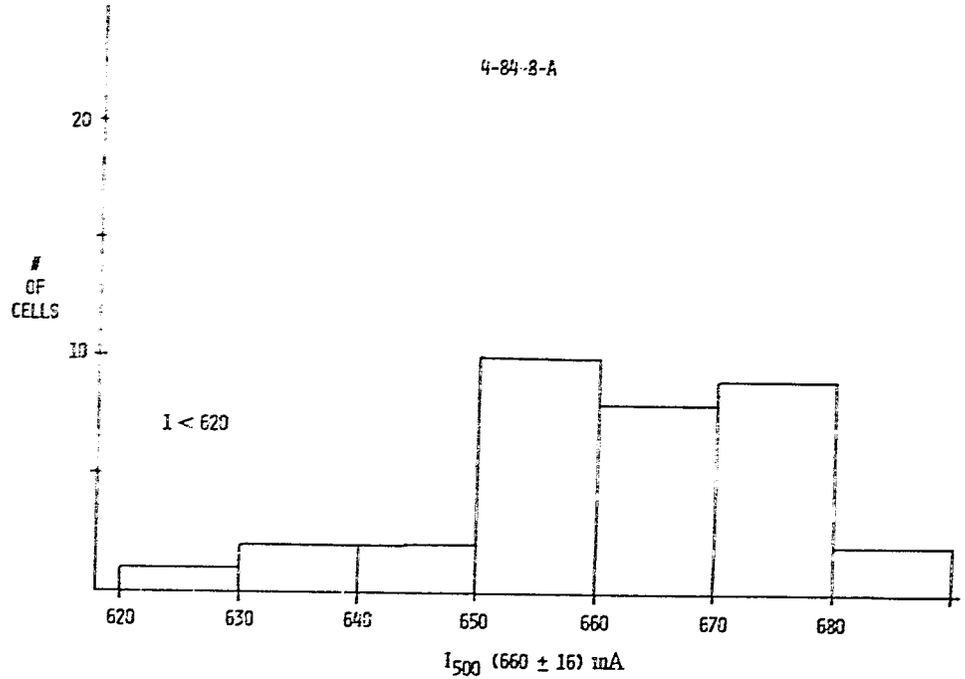

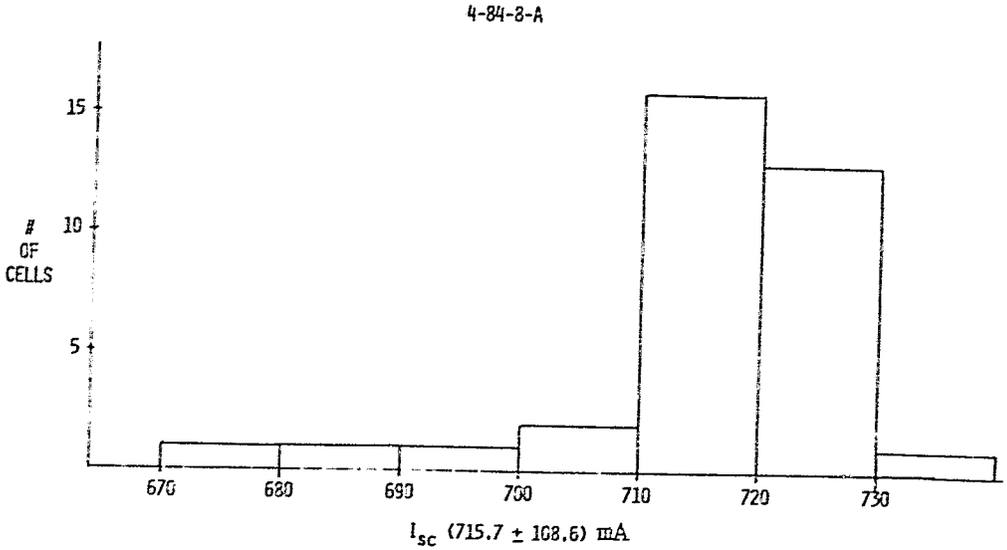

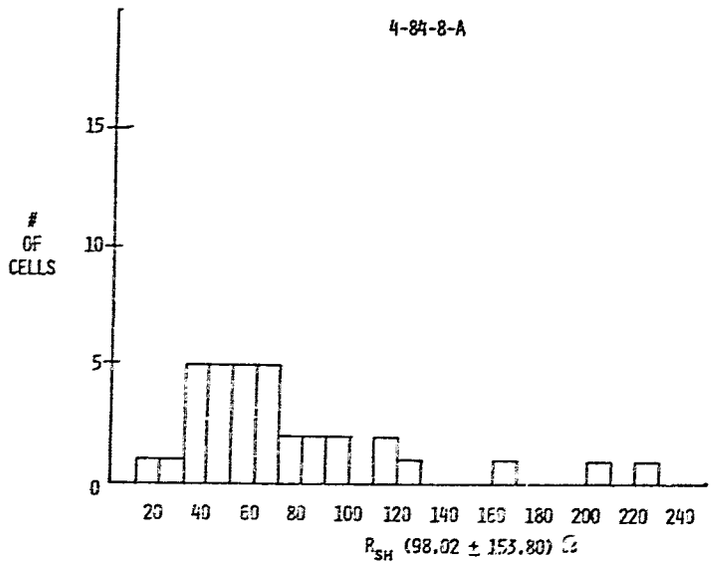

Figure 3.21-C. HISTOGRAM OF CELLS DIFFUSED FOR 13 MINUTES AT 900°C

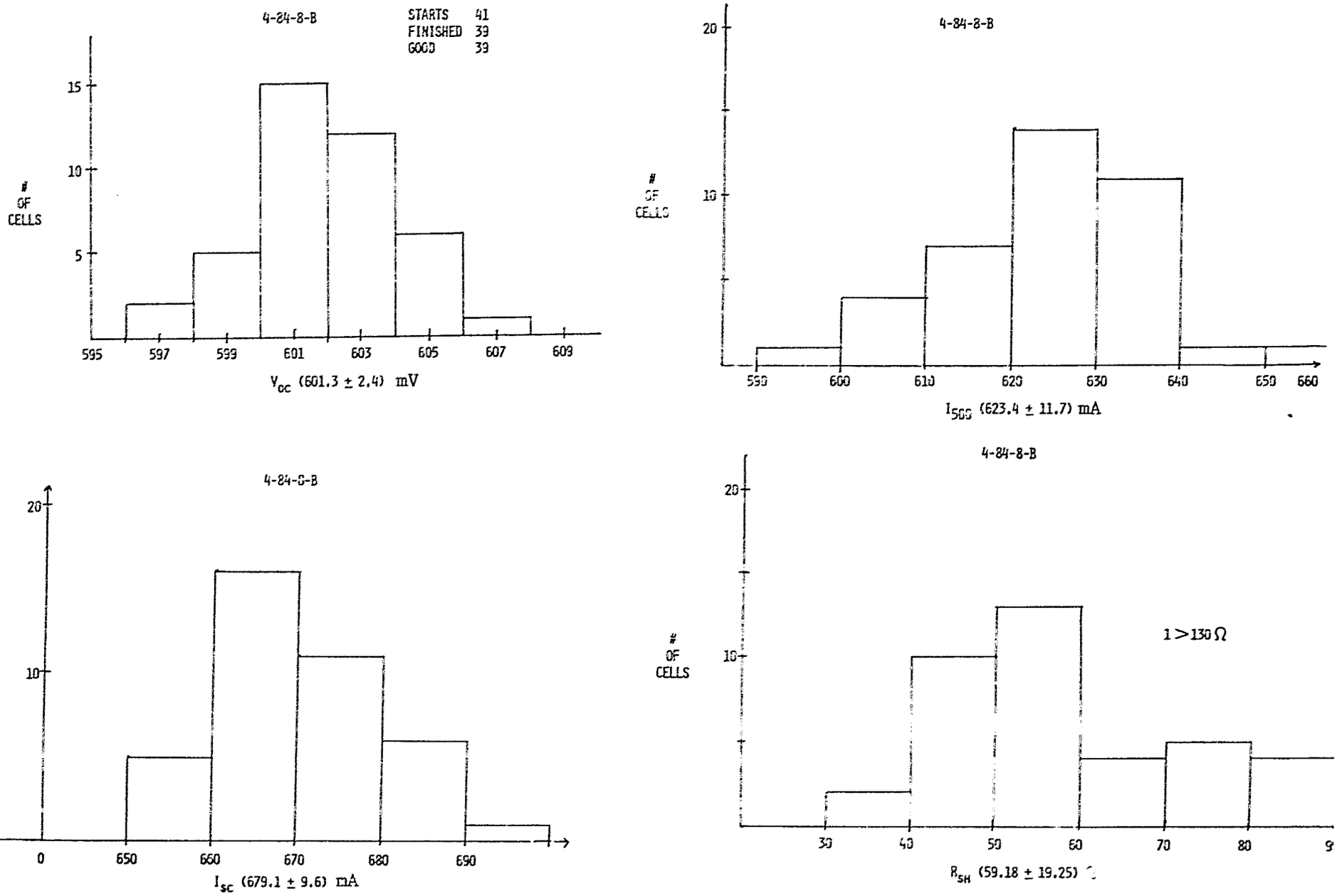

Figure 3.21-D. HISTOGRAM OF CELLS DIFFUSED FOR 6 MINUTES AT 925°C

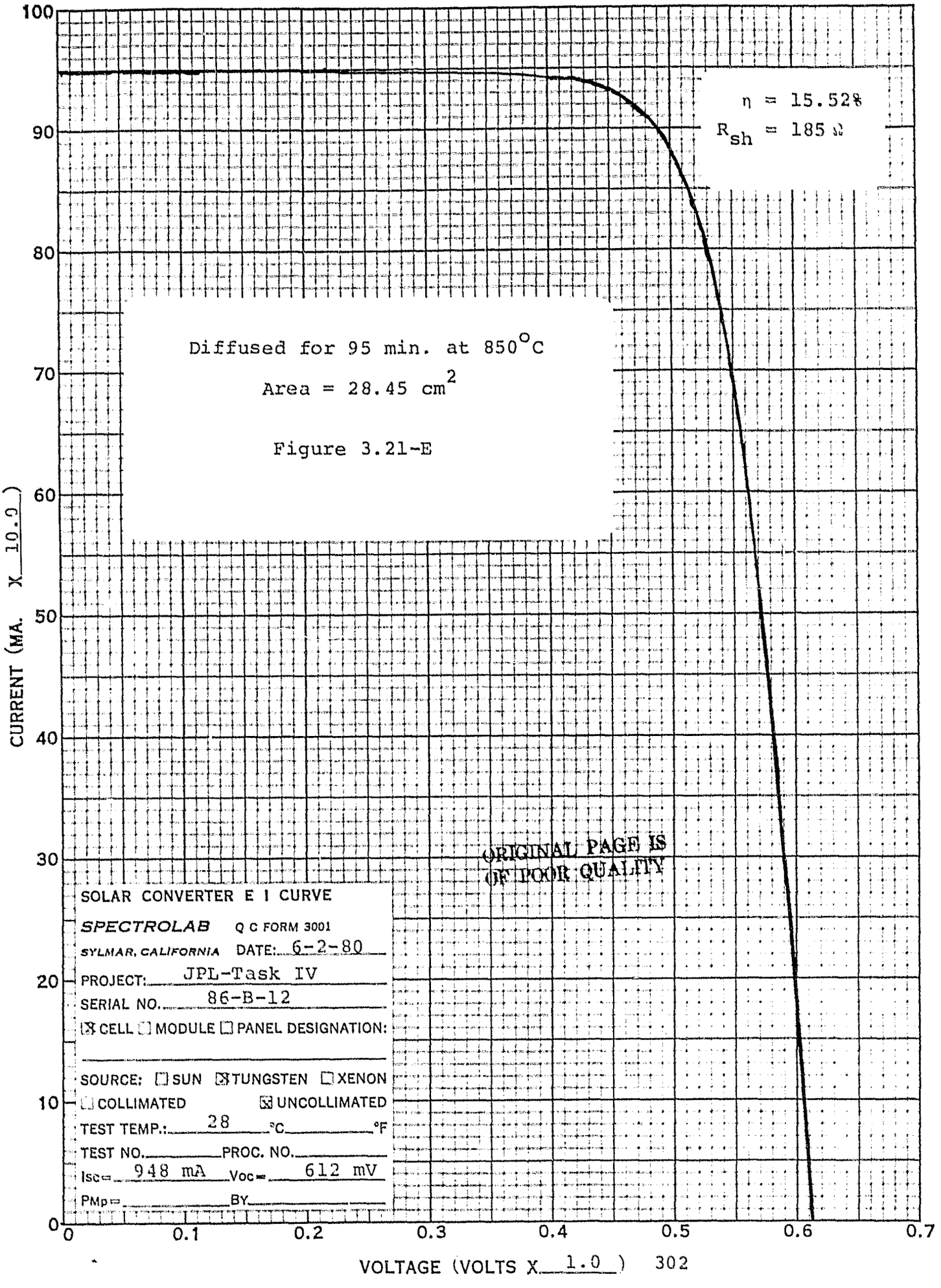

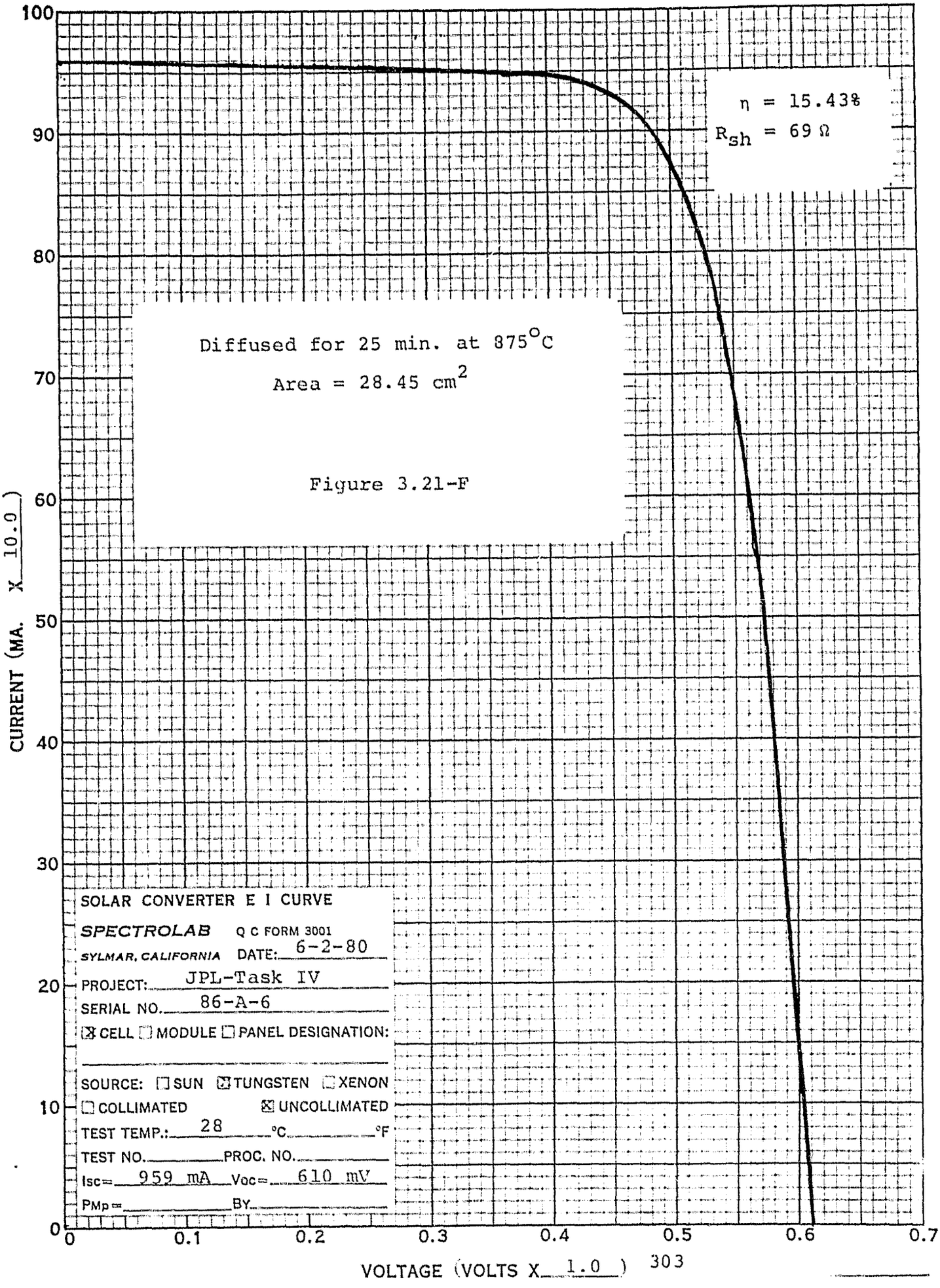
η = 15.43%
R_{sh} = 69 Ω
Diffused for 25 min. at 875°C
Area = 28.45 cm²
Figure 3.21-F
SOLAR CONVERTER E I CURVE
SPECTROLAB Q C FORM 3001
SYLMAR, CALIFORNIA DATE: 6-2-80
PROJECT: JPL-Task IV
SERIAL NO. 86-A-6
☒ CELL ☐ MODULE ☐ PANEL DESIGNATION:
SOURCE: ☐ SUN ☒ TUNGSTEN ☐ XENON
☐ COLLIMATED ☒ UNCOLLIMATED
TEST TEMP.: 28 °C °F
TEST NO. PROC. NO.
Isc= 959 mA Voc= 610 mV
PMp= BY
CURRENT (MA. X 10.0)
VOLTAGE (VOLTS X 1.0)
0
10
20
30
40
50
60
70
80
90
100
0
0.1
0.2
0.3
0.4
0.5
0.6
0.7

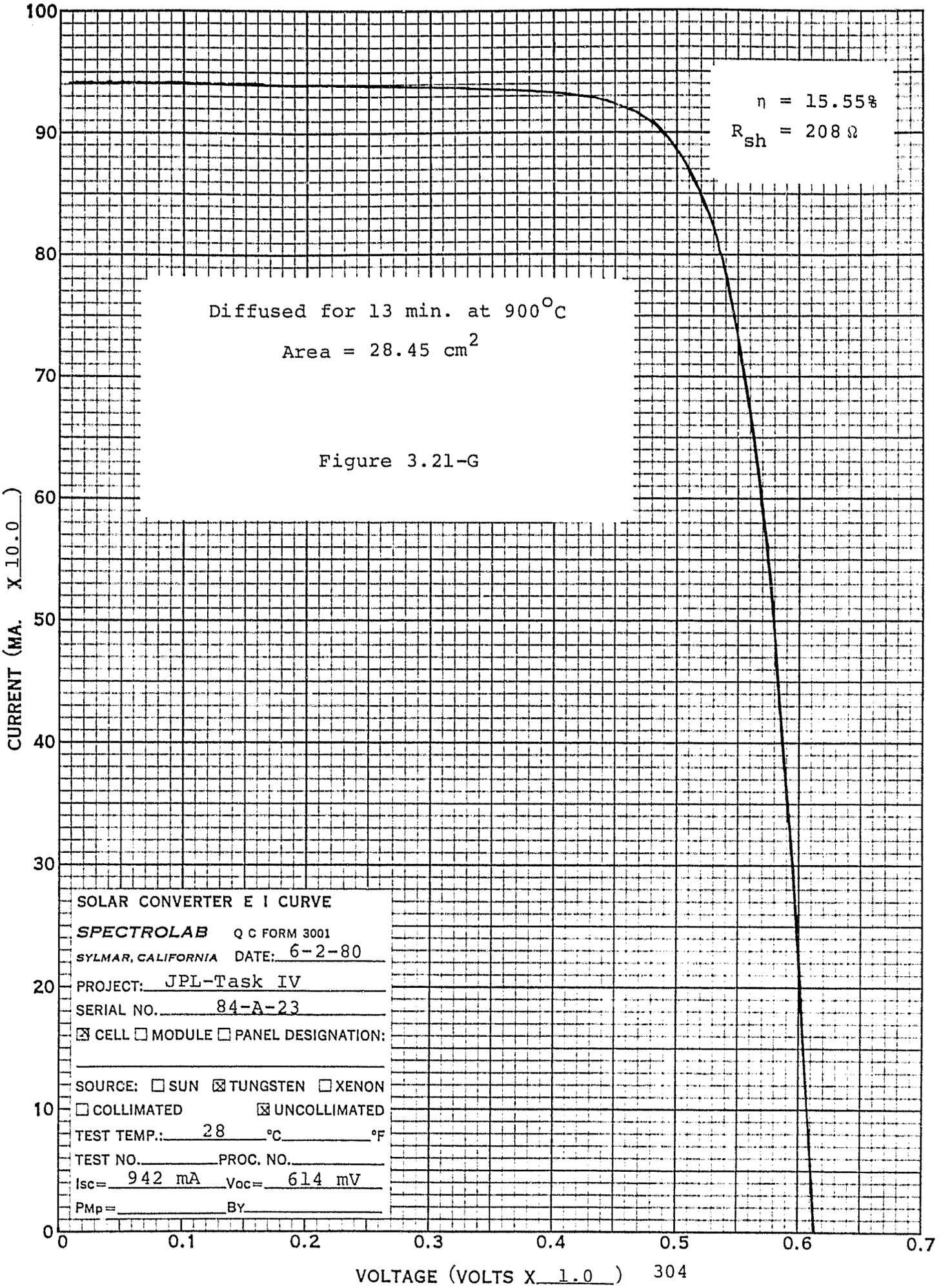
η = 15.55%
R_{sh} = 208 Ω
Diffused for 13 min. at 900°C
Area = 28.45 cm²
Figure 3.21-G
CURRENT (MA. X 10.0)
VOLTAGE (VOLTS X 1.0)
0
10
20
30
40
50
60
70
80
90
100
0
0.1
0.2
0.3
0.4
0.5
0.6
0.7
SOLAR CONVERTER E I CURVE
SPECTROLAB Q C FORM 3001
SYLMAR, CALIFORNIA DATE: 6-2-80
PROJECT: JPL-Task IV
SERIAL NO. 84-A-23
☒ CELL ☐ MODULE ☐ PANEL DESIGNATION:
SOURCE: ☐ SUN ☒ TUNGSTEN ☐ XENON
☐ COLLIMATED ☒ UNCOLLIMATED
TEST TEMP.: 28 °C °F
TEST NO. PROC. NO.
Isc= 942 mA Voc= 614 mV
PMp= BY

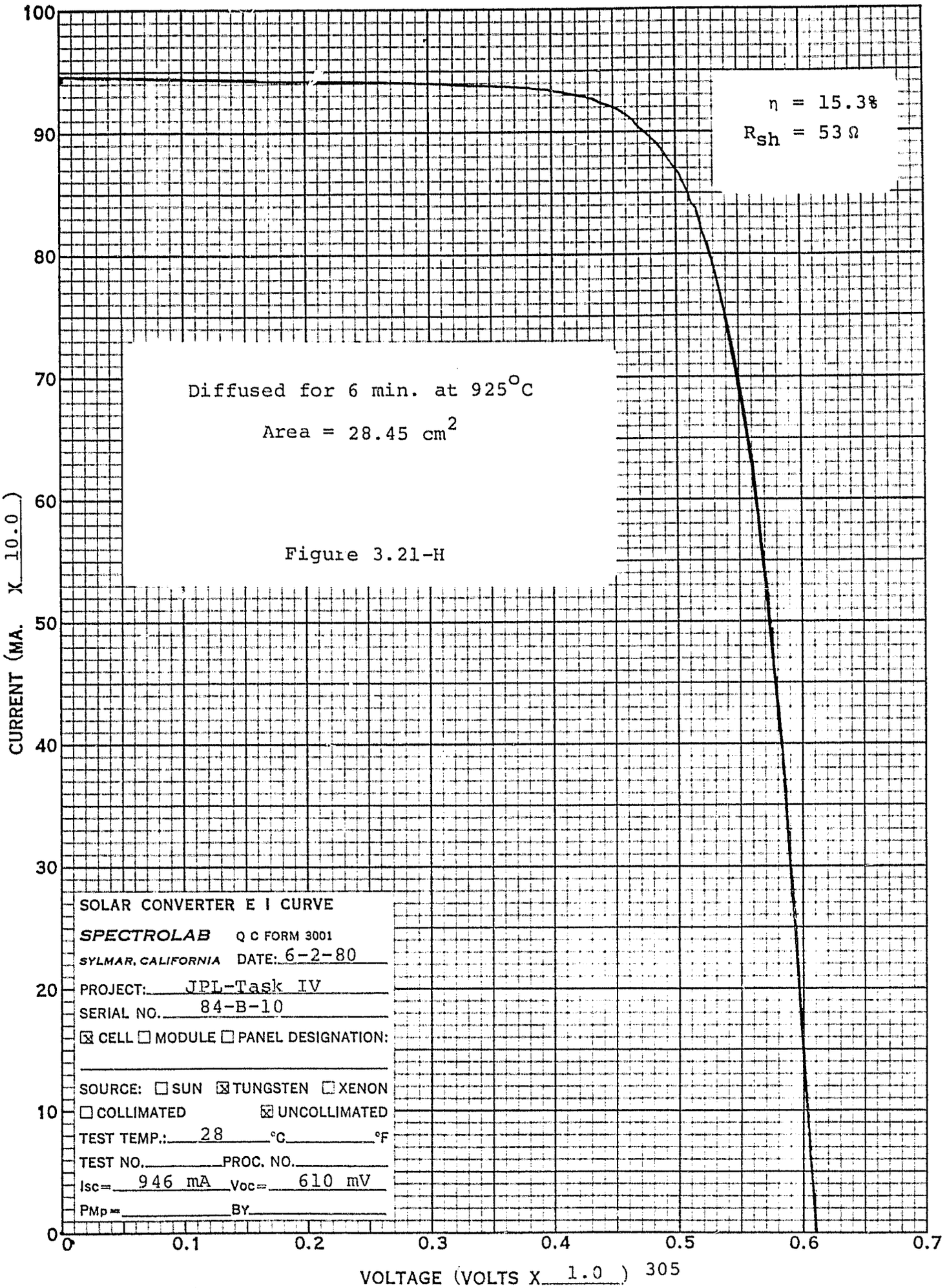
η = 15.3%
R_{sh} = 53 Ω
Diffused for 6 min. at 925°C
Area = 28.45 cm²
SOLAR CONVERTER E I CURVE
SPECTROLAB Q C FORM 3001
SYLMAR, CALIFORNIA DATE: 6-2-80
PROJECT: JPL-Task IV
SERIAL NO. 84-B-10
☒ CELL ☐ MODULE ☐ PANEL DESIGNATION:
SOURCE: ☐ SUN ☒ TUNGSTEN ☐ XENON
☐ COLLIMATED ☒ UNCOLLIMATED
TEST TEMP.: 28 °C °F
TEST NO. PROC. NO.
Isc= 946 mA Voc= 610 mV
PMp= BY
CURRENT (MA. X 10.0)
VOLTAGE (VOLTS X 1.0)
0
10
20
30
40
50
60
70
80
90
100
0
0.1
0.2
0.3
0.4
0.5
0.6
0.7

Figure 3.21-H

Processing problems seem to be indicated by current at load variations between different lots diffused at the same temperature, and by large standard deviations of the low lots. The cell lot diffused at 925°C for four minutes had a very thin aluminum back surface which made electrical testing very difficult and makes the data questionable. Although some problems did arise during these verification runs, most lots resulted in high yield (for a non-mechanized process) and high average efficiency (> 14%) cells. It is believed that the process sequence described in Table 3.21-1 is capable of producing 15% cells with a 90% yield.

Two additional verification runs were performed with 100 (7-14 Ω-cm) wafers each. These lots were utilized to fabricate a 200 cell panel. The cell processing was the same as that of the first run and an AR coating was applied by evaporating SiO_x. An average efficiency in excess of 14% was achieved with both verification runs, using this process sequence. These two hundred wafers were processed in accordance with Table 3.21-1 except for the AR coating. The following paragraph is a detailed explanation of this sequence.

The first processing step is surface preparation which consists of placing the wafers in 30% NaOH for 20 minutes, followed by 20% HCl for 15 minutes. Junction formation is achieved by spinning on PX-10 diffusion source, followed by drying for 15 minutes at 150°C, and diffusing at 400°C for a total time of 13 minutes. The aluminum P^+ back is printed, and then IR dried and fired at a belt speed of 36"/min., with the four zones set at 500°C, 800°C, 875°C, and 875°C, respectively. Following this step, the aluminum back is cleaned in 10% HF for 4 minutes followed by 2% NH_4OH for 30 seconds. The excess aluminum was removed by brushing. The

next processing step is laser scribing to isolate the junction, followed by a front surface cleaning step to remove excess aluminum particles. The front Ag contacts are printed, and the IR dried and fired at a belt speed of 48"/min., with the four zones set at 0, 800°C, 750°C, and 750°C, respectively. The SiO_x AR coating is applied to the cells by evaporation. This completes the cell fabrication sequence utilized in the verification runs.

After the completion of the verification runs, electrical performance data was obtained and statistically evaluated. Histograms of I_{sc}, V_{oc}, I_{500} and R_{sh} for the two lots are presented in Figures 3.21-I and 3.21-J, respectively.

A final verification run was performed with 500 wafers. This lot was processed identically to the preceding two lots, discussed above. During IR firing of the aluminum P^+ back, it was discovered that the firing temperature had been set too low. A total of 132 wafers were fired incorrectly before the temperature variation was disclosed. The remaining wafers were processed in accordance with our process sequence. Table 3.21-4 lists the percentage yield during the process sequence. The as-sawed wafers had fractures along the edges which has the influence of reducing the yield.

Some of the processed cells were selected for AR coating and soldering of front tabs, some were only AR coated while some were not AR coated at all (at the request of JPL). These cells have been sent to JPL for evaluation. Table 3.21-5 lists the V_{oc}, I_{sc}, I_{500} and R_{sh} of all the cells prior to AR coating and the selected cells that were AR coated; Figure 3.21-K is the histogram of the AR coated cells.

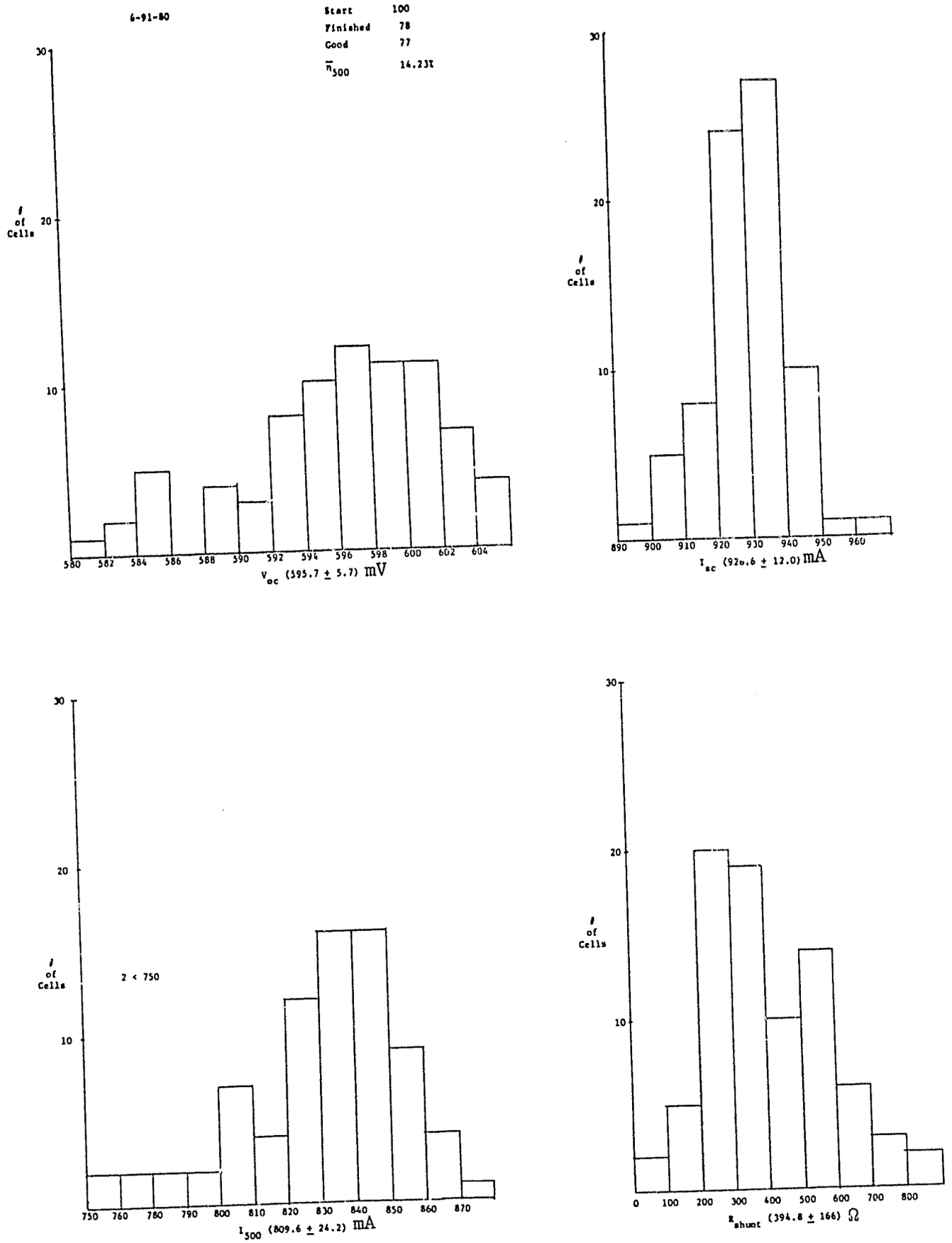
6-91-80
Start 100
Finished 78
Good 77
$\bar{\eta}_{500}$ 14.23%
# of Cells
V_{oc} (595.7 ± 5.7) mV
I_{sc} (926.6 ± 12.0) mA
2 < 750
I_{500} (809.6 ± 24.2) mA
R_{shunt} (394.8 ± 166) Ω

Figure 3.21-I

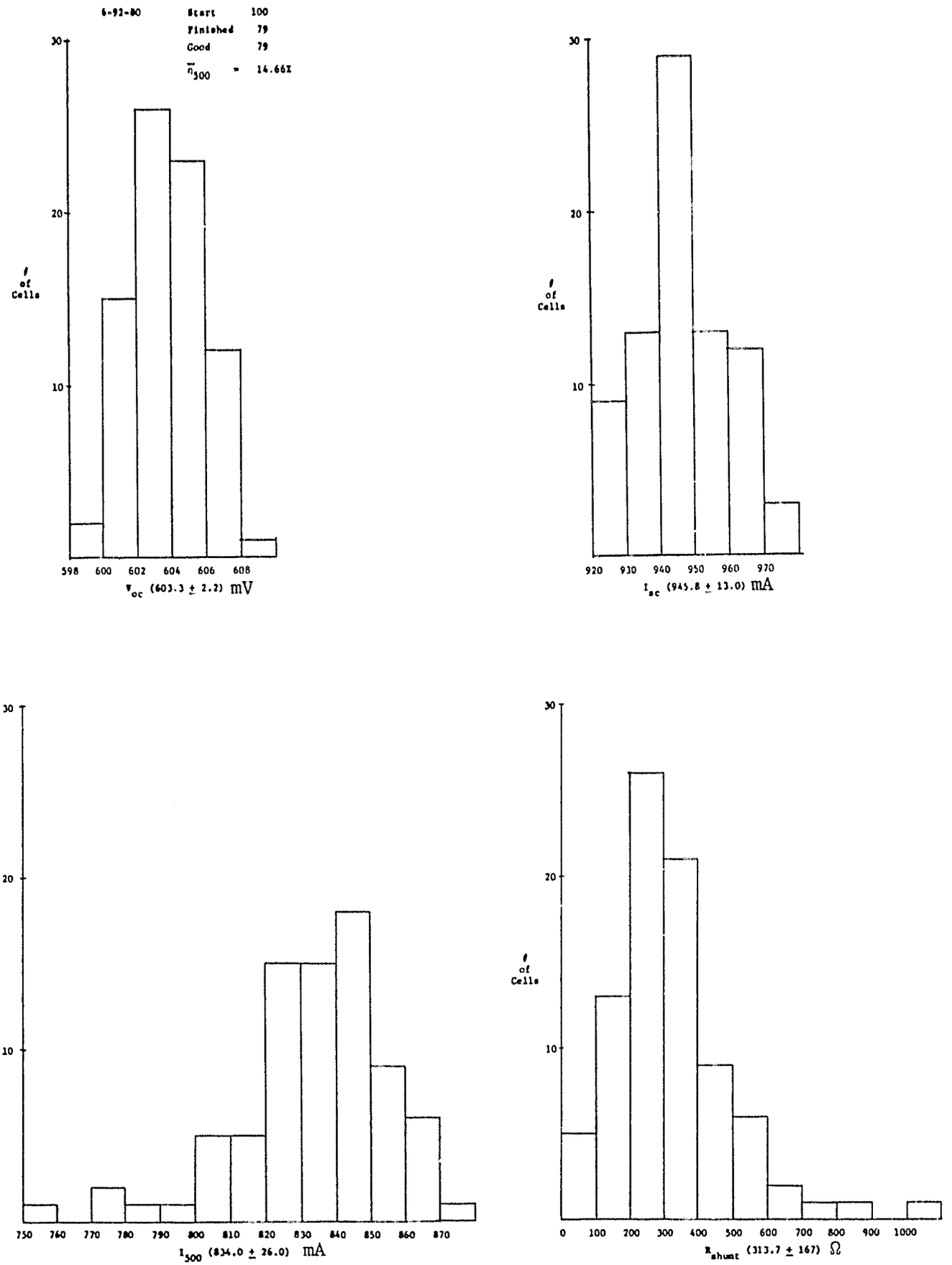
6-92-80
Start 100
Finished 79
Good 79
$\bar{\eta}_{500}$ = 14.66%
# of Cells
V_{oc} (603.3 ± 2.2) mV
I_{sc} (945.8 ± 13.0) mA
I_{500} (834.0 ± 26.0) mA
R_{shunt} (313.7 ± 167) Ω

Figure 3.21-J

Table 3.21-4

PROCESS SEQUENCE

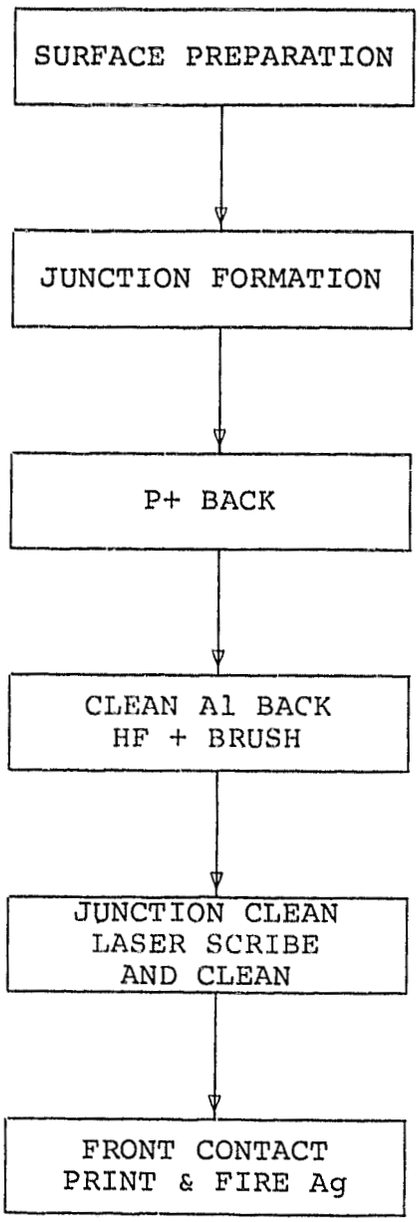

	% Yield
SURFACE PREPARATION	98.6
JUNCTION FORMATION	98.8
P+ BACK	97.5
CLEAN Al BACK HF + BRUSH	99.4
JUNCTION CLEAN LASER SCRIBE AND CLEAN	97.1
FRONT CONTACT PRINT & FIRE Ag	99.1

Table 3.21-5

	V_{oc} (mV)	I_{sc} (mA)	I_{500} (mA)	R_{sh} (Ω)
	No AR Coating			
Average	575.4	715.7	598.9	383
$\hat{\sigma}$	13.2	33.2	40.0	284
	AR Coated			
Average	582.4	945.8	794.2	405
$\hat{\sigma}$	12.2	21.2	47.3	284

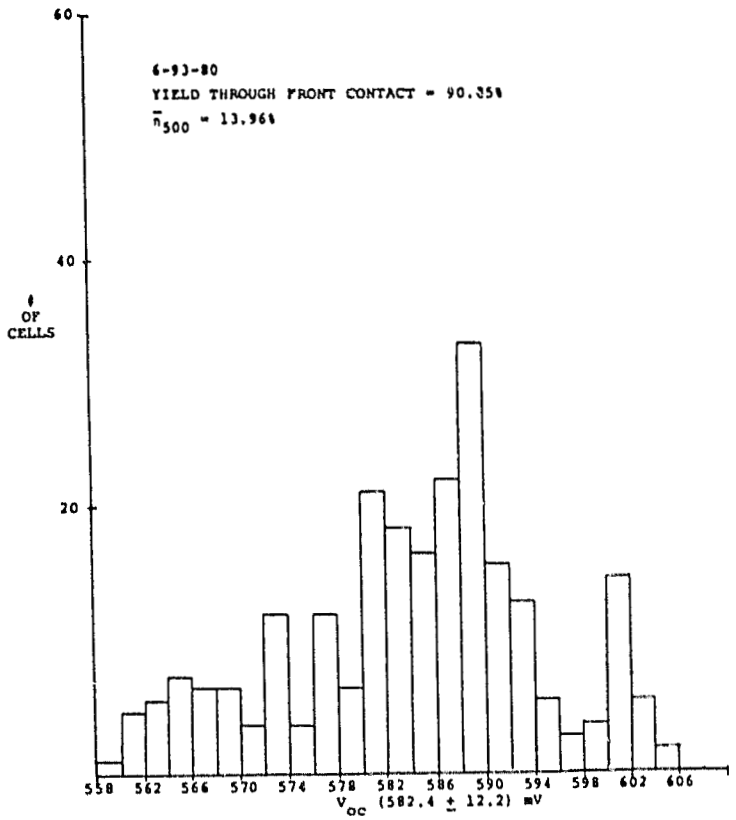
6-93-80
YIELD THROUGH FRONT CONTACT = 90.35%
$\bar{\eta}_{500}$ = 13.96%
60
40
20
OF CELLS
558 562 566 570 574 578 582 586 590 594 598 602 606
V_{oc} (582.4 ± 12.2) mV

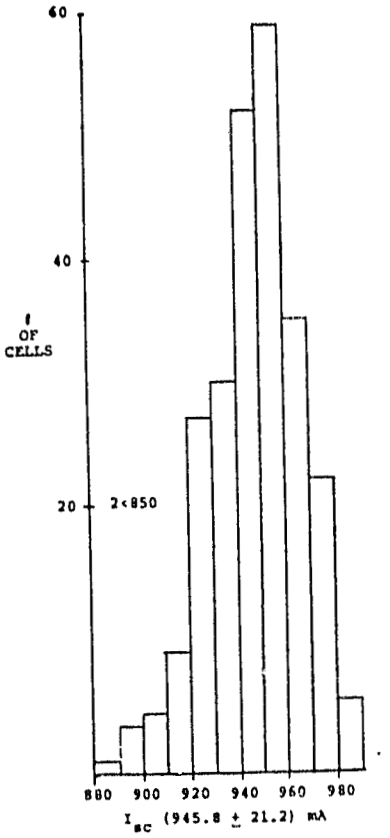
60
40
20
OF CELLS
2<850
880 900 920 940 960 980
I_{sc} (945.8 ± 21.2) mA

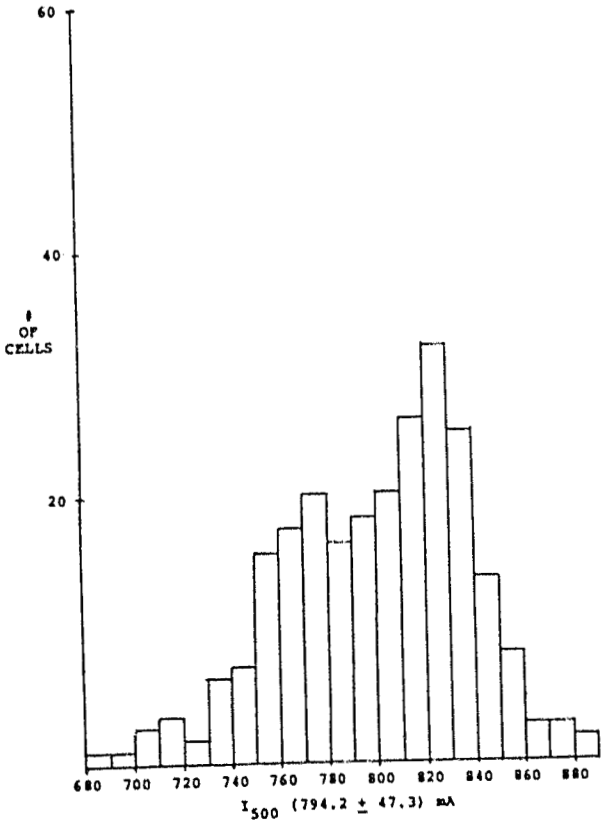
60
40
20
OF CELLS
680 700 720 740 760 780 800 820 840 860 880
I_{500} (794.2 ± 47.3) mA

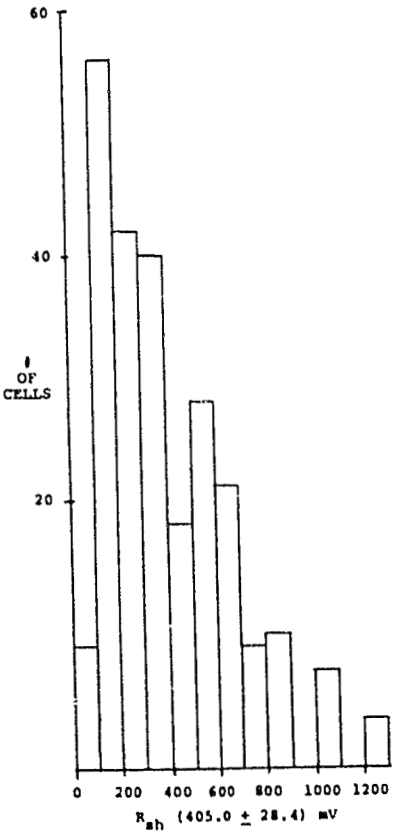
60
40
20
OF CELLS
0 200 400 600 800 1000 1200
R_{sh} (405.0 ± 28.4) mV

Figure 3.21-K

Some of the cells have very low V_{oc}'s (these cells were not chosen to be AR coated). These cells are believed to be indicative of the temperature response of the IR furnace under heavy load. The optimum firing conditions for aluminum P^+ back contacts were arrived at with small lots (less than fifty wafers) and may not be the optimum conditions for concinuous firing of P^+ contacts.

3.22 ECONOMIC EVALUATION

Of the processes studied we have recommended that the following be retained:

Spray on diffusion
Print and fire aluminum P^+ back
Clean
Print and fire silver front contact
Apply tin pad to aluminum back

These process steps are evaluated in this section using the IPEG equation. The analysis is summarized in Table 3.22-1. All costs and prices are expressed in 1975 dollars. The total cost for the five process steps considered is $0.0625 per peak watt at 100% yield. Assuming a budget of $0.15 for cell fabrication, $0.0875 is left for the missing processes of:

Surface preparation
Junction cleaning
AR coating
Testing

and yield losses. The assumptions and inputs to Table 3.22-1 are discussed in the following paragraphs.

3.22.1 General Assumptions

It is assumed that the solar cells being produced are 4 inch squares with an encapsulated efficiency of 13%. The peak output per cell is therefore 1.34 watts. The factory is assumed to operate 7 days per week, 50 weeks per year. During this operating period all processes are assumed to have a machine "up" time ratio of 0.90 operating minutes per minute. A shift factor of 4 has been used to convert labor requirements per shift to that required for the specified operating mode.

Input costs (other than capital equipment) were taken wherever possible from the SAMICS catalog. When costs were not available

Table 3.22-1

DOLLARS PER WATT CONTRIBUTION OF FIVE CELL PROCESS STEPS

	DIFFUSION	AL BACK	CLEAN	FR. CONTACT	TIN PAD	
QUAN.	45.6	15.2	30.4	15.2	15.2	MW_{PK} / YR.
EQUIP.	.0043 * 405,000	.0015 48,000	.0008 51,250	.0012 36,500	.0007 22,750	$(1975)
FLOOR SP.	.0035 1,640	.0022 350	.0009 300	.0020 320	.0019 300	SQUARE FEET
LABOR	.0038 83,460	.0034 24,565	.0038 55,370	.0034 24,565	.0043 31,145	$(1975) / YR
MATERIALS	.0001 3,675	.0022 25,140	.0022 51,325	.0171 200,515	.0002 2,250	$(1975) / YR
UTIL.	.0018 63,640	.0004 4,550	205	.0004 4,770	340	$(1975) / YR
P (IPEG)	0.0136	.0097	.0078	.0242	.0072	.0625 $(1975)/ WP

* $(1975) PER WATT CONTRIBUTION FOR THIS ELEMENT.

in the catalog, use was made of actual purchases or vendor quotes. Inputs and their prices are given in Table 3.22-2. Equipment and equipment costs are identified in the text. Equipment costs are based on discussions with vendors where comparable equipment exists. Adjustments were estimated for anticipated modifications. Where this could not be done, estimates of equipment costs were made by Spectrolab. Equipment costs have been adjusted to include estimated installation costs and salvage value. All input costs were reduced to 1975 dollars using an average annual inflation rate of 8.75%.

3.22.2 Diffusion

The diffusion station consists of a Zicon source spray system feeding seven belt diffusion furnaces with an output rate of 75 cells per operating minute. The annual output of the station is 34,020,000 cells or 45.6 MW_{pk} per year.

The equipment cost is estimated to be $160,000 for the spray station and $35,000 per furnace equipment (including transfer mechanisms). The total equipment cost is therefore $405,000.

The spray station will require 450 square feet of floor space. The furnace belts are assumed to be 26" wide to handle 6 cells side by side. The thruput rate is 10.7 cells per minute, requiring a belt speed of 7.143 inches per minute. If the dwell time is 30 minutes the furnace length is required to be 18 feet. Allowing an extra 10 feet for ramp, loading and unloading and a width of 6 feet gives a space requirement of 170 square feet per furnace or 1190 square feet for 7 furnaces. The total space required is therefore 1640 square ft.

Labor requirements are estimated to be 0.5 person/shift of assembly operator labor for the spray station and 0.214 persons per shift for each diffusion furnace or a total of 8 person years. Maintenance personnel requirements are estimated to be 0.1 person/shift for the spray station and 0.04 person/shift for each furnace, or a total of 1.5 person years. It is estimated that 0.25 person/shift will be required for inspection of the combined diffusion process, or 1 person year. The total annual labor cost is then:

Table 3.22-2

INPUTS (OTHER THAN CAPITAL EQUIPMENT)
FOR PROCESS SEQUENCE AND THEIR PRICES

SQUEEGEE	E 1624 D	$	0.40 EA	(1977)
ALUMINUM PASTE	E P 27 D		0.79 /LB	(1978)
SCREENS	E 1576 D		5.00 EA	(1977)
ELECTRICITY	C 1032 B		0.32 /KW HR	(1977)
SEMICONDUCTOR ASSEMBLER	B 3096 D		8,100 /YR	(1976)
ELECTRONICS MAINTENANCE	B 3688 D		11,000 /YR	(1976)
MECHANICAL MAINTENANCE	B 3736 D		11,800 /YR	(1976)
CHEMICAL OPERATOR II	B 3672 D		10,050 /YR	(1976)
INSPECTOR	B 3720 D		8,250 /YR	(1976)
DEIONIZED WATER	C 1144 D		0.1869 CU FT	(1977)
HYDROFLORIC ACID	E 1328 D		0.52 /LB	(1977)
AMMONIUM HYDROXIDE	E 1110 D		0.26 /CU FT	(1977)
ACETIC ACID	E 1016 D		0.30 /LB	(1977)
LIQUID NITROGEN	A 1160 I		0.39 /CU FT	(1977)
LIQUID OXYGEN	A 1176 I		0.10 /CU FT	(1977)
SILVER PASTE	SPECTROLAB		0.17 /GM	(1975)
DIFFUSION SPRAY ON SOURCE	EG1210 D		6.00 /L	(1978)
TIN - 2% ZINC ALLOY WIRE	SPECTROLAB		0.12 /GM	(1978)

8	x $ 7450	= $59600	for operators
1.5	x 10850	= 16275	for maintenance
1	x 7585	= 7585	for inspection
TOTAL		$83460	

Assuming a spray-on layer of diffusion source 0.2 μ thick and a 30% spray loss, $(4^2 \times 2.54^2 \times 2 \times 10^{-5} \times 75 \div 0.7) = 0.22$ cc/min. or 100 liters per year are required at an estimated cost of $6 per liter or $600 per year. Nitrogen gas requirements are estimated to be 0.5 cubic feet per minute for the spray station and 1.5 cubic feet per minute for each furnace, for a total of 11 cubic feet per minute or 5,544,000 cubic feet per year. The equivalent amount of liquid nitrogen is 8580 cubic feet (density of liquid = 0.8081 gm. per cc, density of gas = 1.2506 gm. per l.). At a price of $0.33 per cubic foot, the annual cost for nitrogen gas will be $2850. In a like fashion the requirement of 0.15 cubic feet per minute of oxygen for each furnace translates into 550,000 cubic feet per year. This is equivalent to 684 cubic feet of liquid oxygen. At $0.33 per cubic feet the annual cost for oxygen is $225. Total material cost is therefore $3675.

Electric power consumption is estimated at 40 kW per hour per furnace or 2,352,000 kW hours per year. At $0.027 per kilowatt hr. the annual electrical cost will be $63,640.

Applying this data to the IPEG equation gives a total cost of

$$(.49 \times 405{,}000 + 97 \times 1640 + 2.1 \times 89550 + 1.3 \times 4220 + 1.3 \times 75264) / (45.6 \times 10^6) = 0.014 \text{ per peak watt.}$$

3.22.3 Aluminum Back Contact

The aluminum back contact station consists of an automatically fed screen printer which automatically discharges into an infra-red belt furnace. After firing, the wafers are loaded into a cassette. The output rate is 25 cells per operating minute with a machine "up" time ratio of 0.90. The annual output is 11,340,000 cells, or 15.2 MW_{pk} per year.

The equipment costs are estimated to be:

Printer	$17,000
IR Furnace	19,500
Cassette Loader	12,500
Total	$48,000

Floor space requirement is estimated to be 350 square feet.

Labor requirement is estimated to be 0.33 assembly operators per shift. Maintenance personnel requirements are estimated to be 0.2 maintenance technicians per shift. It is estimated that 0.2 persons per shift will be required for inspection. Labor cost is therefore:

1.32 x 7450	=	$ 9,835	for operators
0.8 x 10825	=	8,660	for maintenance
0.8 x 7585	=	6,070	for inspections
TOTAL		$24,565	

Material inputs for the aluminum back process consist of aluminum paste, squeegees and printing screens. Using a coverage factor of 1.50 grams of aluminum paste per 100 square centimeters gives a requirement of 1.54 grams per wafer or 17,500,000 grams per year. At a cost of $1.35 per kilogram, the annual cost would be $23,625. Squeegee requirements are estimated to be 2 per week and screens, 1 per day . 100 squeegees and 350 screens will be required per year. The annual costs would be $35 for squeegees and $1480 for screens. Total material cost per year would therefore be $25,140.

Power requirements are estimated at 20 kilowatts, totaling 168,000 kW hrs per year for $4550.

Applying the IPEG equation gives a cost contribution of $0.0099 for this process step.

3.22.4 Clean Aluminum Back and Remove Oxide

The cleaning station is comprised of 5 chemical and rinse tanks with automatic transfer, two rinse and dry spinners, a vacuum brush and cassette loading station. Output rate is estimated to be 50 wafers per operating minute generating an annual output of 30.4 MW_{pk}

Equipment cost is estimated to be:

Tank Assembly	$12,750
2 Spinners	11,000
Vacuum Brush	15,000
Cassette Loader	12,500
TOTAL	$51,250

Floor space allocation is 300 sq. ft. Labor requirements are projected to be:

Chem. Operator	1 person/shift
Maintenance	0.25 person/shift
Inspection	0.25 person/shift

The annual labor cost is then:

4 x 9240	=	$36,960	for operators
1 x 10825	=	10,825	for maintenance
1 x 7585	=	7,585	for inspection
TOTAL		$55,370	

Materials consumptions per operating minute is estimated to be 0.6 cubic feet of deionized water, 0.03 pounds per minute of Hydrofloric acid, 0.06 cubic feet per minute of ammonium hydroxide, 0.006 pounds per minute of acetic acid and 71.7 cubic feet per minute of nitrogen gas. These translate into the following annual requirements and costs:

Deionized Water	136,080	cu. ft.	$21,500
Hydrofloric acid	13,608	lbs	5,980
Ammonium hydroxide	27,216	cu. ft.	6,575
Acetic acid	2,722	lbs.	670
Liquid nitrogen	50,332	cu. ft.	16,600
Total material cost			$51,325

Power requirement is estimated to be 1 kW or 7560 kW hr. per year, at a cost of $205.

3.22.5 Front Contacts

The processing station for applying front contacts consists of an automatic screen printer feeding into an infra-red belt furnace.

Output rate is estimated at 25 per operating minute leading to an annual output of 15.2 MW_{pk}. Equipment cost is estimated to be $17,000 for the printer and 19,500 for the infra-red furnace. Floor space requirement is estimated at 320 square feet.

Labor requirement for this printing process is the same as that for the aluminum back contact process (paragraph 3.21.3), $24,565 per year.

Material inputs consist of silver paste, printer squeegees and screens. Using a coverage ratio of 80 square centimeters per gram of silver paste and a factor of 0.08 for coverage of the front surface gives a requirement of 0.10 grams of silver paste per cell or 2.58 grams per operating minute. A squeegee replacement rate of 2 per week and a screen replacement rate of 1 per day are assumed. The annual materials costs are therefore:

Silver paste	1,170,578 grams	$199,000
Squeegees	100 ea.	35
Screens	350 ea.	1,480
TOTAL		$200,515

Power requirements are estimated to be 15 kW or 126,000 kW hrs per year for a total cost of $4770.

3.22.6 Apply Tin Alloy Solder Pad

The station for applying the tin alloy pad to the aluminum back consists of an ultrasonic solder head mounted on a heated platon. The station is fed by an automatic pick and place mechanism from the preceding station and discharges to the succeeding station by a similar mechanism. Output rate is 25 cells per minute for an annual production of 15.2 MW_{pk}. The cost of a station is estimated to be $12750 plus $10,000 for automatic station transfer mechanisms. The space requirement is estimated to be 300 square feet.

Labor requirements are estimated to be 0.5 semiconductor assembler per shift, 0.2 maintenance technicians per shift and 0.25 inspectors per shift. The annual labor cost is thus:

2 x	7450 =	$14,900	for operators
0.8 x	10825 =	8,660	for maintenance
1 x	7585 =	7,585	for inspection
	TOTAL	$31,145	

Material input consists of 0.055 grams of tin - 2% zinc alloy per wafer. The annual usage is 24,950 grams per year with a cost of $2550.

Power requirements are estimated to be 1.5 kW for an annual usage of 12600 kW hrs at a cost of $340.

4.0 CONCLUSIONS

4.1 INTRODUCTION

Detailed technical conclusions and recommendations relating to the processes investigated are included in the appropriate sections of Chapter 3. In this chapter discussions will be limited to salient features regarding technological readiness and cost effectiveness of the entire process sequence.

4.2 CELL FABRICATION

The use of a condensed phase polymeric diffusion source was shown to be satisfactory for junction formation from both technology readiness and cost effectiveness. The use of a printed dielectric diffusion mask was found to be unsatisfactory because of technical deficiencies.

The use of a P+ back surface formed by firing printed paste aluminum and using the aluminum for the back contact was found to be cost effective. Use of the residual aluminum for the back contact requires the introduction of a cleaning process for the aluminum and the application of a tin pad to which soldered interconnect contacts can be made. Satisfactory processes for these purposes were developed, although the wet chemistry/brushing process for cleaning the aluminum can perhaps be improved on by some dry process such as plasma etching.

Screen printed silver front contacts were further developed to a state of technology readiness. This process was found to be cost effective. However, the high and rising price of silver makes the development of a suitable base metal printing ink desirable. The associated processes using printed wraparound insolation dielectric and conductors were rejected because of technical deficiencies in the printed dielectric.

Retention of the diffusion oxide to serve as an antireflective coating was found to be not feasible because of inability of the printed metal to make satisfactory contact to the silicon. This failure, together with failure of the printed dielectric diffusion mask, requires the introduction of processes for junction cleaning and AR coating into the process sequence. Laser scribing or plasma etching for junction cleaning and the use of a spray-on polymeric source converted by oxidative firing for AR coating are believed to be suitable processes injectable into the screen printing process sequence. The use of a chemical vapor deposited AR coating is an alternative possibility.

Sheet material which will be available in 1986 may not have an orientation suitable for forming a textured surface. Surfaces of these materials may be formed during the sheet growth process, eliminating the need for a damage removal etch. It will, however, be desirable to have a surface treatment immediately prior to introducing the sheet material into the diffusion process which produces a "standard" surface condition, thereby eliminating one source of variability. We recommend that plasma etching be considered for this purpose.

The cell fabrication sequence shown in Table 4.2-1 incorporates the conclusions and recommendations stemming from the work described in this report. It is recommended that this process sequence be further developed and integrated.

4.3 MODULE DESIGN AND FABRICATION

The module assembly process investigated (adhesive attachment of cells to glass superstrate followed by application of a protective polymeric coating) is a technically feasible process. The lack of a suitable adhesive other than silicone compounds limits the method to the use of these relatively expensive materials for both adhesive

Table 4.2-1

PROCESS' SEQUENCE

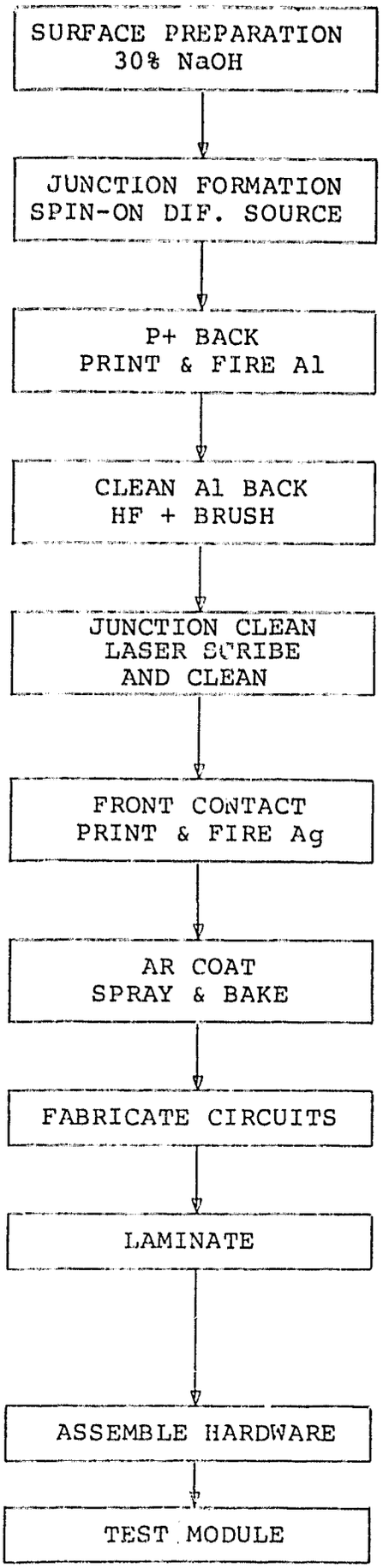

and protective coating. We have therefore recommended that attention be shifted to assembly by lamination to a glass superstrate using ethylene vinyl acetate as the laminating and encapsulating medium.

Use of an antireflective surface for the glass superstrate offers substantial benefit. We conclude, however, that the processes presently available are not sufficiently controllable to be considered for use in a high volume, low cost production operation.

5.0 REFERENCES

1. Bickler, D., "LSA Project cost and volume goals", Proceedings: 10th Project Integration Meeting - Low Cost Solar Array Project, August 16-17, 1978, p. 4-41.

2. Ross, R.G. Jr., "Photovoltaic Design Optimization for Terrestrial Applications", Thirteenth IEEE Photovoltaic Specialists Conference 1978, June 5-8, 1978, pp. 1067-1073.

3. Hansen, M., "Constitution of Binary Alloys", McGraw Hill Book Co., Inc., (New York City) 1958.

4. Taylor, W.E., Kimberly, W., Maidesich, N., and Pepe, A., "Array Automated Assembly Phase 2", Quarterly Report JPL Contract No. 954853, October 1978.

5. Pastirik, E.M., Sparks, T.G. and Coleman, M.G., "Studies and Testing of Antireflective (AR) Coatings for soda-lime glass", Motorola Report No. 2335/1, May 1978.

APPENDIX A

CALCULATION OF OPTIMUM WAFER SHAPE FROM CYLINDRICAL CRYSTALS

An analysis was made of the optimum shaping of squared wafers from cylindrical Czochralski crystals as a function of the relative costs of silicon material and photovoltaic module and system related costs. For the purposes of this analysis it was assumed that the shaping would be accomplished by slabbing off four sides of the crystal to form a square section with truncated (rounded) corners. This procedure eliminates the cell processing costs which would be associated with the discarded silicon if the cells were shaped after processing. It also provides the maximum salvage value for the discarded silicon.

The module geometry associated with one cell is shown in Figure A-1. The circular segments, A_S, outside of the square correspond to the areas of discarded silicon. The corners of the square, A_I, which are truncated by the circle, correspond to interstitial areas which incur module and system related costs, but which do not generate any power.

For interpretive purposes it is convenient to consider the ratio of the size of the circle to that of the square rather than the angle θ as a measure of the degree or extent of shaping:

$$\alpha = \frac{R}{y_o} = \frac{1}{\cos\theta} \qquad (1)$$

The range of α will be from 1 (perfect circle, no shaping) to 1.414 (perfect square).

The total cost per watt will be

$$C_W = C_W^o + S_W^o A_S' + M_W^o A_I' \qquad (2)$$

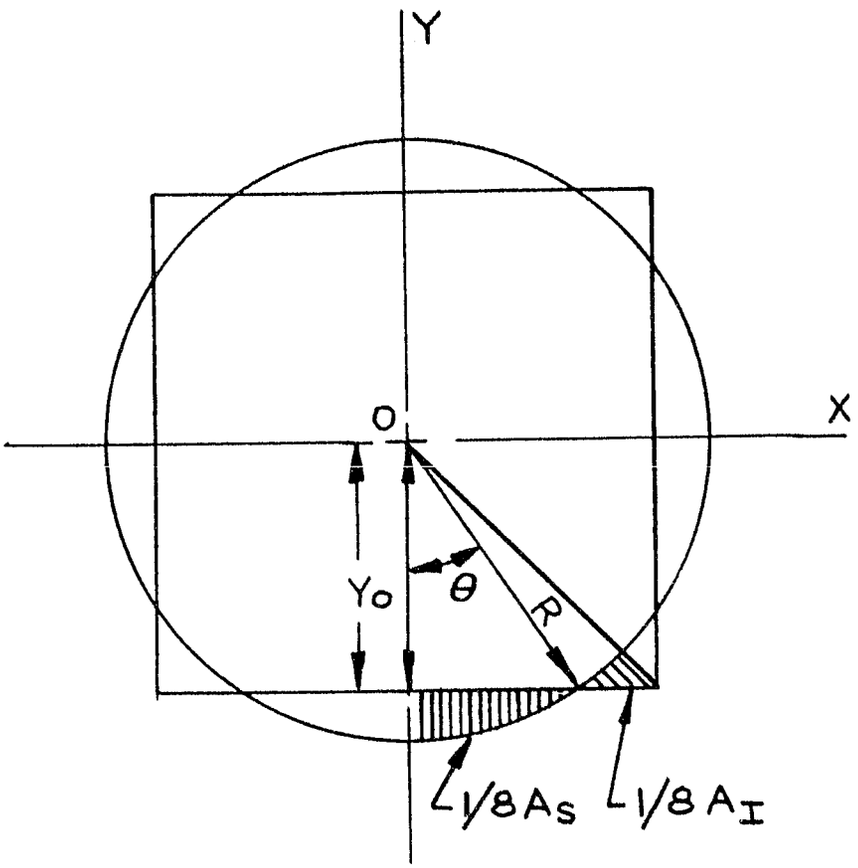

Figure A-1. MODULE GEOMETRY OF UNIT CELL

where C_w^o = Cost per watt assuming perfect nesting without shaping costs

S_w^o = Cost per watt for silicon

A_S' = Fractional area of silicon discarded

M_w^o = Module and system associated cost per watt

A_I' = Fractional area of module not occupied

and where the superscript o indicates costs assuming perfect nesting without shaping costs.

It can be shown that

$$A_S' = 4R^2 \ (\theta - \sin\theta\cos\theta) \tag{3}$$

$$\text{and} \quad A_I' = 4R^2 \ (\cos^2\theta - \sin\theta\cos\theta - \tfrac{\pi}{4} + \theta) \tag{4}$$

where θ is defined in Figure A-1.

The incremental costs associated with shaping will be

$$\frac{\Delta C_w}{S_w^o} = A_S' + \beta A_I' \tag{5}$$

$$\text{Where } \beta = M_w^o / S_w^o \tag{6}$$

Substitution of equations (2) and (3) into (4) gives

$$\frac{\Delta C_w}{S_w^o} = 4R^2 \ (\theta - \sin\theta\cos\theta) + \beta \ 4R^2 \ (\cos^2\theta - \sin\theta\cos\theta - \frac{\pi}{4} + \theta) \tag{7}$$

Shaping will be favored if the silicon cost is small compared to the module associated costs (i.e., large β), however, cost projections suggest that it is unlikely β will ever be larger than 1. For example one estimate of the cost allocation required to meet the 1986 goal of $50/kW allots $25 to silicon sheet and $10 to module assembly and encapsulation[1].

For interpretive purposes it is convenient to use a ratio of the size of the circle to that of the square rather than the angle θ:

$$\alpha = \frac{R}{y_o} = \frac{1}{\cos\theta} \tag{8}$$

The incremental cost normalized to silicon costs (equation 5) is plotted against the ratio α in Figure A-2 for β = 0.5 and β = 1.0.

The minimum in incremental cost will occur when

$$\frac{d}{d\theta}\left(\frac{C_w}{S_w^o}\right) = \frac{dA_S'}{d\theta} + \beta\frac{dA_I'}{d\theta} = 0$$

or

$$\beta = -\frac{\frac{dA_S'}{d\theta}}{\frac{dA_I'}{d\theta}} \tag{9}$$

From equations (3) and (4) it can be shown that

$$\frac{dA_S'}{d\theta} = 4R^2\ (2\sin^2\theta) \tag{10}$$

and

$$\frac{dA_I'}{d\theta} = 4R^2\ (2\sin^2\theta - 2\cos\theta\sin\theta) \tag{11}$$

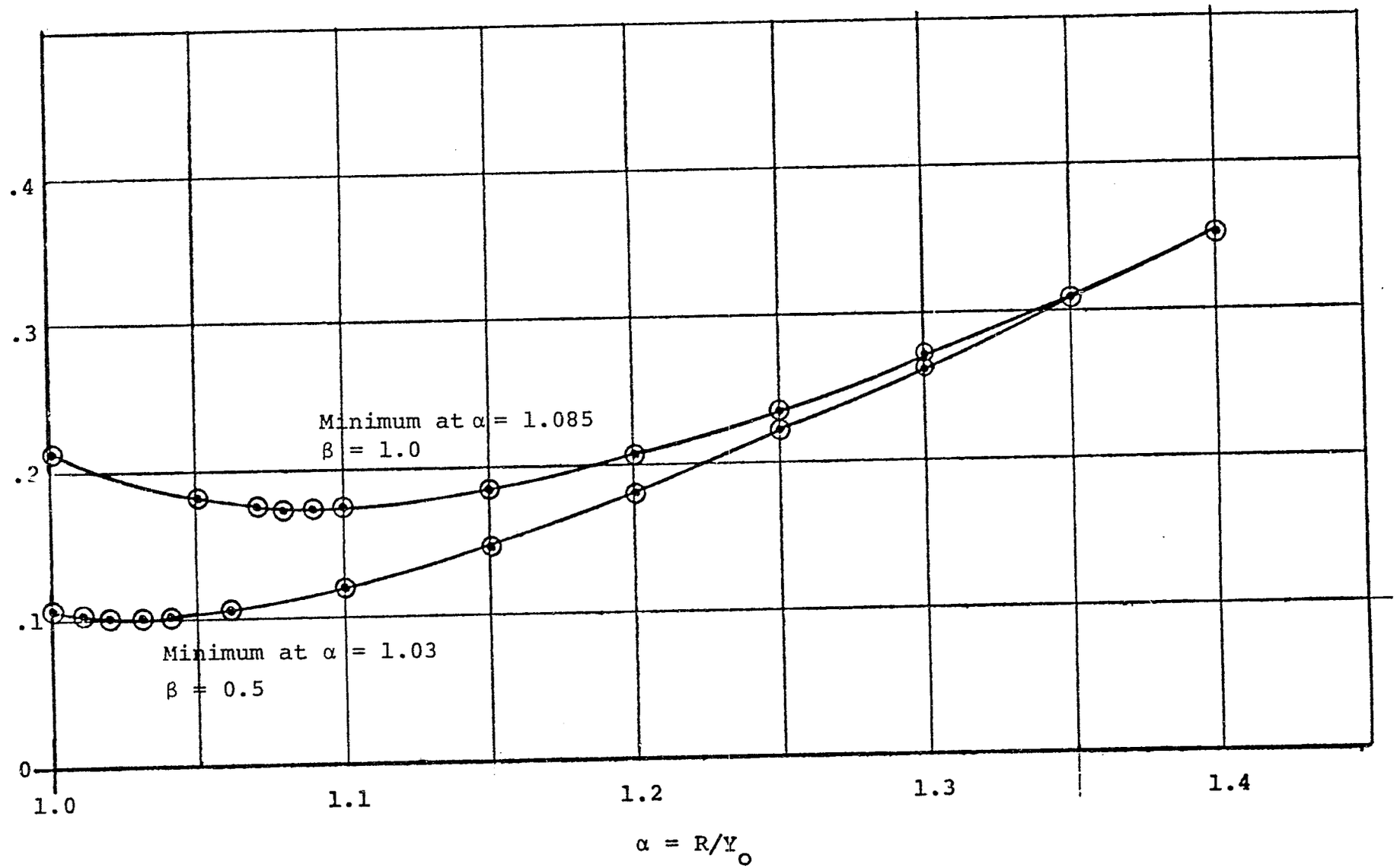

Figure A-2. INCREMENTAL COSTS ASSOCIATED WITH SHAPING MODIFIED SQUARES FROM CIRCULAR CRYSTALS

from which it follows that the condition for the minimum is

$$\beta = - \frac{2\sin^2\theta}{2\sin^2\theta - 2\cos\theta\sin\theta} \qquad (12)$$

The location of the minimum in terms of α is plotted in Figure A-3.

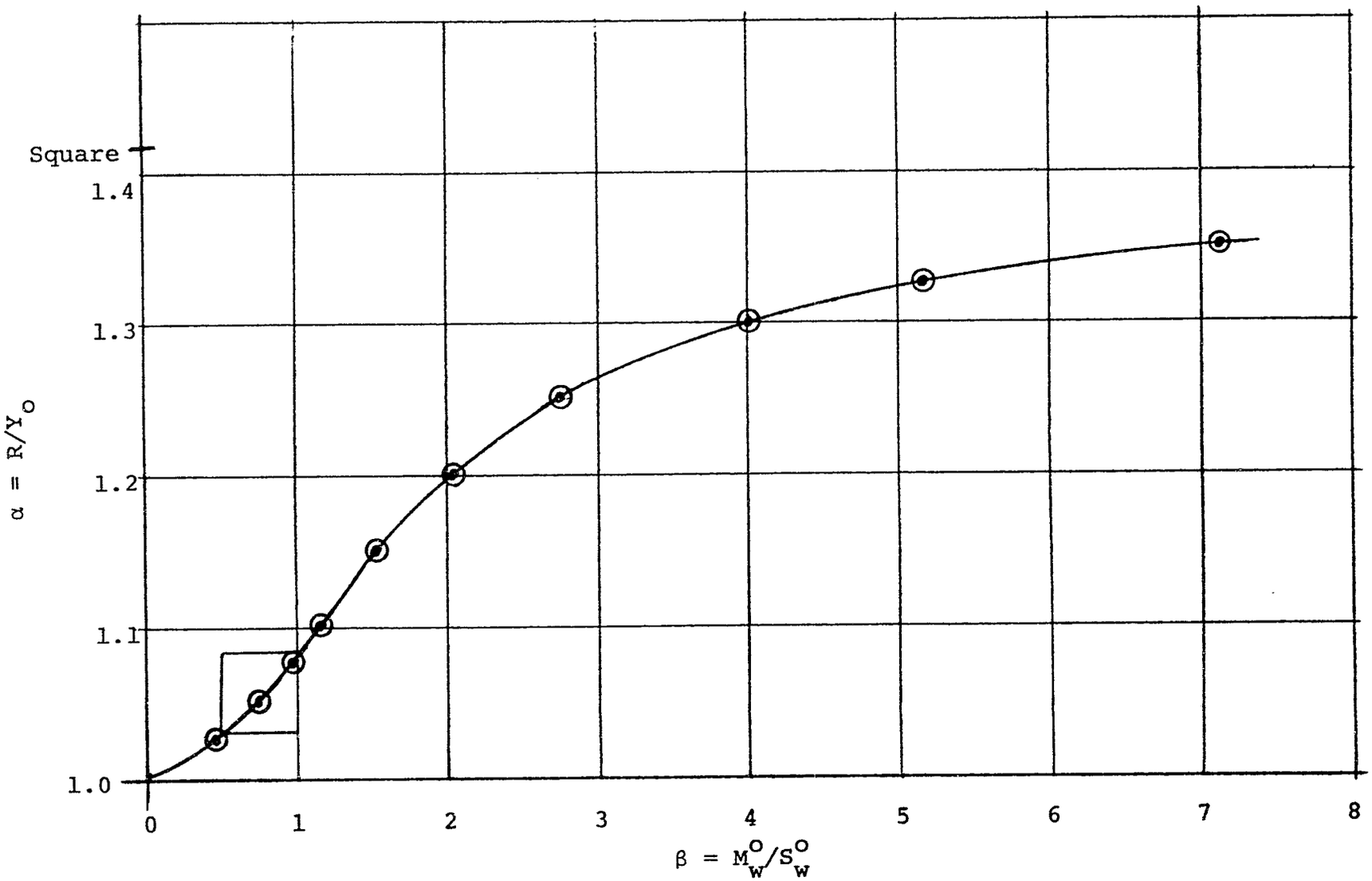

Figure A.3. α LOCATION OF THE MINIMUM INCREMENTAL COST FOR SHAPING MODIFIED SQUARES FROM CIRCULAR CRYSTALS AS A FUNCTION OF THE RATIO OF MODULE TO SILICON COSTS.

APPENDIX B*

VARIATIONS IN DIELECTRIC PASTE

The following criteria were selected for guiding the development of the diffusion masking dielectric:

1. Maturation (firing temperature = 850-900^{o}C)
2. Barrier to phosphorus migration
3. Thermal coefficient of linear expansion, 3.9 to 4.6 x 10^{-6} per ^{o}C
4. Good melting properties
5. Stability with respect to water
6. Stability with respect to silicon at the maturation temperature
7. Structural and chemical stability with respect to thermal cycling in subsequent processing

The low expansion coefficient of silicon (3.9 to 4.6 x $10^{-6}/^{o}$C) dictates the use of glasses whose compositions can be modified to obtain expansion values below 4 x $10^{-6}/^{o}$C. The glasses must mature within the selected temperature ranges and exhibit the required physical characteristics when applied to silicon. In general the expansion coefficients of glasses are inversely proportional to the maturation temperature. Low expansion glasses usually have high maturation temperatures.

The glass systems investigated were selected on the following considerations:

1. Those with low expansion coefficients which would mature within the required temperature limits; and

*For recommendations see Section 3.5.

2. Coating systems with acceptable maturation temperatures and composition which can be altered to reduce the expansion coefficient and not affect the firing characteristics.

Based on criteria (1), (2), and (3), five families of glasses were selected as potential candidates. The initial compositions are shown in Table B-1.

Series 1 - Beta-Spodumene Glasses

This series of glasses was originally compounded for application to slip-cast-fused silica, which has an expansion coefficient of $0.3 \times 10^{-6}/^{o}C$. Maturation temperature is about $1150^{o}C$. These glasses, upon maturation, devitrify to form keatite ($Li_2O \cdot Al_2O_3 \cdot 5SiO_2$) and spodumene ($Li_2O \cdot Al_2O_3 \cdot 4SiO_2$).

The original formulation, 1E-1, was modified (Table B-2) to increase expansion, promote devitrification and reduce maturation temperature. Composition 1E-6 did not form a melt after smelting at $1360^{o}C$ for 30 minutes. Composition 1E-7 formed a melt at $1360^{o}C$, but was highly viscous. A low viscosity melt was obtained with Composition 1E-8.

The latter composition was overfired at $900^{o}C$ when fired on silicon for either 7 minutes or one minute. Firing temperature was reduced until a vitrified surface was obtained at $700^{o}C$. This glass at $700^{o}C$ exhibited a possible two phase system, however, surface tension was high and the glass tended to form beads.

The composition was further altered by reducing the P_2O_5 content to 29.71 mol percent and adding B_2O_3 to constitute 7.43 mol percent. This composition, designated as 1E-11 (Table B-3), formed a low viscosity melt, but did not mature at a firing temperature of $800^{o}C$. The wetting angle did not decrease appreciably. Substitution of LiF for Li_2O and NaF for Na_2O in the 1E-8 (1E-12) reduced the

Table B-1

STARTING COMPOSITIONS OF DIFFUSION MASKING DIELECTRICS

Series	1E-1	2E-1	3E-1	5E-1	7E-1
Oxide			Equivalents		
BaO	-	-	0.133	-	0.395
Li_2O	0.811	-	-	0.149	-
MgO	0.189	0.875	0.783	-	0.436
CaO	-	0.125	0.043	0.080	0.085
ZnO	-	-	0.041	0.055	0.084
Na_2O	-	-	-	0.505	-
K_2O	-	-	-	0.211	-
Total	1.000	1.000	1.000	1.000	1.000
B_2O_3	-	1.382	1.753	0.644	0.766
Al_2O_3	0.282	0.330	-	-	-
P_2O_5	0.340	-	-	-	-
	-	-	-	-	-
SiO_2	3.023	2.334	1.016	2.669	0.857
TiO_2	-	-	-	1.178	-
			Mol Percent		
BaO	-	-	3.52	-	15.06
Li_2O	17.46	-	-	2.71	-
MgO	4.07	17.34	20.79	-	16.62
CaO	-	2.48	1.14	1.46	3.24
ZnO	-	-	1.09	1.00	3.20
Na_2O	-	-	-	9.20	-
K_2O	-	-	-	3.84	-
B_2O_3	-	27.39	46.51	11.73	29.20
Al_2O_3	6.07	6.54	-	-	-
P_2O_5	7.32	-	-	-	-
SiO_2	65.08	46.25	26.96	48.61	32.67
TiO_2	-	-	-	21.45	-

Table B-2

COMPOSITION (mol %) OF BETA-SPODUMENE GLASSES

Oxide	1E1	1E6	1E7	1E8
Li_2O	17.46	15.29	24.25	19.22
MgO	4.07	3.56	5.64	4.47
Na_2O	--	4.71	7.47	5.92
Al_2O_3	6.07	5.33	8.45	6.69
P_2O_5	7.32	13.20	20.93	37.32
SiO_2	65.08	56.97	31.76	25.18
SnO_2	--	0.94	1.49	1.18

Table B-3

COMPOSITIONS (mol %) OF 1E SERIES

Oxide	1E-2	1E-8	1E-11	1E-12	1E-13	1E-14
Li_2O	17.27	19.22	19.28	19.22(1)	14.66(3)	19.34(5)
MgO	4.03	4.47	4.49	4.47	5.04	3.81
Na_2O	-	5.92	5.94	5.92(2)	4.53(4)	6.00(6)
Al_2O_3	6.01	6.69	6.71	6.69	5.14	6.76
P_2O_5	7.24	37.32	29.71	37.32	26.19	37.48
B_2O_3	-	-	7.43	-	-	
SiO_2	64.39	25.18	25.25	25.18	19.29	25.42
SnO_2	1.06	1.18	1.19	1.18	0.92	1.19

(1) Li_2O added as LiF
(2) Na_2O added as NaF
(3) Li_2O added as LiF
(4) Na_2O added as NaF
(5) Li_2O added as LiF
(6) Na_2O added as NaF

wetting angle, however, the actual maturation and range of maturation temperature was reduced as compared to 1E-8. At 650°C for five minutes, the coating was underfired, whereas at 740°C for the same time period, the coating was overfired.

Composition 1E-13, in which the MgO content of 1E-12 increased to 0.120, resulted in a refractory coating system.

It was concluded that the maturation temperature of this coating was too low and difficult to control.

Series 2 - $MgO \cdot Al_2O_3$ Borosilicate Glasses

The composition of this series was based on a commercial glaze which had a calculated coefficient of expansion of $3.9 \times 10^{-6}/°C$ (2E-1, Table B-4). The glass did not form a melt at a smelting temperature of 1400°C. Subsequent additions of B_2O_3 (2E-2), and subtractions of MgO (2E-3) to reduce the maturation temperature resulted in a low viscosity melt. Composition 2E-3 exhibited a partially vitrified surface when fired on silicon at 900°C for 7 minutes. Further increasing the B_2O_3 content to 5.200 equivalents, did not result in liquid formation during smelting. The development of this coating system was terminated.

Series 3 - Baria Glasses

The composition of these glasses is based on a $BaO \cdot 3.58SiO_2$ eutectic at 850°C. Compositions were modified to increase expansion and increase fluidity as shown in Table B-5. All of these compositions formed high viscosity melts and were too refractory for use as a coating which would mature at 880°C. Further work was continued with modifications of this coating system (Series 7), and is discussed below.

Table B-4

COMPOSITIONS (Mol %) OF $MgO \cdot Al_2O_3$ BOROSILICATE GLASSES

Oxide	Series Number		
	2E-1	2E-2	2E-3
CaO	2.48	2.07	2.25
MgO	17.34	14.47	7.18
Al_2O_3	6.54	5.46	5.93
B_2O_3	27.39	39.40	42.73
SiO_2	46.25	38.60	41.90

Table B-5

COMPOSITIONS (mol %) OF BARIA GLASSES

Oxide	3E-1	3E-2	3E-3
BaO	3.52	4.44	5.33
ZnO	1.09	1.38	1.66
CaO	1.14	1.44	0.94
MgO	20.79	--	--
B_2O_3	46.51	58.71	70.39
SiO_2	26.96	34.03	21.68

Series 5 - Titania Glasses

This coating series, containing dissolved titania as rutile, when smelted and quenched quickly (as when quenched in water) is a clear glass. However, when the glass is reheated and quenched slowly (air quench), through the temperature range of 590 to 650°C, the titania crystallizes primarily as anatase. Upon further reheating the anatase converts to rutile. These glasses are highly stable when subjected to thermal excursions, and are therefore, based upon thermal characteristics, an excellent system for the masking dielectric.

The original composition (5E-1), as shown in Table B-6, exhibited a calculated expansion coefficient of $9.9 \times 10^{-6}/^{\circ}C$. As the expansion was too high for coatings applied to silicon, changes in the composition were made to obtain more compatible expansion values as in 5E-7 and 5E-8. These latter compositions matured to a high gloss, smooth finish when fired at 880°C for 7 minutes.

Coatings 5E-7 and 5E-8 were evaluated as diffusion barriers by subjecting P-type silicon wafers to a diffusion cycle using Emulsitone N-250 phosphorus source. The silicon surface under barrier coated areas was tested by staining techniques and resistivity measurement with no evidence of phosphorus penetration being detected.

Coatings 5E-7 and 5E-8 were further evaluated for their purpose by fabrication of cells after application of the coating. These preliminary experiments yielded cells of poor quality. This result was interpreted as being due to contamination of the silicon from the paste during the diffusion step. The titania being suspected as the source of contamination, coating 5E-7-1 was compounded for evaluation. The titania in this coating was replaced entirely by silica. To further identify the contaminant, batches were made in

Table B-6

COMPOSITIONS (mol %) OF TITANIA GLASSES

Oxide	5E-1	5E-2	5E-3	5E-7	5E-8	5E-7-1
Na_2O	9.20	5.87	6.23	2.16[1]	1.65	2.16[1]
K_2O	3.84	1.95	2.07	0.70	0.70	0.70
CaO	1.46	1.57	1.66	1.73[2]	1.77	1.73[2]
Li_2O	2.71	1.95	2.07	2.21	2.20	2.21
ZnO	1.00	1.08	1.15	1.20	1.22	1.20
B_2O_3	11.73	19.59	20.70	22.05	22.14	22.05
TiO_2	21.45	15.68	10.56	11.16	11.24	-
SiO_2	48.61	52.29	55.47	58.78	59.07	69.94
Expansion Coefficient ($\times 10^{-6}/^{o}C$)	9.9		7.0	5.2	5.2	3.5

(1) Na_2O added as NaF

(2) Li_2O added as LiF

a platinum crucible and a clay crucible. Tests of these materials by cell fabrication showed no improvement over the original composition, and were possibly even inferior.

In another attempt to isolate the contaminant, compositions 5E-7-2 through 5E-7-5 (shown in Table B-7) were compounded. The ZnO, Na_2O and Li_2O content was replaced by P_2O_5 (5E-7-2). This composition did not form a melt. Consequently, the silica content was incrementally reduced in series 5E-7-3 through 5E-7-5.

The viscosity characteristics for fusion flow of the Series 5 glasses were determined. The test is conducted as follows:

A one gram sample of -400 mesh powdered glass is formed into a 9.5 mm (3/8 in.) diameter pellet at a minimum pressure of 28,500 psi (1000 lbs load). The pellet is placed on a silicon wafer and fired at 980°C (100°C above the maturation temperature), in a horizontal position for 1.5 minutes. Without removing from the furnace, the wafer is tilted 90° and the pellet is fired for 7.0 minutes in the vertical position. The flow of the melted glass is measured to the nearest 0.5 mm.

The fusion flow characteristics of the 5E-7, 5E-8, 5E-7-1 and 5E-7-1-P samples are shown in Table B-8. It can be noted that Series 5E-7 has a longer fusion flow than 5E-8, due to the higher Na_2O content. A major point of interest is the higher fusion flow of 5E-7-1-P as compared to 5E-7-1. Both series are the same composition, except that 5E-7-1 was smelted in a clay crucible, whereas 5E-7-1-P was smelted in a platinum crucible. The observed difference indicates solubility of the clay crucible in the melt. Additionally, the results of substituting silica for titania (5E-7 and 5E-7-1) can be noted.

Table B-7

SERIES 5E COMPOSITIONS (mol %) WITH ADDED P_2O_5

Oxide	5E-72	5E-73	5E-7-4	5F-7-5
K_2O	0.55	0.86	1.01	1.22
CaO	1.36	2.12	2.49	3.02
B_2O_3	17.31	26.95	31.67	38.40
SiO_2	74.06	59.62	52.55	42.47
P_2O_5	6.71	10.45	12.28	14.89
Expansion Coefficient ($\times 10^{-6}/^{o}C$)	3.3	3.4	3.5	3.7

Table B-8

FLOW OF SFRIES 5
AT 980^{O} AND 7 MINUTES

Test	Series Number	Flow (mm)	Remarks
1	5E-7	29.5	
2	5E-8	23.5	Lower Na_2O content than 5E-7
3	5E-7-1	24.3	*Smelted in clay crucible
4	5E-7-1-P	39.3	*Smelted in platinum crucible
No titania in 5E-7-1 and 5E-7-1-P			

*Compositions are the same

This testing can be valuable in assessing the effect of changes in composition upon maturing temperature. This application of the test will be illustrated in the discussion of the Series 7 glasses.

Coatings 5E-7 and 5E-8 were evaluated for thermal endurance. The coatings were cycled ten times from room temperature to 880°C and back to room temperature (Series A). The color of the coatings changed from a blue white to a yellow white, indicating that the crystallized titania was converted from anatase to rutile. Cursory examination of the exposed silicon adjacent to the coating indicated a blue haze which became more pronounced as the thermal cycling progressed. The coatings were also sequentially cycled from room temperature to 880, 800, 700, 600 and 500°C (Series B).

Series 7 - Modified Baria Glasses

The study of this series, a modification of Series 3 with increased baria and reduced magnesia content, was initiated as a back-up to Series 5. These coatings, as shown in Table B-9, are free of Na_2O and Li_2O. The initial compositions (7E-1 and 7E-3) evaluated for degree of maturation at a firing temperature of 880°C for 7 minutes indicated an overfired condition. Additionally, the expansion coefficient (calculated) was too high for application to silicon. The magnesia content was increased in 7E-3 to obtain a reduced coefficient of expansion and at the same time increase the maturation temperature. From examination of Table B-9 the reduction in expansion coefficient can be noted.

Based on the work on Series 5 discussed above, it was decided that the Series 7 glasses should exhibit a fusion flow length between 20 and 30 millimeters at an exposure of 980°C, with 1½ minutes in the horizontal position and 7 minutes vertically. Based on the data shown in Table B-10 all of the glasses, with the exception of 7E-8, would be overfired at a temperature of 880°C. Coating 7E-8 would be underfired. As the magnesia content was increased above that shown

Table B-9

SERIES 7 COMPOSITIONS

Oxide	7E-1	7E-3	7E-4	7E-5	7E-6	7E-7	7E-8	7E-9
				Equivalents				
BaO	0.412	0.395	0.395	0.359	0.329	0.304	0.198	0.260
ZnO	0.088	0.084	0.084	0.076	0.070	0.065	0.042	0.055
CaO	0.089	0.085	0.085	0.077	0.071	0.065	0.042	0.056
MgO	0.412	0.436	0.436	0.487	0.530	0.566	0.718	0.629
Total	1.001	1.000	1.000	0.999	1.000	1.000	1.000	1.000
Al_2O_3	0.014	-	-	-	-	-	-	-
B_2O_3	0.634	0.766	0.766	0.696	0.638	0.489	0.386	0.506
SiO_2	0.895	0.857	0.657	0.597	0.548	0.505	0.329	0.433
ZnO_2	0.029	-	-	-	-	-	-	-
				Mol %				
BaO	16.01	15.06	16.30	15.66	15.05	14.52	11.52	13.41
ZnO	3.42	3.20	3.47	3.32	3.20	3.10	2.45	2.85
CaO	3.46	3.24	3.51	3.36	3.25	3.10	2.48	2.89
MgO	16.01	16.62	17.99	21.25	24.25	27.03	41.88	32.43
Al_2O_3	0.54	-	-	-	-	-	-	-
B_2O_3	24.64	29.20	31.61	30.37	29.19	28.13	22.51	26.09
SiO_2	34.78	32.67	27.12	26.45	25.07	24.12	19.16	22.32
ZnO_2	1.13	-	-	-	-	-	-	-
Expansion Coefficient ($\times 10^{-6}/^{o}C$)	5.2	4.9	5.0	4.6	4.5	4.4	3.9	4.3

Table B-10

FLOW OF SERIES 7

AT VARIOUS TIMES AND TEMPERATURES

Test	Series Number	Temp (°C)	Time (min)	Flow (mm)	Remarks
1	7E-2	980	4	>46.0	
2	7E-3	980	3	27.0	
3	7E-4	980	2	>46.0	
4	7E-7	980	7	>51.0	
5	7E-8	980	7	13.5	(devitrified)
6	7E-5	900	4	40.8	
7	7E-6	900	4	36.8	
8	7E-7	900	4	32.3	
9	7E-8	900	4	17.8	

in 7E-5, adherence decreased drastically. The adherence was restored upon the addition of 5 parts of lead fluoride (PbF_2) to 100 parts by weight of glass.

Mixtures of glasses 7E-6, 7E-7 and 7E-8 were made to determine the optimum magnesia and lead fluoride content to obtain good adherence and maturation at 880°C (Table B-11). Adherence was noted only at lead fluoride contents of 5 parts per 100 parts by weight of glass. The composition of 7E-8-1 was determined on the basis of tests 4, 5 and 10 through 17. An anomaly exists in tests 19 through 21. It would be expected that an increasing lead fluoride content should increase the fusion flow; however, since lead fluoride contents less than 5.0 did not result in adherence, the reasons for the anomaly may be academic.

Evaluation of composition 7-8-1A, Table B-12, formulated on the basis of previously reported fusion flow tests, indicated excessive refractoriness (underfiring). The series 7 glasses were further compounded to decrease maturation temperature and expansion coefficient. The compositions shown in Table B-12 were compounded and evaluated. Maturing temperature of these coatings was between 700 and 750°C. The surfaces were free of bubbles. It was then discovered that the original difficulty was overfiring rather than underfiring.

A number of 7E series glasses were formulated (primarily varying the relative amounts of the B_2O_3 and Al_2O_3 constituents) with the goal of attaining a maturation temperature of 880°C. Compositions of the various formulations are given in Table B-13.

The first of these compositions 7E-17 formed by adding 0.300 equivalents of Al_2O_3 to 7E-8-1A was far too refractory (no fusion at 950°C). Other variations in the composition of 7E-8-1A shown in Table B-13 include:

Table B-11

FLOW OF SERIES 7 @ 980°C, 7 MIN.

Test No.	7E-6	7E-7	7E-8	7E-8-1	PbF_2*	Flow (mm)	
4	-	100	-	-	0	51.0	
5	-	-	100	-	0	13.5	(divitrified)
10	-	50	50	-	0	19.0	
11	-	70	30	-	0	34.0	
12	-	70	30	-	2.5	47.5	
13	-	70	30	-	5.0	48.5	
14	-	-	100	-	5.0	0	
15	40	-	60	-	5.0	18.0	
16	45	-	55	-	5.0	20.5	
17	50	-	50	-	5.0	48.5	
18	-	-	-	100	0.0	46.8	
19	-	-	-	100	5.0	22.0	
20	-	-	-	100	4.5	33.5	
21	-	-	-	100	4.0	24.5	

Table B-12

COMPOSITION OF SERIES 7 DIFFUSION MASKING DIELECTRICS

(Equivalents)

Oxide	7E-8-1	7E-8-1A	7E-12	7E-13	7E-14	7E-15	7E-16	7E-17
BaO	0.260	0.253	0.403	0.285	0.285	0.253	0.270	0.253
ZnO	0.055	0.054	---	0.061	0.061	0.054	0.059	0.054
CaO	0.056	0.054	0.081	0.061	0.061	0.054	---	0.054
MgO	0.629	0.612	0.494	0.563	0.563	0.612	0.671	0.612
PbO	---	0.027	0.022	0.030	0.030	0.027	0.030	0.027
Total	1.000	1.000	1.000	1.000	1.000	1.000	1.000	1.000
Al_2O_3	---	---	---	---	---	---	---	0.300
B_2O_3	0.506	0.492	0.397	0.619	0.780	0.550	0.539	0.492
SiO_2	0.433	0.421	0.345	0.474	0.474	0.421	0.462	0.421

Compositional Changes

7E-12 In 7E-8-1-A, increased BaO to 0.500 equivalents, eliminated ZnO, increased CaO to 0.100 equivalents.

7E-13 In 7E-8-1-A, increased B_2O_3 to 0.550 equivalents, reduced MgO to 0.50 equivalents.

7E-14 In 7E-13, increased B_2O_3 to 0.780 equivalents.

7E-15 In 7E-8-1-A, increased B_2O_3 to 0.55 equivalents.

7E-16 In 7E-8-1-A, removed CaO.

7E-17 In 7E-8-1-A, added 0.3000 equivalents of Al_2O_3.

Table B-13

COMPOSITIONS OF SERIES 7E - MASKING DIELECTRICS

(Equivalents)

	7E-8-1A	7E-17	7E-18	7E-19	7E-20	7E-21	7E-22	7E-23	7E-24	7E-25
BaO	.253	.253	.253	.253	.253	.253	.204	.213	.253	.253
ZnO	.054	.054	.054	.054	.054	.054	.044	--	.054	.054
CaO	.054	.054	.054	.054	.054	.054	.044	.046	.054	.054
MgO	.612	.612	.612	.612	.612	.612	.687	.718	.612	.612
PbO	.027	.027	.027	.027	.027	.027	.022	.023	.027	.027
Total	1.000	1.000	1.000	1.000	1.000	.1000	1.001	1.001	1.000	1.000
B_2O_3	.492	.492	.492	.492	.450	.400	.397	.415	.491	.400
Al_2O_3	--	.300	.060	.075	--	--	--	--	--	--
SiO_2	.421	.421	.421	.421	.421	.421	.340	.355	.600	.421

Composition Changes to 7E-8-1-A

7E-17 Added 0.300 equivalents of Al_2O_3 for basic glass

7E-18 20 w/o 7E-17 and 80 w/o 7E-8-1-A

7E-19 25 w/o 7E-17 and 75 w/o 7E-8-1A

7E-20 Reduced B_2O_3 in 7E-8-1-A to 0.450 equivalents

7E-21 Reduced B_2O_3 in 7E-8-1-A to 0.400 equivalents

7E-22 Increased MgO in 7E-8-1-A to 0.850 equivalents

7E-23 Removed ZnO from 7E-22

7E-24 Increased SiO_2 in 7E-8-1-A to 0.600 equivalents

7E-25 Decreased B_2O_3 in 7E-24 to 0.400 equivalents

1. Reduction in B_2O_3 content 7E-20 and 7E-21
2. Increase in MgO content 7E-22
3. Elimination of ZnO 7E-23
4. Increase in SiO_2 7E-24 and 7E-25

All coatings were blended with the screening vehicle using an alumina mortar and pestle. This procedure was followed to avoid iron contamination, which could be introduced by processing through the three-roll mill used heretofore. Additional variations were: (1) the use of a platinum crucible for making some of the glass melts, and (2) zirconia instead of alumina grinding media in the ball mill for initial particle reduction of the glass frit.

The use of zirconia grinding media exhibited a tendency to lower the maturation temperature of the coating. Smelts containing PbO, derived from PbF_2, turned black when melted in a platinum crucible. It was determined that the PbF_2 was reduced by the platinum.

The effects on fusion flow and maturation caused by the variations in composition and processing are summarized in Table B-14. The most promising formulations were 7E-20 and 7E-24.

Table B-14

TEST RESULTS OF SERIES 7E

Composition	Crucible Material	Milling Media	Flow Characteristics			Maturing Temp. (°C)
			Temp (°C)	Time (Min)	Flow (mm)	
7E-8-1-A	Clay	Al_2O_3	900	7	46.5	800
	Pt	ZrO_2	800	7	42.0	750
			900	7	17.0	
7E-18	Clay	Al_2O_3	980	7	0	830
			880	7	17.0	
7E-19	Clay	Al_2O_3	980	7	22.0	830
			880	7	22.0	
7E-20	Clay	Al_2O_3	980	7	20.5	880
			880	7	33.0	
7E-21	Clay	Al_2O_3	980	7	0	880
			880	7	16.0	
7E-22	Pt	Al_2O_3	800	7	36.0	800
		ZrO_2	800	7	8.5	750
			900	7	0	
7E-23	Pt	Al_2O_3	800	7	25.0	800
		ZrO_2	800	7	21.5	800
			900	7	0	
7E-24	Clay	Al_2O_3	TBD			880
	Pt	Al_2O_3	TBD			800
7E-25	Clay	Al_2O_3	TBD			800
	Pt	Al_2O_3	TBD			800

APPENDIX C*

ISOLATION DIELECTRICS

The specific requirements for these glasses are as follows:

(1) Maturation temperature between 550 and 650°C

(2) Thermal expansion coefficient between 3.9 and $4.6 \times 10^{-6}/^{\circ}C$.

(3) Freedom from bubbles and pinholes.

Four families of glasses have been explored for this application. These families are specifically: (1) phosphate glasses (Series 4I), (2) germania/tantalum and silica/tantalum glasses (Series 6I), (3) baria-magnesia borosilicate glasses (Series 7I), and (4) modified titania precipitated glasses (Series 9I).

Series 4I Glasses

Series 4I-1 through 4I-11 all exhibited lack of maturity at temperatures as high as 880°C. Additionally, the calculated expansion coefficients were considered too high as shown in Table C-1. These compositions were altered in Series 4I-12 through 4I-15 to reduce maturation temperature and expansion as shown in Table C-2. These coatings matured between 650 and 700°C, but still had excessively large expansion coefficients. Moreover, they were found to be moisture sensitive and for these reasons were dropped from further consideration.

Series 6I Glasses

The starting composition of the germania-tantalum series (Table C-3) was applied to silicon and fired at 650°C. This composition was deemed as too refractory. Increasing the germania content to 1.000 equivalents did not reduce the maturing temperature. Substitution

*For recommendations see Section 3.10.

Table C-1

TYPICAL COMPOSITIONS OF INITIAL SERIES 4 GLASSES

Oxide	4I-1	4I-3	4I-7	4I-8
	Equivalents			
Li_2O	←	0.485	→	
K_2O	←	0.515	→	
Total	←	1.000	→	
P_2O_5	←	2.976	→	
B_2O_3	---	---	1.250	1.250
SiO_2	---	1.000	1.250	0.500
	Mol Percent			
Li_2O	12.20	9.75	7.49	8.47
K_2O	12.95	10.35	7.95	8.99
P_2O_5	74.85	59.81	45.95	51.97
B_2O_3	---	---	19.30	21.83
SiO_2	---	20.10	19.30	8.73
Expansion Coefficient ($x10^{-6}/^oC$)				
	9.8	9.0	7.7	8.1

Table C-2

COMPOSITIONS OF REVISED SERIES 4 GLASSES

Oxides	4I-12	4I-13	4I-14	4I-15
	Equivalents			
Na_2O	←	0.500	→	
Li_2O	←	0.150	→	
NaF	←	0.350	→	
Total	←	1.000	→	
P_2O_5	←	0.200	→	
B_2O_3	0.500	1.500	2.000	2.500
SiO_2	0.800	0.800	1.000	1.200
	Mol Percent			
Na_2O	20.00	14.29	11.90	10.20
Li_2O	6.00	4.29	3.57	3.06
NaF	14.00	10.00	8.33	7.14
P_2O_5	8.00	5.71	4.76	4.08
B_2O_3	20.00	42.86	47.62	51.02
SiO_2	32.00	22.86	23.81	24.49
Expansion Coefficient ($x10^{-6}/^oC$)				
	---	8.3	7.1	6.2

Table C-3

COMPOSITIONS OF SERIES 6I-1 GERMANIA-TANTALUM GLASSES

Oxide	6I-1	6I-1-1	6I-1-2
	Equivalents		
Li_2O	0.740	0.740	---
ZnO	0.360	0.260	except that LiF for Li_2O.
Al_2O_3	0.043	0.043	
B_2O_3	4.277	4.277	
Ta_2O_5	0.039	0.039	
GeO_2	0.600	1.000	
P_2O_5	---	---	
	Mol Percent		
Li_2O	12.41	11.63	Same as 6I-1 was substituted
ZnO	4.39	4.09	
Al_2O_3	0.71	0.68	
B_2O_3	71.73	67.26	
Ta_2O_5	0.66	0.61	
GeO_2	10.10	15.72	
P_2O_5	---	---	---

of LiF for the Li_2O resulted in bubble formations without affecting the maturation temperature. It was decided that this coating system be set aside due to its refractory characteristics, and the analogous silica series explored.

The silica-tantalum glasses, as shown in Table C-4 are germania-free borosilicates with Li_2O and Ta_2O_5. Composition 6I-2-2 was judged best in obtaining maturity at temperatures between 650 and 700°C. Variations in the composition of the silica-tantalum glasses were made to obtain glasses which were (1) smooth and glossy when fired, and (2) compositions free of Ta_2O_5. All of the glasses exhibited bubble formation when compounded free of Ta_2O_5. The addition of 5 parts of PbF_2 per 100 parts by weight to the as ground glass powder did not reduce bubble formation. The effects of these variations are summarized in Table C-5.

Because of the problems with the silica-tantalum series, the composition of the original germania-tantalum series was substantially altered by decreasing B_2O_3 and increasing GeO_2 and Ta_2O_5 in an attempt to overcome its refractory character (Table C-6). The initial composition of this series (6I-3) resulted in an underfired condition at 700°C, however, this condition was remedied by increasing the B_2O_3 content to 4.500 equivalents. The elimination of Ta_2O_5 in this system caused bubbling of the surface. The effects of the compositional variations are summarized in Table C-7.

One additional compositional variant of the germania-tantalum glasses (Series 6I-4) was investigated (Table C-8), extending the compositional modifications of Series 6I-3 still further. This coating system exhibited a high wetting angle and an overfired condition. The germania content of 6I-4 was reduced appreciably (6I-4-1) without affecting the wetting angle, but maturation occurred at a firing temperature of 650°C. Elimination of Ta_2O_5 resulted in bubble formation upon application to silicon and firing at 650°C. The effects of compositional variations within the 6I-4 series are summarized in Table C-9.

Table C-4

COMPOSITION OF SERIES 6I-2 SILICA/TANTALUM GLASSES

Oxides	6I-2	6I-2-1	6I-2-2	6I-2-3	6I-2-4	6I-2-5	6I-2-6
	Equivalents						
Li_2O	0.575	0.575	0.605	0.575 (1)	0.575 (1)	0.575 (1)	0.605
ZnO	0.425	0.425	0.395	0.425	0.425	0.425	0.395
Al_2O_3	0.282	0.282	0.186	0.282	0.282	0.282	0.186
B_2O_3	4.954	5.400	4.608	4.954	4.954	4.954	4.608
Ta_2O_5	0.103	0.103	0.096	0.103	---	---	---
SiO_2	1.724	1.724	1.395	1.724	1.724	1.724	1.395
P_2O_5	---	---	---		---	0.103	---
	Mol Percent						
Li_2O	7.13	6.76	8.30	7.13	7.22	7.13	8.42
ZnO	5.27	4.99	5.42	5.27	5.34	5.27	5.49
Al_2O_3	3.50	3.31	2.55	3.50	3.54	3.50	2.59
B_2O_3	61.44	63.46	63.25	61.44	62.24	61.44	64.10
Ta_2O_5	1.28	1.21	1.32	1.28	---	---	---
SiO_2	21.38	20.26	19.15	21.38	21.66	21.38	19.40
P_2O_5	---	---	---	---	---	1.28	---

Table C-5

COMPOSITIONAL CHANGES IN 6I-2 SERIES

Coating	Changes	Remarks
6I-2-1	Increased B_2O_3 content of 6I-2 to 5.400 equivalents.	Refractory characteristics not eliminated
6I-2-2	Increased Li_2O content to 0.65 equivalents. Decreased Al_2O_3 content to 0.200 equivalents. Reduced SiO_2 to 1.500 equivalents.	Matured to a smooth coating at 700°C. Under fired at 650°C.
6I-2-3	Substituted LiF for Li_2O in 6I-2.	Formed bubbles on surface.
6I-2-4	Eliminated Ta_2O_5 from 6I-2-3.	Formed bubbles.
6I-2-5	Substituted P_2O_5 for Ta_2O_5 in 6I-2-3.	Formed bubbles

Table C-6

COMPOSITION OF SERIES 6I-3 GERMANIA/TANTALUM GLASSES

Oxide	6I-1	6I-3	6I-3-1	6I-3-2	6I-3-3	6I-3-4	6I-3-5
	Equivalents						
Li_2O	0.740	0.448	0.448	--	0.448 (1)	0.448 (1)	0.448
ZnO	0.260	0.552	0.552		0.552	0.552	0.552
Al_2O_3	0.043	0.220	0.220		0.220	0.220	0.220
B_2O_3	4.277	3.605	4.500		3.592	3.592	4.500
Ta_2O_5	0.039	0.081	0.081		---	---	---
GeO_2	0.600	0.771	0.771		0.771	0.771	0.771
P_2O_5	---	---			---	0.081	---
	Mol Percent						
Li_2O	12.41	7.89	6.82	Same as 6I-3 except that LiF was substituted for Li_2O	8.02	7.91	6.90
ZnO	4.39	9.72	8.40		9.89	9.75	8.50
Al_2O_3	0.71	3.88	3.35		3.94	3.88	3.39
B_2O_3	71.73	63.50	68.47		64.33	63.42	69.33
Ta_2O_5	0.66	1.43	1.23		---	---	---
GeO_2	10.10	13.58	11.73		13.81	13.61	11.878
P_2O_5	---	---	---		---	1.43	---

(1) Li_2O added as LiF

Table C-7

COMPOSITION CHANGES IN 6I-3 SERIES

Coating	Changes	Remarks
6I-3-1	Increased B_2O_3 content of 6I-3 to 4.500 equivalents	Good maturation between 650 and 700°C.
6I-3-2	Substituted LiF for Li_2O in 6I-3	Bubbles formed, good coating.
6I-3-3	Eliminated Ta_2O_5 from 6I-3-2.	Formed coating with high quantity of bubbles at 650 and 700°C.
6I-3-4	Substituted P_2O_5 for Ta_2O_5 in 6I-3-2.	Formed very rough surface at 650 and 700°C
6I-3-5	Eliminated Ta_2O_5 in 6I-3-1	Excessive bubbles

Table C-8

COMPOSITION OF SERIES 6I-4 GERMANIA/TANTALUM GLASSES

Oxide	6I-1	6I-3	6I-4	6I-4-1	6I-4-2	6I-4-3	6I-4-4
	Equivalents						
Li_2O	0.740	0.448	0.575	0.575	Same as 6I-4 except that LiF was substituted for Li_2O	0.575(1)	0.575(1)
ZnO	0.260	0.552	0.425	0.425		0.425	0.425
Al_2O_3	0.043	0.220	0.563	0.563		0.563	0.563
B_2O_3	4.277	3.605	2.891	2.891		2.874	2.874
Ta_2O_5	0.039	0.081	0.103	0.103		---	---
GeO_2	0.600	0.771	2.086	1.500		2.086	2.086
P_2O_5	---	---	---	---		---	0.052
	Mol Percent						
Li_2O	12.47	7.89	8.66	9.49		8.81	8.75
ZnO	4.39	9.72	6.40	7.02		6.52	6.46
Al_2O_3	0.71	3.88	8.48	9.30		8.63	8.55
B_2O_3	71.73	63.50	43.52	47.73		44.06	43.71
Ta_2O_5	0.66	1.43	1.55	1.70		---	---
GeO_2	10.10	13.58	31.40	24.76		31.98	31.73
P_2O_5	---	---	---	---		---	0.79

(1) Li_2O added as LiF

Table C-9

COMPOSITION CHANGES IN 6I-4 SERIES

Coating	Changes	Remarks
6I-4-1	Decreased GeO_2 content of 6I-4 to 1.500	Retained high wetting angle, but matured at 650°C
6I-4-2	Replaced Li_2O with LiF in 6I-4	Formed bubbles on surface
6I-4-3	Eliminated Ta_2O_5 from 6I-4-2	Formed bubbles on surface
6I-4-4	Substituted P_2O_5 for Ta_2O_5 in 6I-4-2	Had bubbles, cracks and voids

A study of the fusion-flow characteristics of the Series 6 glasses was carried out. In this test a one gram sample of -400 mesh powdered glass is formed into a 9.5 mm (3/8 in.) diameter pellet at a minimum pressure of 28500 psi (1000 lbs load). The pellet is placed on a silicon wafer and fired at 980°C (100°C above the maturation temperature), in a horizontal position for 1.5 minutes. Without removing from the furnace, the wafer is tilted 90° and the pellet is fired in the vertical position. The flow of the melted glass is measured to the nearest 0.5 mm. Positive results were obtained only with the compositions shown in Table C-10.

In a further attempt to improve the bubble condition the most promising compositions, 6I-2-2 and 6I-3-1, were modified by increasing the B_2O_3 content (Table C-11). This result was not successful with the compositions 6I-X-6 and 6I-X-7 (X = 2 or 3), however some reduction in bubble formation was achieved by complete elimination of Al_2O_3 (6I-X-8). The effect of the compositional variations is summarized in Table C-12.

The tendency to form bubbles was reduced by dry grinding of 6I-2-2 and 6I-3-1. These coatings matured when fired at 650° for seven minutes. Coatings of 6I-2-2 and 6I-3-3, when ground dry, exhibited increasing bubble size as a function of temperature when fired at 600, 650 and 700°C for seven minutes.

Series 7I Glasses

In view of the excellent firing obtained with baria-magnesia borosilicate Series 7E composition as a diffusion mask, the compositions were altered in an attempt to reduce the fusion temperatures from 860 to 650°C. Compositions 7I-1 and 7I-2 (Table C-13) did not flow during fusion flow tests at 750 and 850°C.

Table C-10

FUSION FLOW CHARACTERISTICS OF SERIES 6 GLASSES

Series Number	Temp. (°C)	Time[1] (min)	Flow Length (mm)
6I-3-2	700	4	17.0
6I-3-2	700	7	21.5
6I-3-2	750	4	26.5
6I-4-3	750	4	24.0
6I-4-2	700	7	20.0
6I-4-2	750	4	23.5

(1) Time in the vertical position. All samples held 1-1/2 minutes in the horizontal position.

Table C-11

COMPOSITIONS OF MODIFIED 6I-2-2 AND 6I-3-1
SILICA-TANTALUM AND GERMANIA-TANTALUM GLASSES

Oxides	6I-2-2	6I-2-6	6I-2-7	6I-2-8	6I-3-1	6I-3-6	6I-3-7	6I-3-8
	Equivalents		except that as LiF instead	Equivalents			except that as LiF instead	
Li_2O	0.605	0.605		0.605	0.448	0.448		0.448
ZnO	0.395	0.395		0.395	0.552	0.552		0.552
Al_2O_3	0.186	0.100		---	0.220	0.220		---
B_2O_3	4.608	5.000		4.795	4.500	5.500		4.722
Ta_2O_5	0.096	0.096		0.096	0.081	0.081		0.081
SiO_2	1.395	1.200		1.395	---	---		0.771
GeO_2	---	---		---	0.771	0.771		0.771
			MOL PERCENT					
Li_2O	8.30	8.18	Same as 6I-3-6 Li_2O introduced of Li_2CO_3	8.30	6.82	5.92	Same as 6I-3-6 Li_2O introduced of Li_2CO_3.	6.82
ZnO	5.42	5.34		5.42	8.40	7.29		8.40
Al_2O_3	2.55	1.35		---	3.55	2.91		---
B_2O_3	63.25	67.60		65.81	68.47	72.63		71.83
Ta_2O_5	1.32	1.30		1.32	1.23	1.07		1.23
SiO_2	19.15	16.22		0.16	---	---		---
GeO_2	---	---		---	11.73	10.18		11.71

Table C-12

COMPOSITION CHANGES IN 6I-2-2 AND 6I-3-1 GLASSES

Coating	Changes	Remarks
6I-2-6	Increased B_2O_3 content of 6I-2-2 to 5.000 eq.	No effect on bubble formation
6I-2-7	In 6I-2-6, replaced Li_2CO_3 with LiF	No effect on bubble formation
6I-2-8	In 6I-2-2, replaced Al_2O_3 with B_2O_3	Reduced bubble formation
6I-3-6	Increased B_2O_3 Content of 6I-3-2 to 5.500 eq.	No effect on bubble formation
6I-3-7	In 6I-3-6, replaced Li_2CO_3 with LiF	No effect on bubble formation
6I-3-8	In 6I-3-2, replaced Al_2O_3 with B_2O_3	Reduced bubble formation

Table C-13

COMPOSITIONS OF BARIA-MAGNESIA BOROSILICATE GLASSES MODIFIED FOR LOWER MATURATION TEMPERATURE

Oxide	7E-8-1	7I-1	7I-2
	Equivalents		
BaO	0.260	0.714	0.714
ZnO	0.055	0.143	---
CaO	0.056	0.143	0.143
MgO	0.629	---	---
PbO	---	---	0.143
Total	1.000	1.000	1.000
B_2O_3	0.506	2.237	2.237
SiO_2	0.433	1.524	1.524
	Mol Percent		
BaO	13.41	15.00	15.00
ZnO	2.85	3.00	3.00
CaO	2.89	3.00	---
MgO	32.43	---	3.00
PbO	---		
B_2O_3	26.09	46.99	46.99
SiO_2	22.32	32.01	32.01

Series 9I

The study of this series was initiated to reduce the maturing temperature of Series 5E (diffusion mask dielectric) from 880 to 650°C. Compositions 9I-1 through 9I-5 (Table C-14) were evaluated in this report period. The compositional changes made in this series are summarized in Table C-15.

Good maturity was obtained in coating 9I-4 at 700°C. As the calculated expansion coefficient of this coating is too large ($6.8 \times 10^{-6}/^{\circ}C$), the B_2O_3 and SiO_2 were increased with negative effects on the maturation temperature.

Coatings 9I-6 through 9I-8 were smelted trying to improve these characteristics. Although some success has been achieved (Table C-15), the desired goal has not been reached.

As expansion is reduced by increasing the B_2O_3 and SiO_2, maturing temperature increases. It is planned to alter the compositions by additions of lithia until a maturing temperature of 550°C is reached. This procedure will increase the thermal expansion. To offset this trend, B_2O_3 will be substituted for Li_2O in small increments to reduce the expansion. On a normalized weight percent basis the expansion contribution of B_2O_3 is 1/120 that of lithia.

The effort during this reporting period was concentrated on reducing the maturation temperature of the 6I2-2 (isolation) glass. This composition has a maturation temperature of 700°C. Compositions of experimental glasses which were evaluated are given in Table C-16.

The first modification, 6I2-2-A, retained the same composition as 6I2-2 but derived the Li_2O from Li_2CO_3 instead of from LiF. The

Table C-14

COMPOSITIONS OF SERIES 9 ISOLATION DIELECTRICS

Oxide	5E-7	9I-1	9I-2	9I-3	9I-4	9I-5	9I-6	9I-7	9I-8
	Equivalents								
Na_2O	.270[1]	.270	.270	.169	.149	.231	.169	.270	.157
K_2O	.088	.088	.088	.055	.049	.075	.056	.088	.052
CaO	.216	.216	.216	.135	.119	.184	---	.216	---
Li_2O	.276[2]	.276	.276	.173	.153	.236	.174	.276	.232
ZnO	.150	.150	.150	---	---	---	---	.150	---
PbO	---	---	---	.469	.530	.273	.602	---	.559
B_2O_3	2.752	2.752	2.752	2.813	2.485	3.843	3.405	3.500	3.162
TiO_2	1.393	---	---	---	---	---	---	---	---
SiO_2	7.338	7.338	5.000	2.813	1.545	3.843	1.754	3.000	1.629
	Mol Percent								
Na_2O	2.16	2.43	3.09	2.55	3.96	2.66			
K_2O	0.70	0.79	1.01	0.83	0.97	0.86			
CaO	1.73	1.95	2.47	2.04	[illegible].37	2.12			
Li_2O	2.21	2.49	3.15	2.61	3.04	2.72			
ZnO	1.20	1.35	1.71	--	--	--			
PbO	--	--	--	7.08	10.54	3.14			
B_2O_3	22.05	24.82	31.44	12.45	49.40	44.24			
TiO_2	11.16	--	--	--	--	--			
SiO_2	58.78	66.17	57.13	42.45	30.72	44.24			

(1) Na_2O added as 0.366 NaF (equivalents)
(2) Li_2O added as .479 LiF (equivalents)

Table C-15

COMPOSITION CHANGES IN SERIES 9 GLASSES

Coating	Changes	Remarks
9I-1	TiO_2 eliminated from 5E7,	No fusion at 750°C
9I-2	Decrease SiO_2 to 5.000 Eq.	No fusion at 750°C
9I-3	Eliminated ZnO, added PbO, further decrease in SiO_2	No fusion at 750°C
9I-4	Increased PbO, decreased SiO_2	Maturation and fusion flow at 700°C
9I-5	Decreased PbO to .273 Eq., increased B_2O_3 and SiO_2	No fusion at 750°C
9I-6	Eliminated CaO from 9I-4, Increased B_2O_3	Expansion coef. reduced from 6.8 to 5.9 x 10^{-6}/°C
9I-7	Increased B_2O_3 in 9I-2 and decreased SiO_2	Refractory, no fusion
9I-8	Increased LiO_2 in 9I-6	Maturing temperature reduced, expansion coefficient 6.1 x 10^{-6}/°C

Table C-16

COMPOSITION OF SERIES 6 ISOLATION GLASSES

Oxide	6I2-2	6I2-8	6I2-9	6I2-10
Li_2O	0.605	0.605	0.605	1.000
ZnO	0.395	0.395	0.395	---
Total	1.000	1.000	1.000	1.000
B_2O_3	4.608	4.795	4.795	7.926
Al_2O_3	0.186	---	---	---
Ta_2O_5	0.096	0.096	---	---
SiO_2	1.395	1.395	1.395	2.306

maturation temperature for this coating was 650°C. Maturation temperatures for the other glass were all above 650°.

Fusion flow measurements which have been made for Series 6 glasses are reported in Table C-17.

Table C-17

FLOW CHARACTERISTICS OF 6I2 SERIES

Coating	Milling Condition	Time (Min.) Hor.	Time (Min.) Vert.	Temp. (°C)	Flow (mm)
6I2-2	Wet	1½	4	750	23.2*
6I2-2	Dry	1½	4	700	34.5
6I2-2	Dry	1½	4	750	Excessive
6I2-3	Wet	1½	4	700	24.5*
6I2-3	Dry	1½	4	750	28.0*
6I2-5	Wet	1½	4	750	Excessive
6I2-6	Wet	1½	4	750	22.5*
6I2-7	Wet	1½	4	700	22.0*
6I2-7	Wet	1½	4	750	21.5*
6I2-8	Dry	1½	4	700	41.5
6I2-8	Dry	1½	4	750	

*Bubbles

APPENDIX D

SERIES RESISTANCE CALCULATIONS FOR FRONT GRID PATTERN

1) Assume 15% efficient cell.

2) Assume peak power point at 500 mV therefore we will have an average current density of 30 mA/cm^2, which includes shadowed areas.

To determine the series resistance we will first calculate the loss in power (ΔP) due to series resistance.

$$\Delta P = I^2R$$

Assume:

#1) The 13 mil base material of 3 Ω-cm

#2) Diffused surface layer 35 Ω/□

#3) Gridlines, that are 6 mils wide and .7 mil thick and a conductivity of 1/3 that of bulk silver

#4) Center ohmic of .7 mil thick and a width of 40 mils to 150 mils

The total resistance will be the sum:

$$R_T = R_B + R_D + R_G + R_{oh}$$

CALCULATION OF SERIES RESISTANCE

A) BASE MATERIAL RESISTANCE

R = resistance (Ω)

ρ_{Si} = resistivity of silicon (Ω-cm)

t = thickness of wafer (cm)

A = area of wafer (cm^2)

$$R_B = \frac{\rho_{Si}\, t}{A} \qquad (1)$$

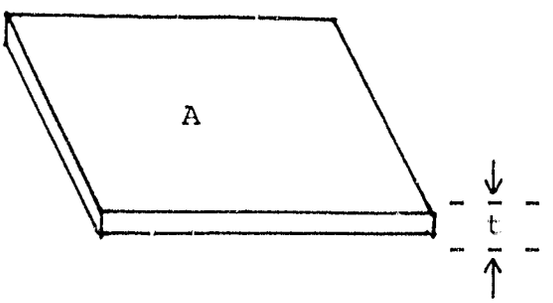

B) RESISTANCE OF DIFFUSED SURFACE LAYER

ρ_s = surface resistivity Ω/□

l_o = length of grid line (assuming grid lines go to edge of wafer)

x_o = half distance between grid lines

j = current density* ohms/cm^2

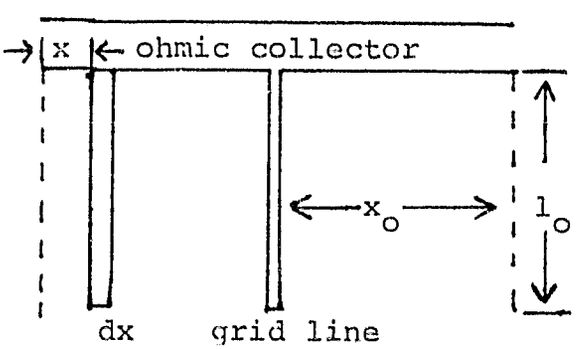

The element of power loss (p) over an element of silicon dx, is the square of the current entering that element times the resistance of that element dx.

$$dp = (j l_o x)^2 \cdot (\rho_s \frac{dx}{l_o}) \qquad (2)$$

$$dp = j^2 l_o \rho_s x^2 dx \qquad (3)$$

integrating over the half distance between grid lines (x_o) gives the total voltage drop to the midpoint.

*As a first approximation of power loss, the current density (j) is assumed to be independent of distance from gridline.

$$\Delta p = j^2 \rho_s l_o \int_o^{x_o} x^2 dx$$

$$= 1/3\ j^2 \rho_s l_o\ x^3 \Big|_o^{x_o}$$

$$\Delta p = 1/3\ j^2 \rho_s l_o\ x_o^3 \qquad (4)$$

The total resistance over the half distance between grid lines is;

$$R = \frac{\Delta p}{j^2 l_o^2\ x_o^2} \qquad (5)$$

$$= \frac{\rho_s\ x_o}{3 l_o} \qquad (6)$$

These areas of half distance between grid lines are all in parallel.

$$R_D \text{ (total)} = \frac{\rho_s\ x_o}{3 l_o} \div \text{number of areas} \qquad (7)$$

C) RESISTANCE OF GRID LINES

ρ_{Ag} = resistivity of silver paste (Ω-cm)

l_o = length of grid lines (assuming grid lines go to edge of wafer) (cm)

W = width of grid line (cm)

H = height of grid line (cm)

x_o = half distance between grid lines (cm)

j = current density (amps/cm)

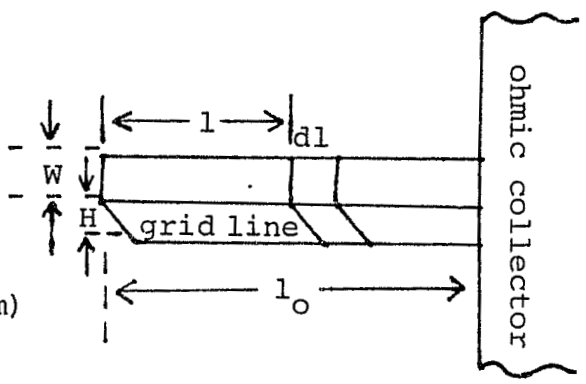

The element of power loss over an element of grid line dl, is the square of the current entering that element times the resistance of that element dl.

$$dp = (2\ x_o\ j\ l)^2 \cdot \left(\frac{\rho_{Ag}\ dl}{WH} \right) \qquad (8)$$

$$dp = \frac{4j^2\ \rho_{Ag}\ x_o^2\ l^2 dl}{WH} \qquad (9)$$

integrating over the grid line gives the total power loss for the grid line.

$$\Delta P = \frac{4j^2 \rho_{Ag}\ x_o^2}{WH} \int_o^{l_o} l^2 dl$$

$$\Delta P = \frac{4j^2\ \rho_{Ag}\ x_o^2\ l_o^3}{3\ WH} \qquad (10)$$

The total resistance over the grid lines is:

$$R = \frac{\Delta P}{4\ x_o^2\ j^2\ l_o^2}$$

$$= \frac{\rho_{Ag}\ l_o}{3\ WH} \qquad (11)$$

The grid lines are in parallel, therefore

$$R_G\ (\text{total}) = \frac{\rho_{Ag}\ l_o}{3\ WH} : \text{number of grid lines} \qquad (12)$$

D) OHMIC COLLECTOR

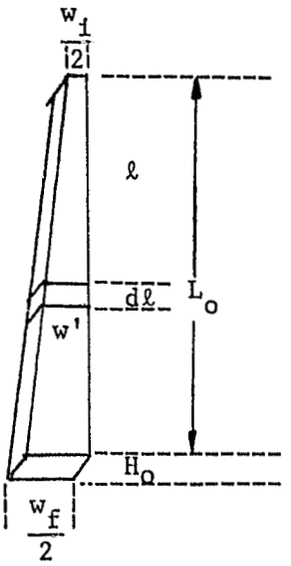

ρ_{Ag} = resistivity of silver paste

l_o = average distance between ohmic and edge of cell

w_i = minimum width of ohmic collector

w_f = maximum width of ohmic collector

L_o = length of ohmic collector

j = current density

Considering one half the cell, the element of power loss over an element of ohmic collector $d\ell$, is the square of the current entering that element times the resistance of the element $d\ell$.

$$dP = (l_o \ell j)^2 \cdot \left(\frac{\rho_{Ag}\, d\ell}{w' H_o}\right) \tag{13}$$

w' can be expressed as

$$w' = \frac{\ell(w_f - w_i) + L_o\, w_i}{2\, L_o} \tag{14}$$

Integrating over the whole ohmic

$$P = \frac{L_o\, l_o^2\, j^2\, \rho_{Ag}}{H_o} \int_o^{L_o} \left[\frac{\ell^2\, d\ell}{L_o\, w_i + \ell(w_f - w_i)}\right] \tag{15}$$

Form of

$$\int_0^C \frac{x^2\,dx}{a + bx} = \frac{x^2}{2b} - \frac{ax}{b^2} + \frac{a^2}{b^3} \ln (a + bx) \qquad (16)$$

(except where b approaches o)

$$P = \frac{4(j^2\, l_o^{\,2}\, L_o^{\,2})\; L_o\, \rho_{Ag}}{H_o(w_f - w_i)} \left[\tfrac{1}{2} - \left(\frac{w_i}{w_f - w_i}\right) + \left(\frac{w_i}{w_f - w_i}\right)^2 \ln \frac{w_f}{w_i} \right] \qquad (17)$$

(except where $W_f \neq W_i$)

Then the resistance over the whole cell becomes:

$$R = \frac{\Delta P}{4j^2\, l_o^{\,2}\, L_o^{\,2}}$$

$$R_o \text{ (Total)} = \frac{\Delta P}{4j^2\, \ell^2\, L_o^{\,2}} = \frac{L_o\, \rho_{Ag}}{H_o\, (w_f - w_i)} \left[\tfrac{1}{2} - \left(\frac{w_i}{w_f - w_i}\right) + \left(\frac{w_i}{w_f - w_i}\right) \ln \frac{w_f}{w_i} \right] \qquad (18)$$

SAMPLE CALCULATION OF SERIES RESISTANCE

FOR GRID PATTERN #6314-08, FIGURE D-1

ρ_{si} = 3.0 Ω-cm

t = 0.033 cm

A = 28.45 cm^2

ρ_s = 35 Ω/□

l_o = 2.54 cm

X_o = 0.145 cm

ρ_{Ag} = 4.77×10^{-6} Ω-cm

w = .0152 cm

H = 1.78×10^{-3} cm

w_i = 0.102 cm

w_f = 0.381 cm

H_o = 1.78×10^{-3} cm

L_o = 5.18 cm

Number of gridlines = 34

A) Base Material Resistance

$$R_B = \frac{\rho_{si}\ t}{A} = \frac{(3.0)(0.033)}{28.45}\ \Omega = 3.48\ m\Omega$$

B) Resistance of Diffused Surface Layer

$$R_o = \frac{\rho_s\ X_o}{3\ l_o} \div 68 = \frac{(35)(0.145)}{3(2.54)}\ \Omega \div 68 = 9.79\ m\Omega$$

C) Resistance of Gridlines

$$R_G = \frac{\rho_{Ag}\, l_o}{3\ WH} \ : \ 34 = \frac{(4.77 \times 10^{-6})(2.54)\ \Omega}{3(.0152)(1.78 \times 10^{-3})} \ : \ 34 = 4.39\ m\Omega$$

D) Resistance of ohmic collector

$$R_o = \frac{\rho_{Ag}\, L_o}{H_o(w_f - w_i)} \left[\tfrac{1}{2} - \frac{w_i}{(w_f - w_i)} + \left(\frac{w_i}{w_f - w_i}\right)^2 \ln \frac{w_f}{w_i} \right]$$

where $w_f \neq w_i$

$$\frac{(4.77 \times 10^{-6})(5.18)}{(1.78 \times 10^{-3})(.279)} \left[\tfrac{1}{2} - \frac{.102}{.279} + \left(\frac{.102}{.279}\right)^2 \ln \left(\frac{.381}{.102}\right) \right]$$

$$R_o = 15.45\ m\Omega$$

Total resistance of contact pattern is:

$$3.48 + 9.79 + 4.39 + 15.45 = 33.11\ m\Omega$$

FIGURE D-1

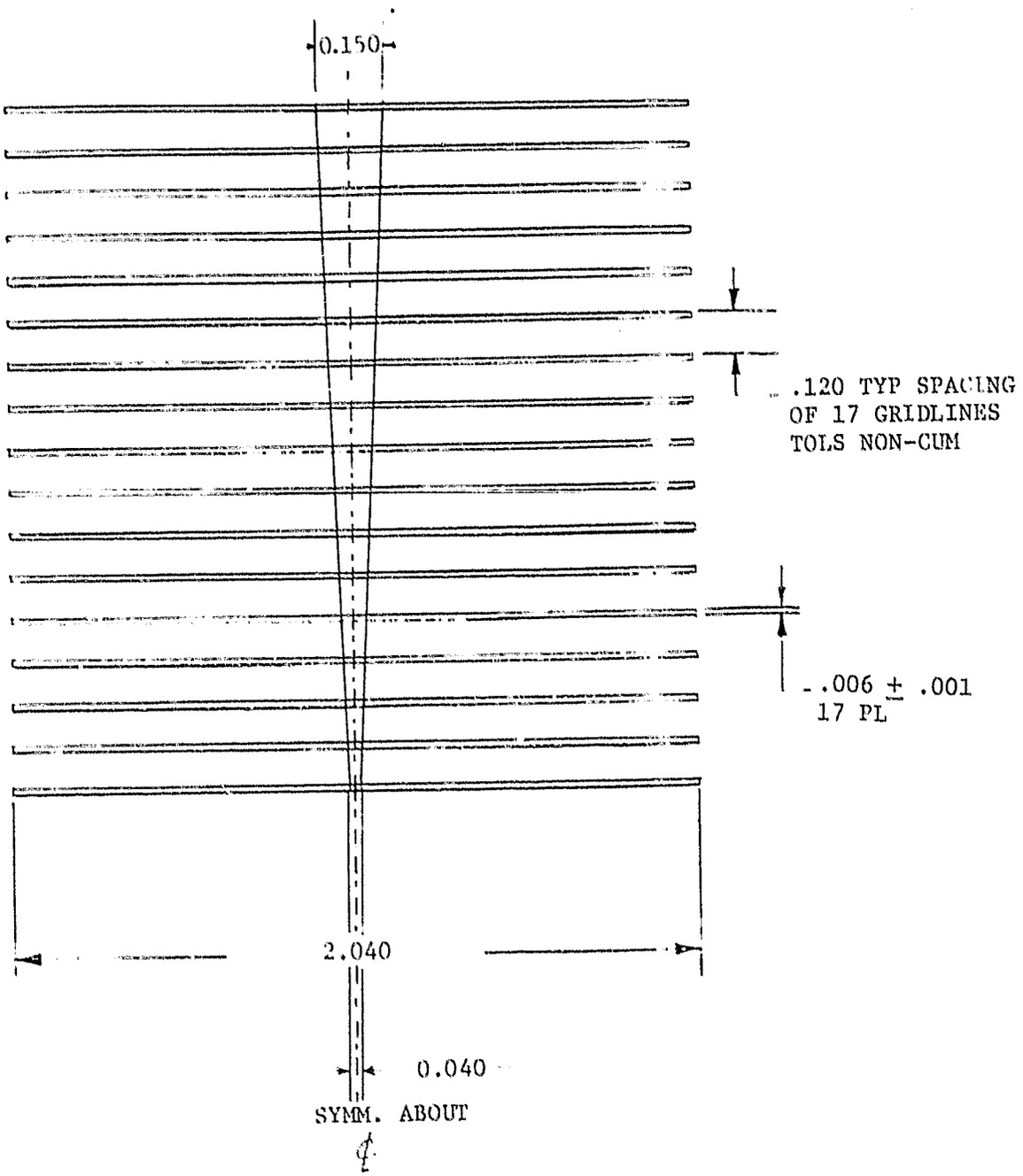

DIMENSIONS ARE IN INCHES

TOLERANCES: .XXX = ± .003

Part No. 6314-08

FRONT CONTACT
GRIDLINE PATTERN
(SCREEN PRINTING)

APPENDIX E

SERIES RESISTANCE CALCULATIONS FOR INTERCONNECTS

Power loss due to resistance. Assume worst case 75°C, 0.8A per cell.

.4" x 3 mil ribbon	8.25 Ω per 1000 ft.
.1" x 2 mil ribbon	49.5 Ω per 1000 ft.

Section	Length	Current	Power Loss
A	2.5"	0.8A	.00110W
B	2.5"	1.6A	.00440
C	2.5"	2.4A	.00990
D	2.5"	3.2A	.01761
E	1.3"	4.0A	.01431
			.04732

x 4 A-E segments per panel .18930W total power loss in bus bars.

200 1/4", 0.8A carrying interconnects .13200W power loss

Total power loss	.32130W
or on 80W panel	0.40%

Sample calculation (Section A)

$$W_L = I^2R$$

$$W_L = (0.8)^2 \times 8.25 \times \frac{1}{1000} \times \frac{1}{12} \times 2.5\ A^2 \cdot \Omega \cdot ft^{-1}\ \frac{ft}{in} \cdot in$$

$$W_L = .00110W$$

Appendix F

PROCESS SPECIFICATIONS

Spectrolab, Inc.

PROCESS SPECIFICATION

SURFACE PREPARATION - POLISH ETCHING

CODE WORD: SURFPREP

6314-0001 Rev A
February 25, 1980

1. SCOPE

The description of all necessary requirements to etch silicon wafers. The purpose of the process to to remove as much material as necessary to eliminate surface damage.

2. INPUT MATERIALS

2.1 Blank Wafers (Spec. #)

3. INPUT SUPPLIES

3.1 Sodium Hydroxide (50%)

3.2 Hydrochloric Acid

3.3 Deionized Water

3.4 City Water

4. EQUIPMENT AND FACILITIES

4.1 The equipment selection and/or design for this operation should be based on the following:

4.1.1 Solution to be used will be of the following composition: 30% (W/V) sodium hydroxide in water.

4.1.2 The reaction that takes place consumes NaOH at the theoretical rate of 2.86 g per gram of etched Si.

4.1.3 The amount of Si to be removed depends on the kind of wafer being etched. Present Cz-grown single crystal wafers (sliced with reciprocating blade saws) appear to yield satisfactory results when a total of approximately 75 μ are removed from the thickness (i.e. approximately 37 μ /side).

4.1.4 Equipment to have capacity for handling 10 cm x 10 cm wafers or 10 cm diameter wafers with expansion capability to 15 cm x 15 cm wafers, .030 to .050 cm thick.

4.2 Equipment required for process sequence as follows:

4.2.1 Wafer carriers.

4.2.2 Sodium Hydroxide etch station.

4.2.3 Rinse station (city water).

4.2.4 Hydrochloric Acid station.

4.2.5 Rinse station (D.I. water).

4.2.6 Drying station.

4.2.7 Automated wafer load-unload and transport system.

4.3 Type A manufacturing space for above equipment.

4.4 Utilities as required for operation of above equipment.

4.5 Heating, air conditioning and equipment to comply with safety standards for above manufacturing space.

4.6 A system to dispose or recover materials for reuse from byproducts, specifically: spent Sodium Hydroxide solution containing Sodium Silicate; used 20% Hydrochloric Acid Solution; Hydrogen gas and rinse waters.

4.7 Process control instrumentation and in-line inspection equipment as follows:

4.7.1 Remote thermometers to constantly monitor solution temperature (a temperature recorder, and an alarm system to indicate when solution temperature is outside of the established range, is recommended).

4.7.2 Automatic equipment to control the composition of the NaOH solution.

4.7.3 Automatic thickness measuring equipment for in-line inspection.

4.7.4 Microscope, 100X, 200X, 400X; binocular, for in-line inspection of wafer topography.

4.7.5 Automatic go/no-go gauge for in-line inspection of wafer outside dimensions.

4.7.6 Automatic resistivity measuring equipment (0.1 to 10 ohm cm range).

4.7.7 Equipment for manual measurement of minority carrier lifetime (range 10 to 500 microseconds).

5. THROUGHPUTS AND LABOR CONTENT

Assuming round-the-clock (3 shifts per day) operation and .90 operating minutes per minute.

5.1 Output rate: 25 polished wafers (10 cm x 10 cm) per operating minute.

5.2 Labor Content:

5.2.1	Semiconductor Assembler: (Cat. # B3096D)	1 person/shift
5.2.2	Electronics Technician: (Cat. # B3704D)	.1 person/shift
5.2.3	Maintenance Mechanic II: (Cat. # B3736D)	.2 person/shift

6. PROCESS SEQUENCE AND PARAMETERS

6.1 Immerse wafers in a solution of 30% ± 1% W/V Sodium Hydroxide in D.I. water.

Temperature of the solution: 85 ± 3°C. As the reaction progresses, Sodium Hydroxide is being consumed and Sodium Silicate is formed as indicated in 4.1.2

Time of immersion: 15-20 minutes (see 4.1.3).

6.2 Rinse in city water until pH of rinse waters is 7 or less.

6.3 Immerse in a 20% solution of Hydrochloric Acid at room temperature for 15 minutes. The purpose of this soaking is to put in solution any iron that the wafers may be contaminated with (from NaOH solution) and to neutralize any NaOH that may have remained in the wafer. An alternative may be to use iron free NaOH, followed by water rinse and then Acetic Acid (30%) rinse to neutralize trapped NaOH (as determined by pH measurement).

6.4 Rinse in deionized water until HCl is completely removed. Dry.

6.5 Transfer wafers to next station

7. BY-PRODUCTS - (Section 5.1.2)

7.1 Sodium Silicate that remains in solution.

7.2 Hydrogen gas that escapes out of solution.

8. PRODUCT REQUIREMENTS & Q.A.

8.1 In-Line Dimensions of incoming wafers shall be as follows: Length 10 cm± , Width 10 cm± , Thickness 0.043 ± , as measured with go/no-go gauge and thickness gauge (100% frequency); resistivity 1 ohm cm min.

8.2 Q.A. Process Control Tests

8.2.1 Inspection of surface under microscope (400X) to verify uniformity of etching as per samples for comparison purposes (2% frequency).

8.2.2 Inspection to verify above in-line inspection for dimensions and etching. (2% frequency.)

8.2.3 Testing to verify solution composition and operating parameters once per hour.

8.2.4 Minority carrier lifetime (1% frequency).

Approved by:

Angel Pepe, Engineer

Approved:

William F. Taylor
Program Manager

SPECTROLAB, INC.

PROCESS SPECIFICATION

JUNCTION FORMATION - DIFFUSED WAFER

#6314-1002
July 28, 1980

CODE WORD: DIFFUSE

1. SCOPE

This specification describes the requirements necessary to form a N+ junction on a P-type silicon wafer using a spin-on polymeric diffusion source. Spin-on emitter diffusion source with a high temperature drive is the basic process.

2. INPUT MATERIALS

2.1 Polished Wafers (Spec. #6314-0001 Rev. A PWAFER)

2.2 Emitter Diffusion Source (Allied Chemicals Accuspin PX-10)

3. INPUT SUPPLIES

3.1 Isopropanol to clean spin equipment.

4. EQUIPMENT AND FACILITIES

4.1 Application of polymeric diffusion source should be based on the following:

4.1.1 Spinning equipment to apply polymeric source onto only one side of the wafer (preventing wicking of source around edge of wafer). (Apply approximately 1.8 ml per wafer.)

4.1.2 I.R. drying equipment, to drive off solvents from sprayed wafers (see 6.1.3).

4.2 Firing equipment to drive emitter diffusion source into wafer 800°C to 1000°C, 5 to 30 minutes, nitrogen and air atmosphere (see 6.2).

4.3 All equipment to have capacity for handling 10 cm x 10 cm square and 10 cm diameter round wafers with expansion capability to 15 cm x 15 cm wafers, 0.020 to 0.050 cm thick.

4.4 Type A manufacturing space for above equipment.

4.5 Utilities for above equipment.

4.6 Heating, air conditioning and equipment to comply with safety standards for above manufacturing space.

4.7 Waste disposal containers for collection of solids (paper, jars, etc.) and liquids (waste solvents, etc.).

5. THROUGHPUT AND LABOR CONTENT

Assuming round-the-clock (3 shifts/day) operating and .90 operating minutes per minute.

5.1 Output rate 24 diffused wafers (10 cm x 10 cm)/operating minute.

5.2 Labor content:

5.2.1	Semiconductor Assembler:	8 - Spin diffusion source:	.2 persons/shift/machine
		IR Drying oven:	.20 persons/shift/machine
		2 - Diffusion furnace:	.20 persons/shift/machine
5.2.2	Electron Technician: (Cat. #B3704D)	.02 person/shift/spin machine .05 person/shift/drying oven .05 person/shift/diffusion furnace	
5.2.3	Maintenance Mechanic II: (Cat. #B3736D)	.05 person/shift/spin machine .05 person/shift/drying oven .05 person/shift/diffusion furnace	

6. PROCESS SEQUENCE AND PARAMETERS

6.1 Spin-on emitter diffusion source.

6.1.1 Place wafer on pedastal.

6.1.2 Apply diffusion source onto wafer.

6.1.3 Spin wafer. (3000 rpm, 10 sec.)

6.2 IR Bake for 3 minutes @ 300°C ± 20°C.

6.3 Diffuse wafers 10 minutes in nitrogen atmosphere @ 900°C ± 5 and 5 minutes in air atmosphere @ 900° ± 5°C.

6.4 Allow wafers to cool to room temperature.

6.5 Transfer wafers to next station.

7. BY-PRODUCTS

7.1 Solvents that evaporate from diffusion source.

8. PRODUCT REQUIREMENT AND Q.A.

8.1 In-Line sheet resistance measurements of diffused surfaces will be performed just after aluminum cleaning, CLNBACK.

Prepared by:

Nick Mardesich

Nick Mardesich, Sr. Engineer

Approved by:

William E. Taylor

William E. Taylor
Program Manager

SPECTROLAB, INC.

PROCESS SPECIFICATION

PRINT AND FIRE BACK SURFACE FIELD SOURCE

CODE WORD: BACKCONT

6314-0003 Rev. A
June 22, 1979

1. SCOPE

This specification describes the requirements necessary to obtain a P+ back surface on an N+ diffused wafer using screen printed and fired aluminum paste.

2. INPUT MATERIALS

2.1 Diffused Wafers (Spec. #6314-1002 DWAFER)

2.2 Aluminum Printing Paste (Spec. #6314-2001)

3. INPUT SUPPLIES

3.1 Screens (Cat. # E 1576D)

3.2 Squeegee (Cat. # E1624D)

3.3 Terpinol

3.4 Butyl Carbutol

3.5 Xylene

4. EQUIPMENT AND FACILITIES

4.1 Screen printing system, automatic; capable of printing a 3.9" x 3.9" image on a 4" x 4" wafer. Must be adaptable for wafers up to 6" x 6".

4.2 Drying equipment; to drive off solvents from paste-printed substrates (see 6.2).

4.3 Firing equipment; to fire paste on coated wafers (see 6.3), 700-950°C, 10-60 second dwell time, 5 second max. temperature (environment) transition time up and down.

4.4 Automated cassette loader.

4.5 Equipment for testing P+ back surface field.

4.6 Environmental test equipment (100% RH @ 70°C).

4.7 Type A manufacturing space for above equipment.

4.8 Utilities for above equipment.

4.9 Heating, air conditioning, and equipment to comply with safety standards for above manufacturing space.

4.10 Waste disposal or recovery of solids (paste residues, paper, jars, etc.) and liquids (waste solvent, thinner, vehicles, etc.).

5. THROUGHPUT AND LABOR CONTENT

Assuming round-the-clock (3 shifts per day) operation and .90 operating minutes per minute.

5.1 Minimum output rate: 25 back surface field wafers (4" x 4") per operating minute.

5.2 Labor content:

5.2.1	Semiconductor Assembler (Cat. # B3096D)	.20 persons/shift/machine
5.2.2	Electronics Technician (Cat. # B3704D)	.10 persons/shift/machine
5.2.3	Maintenance Mechanic II (Cat. # B3736D)	.10 persons/shift/machine

6. PROCESS PROCEDURES AND PARAMETERS

6.1 Print wafers with aluminum paste (approximately 1 mil thick when applied).

6.2 Dry applied paste; 15 ± 1 minutes @ 200 ± 5°C in air.

6.3 Fire dried paste; 45 ± 1.5 seconds @ 850 ± 2°C in air, 5 sec. max. transition. (See Note 9.6)

6.4 Allow wafers to cool to room temperature, 5 sec. max. transition.

6.5 Load wafers into cassette.

6.6 Transfer wafers to next station.

7. BY-PRODUCTS

7.1 Paste thinner vapors at printer.

7.2 Paste vehicle and thinner vapors at drying and firing.

7.3 Cleaning-solvent vapors when cleaning equipment and supplies.

7.4 Total estimated amount of fumes: 5.54 cu. ft./operating minute.

7.5 Waste paste.

8. PRODUCT REQUIREMENTS AND Q.A.

8.1 In Line Backfield surface to be P+ as indicated by open circuit voltage of 0.6 volts min. with 100 mW/cm^2 illumination (10% frequency). To be done after CLN back.

9. NOTES

9.1 There are three options on screen mesh materials; polyester with exceptionally long life, nylon for difficult contours and stainless steel for better line definition and overall print consistency.

9.2 On stainless steel screens a 70 Durometer squeegee @ 4 to 6 lbs. of pressure should be the choice; with polyester screens a 60 Durometer flexible squeegee with 3 to 4 lbs. of pressure is recommended.

9.3 Presently available screen printing equipment is capable of making 3,000 impressions per hour; however, it will only do a little better than 1,500/hr. when the substrate size is as large as the one in this specification.

9.4 TV monitoring of the printe cycle is also presently available.

9.5 Drying and firing equipment could be an infrared conveyor furnace with two sections, one for drying and the other for firing.

9.6 The firing parameters given in Paragraph 6.3 were determined for a particular case. The exact firing parameters for the dried aluminum paste must be emperically determined for the particular furnace, furnace load and wafer configuration.

Approved by:

Nick Mardesich

Nick Mardesich, Engineer

Approved:

William E. Taylor

William E. Taylor
Program Manager

Spectrolab, Inc.

PROCESS SPECIFICATION

REMOVE OXIDE AND CLEAN ALUMINUM BACK

CODE WORD: CLNBACK

6314-0004 Rev. B
February 25, 1980

1. SCOPE

All the necessary requirements to remove the oxide layer from the front surface of wafers, and to clean off the excess aluminum from the back contact surface of the same wafers are described in this specification.

2. INPUT MATERIALS

2.1 Back Surface Field Wafers (Spec. #6314-0003, Rev. A BWAFER)

3.0 INPUT SUPPLIES

3.1 Hydrofluoric Acid

3.2 Hydrochloric Acid

3.3 Ammonium Hydroxide

3.4 Acetic Acid

3.5 Deionized Water

4. EQUIPMENT AND FACILITIES

4.1 The purpose of the equipment to be selected or designed for this operation is to remove the unsintered aluminum from the surface of the cells after a treatment (see 6.0) that loosens the powder.

4.1.1 Removal of the unsintered aluminum should preferably be accomplished by a brushing or other equivalent operation. Care should be taken in the design of the cell handling part of the equipment.

4.1.2 It is important to note that a hydrofluoric acid solution is used in this operation, therefore, special safety precautions should be taken in the design of the equipment due to the nature of the acid.

4.2 Hydrofluoric acid solution composition should be: 5% ± 1% HF. This may be prepared by mixing 10% ± 2% of a concentrated 50% HF solution with deionized water.

4.3 Equipment to have capacity for handling 10 cm x 10 cm square or 10 cm diameter round wafers, with expansion capability up to 15 cm x 15 cm wafers.

4.4 Equipment required as per process sequence.

4.5 Type A manufacturing space for above equipment.

4.6 Utilities as required for operation of above equipment.

4.7 Heating, air conditioning and equipment to comply with safety standards for above manufacturing space.

4.8 A system to dispose or recover materials for reuse from by-products: Aluminum powder, spent HF solution, etc.

5. THROUGHPUT AND LABOR CONTENT

Assuming round-the-clock (3 shifts per day) operation and .90 operating minutes per minute.

5.1 Output rate: 25 clean back surface field wafers (10 cm x 10 cm) per operating minute.

5.2 Labor Content.

5.2.1 Semiconductor Assembler: (Cat.# B3096D) 1 person/shift

5.2.2 Electronics Technician: (Cat.# B3704D) .1 person/shift

5.2.3 Maintenance Mechanic II: (Cat. # B3736D).1 person/shift

6. PROCESS SEQUENCE AND PARAMETERS

6.1 Immerse wafers in a 5% Hydrofluoric Acid solution (see 4.2)
Time: 4 ± .2 minutes
Temperature: Room ($25^{o}C \pm 5^{o}C$)

6.2 Rinse in deionized water. (Time of transfer should be minimized to avoid contact of HF-wetted wafers with air.) This is a quick rinse, so it could possibly be accomplished by spraying D.I. water while wafers are transferred from 6.1 to 6.3 solution.
Time: 5 + 1 second
Temperature: Room

6.3 Immerse in a 3% (2-4%) ammonium hydroxide solution.
Time: 2 + .2 minutes
Temperature: Room

6.5 Dry

6.6 Bake for 5 ± .5 minutes at $105^{o}C$ in air.

6.7 Remove loose aluminum powder from surface.

6.8 Immerse wafers in 10% hydrochloric acid solution.
Time: 1± .1 minutes
Temperature: Room (25% ± 5°C)

6.9 Immerse wafers in 10% hydrofluoric acid solution.
Time: 1 ± .1 minutes
Temperature: Room (25°C ± 5°C)

6.10 Immerse in concentrated acetic acid
Time: 1 ± .1 minutes
Temperature: Room

6.11 Rinse in deionized water.
Time: 2 ± .2 minutes
Temperature: 25°C ± 5°C

6.12 Dry.

6.13 Transfer wafers to next station.

7. BY-PRODUCTS

7.1 Aluminum powder from the back of wafers.

7.2 Exhausted hydrofluoric acid solution.

7.3 Exhausted ammonium hydroxide solution.

7.4 Exhausted acetic acid solution.

7.5 Acidic and basic rinse wafers.

7.6 Exhausted hydrochloric acid solution.

8. PRODUCT REQUIREMENTS AND Q.A.

8.1 In Line visual inspection to determine whether or not all unsintered aluminum has been removed.

8.2 Q.A. Process Control Tests

8.2.1 Aluminum layer should pass a 90° pull test of at least 500 gms. when a #22 gauge solid copper wire is soldered to a tinned pad (1 cm x 1 cm) that has been applied to the surface with an ultrasonic soldering iron. One test cell run once per hour. (1/1350 frequency)

Should pass same test as above after 1 week of environmental exposure (70°C and 100% humidity). Ten test cells run once per week (10/162,000 frequency).

8.2.2 In Line sheet resistivity measurement of diffused surface, 35 to 45 Ω/□ (100% frequency) must be done after cell cleaning.

8.2.3 In Line backfield surface to be P+ as indicated by open circuit voltage of 0.6 volts min. with 100 mW/cm^2 illumination (10% frequency). To be done after CLN back.

9. NOTES

9.1 The firing of the printed aluminum, as described in Process #6314-0003 B CONT, alloys it to the silicon. However a good portion remains unsintered, as it is referred to throughout the present specification. This unsintered aluminum has to be removed before proceeding to the next step in the manufacturing process.

9.2 This powder is very fine and loose on the surface, but not easy to remove completely. A brushing in conjunction with suction is the technique used for laboratory scale operations.

9.3 Step 6.6 of the process sequence is presently being used to facilitate removal, however it may not be necessary if a different technique is used.

9.4 The purpose of the hydrochloric,hydrofluoric acetic acid and hot deionized water to rinse is to eliminate any aluminum fluoride that may have formed, as well as to prepare the front surface for the application of contacts with good adherence to the silicon surface.

9.5 IMPORTANT: If necessary to store wafers in process it should be done before Step 6.8 of the process sequence. Steps 6.8 through 6.13 should immediately be followed by the next operation. 2 hrs. maximum delay time.

Prepared by:

Nick Mardesich

Nick Mardesich
Engineer

Approved by:

William E. Taylor
Program Manager

SPECTROLAB, INC.

PROCESS SPECIFICATION

JUNCTION CLEAN - LASER SCRIBE

#6314-1007
July 28, 1980

CODE WORK: J CLEAN

1. SCOPE

This specification describes the requirements for cell junction isolation by laser scribing through the p+ back layer and breaking.

2. INPUT MATERIALS

2.1 Remove oxide and cleaned aluminum back (Spec. #6314-0004 Rev. B CLNBACK).

3. INPUT SUPPLIES

3.1 Deionized water 10 c.c./hr.

3.2 Cooling water 3 gal/min.

3.3 Krypton arc lamps (200 hr. life)

3.4 Illumination lamp (50 hr. life)

3.5 Filters for particle vacuum exhaust system

4. EQUIPMENT AND FACILITIES

4.1 Nd-YAG laser scribe system capable of scribing a rectangular pattern up to 10 cm x 10 cm in TEMoo laser mode.

4.2 Cassette to cassette load and unload.

4.3 All equipment to have capacity for handling 10 cm x 10 cm square wafers or 10 cm diameter round wafers with expansion capability to 15 cm x 15 cm wafers.

4.4 Type A manufacturing space for above equipment.

4.5 Utilities for above equipment.

4.6 Heating, air conditioning and equipment to comply with safety standards for above manufacturing space.

4.7 Waste disposal containers for collection of particles.

5. THROUGHPUT AND LABOR CONTENT

Assuming round-the-clock (3 shifts/day) operating and .90 operating minutes per minute.

5.1 Output rate 8.33 or 12.5 diffused wafers (10 cm x 10 cm)/ operating minute.

5.2 Labor content:

5.2.1 Semiconductor Assembler: 0.5 person/shift/machine (Cat. #B3096D).

6. PROCESS SEQUENCE AND PARAMETERS

6.1 Load wafer onto vacuum hold-down chuck.

6.2 Engage vacuum.

6.3 Start cycle.

6.4 Unload wafer from vacuum chuck.

6.5 Break edge of wafer.

7. BY-PRODUCTS

7.1 Silicon particles.

8. PRODUCT REQUIREMENTS AND Q.A.

8.1 In-Line none.

8.2 Q.A. Process Control Tests

8.2.1 Scribed groove must be not more than 0.025 cm from wafer edge. Test 1 cell/hour (1/1350 frequency).

9. NOTES

Prepared by:

Nick Mardesich, Sr. Engineer

Approved by:

William E. Taylor
Program Manager

SPECTROLAB, INC.

PROCESS SPECIFICATION

PRINT AND FIRE FRONT CONTACT

CODE WORD: FRONTCONT

6314-0005 Rev.A
June 22, 1979

1. SCOPE

This specification describes the requirements necessary to obtain a collector grid on the N+ diffused wafer using screen printed silver paste.

2. INPUT MATERIALS

2.1 Junction Clean Wafer (Spec. #6314-1007 JCWAFER)

2.2 Silver Printing Paste, (Spec. # 6314-2002)

3. INPUT SUPPLIES

3.1 Printing Screens

3.2 Squeegee

3.3 Butyl Carbitol

3.4 Xylene

3.5 #600 Scotch tape

4. EQUIPMENT AND FACILITIES

4.1 Screen printing systems, automatic; capable of printing a 4" x 4" image on a 4" x 4" wafer. Must be adaptable for wafers up to 6" x 6".

4.2 Drying equipment; to drive off solvents from paste printed wafers (see 6.2).

4.3 Firing equipment; to fire paste on coated wafers 600 to 800°C, 20 to 60 seconds with 5 second ramp from 400°C to peak, air atmosphere (see 6.5).

4.4 Type A manufacturing space for above equipment.

4.5 Utilities for above equipment.

4.6 Heating, air conditioning, and equipment to comply with safety standards for above manufacturing space.

4.7 Waste disposal containers or recovery of solids (paste residues, paper, jars, etc.) and liquids (waste solvent, thinner, vehicles, etc.).

4.8 Pull test equipment.

5. THROUGHPUT AND LABOR CONTENT

Assuming round-the-clock (3 shifts/day) operation and .90 operating minutes per minute.

5.1	Output rate 25 front contacted wafers (4" x 4")/operating minutes	
5.2	Labor Content:	
5.2.1	Semiconductor Assembler: (Cat. # B3096D)	.20 persons/shift machine
5.2.2	Electronic Technician: (Cat. # B3704D)	.10 persons/shift machine

6. PROCESS SEQUENCE AND PARAMETERS

6.1 Print front grids on wafers with silver paste (approximately 1 mil thick when applied), (6 mil wide lines).

6.2 Dry applied paste 10 ± 1.0 minutes @ 125 ± 10°C in air.

6.3 Fire dried paste 20-25 seconds @ 700 ± 2°C air atmosphere.

6.4 Allow wafers to cool to room temperature.

6.5 Transfer wafers to next station.

7. BY-PRODUCTS

7.1 Paste thinner vapors at printer.

7.2 Paste vehicles and thinner vapors when drying and firing.

7.3 Cleaning solvent vapors when cleaning equipment and supplies.

7.4 Total estimated amount of fumes: 0.1 cu. ft. /operating minute.

7.5 Waste silver paste.

8. PRODUCT REQUIREMENTS AND Q.A.

8.1 In Line None.

8.2 Q.A. Process Control Tests

8.2.1 Front grid pattern:

8.2.1.1 Silver must be adherent and be able to pass #600 scotch tape test Spec. # (ASTM #).

8.2.1.2 Should pass same test as above after 2 weeks of environmental exposure (70°C and 100% humidity). Ten test cells run once per week (10/162,000 frequency).

8.2.2 Ohmic solder pads:

8.2.2.1 Silver contact pad must be solderable with 62 Sn, 36 Pb, 2 Ag solder.

8.2.2.2 Silver contact pad should pass a 90° pull test of at least 500 grams when a #22 gauge solid copper wire is soldered to it. One test cell run once per hour (1/1350 frequency).

8.2.2.3 Should pass same test as above after 1 week of environmental exposure (70°C and 100% humidity). Ten test cells run once per week (10/162,000 frequency).

9. NOTES

9.1 There are three options on screen mesh materials; polyester with exceptionally long life, nylon for difficult contours and stainless steel for better line definition and overall print consistency.

9.2 On stainless steel screens, a 70 Durometer squeegee @ 4 to 6 pounds of pressure should be the choice; with polyester screens a 60 Durometer flexible squeegee with 3 to 4 pounds of pressure is recommended.

9.3 Presently available screen printing equipment is capable of making 3,000 impressions per hour; however, it will only do a little better than 1,500/hr. when the substrate size is as large as the one in this specification.

9.4 TV monitoring of the printing cycle is also presently available.

9.5 Drying and firing equipment could be an infrared conveyor furnace with two sections, one for drying, and the other for firing.

Approved by:

Nick Mardesich

Nick Mardesich, Engineer

Approved:

William E. Taylor

William E. Taylor
Program Manager

SPECTROLAB, INC.

PROCESS SPECIFICATION

ANTI-REFLECTIVE COATING

#6314-1008
July 28, 1980

CODE WORK: AR COAT

1. SCOPE

This specification describes the requirements for evaporated anti-reflective film on front contacted wafer.

2. INPUT MATERIALS

2.1 Front contacted wafer (Spec. #6314-0005 Rev. A, FWAFER)

2.2 Silicon monoxide (SiO) powder

3. INPUT SUPPLIES

3.1 Nitrogen gas
3.2 Nitrogen liquid
3.3 Cooling water

4. EQUIPMENT AND FACILITIES

4.1 Application of AR evaporated coating should be based on the following:

4.1.1 High vacuum deposition system

4.1.2 Domed Planetary fixturing system

4.1.3 Automatic deposition monitoring system

4.1.4 In-line micron filtering aparatus

4.2 All equipment to have capacity for handling 10 cm x 10 cm square or 10 cm diameter round wafers with expansion capability to 15 cm x 15 cm wafers.

4.3 Type A manufacturing space for above equipment

4.4 Utilities for above equipment (water and nitrogen)

4.5 Heating, air conditioning and equipment to comply with safety standard for above manufacturing space.

4.6 Waste disposal container for collection of solids (paper, jars, etc.)

5. THROUGHPUT AND LABOR CONTENT

5.1 Output rate 3.0 cells (10 cm x 10 cm)/operating minute

5.2 Labor content:

5.2.1 Semiconductor Assembler: 5.2 persons/shift/machine

6. PROCESS SEQUENCE AND PARAMETERS

6.1 Load cells

6.1.1 Load cells into planetary fixture.

6.1.2 Load planetary system into deposition system.

6.2 Deposit AR coating.

6.2.1 Close chamber and pump down to 5×10^{-6}.

6.2.2 Evaporate silicon monoxide @ 750Å.

6.2.3 Open chamber.

6.3 Unload cells

6.3.1 Remove planetary system from deposition system.

6.3.2 Unload cells from planetary fixture.

6.4 Transfer wafer to next station.

7. BY-PRODUCTS

7.1 Unusable silicon monoxide powder

8. PRODUCT REQUIREMENTS AND Q.A.

8.1 Q.A. Process Control Test

8.1.1 Visual inspection for uniformity of thickness and color.

8.1.2 Measure index of refraction 1 cell/hour.

8.1.3 Test 1 cell/hour.

Prepared by:

Nick Mardesich, Sr. Engineer

Approved by:

William E. Taylor
Program Manager

SPECTROLAB, INC.

PROCESS SPECIFICATION

CELL TEST

#6314-0017

CODE WORD: CELL TEST

1. SCOPE

This specification describes the process required for testing of the cells prior to starting the interconnecting process.

2. INPUT MATERIAL

Finished Cell (Spec. #6314-1008 FCELL)

3. INPUT SUPPLIES

3.1 Cooling Water

4. EQUIPMENT AND FACILITY

4.1 Transport: The equipment shall be able to move cells to the transfer position and after testing to the end of this station.

4.2 Transfer: This equipment shall be able to transfer cells to the test position.

4.3 Simulator: This simulator shall test cells up to a size of 4" square under AM1 conditions. There shall be provisions to test cells at a given preselected temperature.

4.4 Sorter: This equipment shall sort cells after testing according to voltage at a given current output level. The cells shall be loaded into designated cassettes for transfer to the next process station.

4.5 Manufacturing floor space for the above equipment:

Light House	5' x 4'	20 sq. ft.
Transport, Buffer Storage	10' x 7'	70 sq. ft.
Sorter, Storage	10' x 7'	70 sq. ft.
Total		160 sq. ft.

4.6 Utilities for the above equipment.

5. THROUGHPUT AND LABOR CONTENT

Assuming round the clock (3 shifts per day) operating .97 operating minutes per minute.

5.1 Output Rate: 25 cells per operating minute.

5.2 Labor Content:

5.2.1 Electronics component tester
CAT #B3768D: 1.0 person/shift

5.2.2 Electronic maintenance
CAT #B3688D: .20 person/shift

5.2.3 Maintenance mechanic II
CAT #B3736D: .10 person/shift

6. PROCESS SEQUENCE AND PARAMETERS

6.1 Load cells onto belt.

6.2 Transfer cells from belt to test station (vacuum fixture) for transfer plus vacuum hold down while testing.

6.3 Test cells at AM1, 28^{o}C, fixed current.

6.4 Sort cells according to voltage and load into pre-designated cassettes.

7. BY-PRODUCTS

Used cooling water.

8. PRODUCT REQUIREMENTS AND Q.A.

8.1 In Line: None

8.2 Q.A. Process Control Tests: Set illumination level to AM1 against JPL standard cells at the beginning and at the midpoint of each shift. Check water temperature once per day.

9. NOTES

Prepared by:

Nick Mardesich, Sr. Engineer

Approved by:

William E. Taylor
Program Manager

SPECTROLAB, INC.

PROCESS SPECIFICATION

LEAD CELL

#6314-0010 Rev. B
February 25, 1980

CODE WORD: LEAD

1. SCOPE

This specification describes the process requirement for attachment of interconnect leads to individual solar cells as necessary prior to module assembly.

2. INPUT MATERIALS

2.1 Tested Solar Cells (Spec. #6314-1017 TCELL)

2.2 Interconnect Ribbon (OFHC annealed copper, 0.5 mils solder plate, fused, 2 mil thick, total ribbon width in inches = $0.025\ A_c$ where A_c = cell area in $inch^2$).

3. INPUT SUPPLIES

3.1 Cleaning Solvent (Freon (R) TMC or equivalent).

3.2 Solder Flux (Alpha 611 or equivalent).

4. EQUIPMENT AND FACILITIES

4.1 Lead Soldering System: The equipment shall have the capability to place and solder I/C material on front side metallized solder pads of silicon solar cells. The cut length of the I/C shall be steplessly adjustable over the range of 1/2" to 3". Solder melting tool temperature shall be controlled $\pm$ 10°C over a range of 1 second to 4 seconds. Means shall be provided for hold down of I/C during solidification. Equipment shall have the capability of applying a 500 gram proof test load to each soldered I/C in the plane of the cell and the direction of the I/C. Equipment shall automatically reject leaded cells failing proof test.

4.2 Flux removal equipment; to dissolve and remove flux and residues from cell and panel assembly. Chamber shall be closed with distillation and vapor condensation provisions.

4.3 Handling system to feed cells to soldering machinery.

4.4 Handling system to move leaded cells into and out of flux removal equipment.

4.5 Type A manufacturing space for above equipment.

4.6 Utilities for above equipment.

4.7 Heating, air conditioning and equipment to comply with safety standards for above manufacturing space.

4.8 Waste disposal for solids (solder scrap, I/C scrap) and liquids (loaded solvent).

5. THROUGHPUT AND LABOR CONTENT

Assuming round-the-clock (3 shifts per day) operating and .90 operating minutes per minute.

5.1 Minimum output rate 720 cells with interconnect leads attached (10cm x 10cm) per operating hour.

5.2 Labor content:

5.2.1 Machine Operator: .50 persons/shift/machine (Cat. #B3752D)

6. PROCESS SEQUENCE AND PARAMETERS

6.1 Transfer cells from previous process step (see 2.1).

6.2 I/C Soldering.

6.2.1 Feed I/C material (see 2.3) from supply reel.

6.2.2 Position I/C over cell soldering pad and apply solder melting tool.

6.2.3 Apply hold-down apparatus to keep I/C flat while solder joint solidifies.

6.2.4 Cut I/C to length.

6.3 Transfer cells to flux removal equipment.

6.4 Immerse or spray clean cells and allow to dry.

6.5 Proof test and retest if failure.

6.6 Transfer cells to next position.

7. BY-PRODUCTS

7.1 Flux smoke and fumes at soldering machine(s).

7.2 Cleaning solvent vapors from flux removal equipment and from cleaning solder machines. Total estimated amount of fumes: 5 cu.ft./operating minute.

7.3 Liquids (loaded solvents).

8. PRODUCT REQUIREMENTS AND Q.A.

8.1 In Line

8.1.1 Visual inspection, random for proper operation of soldering equipment by comparison of results to Reflow Solder Criteria (2% frequency).

8.1.2 Tensile testing soldered I/C with 500 gram proof-test load (see 4.1) (100% frequence).

8.2 Q.A. Process Control Tests: One test cell run once per shift (1/2880 frequency) and subjected to following tests: Visual examination; Tensile shear test.

9. NOTES

9.1 Liquid flux (see 3.2) may be used in place of or in addition to flux-cored solder.

9.2 Water-base flux may be used as an alternative to solvent base, in which event the flux removal equipment (4.2) may be an open, water washing station.

9.3 Hot-ram soldering equipment is recommended. Heat is supplied to the solder area by a non-wetting block containing a heater cartridge and a thermocouple for temperature control.

9.4 Optical recognition equipment might be considered for continuous monitoring of solder joint configuration.

9.5 Cell will have a minimum of two leads on the front. In 2.2 total ribbon width refers to the sum of leads widths.

Prepared by:

Alexander Garcia III

Alexander Garcia III, Engineer

Approved by:

William E. Taylor

William E. Taylor
Program Manager

SPECTROLAB, INC.

PROCESS SPECIFICATION

STRING ASSEMBLY

#6314-0019
February 25, 1980

CODE WORD: A-STRING

1. SCOPE

This specification describes the process requirement for assembly of front leaded cells into strings by ultrasonic soldering.

2. INPUT MATERIAL

2.1 Leaded Cells (Spec. #6314-0010 Rev. B, LEAD)

3. INPUT SUPPLIES

3.1 Tin/Zinc Eutectic Solder

4. EQUIPMENT AND FACILITIES

4.1 The equipment shall have the capability to place leaded cells in the proper orientation and ultrasonically solder the front lead of one cell to the Al back of another. The distance between cells once connected shall be held to 1.3 mm $\pm$ 0.1 mm. Soldering shall be done by an ultrasonical process which first entails the wetting of the Al back with a tin/zinc eutectic solder followed by the soldering of the lead (see Spec. #6314-0010, paragraph 2.2) to this area. The cell to which the soldering is done must be kept at 120°C $\pm$ 10°C for the duration of the operation. The solder melting tool shall be controlled $\pm$ 10°C over a range of 0.5 - 5 seconds. Means shall be provided to hold down the joint during solidification. Equipment shall have the capability of applying a 500 gram proof test load to each soldered joint in the plane of the cell and the direction of the lead. Equipment should automatically reject strings failing proof test. The equipment shall be able to integrate cells with different lead lengths into a specific cell pattern (e.g. every third cell will have a 1/2" cm portion of the lead extending past the solder joint on the back of the cell).

4.2 Handling system to feed leaded cells to soldering machinery and transfer strings to next process.

4.3 Type A manufacturing space for above equipment.

4.4 Utilities for above equipment.

4.5 Heating, air conditioning and equipment to comply with safety standards for above manufacturing space.

4.6 Waste disposal for solids (solder scrap, lead scrap).

5. THROUGHPUT AND LABOR CONTENT

Assuming round-the-clock (3 shifts per day) operating and 0.90 operating minutes per minute.

5.1 Minimum output rate 66-cell strings containing 11 10cm x 10cm cells per operating hour, or 72-cell strings containing 10 10cm diameter round cells.

5.2 Labor content as required to support above equipment.

6. PROCESS SEQUENCE AND PARAMETERS

6.1 Transfer cells from previous process step.

6.2 Solder

6.2.1 Heat cell to be soldered to a temperature of 120°C.

6.2.2 Wet soldering area on cell with tin/zinc eutectic via ultrasonics and heat.

6.2.3 Solder front lead from other cell to this area.

6.2.4 Proof test and reject if failure.

6.2.5 Transfer cell/string for next operation.

6.3 Transfer string to next position.

7. BY-PRODUCTS

7.1 Solids (solder scrap, lead scrap).

8. PRODUCT REQUIREMENTS AND Q.A.

8.1 In Line

8.1.1 Visual inspection (2% frequency).

8.1.2 Tensile testing with 500 grams proof test load (100% frequency).

8.2 Q.A. Process Control Tests as required.

9. NOTES

Approved by:

William E. Taylor
Program Manager

Prepared by:

Alexander Garcia, III, Engineer

SPECTROLAB, INC.

PROCESS SPECIFICATION

CIRCUIT ASSEMBLY #6314-0020
February 25, 1980

CODE WORD: A-CIRCUIT

1. SCOPE

This specification describes the process requirement for assembly of strings into complete circuits using soldering techniques.

2. INPUT MATERIALS

2.1 Cell String (Spec. #6314-1019, STRING)

2.2 Interconnect Ribbon (See Spec. #6314-0010 2.2)

2.3 Bus Bar Ribbon (OFHC annealed copper, 0.5 mils solder plate, fused, 5 mil thick, 0.4-0.8" thick.

3. INPUT SUPPLIES

3.1 Cleaning solvent (Freon(R) TMC or equivalent).

3.2 Solder Flux (Alpha 611 or equivalent).

4. EQUIPMENT AND FACILITIES

4.1 String transfer and placement.

The equipment shall have the capability to transfer cell strings composed of 11 cells, 10cm x 10cm square or 10cm diameter round. The string shall be placed to form a circuit of 11 parallel cells in the square case or 13 parallel 10 cell strings in the round case.

4.2 Electrical interconnection will be made with the bus bar ribbon at the two ends of the circuit. The interconnect ribbon is used at mid circuit points. Mid circuit parallel may be at any point in the circuit. A soldering process will be used.

4.3 N-contact termination. Provisions to bend the N-contact lead to the back of the cell must be made. A dielectric strip must then be placed before the bus bar is bent into a planar configuration.

4.4 Flux removal. The circuit must be cleaned of any excess flux and dried.

4.5 Circuit transfer. The completed circuit must be transferred to the next station.

4.6 Type A manufacturing space for above equipment.

4.7 Utilities for the above equipment.

4.8 Heating, air conditioning and equipment to comply with safety standards for above manufacturing space.

4.9 Waste disposal for the above process.

5. THROUGHPUT AND LABOR CONTENT

Assuming round-the-clock (3 shifts per day) operating and 0.90 operating minutes per minute.

5.1 Minimum output rate 6 complete circuits per operating hour. A circuit will consist of 121 cells in the square case and 130 cells in the round case.

5.2 Labor content. As required for process.

6. PROCESS SEQUENCE AND PARAMETERS

6.1 Transfer string from previous process step.

6.2 Feed interconnecting and bus bar ribbon and adjust leads for soldering.

6.3 Flux and solder.

6.4 Remove excess flux and dry.

6.5 Place dielectric material where needed.

6.6 Bend over interconnect at bus bar region as necessary.

6.7 Transfer complete circuit to next process step.

7. BY-PRODUCTS

7.1 Flux smoke and fumes.

7.2 Waste solvent and vapor.

8. PRODUCT REQUIREMENTS AND Q.A.

8.1 Circuit output at 5.25 volts should be 3.5 $\pm$ amps for square cells. For round cells circuit output at 4.8 volts should be 3.25 $\pm$ amps.

9. NOTES

9.1 See Figures 1 and 2 for module concepts in the square and round cases.

Prepared by:

Alexander Garcia, III, Engineer

Approved by:

William E. Taylor
Program Manager

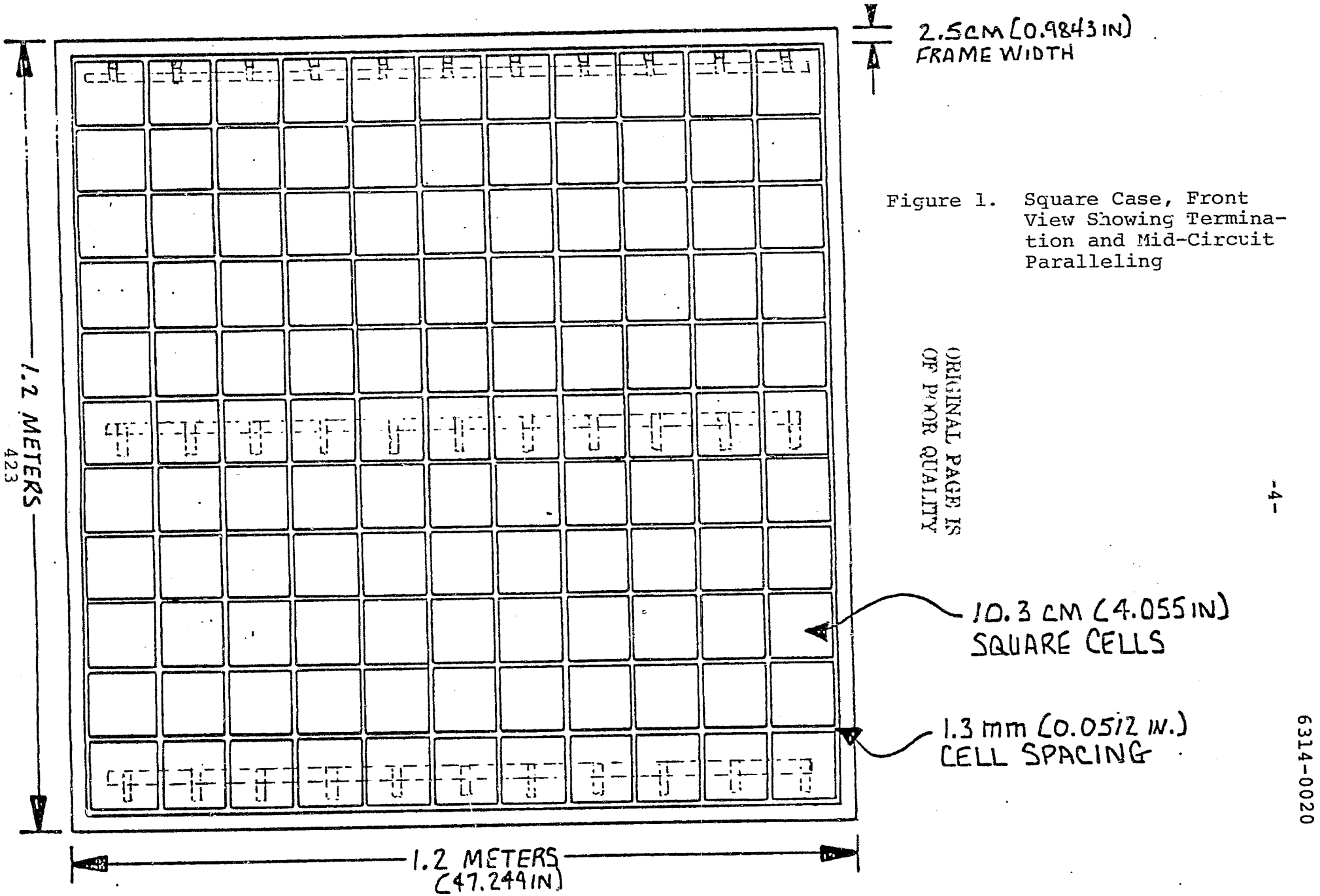

Figure 1. Square Case, Front View Showing Termination and Mid-Circuit Paralleling

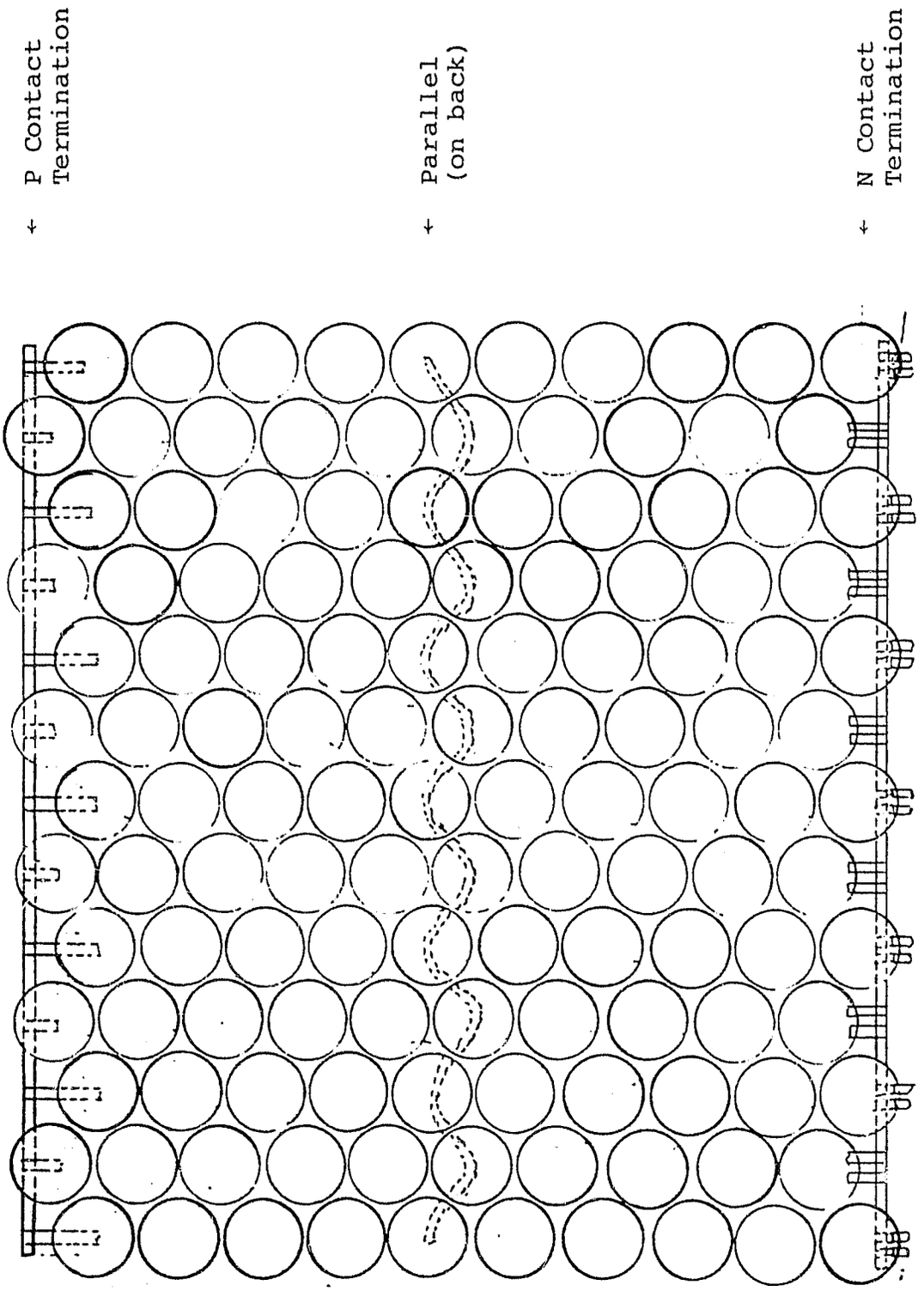

Figure 2. Round Case, Front View Showing Termination and Mid-Circuit Paralleling

SPECTROLAB, INC.

PROCESS SPECIFICATION

LAMINATE CIRCUIT

#6314-0021
February 25, 1980

CODE WORD: LAMINATE

1. SCOPE

This specification describes the process requirement for the lamination of circuits into encapsulated modules.

2. INPUT MATERIALS

2.1 Circuits (Spec. #6314-0020, CIRCUIT)

2.2 Ethylene Vinyl Acetate (EVA) sheet material, clear and white, 1.2m wide.

2.3 Crane-Glas 250, 5 mil thick, 1.2m wide.

2.4 0.5 mil Al foil/0.5 mil white pigmented polyester laminated film 1.2m wide.

2.5 Tempered glass, 3/16" thick, 1.2m x 1.2m square.

3. INPUT SUPPLIES

3.1 Silane primer GE SS 4179

3.2 Solvent for above primer.

4. EQUIPMENT AND FACILITIES

4.1 Glass clean and prime: The equipment shall have the capability to clean and dry a 1m x 1m piece of 3/16" tempered glass and then apply a thin layer of silane primer in an organic vehicle.

4.2 Cutting equipment. The equipment shall be able to cut 1.2m x 1.2m piece of EVA from a roll of material and then cut small openings as required for electrical connection areas of the circuit. The equipment shall be able to handle white EVA, clear EVA, Crane-Glas, and metal foil.

4.3 Transfer equipment. The equipment shall handle the transfer of cut materials as well as the circuit to an assembly process.

4.4 Assembly equipment. The equipment shall be able to assemble the cut pieces into a layup assembly. A typical layup pattern would be glass, Crane-Glas, EVA clear, circuit, Crane-Glas, EVA white, Crane-Glas, and Al foil laminate.

4.5 Transfer equipment. To transfer the assembled layup to the laminator.

4.6 Laminator. The equipment shall be capable of heating the assembly within a double vacuum chamber which consists of two vacuum chambers with a vlexible diaphram between. Both chambers should have individual vacuum controls. The assembly layup would be placed in the lower chamber and heated to 150°C within 30 minutes while under vacuum.

4.7 Final transfer. The equipment shall take the module and transfer it to the next process step.

5. THROUGHPUT AND LABOR CONTENT

Assuming round-the-clock (3 shifts per day) operating and 0.90 operating minutes per minute.

5.1 Minimum output rate. 12 modules per operating hour.

5.2 Labor content. As required.

6. PROCESS SEQUENCE AND PARAMETERS

6.1 Transfer Circuit

6.2 Clean and prime glass.

6.3 Cut materials.

6.4 Assemble layup.

6.5 Transfer layup.

6.6 Laminate layup; heat to 105°C, remove top vacuum, heat to 150°C, cool.

6.7 Transfer module.

7. BY-PRODUCTS

7.1 Vacuum pump oil.

7.2 Solid scrap EVA, Crane-Glas.

7.3 Solvent fumes from priming operation.

7.4 Water and MEK from cleaning operation.

8. PRODUCT REQUIREMENT AND Q.A.

As required

9. NOTES

Prepared by:

Alexander Garcia, III, Engineer

Approved by:

William E. Taylor
Program Manager

SPECTROLAB, INC.

PROCESS SPECIFICATION

FRAME MODULE

#6314-0022
February 25, 1980

CODE WORD: FRAME

1. SCOPE

This specification describes the process requirement for the framing and termination connection of the module.

2. INPUT MATERIALS

2.1 Module (Spec. #6314-0021, SUPERST)

2.2 Al extension for frame.

2.3 J-Box with connectors.

2.4 Misc. hardware.

2.5 Waterproof sealant.

2.6 Rubber gasket.

3. INPUT SUPPLIES

3.1 Solder

3.2 Solder flux

3.3 Cleaning solvent

4. EQUIPMENT AND FACILITIES

4.1 Frame Cutter. This equipment shall take Al extrusions and cut them to the desired length for framing and transfer them to correct position in processing line.

4.2 J-Box to Frame. This equipment will connect the J-Box to the correct place in the frame and perform necessary transfers.

4.3 Framing. This equipment shall load module and place any gaskets necessary on the edges. The frame parts will then be attached to the module and fastened.

4.4 Termination electrical interconnection. This equipment will solder the J-Box leads to the module and clean any excess flux.

4.5 J-Box sealing. This equipment will seal the J-Box top and bottom for a water-tight seal.

4.6 Final transfer. This equipment will move completed module to next processing step.

5. THROUGHPUT AND LABOR CONTENT

Assuming round-the-clock (3 shifts per day) operating and 0.90 operating minutes per minute.

5.1 Minimum output rate 12 complete framing operations per operating hour. Framed module will be approximately 1.2m x 1.2m size.

6. PROCESS SEQUENCE AND PARAMETERS

6.1 Cut extrusion to proper size

6.2 Attach J-Box.

6.3 Transfer module to frame.

6.4 Apply gasket to module.

6.5 Apply frame to module aid fasten.

6.6 Solder termination to J-Box and clean.

6.7 Seal J-Box.

6.8 Transfer module.

7. BY-PRODUCT

7.1 Al from cutting operation.

7.2 Solid scraps Al, gasket

7.3 Loaded solvent from flux cleaning.

8. PRODUCT REQUIREMENTS AND Q.A.

As required

9. NOTES

Prepared by:

Alexander Garcia, III, Engineer

Approved by:

William E. Taylor
Program Manager

SPECTROLAB, INC.

PROCESS SPECIFICATION

FINAL TEST

#6314-0023
February 25, 1980

CODE WORD: F-TEST

1. SCOPE

This specification describes the process required for the final testing of the modules for power output.

2. INPUT MATERIAL

2.1 Framed module (Spec. #6314-0022 PANEL 1)

3. INPUT SUPPLIES

None required.

4. EQUIPMENT AND FACILITIES

4.1 Transfer. The equipment shall be able to transfer modules to test position and then after test transfer modules to end of line.

4.2 Solar Simulator. The equipment shall be able to test the 1.2m x 1.2m module at AM1.

4.3 Type A manufacturing space for above equipment.

4.4 Utilities for above equipment.

4.5 Heating, air conditioning and equipment to comply with safety standards for above manufacturing space.

5. THROUGHPUT AND LABOR CONTENT

Assuming round-the-clock (3 shifts per day) operation and 0.90 operating minutes per minute.

5.1 Minimum output is 40 modules per operating hour.

5.2 Labor content as required for process.

6. PROCESS SEQUENCE AND PARAMETERS

6.1 Transfer module to test position.

6.2 Test.

6.3 Final transfer to end of line.

7. BY-PRODUCTS

None

8. PRODUCT REQUIREMENT AND Q.A.

As required.

9. NOTES

Prepared by:

Alexander Garcia, III, Engineer

Approved by:

William E. Taylor
Program Manager

SPECTROLAB, INC.

MATERIALS SPECIFICATION

ALUMINUM PRINTING PASTE

6314-2001 Rev.A
June 22, 1979

1. SCOPE

This specification describes the composition and materials used to prepare aluminum printing paste.

2. INPUT MATERIALS

2.1 Aluminum powder (Cat. #)

2.2 Alpha Terpinol (Cat. #)

2.3 Butyl Carbitol Acetate (Cat. #E11280)

2.4 Ethyl Cellulose (Cat. #)

2.5 Thixatrol St (Cat. #)

3. COMPOSITION

3.1 Vehicle

3.1.1 44.3% Alpha Terpinol

3.1.2 44.3% Butyl Carbitol Acetate

3.1.3 9.9% Ethyl Cellulose

3.1.4 1.5% Thixatrol ST

3.2 Aluminum Paste

3.2.1 68% Aluminum Powder

3.2.2 29% Vehicle

3.2.3 3% Butyl Carbitol Acetate

4. NOTES

In preparing aluminum paste the viscosity can be altered by increasing or reducing the amount of Butyl Carbitol Acetate in the final paste composition to achieve 60-80 kcps.

5. MATERIAL SUPPLIERS

Cat. # - Aluminum
Atomized aluminum powder (AMPAL 631)
Supplied by: Atomized Metal Powders, Inc.
P.O. Box 31
Flemington, NJ 08822

Cat. # - Alpha Terpinol
Supplied by: Matheson Coleman & Bell
Manufacturing Chemists
Norwood, Ohio 45212

Cat. #E11280 - Butyl Carbitol Acetate
Supplied by: Matheson Coleman & Bell
Manufacturing Chemists
Norwood, Ohio 45212

Cat. # - Ethyl Cellulose
Ethyl Cellulose (N-14)
Supplied by: Hercules Inc.
Wilmington, Delaware

Cat. # - Thixatrol ST
Supplied by: NL Industries
Industrial Chemical Division
Hightstown, NJ 08520

Prepared by:

Nick Mardesich

Nick Mardesich, Engineer

Approved:

William E. Taylor
Program Manager

Spectrolab, Inc.

PROCESS SPECIFICATION

SILVER PRINTING PASTE # 6314-2002
June 22, 1979

1. SCOPE

This specification describes the composition and materials used to prepare modified silver printing paste.

2. INPUT MATERIALS

2.1 Commercial silver paste

2.2 Emitter diffusion source

3. COMPOSITION

3.1 Silver paste

3.1.1 98% commercial silver paste

3.1.2 2% emitter diffusion source

4. MATERIAL SUPPLIERS

P.2.1 - Commercial silver paste
Conductrox 3347 Ag
Supplied by: Thick Film Systems, Inc.
324 Palm Avenue
Santa Barbara, Ca. 93101

P.2.2 - Emitter diffusion source
N-Diffusol
Supplied by: Transene Co.
Rowley, Mass.

Prepared by:

Nick Mardesich
Nick Mardesich, Engineer

Approved:

William E. Taylor
William E. Taylor
Program Manager

Appendix G

FORMAT A's FOR SAMICS CALCULATIONS

FORMAT A

JET PROPULSION LABORATORY
California Institute of Technology
4800 Oak Grove Dr. / Pasadena, Calif. 91103

PROCESS DESCRIPTION

Note: Names given in brackets [ ] are the names of process attributes requested by the SAMICS III computer program.

A1 [Process Referent] SURFPREP

A2 [Descriptive Name] Polish Etch Wafer

PART 1 -- PRODUCT DESCRIPTION

A3 [Product Referent] PWAFER

A4 Descriptive Name [Product Name] Etched Wafer

A5 Unit Of Measure [Product Units] Wafer

PART 2 -- PROCESS CHARACTERISTICS

A6	[Output Rate] (Not Thruput)	25	Units (given on line A5) Per Operating Minute
A7	Average Time at Station [Processing Time]	45	Calendar Minutes (Used only to compute in-process inventory)
A8	Machine "Up" Time Fraction [Usage Fraction]	90	Operating Minutes Per Minute

PART 3 -- EQUIPMENT COST FACTORS [Machine Description]

A9	Component [Referent]	Loader	Test W	Etch Stat
A9a	Component [Descriptive Name] (Optional)	Wafer Transp	Thickness Dimens Resist	HCL And NAOH Cleaning Tanks
A10	Base Year For Equipment Prices [Price Year]	1980	1980	1980
A11	Purchase Price ($ Per Component) [Purchase Cost]	6000	20000	225,000
A12	Anticipated Useful Life (Years) [Useful Life]	7	7	7
A13	[Salvage Value] ($ Per Component)	300	200	200
A14	[Removal and Installation Cost] ($/Component)	500	500	500

Note: The SAMICS III computer program also prompts for the [payment float interval], the [inflation rate table], the [equipment tax depreciation method], and the [equipment book depreciation method]. In the LSA SAMICS context, use 0.0, (1975, 4.0), DDB, and SL.

Format A: Process Description (Continued)

A15 Process Referent (From Page 1 Line A1) Surfprep

PART 4 – DIRECT REQUIREMENTS PER MACHINE (Facilities) OR PER MACHINE PER SHIFT (Personnel)
[Facilities and Personnel Requirements]

A16 Catalog Number [Expense Item Referent]	A18 Amount Required Per Machine (Per Shift) [Amount per Machine]	A19 Units	A17 Requirement Description
B3096D	0.5	Person/Shift	Semicond. Assembler
B3704D	.10	Person/Shift	Electr. Technican
B3736D	.20	Person/Shift	Maint. Mech.
B3720D	.25	Person/Shift	Systems Insp, Q.C.
A2064D	180	Sq. Ft.	Mgt. Space A

PART 5 – DIRECT REQUIREMENTS PER MACHINE PER MINUTE
[Byproduct Outputs] and [Utilities and Commodities Requirements]

A20 Catalog Number [Expense Item Referent]	A22 Amount Required Per Machine Per Minute [Amount per Cycle]	A23 Units	A21 Requirement Description
E1600D	.1674	lbs/min	Sodium Hydroxide
C1144D	.2672	Cu Ft/min	Deionized Water
C1016D	.2672	Cu ft/min	Domestic Water
E1320D	.357	lbs/min	20% Hydrochloric Acid
E1416D	.0354	Cu ft/min	N2 GAS
C1032B	.049	KWHR/min	Electricity
EG0007D	7.76E-6	Each	Teflon Carrier
EW1345	25	Wafers/min	Water HEW 9 mil.
D1032D	.047	Gal/min	Acid Waste
D0001	.002	Gal/min	Alkaline waste
D1048B	1.999	Gal/min	Poluted water

PART 6 – INTRA-INDUSTRY PRODUCT(S) REQUIRED [Required Products]

A24 [Product Reference]	A26 Usable Output Per Unit of Input Product	A27 Units	A25 Product Name
BWAFER	1.0	wafer/wafer	Blank wafer

Prepared by E. Aerni Date 03/03/80

Data Backup on Format A Surfprep original issue.

SOLAR ARRAY MANUFACTURING INDUSTRY COSTING STANDARDS

FORMAT A - PROCESS DESCRIPTION

JET PROPULSION LABORATORY
California Institute of Technology
4800 Oak Grove Dr. / Pasadena, Calif. 91103

A-1 Process [Referent]: DIFFUSEA

Note: Names given in brackets [ ] are the names of process attributes requested by the SAMIS computer program.

A-2 [Descriptive Name] of Process: Spin-on Diff. Source on Wafer

PART 1 - PRODUCT DESCRIPTION

A-3 [Product Referent]	DWAFERA	
A-4 Descriptive Name [Product Name]	Wafer with Diff. Source	
A-5 Unit Of Measure [Product Units]	Wafer	

PART 2 - PROCESS CHARACTERISTICS

A-6 [Output Rate] (Not Thruput)	3	Units (given on line A-5) Per Operating Minute
A-7 [Inprocess Inventory Time]	0.5 min.	Calendar Minutes (Used only to compute in process inventory)
A-8 [Duty Cycle]	.95	Operating Minutes Per Minute
A-8a [Number Of Shifts Per Day]	3	Shifts
A-8b [Personnel Integerization Override Switch]	On	(Off or On)

PART 3 - EQUIPMENT COST FACTORS (Machine Description)

A-9 Component [Referent]	Spin
A-9a Component [Descriptive Name]	Source
A-10 Base Year For Equipment Prices [Price Year]	1980
A-11 [Purchase Cost Vs Quantity Bought Table] (Number Of and $ Per Component)	22,750
A-12 Anticipated [Useful Life] (Years)	7
A-13 [Salvage Value] ($ Per Component)	1,000
A-14 [Removal And Installation Cost] ($/Component)	1,000

Note: The SAMIS computer program also prompts for the [Payment Float Interval], the [Inflation Rate Table], the [Equipment Tax Depreciation Method], and the [Equipment Book Depreciation Method]. In the LSA SAMICS context, use 0.0, (1975 6.0 *), DDB, and SL. (The asterisk is a signal to the computer, not a reference to a footnote.)

A-15 Process Referent (From Front Side Line A-1) DIFFUSEA

PART 4 – DIRECT REQUIREMENTS PER MACHINE (Facilities) OR PER MACHINE PER SHIFT (Personnel)
[Facility. Or. Personnel Requirement]

A-16 Catalog Number (Expense Item Referent)	A-18 Amount Required Per Machine (Per Shift) [Amount. Per. Machine]	A-19 Units	A-17 Requirement Description or Name
A20641D	20	sq. ft.	Manufacturing Space A
B3096D	0.2	person/shift	Semiconductor Assem.
B3704D	.02	"	Electr. Tech.
B3736D	.05	"	Maint. Mech.

PART 5 – DIRECT REQUIREMENTS PER MACHINE PER MINUTE (SAMIS will ask first for Byproducts)
[Byproduct] and [Utility. Or. Commodity Requirement]

A-20 Catalog Number (Expense Item Referent)	A-22 Amount Required Per Machine Per Minute [Amount Per Cycle]	A-23 Units	A-21 Requirement Description or Name
C1032B	.01	kWhr/min.	Electricity
EG1210D	.012	10⁷/min	Diffusion Source
02031D	.001	cu.ft./min.	Compressed air

PART 6 – INTRA-INDUSTRY PRODUCT(S) REQUIRED

A-24 [Required. Product] (Reference)	A-28 [Yield] * (%)	A-26 [Ideal. Ratio] ** Of Units Out/Units In	A-27 Units Of A-26***	A-25 Product Name
PWAFER	99.9	1.0	wafer/wafer	Etched wafer

PREPARED BY N. Mardesich DATE 7/28/80

*100% minus percentage of required product lost in this process.
**Assume 100% yield here.
***Examples: Modules/Cell or Cells/Wafer.

SOLAR ARRAY MANUFACTURING INDUSTRY COSTING STANDARDS

FORMAT A - PROCESS DESCRIPTION

JET PROPULSION LABORATORY
California Institute of Technology
4800 Oak Grove Dr. / Pasadena, Calif. 91103

A-1 Process [Referent]: DIFFUSEB

Note. Names given in brackets [ ] are the names of process attributes requested by the SAMIS computer program.

A-2 [Descriptive. Name] of Process: Dry (Junction Formation)

PART 1 -- PRODUCT DESCRIPTION

A-3	[Product. Referent]	DWAFERB
A-4	Descriptive Name [Product. Name]	Dry Diffusion Source
A-5	Unit Of Measure [Product. Units]	Wafer

PART 2 - PROCESS CHARACTERISTICS

A-6	[Output. Rate] (Not Thruput)	24	Units (given on line A-5) Per Operating Minute
A-7	[Inprocess. Inventory. Time]	3	Calendar Minutes (Used only to compute in-process inventory)
A-8	[Duty. Cycle]	.95	Operating Minutes Per Minute
A-8a	[Number Of Shifts. Per. Day]	3	Shifts
A-8b	[Personnel. Integerization. Override. Switch]	On	(Off or On)

PART 3 -- EQUIPMENT COST FACTORS (Machine Description)

A-9	Component [Referent]	Dry		
A-9a	Component [Descriptive. Name]	Drying Oven		
A-10	Base Year For Equipment Prices [Price. Year]	1980		
A-11	[Purchase. Cost. Vs. Quantity. Bought. Table] (Number Of and $ Per Component)	5,000		
A-12	Anticipated [Useful. Life] (Years)	7		
A-13	[Salvage. Value] ($ Per Component)	200		
A-14	[Removal. And. Installation. Cost] ($/Component)	1,000		

Note: The SAMIS computer program also prompts for the [Payment. Float. Interval], the [Inflation. Rate. Table], the [Equipment. Tax. Depreciation. Method], and the [Equipment. Book. Depreciation. Method]. In the LSA SAMICS context, use 0.0, (1975 6.0 *), DDB, and SL. (The asterisk is a signal to the computer, not a reference to a footnote.)

A-15 Process Referent (From Front Side Line A-1) DIFFUSEB

PART 4 -- DIRECT REQUIREMENTS PER MACHINE (Facilities) OR PER MACHINE PER SHIFT (Personnel)
(Facility, Or, Personnel Requirement)

A-16 Catalog Number (Expense Item Referent)	A-18 Amount Required Per Machine (Per Shift) (Amount, Per, Machine)	A-19 Units	A-17 Requirement Description or Name
A2064D	100	sq. ft.	Manufacturing Space A
B3096D	.20	person/shift	Semiconductor Assem.
B3704D	.05	"	Electr. Tech.
B3736D	.05	"	Maint. Mech.

PART 5 -- DIRECT REQUIREMENTS PER MACHINE PER MINUTE (SAMIS will ask first for Byproducts)
(Byproduct) and (Utility, Or, Commodity Requirement)

A-20 Catalog Number (Expense Item Referent)	A-22 Amount Required Per Machine Per Minute (Amount, Per, Cycle)	A-23 Units	A-21 Requirement Description or Name
C1032B	.03	kWhr/min.	Electricity

PART 6 -- INTRA-INDUSTRY PRODUCT(S) REQUIRED

A-24 (Required, Product) (Reference)	A-28 (Yield)* (%)	A-26 (Ideal, Ratio)** Of Units Out/Units In	A-27 Units Of A-26***	A-25 Product Name
DWAFERA	99.9	1.0	wafer/wafer	Diff. Source Wafer

PREPARED BY Nick Mardesich DATE 7/28/80

*100% minus percentage of required product lost in this process.
**Assume 100% yield here.
***Examples: Modules/Cell or Cells/Wafer.

REVERSE SIDE JPL 3037-S R 5/80

SOLAR ARRAY MANUFACTURING INDUSTRY COSTING STANDARDS

FORMAT A — PROCESS DESCRIPTION

JET PROPULSION LABORATORY
California Institute of Technology
4800 Oak Grove Dr. / Pasadena, Calif. 91103

A-1 Process [Referent]: DIFFUSEC

Note: Names given in brackets [ ] are the names of process attributes requested by the SAMIS computer program.

A-2 [Descriptive. Name] of Process: Diffusion (Junction Formation)

PART 1 – PRODUCT DESCRIPTION

A-3	[Product Referent]	DWAFER
A-4	Descriptive Name [Product. Name]	Diffused Wafer
A-5	Unit Of Measure [Product. Units]	Wafer

PART 2 – PROCESS CHARACTERISTICS

A-6	[Output. Rate] (Not Thruput)	12.5	Units (given on line A 5) Per Operating Minute
A-7	[Inprocess. Inventory. Time]	20	Calendar Minutes (Used only to compute in-process inventory)
A-8	[Duty. Cycle]	.95	Operating Minutes Per Minute
A-8a	[Number. Of. Shifts. Per. Day]	3	Shifts
A-8b	[Personnel. Integerization. Override. Switch]	On	(Off or On)

PART 3 – EQUIPMENT COST FACTORS (Machine Description)

A-9	Component [Referent]	Diffurn		
A-9a	Component [Descriptive. Name]	Belt Furnace		
A-10	Base Year For Equipment Prices [Price. Year]	1980		
A-11	[Purchase. Cost. Vs. Quantity Bought. Table] (Number Of and $ Per Component)	58,000		
A-12	Anticipated [Useful. Life] (Years)	7		
A-13	[Salvage. Value] ($ Per Component)	1,000		
A-14	[Removal. And. Installation. Cost] ($/Component)	2,000		

Note: The SAMIS computer program also prompts for the [Payment. Float. Interval], the [Inflation. Rate. Table], the [Equipment. Tax. Depreciation. Method], and the [Equipment. Book. Depreciation. Method]. In the LSA SAMICS context, use 0.0, (1975 6.0 *), DDB, and SL. (The asterisk is a signal to the computer, not a reference to a footnote.)

A-15 Process Referent (From Front Side Line A-1) DIFFUSEC

PART 4 – DIRECT REQUIREMENTS PER MACHINE (Facilities) OR PER MACHINE PER SHIFT (Personnel)
[Facility, Or, Personnel Requirement]

A-16 Catalog Number (Expense Item Referent)	A-18 Amount Required Per Machine (Per Shift) [Amount, Per, Machine]	A-19 Units	A-17 Requirement Description or Name
B3096D	.20	Person/shift	Semicond. Assembler
B3704D	.05	"	Elect. Tech.
B3736D	.05	"	Maint. Mech.

PART 5 – DIRECT REQUIREMENTS PER MACHINE PER MINUTE (SAMIS will ask first for Byproducts)
[Byproduct] and [Utility, Or, Commodity Requirement]

A-20 Catalog Number (Expense Item Referent)	A-22 Amount Required Per Machine Per Minute [Amount, Per, Cycle]	A-23 Units	A 21 Requirement Description or Name
E1416D	3.40	Cu. ft/min.	Nitrogen Gas
E1448D	.34	"	Oxygen Gas
C1128D	11.00	Gal/min.	Cooling Water
C1032D	.30	kWhr/min.	Electricity
D1160D	11.00	Gal/min.	Used cooling water

PART 6 – INTRA-INDUSTRY PRODUCT(S) REQUIRED

A-24 [Required, Product] (Reference)	A-28 [Yield]* (%)	A-26 [Ideal, Ratio]** Of Units Out/Units In	A-27 Units Of A-26***	A-25 Product Name
DWAFERB	99.9	1.0	wafer/wafer	Dryed Wafer

PREPARED BY: Nick Mardesich DATE: 7/28/80

*100% minus percentage of required product lost in this process.
**Assume 100% yield here.
***Examples: Modules/Cell or Cells/Wafer.

REVERSE SIDE JPL 3037-S R 5/80

SOLAR ARRAY MANUFACTURING INDUSTRY COSTING STANDARDS

FORMAT A

JET PROPULSION LABORATORY
California Institute of Technology
4800 Oak Grove Dr. / Pasadena, Calif. 91103

PROCESS DESCRIPTION

Note: Names given in brackets [ ] are the names of process attributes requested by the SAMICS III computer program.

A1 [Process Referent] BACKCONTA

A2 [Descriptive Name] Print and Fire Back Surface Field Source and Contact

PART 1 – PRODUCT DESCRIPTION

A3 [Product Referent] BWAFER

A4 Descriptive Name [Product Name] Back Printed Wafer

A5 Unit Of Measure [Product Units] Wafer

PART 2 – PROCESS CHARACTERISTICS

A6	[Output Rate] (Not Thruput)	25	Units (given on line A5) Per Operating Minute
A7	Average Time at Station [Processing Time]	20	Calendar Minutes (Used only to compute in-process inventory)
A8	Machine "Up" Time Fraction [Usage Fraction]	.90	Operating Minutes Per Minute

PART 3 – EQUIPMENT COST FACTORS [Machine Description]

A9	Component [Referent]	Screen Prt	Furnace	Load
A9a	Component [Descriptive Name] (Optional)	Print Back Metall	IR Belt Furnace	Cassette Loader
A10	Base Year For Equipment Prices [Price Year]	1980	1980	1980
A11	Purchase Price ($ Per Component) [Purchase Cost]	128,000	40,000	6,000
A12	Anticipated Useful Life (Years) [Useful Life]	7	7	7
A13	[Salvage Value] ($ Per Component)	1000	2000	1000
A14	[Removal and Installation Cost] ($/Component)	2000	2000	1700

Note: The SAMICS III computer program also prompts for the [payment float interval], the [inflation rate table], the [equipment tax depreciation method], and the [equipment book depreciation method]. In the LSA SAMICS context, use 0.0, (1975, 4.0), DDB, and SL.

Format A: Process Description (Continued)

A15 Process Referent (From Page 1 Line A1) Back Cont.

PART 4 – DIRECT REQUIREMENTS PER MACHINE (Facilities) OR PER MACHINE PER SHIFT (Personnel)
[Facilities and Personnel Requirements]

A16 Catalog Number [Expense Item Referent]	A18 Amount Required Per Machine (Per Shift) [Amount per Machine]	A19 Units	A17 Requirement Description
A2064D	200	Sq. Ft.	Mgt. Space Type A
B3096D	.20	Person/Shift	Semiconductor Assem.
B3704D	.10	Person/Shift	Electronic Tech.
B3736D	.10	Person/Shift	Maint. Mech.

PART 5 – DIRECT REQUIREMENTS PER MACHINE PER MINUTE
[Byproduct Outputs] and [Utilities and Commodities Requirements]

A20 Catalog Number [Expense Item Referent]	A22 Amount Required Per Machine Per Minute [Amount per Cycle]	A23 Units	A21 Requirement Description
C1032B	.2 0	KWHR/Min	Electricity
E1128D	.00048	lbs/min	Butyl Acetate
E1576D	.00005	Screens/min	Screens.
E1624D	.00005	Squeegee/min	Squeegee
EP270	.0848 (28.5g)	lbs/min	Al paste
DI016B	5.54	Cu ft/min	Fumes

PART 6 – INTRA-INDUSTRY PRODUCT(S) REQUIRED [Required Products]

A24 [Product Reference]	A26 Usable Output Per Unit of Input Product	A27 Units	A25 Product Name
DWAFER	1.0	Wafer/Wafer	Diffused Wafer
		/	
		/	

Prepared by E. Aerni Date 03/25/80

REVERSE SIDE JPL 3037-S R 7/78

SOLAR ARRAY MANUFACTURING INDUSTRY COSTING STANDARDS

FORMAT A

JET PROPULSION LABORATORY
California Institute of Technology
4800 Oak Grove Dr. / Pasadena, Calif. 91103

PROCESS DESCRIPTION

Note: Names given in brackets [ ] are the names of process attributes requested by the SAMICS III computer program.

A1 Process [Referent] CLNBACK

A2 [Descriptive Name] Clean Excess Al Back And Remove Front

PART 1 – PRODUCT DESCRIPTION

A3 [Product Referent] CBWAFER

A4 Descriptive Name [Product Name] Cleaned Wafer

A5 Unit Of Measure [Product Units] Wafer

PART 2 – PROCESS CHARACTERISTICS

A6 [Output Rate] (Not Thruput) 13.3 Units (given on line A5) Per Operating Minute

A7 Average Time at Station [Processing Time] 30 Calendar Minutes (Used only to compute in-process inventory)

A8 Machine "Up" Time Fraction [Usage Fraction] .90 Operating Minutes Per Minute

PART 3 – EQUIPMENT COST FACTORS [Machine Description]

A9	Component [Referent]	Tanks	Brush	Unloader
A9a	Component [Descriptive Name] (Optional)	Clean. Tanks	Vacuum Brush	Cass. Load Unload
A10	Base Year For Equipment Prices [Price Year]	1980	1980	1980
A11	Purchase Price ($ Per Component) [Purchase Cost]	155,000	150,000	5,000
A12	Anticipated Useful Life (Years) [Useful Life]	7	7	7
A13	[Salvage Value] ($ Per Component)	0	1000	0
A14	[Removal and Installation Cost] ($/Component)	1500	1000	500

Note: The SAMICS III computer program also prompts for the [payment float interval], the [inflation rate table], the [equipment tax depreciation method], and the [equipment book depreciation method]. In the LSA SAMICS context, use 0.0, (1975, 4.0), DDB, and SL.

Format A: Process Description (Continued)

A15 Process Referent (From Page 1 Line A1) Cln Back

PART 4 – DIRECT REQUIREMENTS PER MACHINE (Facilities) OR PER MACHINE PER SHIFT (Personnel)
(Facilities and Personnel Requirements)

A16 Catalog Number (Expense Item Referent)	A18 Amount Required Per Machine (Per Shift) (Amount per Machine)	A19 Units	A17 Requirement Description
A2064D	300	Sq. Ft.	Mgt. Space A
B3096D	1.0	Person/Shift	Semicond. Assembler
B3704D	.10	Person/Shift	Electr. Tech
B3736D	.10	Person/Shift	Maint. Mech.

PART 5 – DIRECT REQUIREMENTS PER MACHINE PER MINUTE
(Byproduct Outputs) and (Utilities and Commodities Requirements)

A20 Catalog Number (Expense Item Referent)	A22 Amount Required Per Machine Per Minute (Amount per Cycle)	A23 Units	A21 Requirement Description
C1032B	.1	KWHR/min	Electricity
C1144D	.30	Cu. ft/min	DI Water
E1328D	.015	lbs/min	Hydrofloric Acid
E1016D	.003	lbs/min	Acetic Acid
E1110D	.03	Cu. ft/min	Ammonium Hydroxide
E1416D	.0353	Cu. ft/min	N2 Gas
D1048D	4.48	Gal/min	Water, Polluted
D1032D	.0037	Gal/min	Acid waste
D0001D	.449	Gal/min	Alkaline waste

PART 6 – INTRA-INDUSTRY PRODUCT(S) REQUIRED (Required Products)

A24 (Product Reference)	A26 Usable Output Per Unit of Input Product	A27 Units	A25 Product Name
BWAFER	1.0	Wafer/Wafer	Back Printed Wafer
		/	
		/	

Prepared by E. Aerni Date 03/25/80

SOLAR ARRAY MANUFACTURING INDUSTRY COSTING STANDARDS

FORMAT A — PROCESS DESCRIPTION

JET PROPULSION LABORATORY
California Institute of Technology
4800 Oak Grove Dr. / Pasadena, Calif. 91103

A-1 Process [Referent]: JCLEAN

Note: Names given in brackets [ ] are the names of process attributes requested by the SAMIS computer program.

A-2 [Descriptive. Name] of Process: Junction Isolation by Laser Scribing and Breaking

PART 1 – PRODUCT DESCRIPTION

A-3 [Product. Referent]: JCWAFER

A-4 Descriptive Name [Product. Name]: Junction Clean Wafer

A-5 Unit Of Measure [Product. Units]: Wafer

PART 2 – PROCESS CHARACTERISTICS

A-6	[Output. Rate] (Not Thruput)	12.5	Units (given on line A-5) Per Operating Minute
A-7	[Inprocess. Inventory. Time]	8.0	Calendar Minutes (Used only to compute in process inventory)
A-8	[Duty. Cycle]	.90	Operating Minutes Per Minute
A-8a	[Number. Of. Shifts. Per. Day]	3	Shifts
A-8b	[Personnel. Integerization. Override. Switch]	On	(Off or On)

PART 3 – EQUIPMENT COST FACTORS (Machine Description)

A-9	Component [Referent]	Nd-YAG	CasLoader	
A-9a	Component [Descriptive. Name]	Scribe System	Cassette Loader	
			Unloader	
A-10	Base Year For Equipment Prices [Price. Year]	1980	1980	
A-11	[Purchase. Cost. Vs. Quantity. Bought. Table] (Number Of and $ Per Component)	98,000	6,000	
A-12	Anticipated [Useful. Life] (Years)	7	7	
A-13	[Salvage. Value] ($ Per Component)	9,000	1,000	
A-14	[Removal. And. Installation. Cost] ($/Component)	1,380	2,000	

Note: The SAMIS computer program also prompts for the [Payment. Float. Interval], the [Inflation. Rate. Table], the [Equipment. Tax. Depreciation. Method], and the [Equipment. Book. Depreciation. Method]. In the LSA SAMICS context, use 0.0, (1975 6.0 •), DDB, and SL. (The asterisk is a signal to the computer, not a reference to a footnote.)

A-15 Process Referent (From Front Side Line A-1)

PART 4 – DIRECT REQUIREMENTS PER MACHINE (Facilities) OR PER MACHINE PER SHIFT (Personnel)
[Facility Or Personnel Requirement]

A-16 Catalog Number (Expense Item Referent)	A-18 Amount Required Per Machine (Per Shift) [Amount Per Machine]	A-19 Units	A-17 Requirement Description or Name
A2064D	250	sq. ft.	Mg. Space Type A
B3096D	1.50	person/shift	Semiconductor Ass.
B3704D	.10	"	Elect. Maint.

PART 5 – DIRECT REQUIREMENTS PER MACHINE PER MINUTE (SAMIS will ask first for Byproducts)
[Byproduct] and [Utility Or Commodity Requirement]

A-20 Catalog Number (Expense Item Referent)	A-22 Amount Required Per Machine Per Minute [Amount Per Cycle]	A-23 Units	A-21 Requirement Description or Name
C1032B	.066	kWhr/min	Electricity
C1144D	.166	Cu. ft/min.	Deionized Water
C1128D	3.0	Gal/min.	Cooling Water
ELA200D	8E-6	Units/min.	Krypton Arc Lamp
ELA50D	2E-6	Units/min.	Illumination layup

PART 6 – INTRA-INDUSTRY PRODUCT(S) REQUIRED

A-24 [Required Product] (Reference)	A-28 [Yield]* (%)	A-26 [Ideal Ratio]** Of Units Out/Units In	A-27 Units Of A-26***	A-25 Product Name
CBWAFER	99.9	1.0	Wafer/Wafer	Cleaned Wafer

PREPARED BY: Nick Mardesich

DATE: 7/28/80

*100% minus percentage of required product lost in this process.
**Assume 100% yield here.
***Examples: Modules/Cell or Cells/Wafer.

SOLAR ARRAY MANUFACTURING INDUSTRY COSTING STANDARDS

FORMAT A

JET PROPULSION LABORATORY
California Institute of Technology
Grace Dr. / Pasadena, Calif. 91103

PROCESS DESCRIPTION

Note: Names given in brackets [ ] are the names of process attributes requested by the SAMICS III computer program.

A1 [Process Referent] FRONTCONT

A2 [Descriptive Name] Print and Fire Front Contact

PART 1 -- PRODUCT DESCRIPTION

A3 [Product Referent] FWAFER

A4 Descriptive Name [Product Name] Front Contacted Wafer

A5 Unit Of Measure [Product Units] Wafer

PART 2 -- PROCESS CHARACTERISTICS

A6	[Output Rate] (Not Thruput)	25	Units (given on line A5) Per Operating Minute
A7	Average Time at Station [Processing Time]	20	Calendar Minutes (Used only to compute in-process inventory)
A8	Machine "Up" Time Fraction [Usage Fraction]	.90	Operating Minutes Per Minute

PART 3 -- EQUIPMENT COST FACTORS [Machine Description]

A9	Component [Referent]	Printer	Furnace	Test Eq.
A9a	Component [Descriptive Name] (Optional)	Unload Print	IR Belt Furnace	Pull Test Facility
A10	Base Year For Equipment Prices [Price Year]	1980	1980	1980
A11	Purchase Price ($ Per Component) [Purchase Cost]	128,000	39,000	40,000
A12	Anticipated Useful Life (Years) [Useful Life]	7	7	7
A13	[Salvage Value] ($ Per Component)	1000	1000	0
A14	[Removal and Installation Cost] ($/Component)	2000	2000	500

Note: The SAMICS III computer program also prompts for the [payment float interval], the [inflation rate table], the [equipment tax depreciation method], and the [equipment book depreciation method]. In the LSA SAMICS context, use 0.0, (1975, 4.0), DDB, and SL.

Format A: Process Description (Continued)

A15 Process Referent (From Page 1 Line A1) Front Cont.

PART 4 – DIRECT REQUIREMENTS PER MACHINE (Facilities) OR PER MACHINE PER SHIFT (Personnel)
[Facilities and Personnel Requirements]

A16 Catalog Number [Expense Item Referent]	A18 Amount Required Per Machine (Per Shift) [Amount per Machine]	A19 Units	A17 Requirement Description
A2064D	320	Sq. Ft.	Mqt. Space A
B3096D	.20	Person/Shift	Semiconductor Ass.
B3704D	.10	Person/Shift	Elect. Maintenance
B3776D	.10	Person/Shift	Maint. Mech.
B3720D	.25	Person/Shift	Inspector, Q.C.

PART 5 – DIRECT REQUIREMENTS PER MACHINE PER MINUTE
[Byproduct Outputs] and [Utilities and Commodities Requirements]

A20 Catalog Number [Expense Item Referent]	A22 Amount Required Per Machine Per Minute [Amount per Cycle]	A23 Units	A21 Requirement Description
C1032B	.20	KWHR/min	Electricity
E1128D	.000753	lbs/min	Butyl Acetate
E1064D	3.0	gm/min	Silver paste
E1576D	.0005	Screens/min	Screens
EG4D	.0002	Gal/min	Toluene
D1016B	.10	Cu. ft/min	Fumes
D1138D	.0002	Gal/min	Used Solvent

PART 6 – INTRA-INDUSTRY PRODUCT(S) REQUIRED [Required Products]

A24 [Product Reference]	A26 Usable Output Per Unit of Input Product	A27 Units	A25 Product Name
JCWAFER	1.0	Wafer/Wafer	Junction Clean Wafer
		/	
		/	

Prepared by E. Aerni Date 03/06/80

REVERSE SIDE JPL 3037-S R7/78

SOLAR ARRAY MANUFACTURING INDUSTRY COSTING STANDARDS

FORMAT A — PROCESS DESCRIPTION

JET PROPULSION LABORATORY
California Institute of Technology
4800 Oak Grove Dr / Pasadena, Calif 91103

A-1 Process [Referent]: ARCOAT

Note: Names given in brackets [ ] are the names of process attributes requested by the SAMIS computer program.

A-2 [Descriptive. Name] of Process: Apply AR Coat to Bare Cell

PART 1 – PRODUCT DESCRIPTION

A-3 [Product. Referent]: FCELL

A-4 Descriptive Name [Product. Name]: Finished Cell

A-5 Unit Of Measure [Product. Units]: Cell

PART 2 – PROCESS CHARACTERISTICS

A-6	[Output. Rate] (Not Thruput)	3.0	Units (given on line A-5) Per Operating Minute
A-7	[Inprocess. Inventory. Time]	12	Calendar Minutes (Used only to compute in-process inventory)
A-8	[Duty. Cycle]	.9	Operating Minutes Per Minute
A-8a	[Number. Of. Shifts. Per. Day]	3	Shifts
A-8b	[Personnel. Integerization. Override. Switch]	ON	(Off or On)

PART 3 – EQUIPMENT COST FACTORS (Machine Description)

A-9	Component [Referent]	DESYSTEM		
A-9a	Component [Descriptive. Name]	Deposition System		
A-10	Base Year For Equipment Prices [Price. Year]	1980		
A-11	[Purchase. Cost. Vs. Quantity. Bought. Table] (Number Of and $ Per Component)	125K		
A-12	Anticipated [Useful. Life] (Years)	7		
A-13	[Salvage. Value] ($ Per Component)	10K		
A-14	[Removal. And. Installation. Cost] ($/Component)	5K		

Note: The SAMIS computer program also prompts for the [Payment. Float. Interval], the [Inflation. Rate. Table], the [Equipment. Tax. Depreciation. Method], and the [Equipment. Book. Depreciation. Method]. In the LSA SAMICS context, use 0.0, (1975 6.0 *), DDB, and SL. (The asterisk is a signal to the computer, not a reference to a footnote.)

Format A: Process Description (Continued)

A-15 Process Referent (From Front Side Line A-1) ARCOAT

PART 4 – DIRECT REQUIREMENTS PER MACHINE (Facilities) OR PER MACHINE PER SHIFT (Personnel)
[Facility. Or. Personnel Requirement]

A-16 Catalog Number (Expense Item Referent)	A-18 Amount Required Per Machine (Per Shift) [Amount. Per. Machine]	A-19 Units	A-17 Requirement Description or Name
A2064D	80	sq ft	Mgt. Space Type A
B3096D	.20	person/shift	Semicond. Assembler
B3764D	.05	"	Elect. Tech.
B3736D	.05	"	Maint. Mech

PART 5 – DIRECT REQUIREMENTS PER MACHINE PER MINUTE (SAMIS will ask first for Byproducts)
[Byproduct] and [Utility. Or. Commodity Requirement]

A-20 Catalog Number (Expense Item Referent)	A-22 Amount Required Per Machine Per Minute [Amount. Per. Cycle]	A-23 Units	A-21 Requirement Description or Name
C1032B	0.17	kWhr/min.	Electricity
C1128D	3.0	gal/min.	Cooling water
C1080D	0.018	cu.ft./min.	N2 liquid
E1416D	0.5	cu.ft./min.	N2 gas

PART 6 – INTRA-INDUSTRY PRODUCT(S) REQUIRED

A-24 [Required. Product] (Reference)	A-28 [Yield] * (%)	A-26 [Ideal. Ratio] ** Of Units Out/Units In	A-27 Units Of A-26***	A-25 Product Name
FWAFER	99.9	1.0	cell/wafer	Front Contacted Cell

PREPARED BY N. Mardesich DATE 7/28/80

*100% minus percentage of required product lost in this process.
**Assume 100% yield here.
***Examples: Modules/Cell or Cells/Wafer.

REVERSE SIDE JPL 3037-S R 5/80

SOLAR ARRAY MANUFACTURING INDUSTRY COSTING STANDARDS

FORMAT A

JET PROPULSION LABORATORY
California Institute of Technology
4800 Oak Grove Dr. / Pasadena, Calif. 91103

PROCESS DESCRIPTION

Note: Names given in brackets [ ] are the names of process attributes requested by the SAMICS III computer program.

A1 Process [Referent] CELLTEST

A2 [Descriptive Name] Test Cells After Processing

PART 1 – PRODUCT DESCRIPTION

A3 [Product Referent] TCELL

A4 Descriptive Name [Product Name] Tested Cell

A5 Unit Of Measure [Product Units] Cells

PART 2 – PROCESS CHARACTERISTICS

A6 [Output Rate] (Not Thruput) 25 Units (given on line A5) Per Operating Minute

A7 Average Time at Station [Processing Time] 2 Calendar Minutes (Used only to compute in-process inventory)

A8 Machine "Up" Time Fraction [Usage Fraction] .95 Operating Minutes Per Minute

PART 3 – EQUIPMENT COST FACTORS [Machine Description]

A9	Component [Referent]			Simulator
A9a	Component [Descriptive Name] (Optional)			Light House and Vacuum Fixture Coolir Prov.
A10	Base Year For Equipment Prices [Price Year]			1980
A11	Purchase Price ($ Per Component) [Purchase Cost]			91,000
A12	Anticipated Useful Life (Years) [Useful Life]			7
A13	[Salvage Value] ($ Per Component)			2000
A14	[Removal and Installation Cost] ($/Component)			500

Note: The SAMICS III computer program also prompts for the [payment float interval], the [inflation rate table], the [equipment tax depreciation method], and the [equipment book depreciation method]. In the LSA SAMICS context, use 0.0, (1975, 4.0), DDB, and SL.

Format A: Process Description (Continued)

A15 Process Referent (From Page 1 Line A1) Cell Test

PART 4 – DIRECT REQUIREMENTS PER MACHINE (Facilities) OR PER MACHINE PER SHIFT (Personnel)
[Facilities and Personnel Requirements]

A16 Catalog Number [Expense Item Referent]	A18 Amount Required Per Machine (Per Shift) [Amount per Machine]	A19 Units	A17 Requirement Description
A2064D	160	Sq. Ft.	Mgt Space Type A
B3768D	1.0	Person/Shift	Electronics Component Tester
B3688D	.20	Person/Shift	Electronic Maintenance
B3736D	.10	Person/Shift	Maintenance Mechanic II

PART 5 – DIRECT REQUIREMENTS PER MACHINE PER MINUTE
[Byproduct Outputs] and [Utilities and Commodities Requirements]

A20 Catalog Number [Expense Item Referent]	A22 Amount Required Per Machine Per Minute [Amount per Cycle]	A23 Units	A21 Requirement Description
C1122D	.2667	Cu. ft/min	Cooling Water
D1160D	2.00	Gal/min	Used Cooling Water
C1032B	.125	KWHR/min	Electricity

PART 6 – INTRA-INDUSTRY PRODUCT(S) REQUIRED [Required Products]

A24 [Product Reference]	A26 Usable Output Per Unit of Input Product	A27 Units	A25 Product Name
FCELL	.95	Cell / Cell	Finished Cell
		/	
		/	

Prepared by E. Aerni Date 03/25/80

SOLAR ARRAY MANUFACTURING INDUSTRY COSTING STANDARDS

FORMAT A

JET PROPULSION LABORATORY
California Institute of Technology
4800 Oak Grove Dr. / Pasadena, Calif. 91103

PROCESS DESCRIPTION

Note: Names given in brackets [ ] are the names of process attributes requested by the SAMICS III computer program.

A1 [Process Referent] ACIRCUIT

A2 [Descriptive Name] Assemble Circuit (includes Lead Cell, String Assembly and Circuit Assembly Process Spec.)

PART 1 – PRODUCT DESCRIPTION

A3 [Product Referent] CIRCUIT

A4 Descriptive Name [Product Name] Assembled Solar Cell Circuit

A5 Unit Of Measure [Product Units] Circuits

PART 2 – PROCESS CHARACTERISTICS

A6	[Output Rate] (Not Thruput)	0.2	Units (given on line A5) Per Operating Minute
A7	Average Time at Station [Processing Time]	28	Calendar Minutes (Used only to compute in-process inventory)
A8	Machine "Up" Time Fraction [Usage Fraction]	.90	Operating Minutes Per Minute

PART 3 – EQUIPMENT COST FACTORS [Machine Description]

A9	Component [Referent]	CIRFAB	FLUX	
A9a	Component [Descriptive Name] (Optional)	Circuit fabricator	Flux Removal	
A10	Base Year For Equipment Prices [Price Year]	1980	1980	
A11	Purchase Price ($ Per Component) [Purchase Cost]	356,000	15,000	
A12	Anticipated Useful Life (Years) [Useful Life]	7	7	
A13	[Salvage Value] ($ Per Component)	0	1,500	
A14	[Removal and Installation Cost] ($/Component)	10,000	500	

Note: The SAMICS III computer program also prompts for the [payment float interval], the [inflation rate table], the [equipment tax depreciation method], and the [equipment book depreciation method]. In the LSA SAMICS context, use 0.0, (1975, 4.0), DDB, and SL.

Format A: Process Description (Continued)

A15 Process Referent (From Page 1 Line A1) A Circuit

PART 4 – DIRECT REQUIREMENTS PER MACHINE (Facilities) OR PER MACHINE PER SHIFT (Personnel) [Facilities and Personnel Requirements]

A16 Catalog Number [Expense Item Referent]	A18 Amount Required Per Machine (Per Shift) [Amount per Machine]	A19 Units	A17 Requirement Description
A2064D	530	Sq. Ft	Mfg. Space A
B3096D	1.0	Person/Shift	Semicond. Assembler
B3704D	.15	Person/Shift	Elect. Maint.
B3736D	.2	Person/Shift	Maint. Mech.

PART 5 – DIRECT REQUIREMENTS PER MACHINE PER MINUTE [Byproduct Outputs] and [Utilities and Commodities Requirements]

A20 Catalog Number [Expense Item Referent]	A22 Amount Required Per Machine Per Minute [Amount per Cycle]	A23 Units	A21 Requirement Description
C1032B	0.1	KWHR/min	Electricity
EG54D	4.00	ft/min	Plated Cu Ribbon
EBR5D	30	in/min	Bus Bar Ribbon
EG2D	2.18	cc/min	Flux
ES005D	.10	cc/min	Tin zinc eutectic
E0002D	.002	lbs/min	TMG (Freon)
D1016B	24	Cu. ft/min	Fumes
D1128B	.00025	Gal/min	Used solvent

PART 6 – INTRA-INDUSTRY PRODUCT(S) REQUIRED [Required Products]

A24 [Product Reference]	A26 Usable Output Per Unit of Input Product	A27 Units	A25 Product Name
TCELL	0.01515	CKTS/Cell	Cell Test
		/	
		/	

Prepared by E. Aerni Date 03/25/80

SOLAR ARRAY MANUFACTURING INDUSTRY COSTING STANDARDS

FORMAT A

JET PROPULSION LABORATORY
California Institute of Technology
4800 Oak Grove Dr. / Pasadena, Calif. 91103

PROCESS DESCRIPTION

Note: Names given in brackets [ ] are the names of process attributes requested by the SAMICS III computer program.

A1 Process [Referent] LAMINATE

A2 [Descriptive Name] Laminating of Circuits to Superstrate glass

PART 1 – PRODUCT DESCRIPTION

A3 [Product Referent] SUPERST

A4 Descriptive Name [Product Name] Superstrate assembly

A5 Unit Of Measure [Product Units] Superstrate

PART 2 – PROCESS CHARACTERISTICS

A6	[Output Rate] (Not Thruput)	0.2	Units (given on line A5) Per Operating Minute
A7	Average Time at Station [Processing Time]	60	Calendar Minutes (Used only to compute in-process inventory)
A8	Machine "Up" Time Fraction [Usage Fraction]	.90	Operating Minutes Per Minute

PART 3 – EQUIPMENT COST FACTORS [Machine Description]

A9	Component [Referent]	Laminator		
A9a	Component [Descriptive Name] (Optional)			
A10	Base Year For Equipment Prices [Price Year]	1980		
A11	Purchase Price ($ Per Component) [Purchase Cost]	415,000		
A12	Anticipated Useful Life (Years) [Useful Life]	10		
A13	[Salvage Value] ($ Per Component)	0		
A14	[Removal and Installation Cost] ($/Component)	10,000		

Note: The SAMICS III computer program also prompts for the [payment float interval], the [inflation rate table], the [equipment tax depreciation method], and the [equipment book depreciation method]. In the LSA SAMICS context, use 0.0, (1975, 4.0), DDB, and SL.

Format A: Process Description (Continued)

A15 Process Reference (From Page 1 Line A1) Laminate

PART 4 – DIRECT REQUIREMENTS PER MACHINE (Facilities) OR PER MACHINE PER SHIFT (Personnel) [Facilities and Personnel Requirements]

A16 Catalog Number [Expense Item Referent]	A18 Amount Required Per Machine (Per Shift) [Amount per Machine]	A19 Units	A17 Requirement Description
A2064D	400	Sq. Ft.	Mfg. Space A
B3048D	1.0	Person/Shift	Encapsulator
B3704D	0.1	Person/Shift	Elect. Maint.
B3736D	0.1	Person/Shift	Maint. Mech

PART 5 – DIRECT REQUIREMENTS PER MACHINE PER MINUTE [Byproduct Outputs] and [Utilities and Commodities Requirements]

A20 Catalog Number [Expense Item Referent]	A22 Amount Required Per Machine Per Minute [Amount per Cycle]	A23 Units	A21 Requirement Description
C1032B	1.0	KWHR/min	Electricity
EVA01D	3.2	Sq. ft/min	Clear EVA 5 mil
EVA02D	3.2	Sq. ft/min	White EVA 5 mil
EVG01D	3.2	Sq. ft/min	Crane Glas
E1721D	(3.2)*2	Sq. ft/min	Metallized milar*
E1828D	3.2	Sq. ft/min	Tempered glass
E5184D	1.2 E-5	lbs/min	Silane primer
E1032D	.10	lbs/min	Acetone
E0001D	.0015	Gal/min	Methyl Alcohol

PART 6 – INTRA-INDUSTRY PRODUCT(S) REQUIRED [Required Products]

A24 [Product Reference]	A26 Usable Output Per Unit of Input Product	A27 Units	A25 Product Name
CIRCUIT	1.0	Superstrate/circuit	Assembled Solar Cell Circuit
		/	
		/	

Prepared by E. Aerni Date 03/25/80

* Catalogue item Al foil at 1¢ per sq. ft. versus 2¢ per sq. ft. of metallized mylar.

SOLAR ARRAY MANUFACTURING INDUSTRY COSTING STANDARDS

FORMAT A

JET PROPULSION LABORATORY
California Institute of Technology
4800 Oak Grove Dr. / Pasadena, Calif. 91103

PROCESS DESCRIPTION

Note: Names given in brackets [ ] are the names of process attributes requested by the SAMICS III computer program.

A1 Process [Referent] FRAME

A2 [Descriptive Name] Framing and Terminating of Module

PART 1 – PRODUCT DESCRIPTION

A3 [Product Referent] PANEL1

A4 Descriptive Name [Product Name] Completed Module

A5 Unit Of Measure [Product Units] Module

PART 2 – PROCESS CHARACTERISTICS

A6	[Output Rate] (Not Thruput)	.20	Units (given on line A5) Per Operating Minute
A7	Average Time at Station [Processing Time]	10	Calendar Minutes (Used only to compute in-process inventory)
A8	Machine "Up" Time Fraction [Usage Fraction]	.90	Operating Minutes Per Minute

PART 3 – EQUIPMENT COST FACTORS [Machine Description]

A9	Component [Referent]	Assy Table	Ext Cut	Framing
A9a	Component [Descriptive Name] (Optional)	Table to Assemble J-Box	Cutting Extrusions To length	Place and attach frame parts to laminate
A10	Base Year For Equipment Prices [Price Year]	1980	1980	1980
A11	Purchase Price ($ Per Component) [Purchase Cost]	1500	5000	35000
A12	Anticipated Useful Life (Years) [Useful Life]	7	10	7
A13	[Salvage Value] ($ Per Component)	0	0	3000
A14	[Removal and Installation Cost] ($/Component)	300	1000	1500

Note: The SAMICS III computer program also prompts for the [payment float interval], the [inflation rate table], the [equipment tax depreciation method], and the [equipment book depreciation method]. In the LSA SAMICS context, use 0.0, (1975, 4.0), DDB, and SL.

Format A: Process Description (Continued)

A15 Process Referent (From Page 1 Line A1) Frame.

PART 4 -- DIRECT REQUIREMENTS PER MACHINE (Facilities) OR PER MACHINE PER SHIFT (Personnel) (Facilities and Personnel Requirements)

A16 Catalog Number (Expense Item Referent)	A18 Amount Required Per Machine (Per Shift) (Amount per Machine)	A19 Units	A17 Requirement Description
A2064D	350	Sq. Ft.	Mgf. Space Type A
B3704D	.025	Person/Shift	Electr. Maint.
B3756D	.10	Person/Shift	Maint. Mech
B3720D	.25	Person/Shift	Insepctor
B3080D	2.00	Person/Shift	Module Assembler

PART 5 -- DIRECT REQUIREMENTS PER MACHINE PER MINUTE (Byproduct Outputs) and (Utilities and Commodities Requirements)

A20 Catalog Number (Expense Item Referent)	A22 Amount Required Per Machine Per Minute (Amount per Cycle)	A23 Units	A21 Requirement Description
C1032B	.10	KWHR/min	Electricity
EG1164D	.06	$/min	Gasket
E1232D	.20	$/min	Edge Sealant
EG3D	.02	$/min	Solder Flux
EG31D	.008	$/min	MEK
EG1283D	.35	$/min	J-Boxes Diodes *
*	.4	Boxes/min	Junction Box
*	.2	diodes/min	Diode

PART 6 -- INTRA-INDUSTRY PRODUCT(S) REQUIRED (Required Products)

A24 (Product Reference)	A26 Usable Output Per Unit of Input Product	A27 Units	A25 Product Name
SUPERST	1.0	Module/Super-/strate	Superstrate Assembly

Prepared by E. Aerni Date 03/25/80

* Expense EG1283D reflects costs of J-Boxes at .75¢ ea. and diodes at .25¢ ea. when utilizing amount per cycle as indicated for each item.

SOLAR ARRAY MANUFACTURING INDUSTRY COSTING STANDARDS

FORMAT A

JET PROPULSION LABORATORY
California Institute of Technology
4800 Oak Grove Dr. / Pasadena, Calif. 91103

PROCESS DESCRIPTION

Note: Names given in brackets [ ] are the names of process attributes requested by the SAMICS III computer program.

A1 [Process Referent] FINALTEST

A2 [Descriptive Name] Test Module For Performance Mechanical Integrity and Electrical Spec Conformity

PART 1 – PRODUCT DESCRIPTION

A3 [Product Referent] MODULE

A4 Descriptive Name [Product Name] Completed Solar Panel, Ready for Shipping

A5 Unit Of Measure [Product Units] Modules

PART 2 – PROCESS CHARACTERISTICS

A6	[Output Rate] (Not Thruput)	.66	Units (given on line A5) Per Operating Minute
A7	Average Time at Station [Processing Time]	1.50	Calendar Minutes (Used only to compute in-process inventory)
A8	Machine "Up" Time Fraction [Usage Fraction]	.90	Operating Minutes Per Minute

PART 3 – EQUIPMENT COST FACTORS [Machine Description]

A9	Component [Referent]	Transfer	Simulator	
A9a	Component [Descriptive Name] (Optional)	Move Equipment to and from test station	Puls Solar simulator	
A10	Base Year For Equipment Prices [Price Year]	1980	1980	
A11	Purchase Price ($ Per Component) [Purchase Cost]	5,000	80,000	
A12	Anticipated Useful Life (Years) [Useful Life]	7	7	
A13	[Salvage Value] ($ Per Component)	0	4000	
A14	[Removal and Installation Cost] ($/Component)	500	500	

Note: The SAMICS III computer program also prompts for the [payment float interval], the [inflation rate table], the [equipment tax depreciation method], and the [equipment book depreciation method]. In the LSA SAMICS context, use 0.0, (1975, 4.0), DDB, and SL.

Format A: Process Description (Continued)

A15 Process Referent (From Page 1 Line A1) Final Test

PART 4 – DIRECT REQUIREMENTS PER MACHINE (Facilities) OR PER MACHINE PER SHIFT (Personnel)
[Facilities and Personnel Requirements]

A16 Catalog Number [Expense Item Referent]	A18 Amount Required Per Machine (Per Shift) [Amount per Machine]	A19 Units	A17 Requirement Description
A2064D	200	Sq.ft	High Space Type A
B3720D	1.0	Person/Shift	Inspector, System
B3704D	.15	Person/Shift	Electronic Maint.
B3080D	1.0	Person/Shift	Module Assembler

PART 5 – DIRECT REQUIREMENTS PER MACHINE PER MINUTE
[Byproduct Outputs] and [Utilities and Commodities Requirements]

A20 Catalog Number [Expense Item Referent]	A22 Amount Required Per Machine Per Minute [Amount per Cycle]	A23 Units	A21 Requirement Description
C1032B	.025	KWHR/min	Electricity

PART 6 – INTRA-INDUSTRY PRODUCT(S) REQUIRED [Required Products]

A24 [Product Reference]	A26 Usable Output Per Unit of Input Product	A27 Units	A25 Product Name
PANEL1	.998	Module/Module	Completed Module
		/	
		/	

Prepared by Aerni Date 03/25/80